
The effect of Coxsackie virus A9 infection on nuclear and nucleolar proteins

Ashjan .A. Shami

A thesis submitted for the degree of Doctor of Philosophy

Department of Biological Sciences.

University of Essex

January 2016

Abstract

Picornaviruses replicate in the cytoplasm, but there is growing evidence that the cell nucleus is affected by infection e.g. transcription factor cleavage, relocation of nuclear proteins and alteration to nucleo-cytoplasmic shuttling. It was previously observed that *Parechovirus* genus members affect the distribution of the nuclear paraspeckle protein PSPC-1, which is an RNA-binding protein involved in splicing and RNA export. To investigate if this is a general feature of picornaviruses infection, coxsackie virus A9 (CAV-9) was studied. This is a typical member of the large and most medically-important picornavirus genera *Enterovirus*, which is genetically divergent from *Parechovirus*. Using an EGFP-PSPC-1 fusion, we found that infection changes the distribution of PSPC-1 from nuclear paraspeckles to cytoplasmic granules that do not seem to correspond to known cytoplasmic foci of RNA-binding proteins e.g. stress granules and P-bodies. They also do not correspond to CAV-9 replication complexes. Two other paraspeckle proteins (PSF and NONO) colocalise with PSPC-1 in these structures. The effect does not seem to be due to cleavage of these proteins by virus proteases, phosphorylation at two sites known to be involved in PSF translocation or sumoylation. It is dependent on part of PSF, between amino acids 452-606, which is also needed for paraspeckle localization and which is involved in key interactions between PSF, PSPC-1 and NONO. There are few reports on the significance of paraspeckle proteins in virus infection. Our results suggest that we have identified a novel cellular compartment, or a structure induced by virus infection. If this is proved to be required by the virus, then it could be a potential drug target for the development of a new class of antiviral agents against this important group of viruses.

Acknowledgements

Though only my name appears on the cover of this thesis, I would never have been able to finish my thesis without the guidance of my lab members, help from friends, and support from my family.

I am most thankful for my dearest parents. They were always supporting me and encouraging me with their best wishes and travelling all this distance to support me by being personally beside me and cheering me up and stood by me through the good and bad times. I would also never forget my grandmother (Nour Kamal, R.I.P) words, prayers and support to accomplish my studies and get the PhD as the first member of the family.

I am very thankful for my both sisters for their support and encouragement.

I would like to thank my beloved fiancé Mr. Remo Zulauf for his support, encouragement, and patience and help to produce my work as thesis.

I would like to express my deepest gratitude to my advisor, Prof. Glyn Stanway, for his kindness, excellent guidance, and patience, and for providing me with an excellent atmosphere for doing research.

I am very thankful and grateful to Dr. Shaia Al Malki, Dr. Arsalan Salimi, Dr Naseebah Baeshen, Miss Cheryl Eno-Ibanga, Mr Ali Khrid, Miss Marina Ioannou, Mrs Natalie Gray and Miss. Hannah Adams for their support and patience during the project.

I would like to thank Mrs Rana Al Ghamdi, who as a good friend was always willing to help and give her best suggestions specially with using microscopes and EndNote x7.

I would like also to thank the Saudi Government and Taif University for their financial sponsoring my PhD.

I would also like to thank Ralf Zwacka, Andrea Moher and their team for helping with Western Blot.

List of Abbreviations

2A ^{pro}	2A proteolytic protein	CVB3	Coxsackie virus B3
3C ^{pro} /3CD ^{pro}	3C/ 3CD proteolytic protein	D1	Domain 1
3D ^{pol}	3D polymerase	DAF	Decay accelerating factor
4E-BPs	eIF4E- binding proteins	DAPI	4',6-Diamidino-2-phenylindole dihydrochloride
APL	Acute promyelocytic leukemia	DBHS	Drosophila Behavior Human Splicing
Arf1	ADP- ribosylation factor 1	DMEM	Dulbecco's Modified Eagle's Medium
AUF1	AU-rich element RNA binding protein factor 1	DNA	Deoxyribonucleic acid
BHV-1	Bovine herpesvirus type 1	dsRNA	Double stranded ribonucleic acid
BRK	Breast tumour kinase	<i>E.coli</i>	<i>Escherichia coli</i>
BSA	Bovine serum albumin	E1	Rubella virus
CAR	Coxsackie adenovirus receptor	EB	Elution buffer
CAV9	Coxsackie virus A9	EGFP	Enhanced green fluorescent protein
CMC	Carboxyl methylcellulose	eIF-4	Human eukaryotic translation initiation factor 4
CNS	Central nervous system	eIF4G	Human eukaryotic translation initiation factor 4G
CPE	Carbapenemase-producing Enterobacteriaceae	eIFs	Canonical initiation factors
Cre	<i>cis</i> -acting replication element	EMCV	Encephalo-myocarditis

ER	Endoplasmic reticulum		Ribonucleoprotein A1
EV71	Enterovirus 71	HPeV	Human parechoviruses
EYFP	Enhanced yellow fluorescent protein	HSV-1	Herpes simplex virus 1
FBP2	Fructose-1,6-Bisphosphatase 2	HT29	Human colon adenocarcinoma cells
FBS	Fetal Bovine Serum	HVS	Herpesvirus saimiri
FITC	Fluorescein isothiocyanate	ICAM1	Intercellular Adhesion Molecule 1
FMD	Foot and mouth disease	ICP27	Infected cell protein 27
G3BP	GTPase-activating protein-binding protein 1	IF4E	Eukaryotic translation initiation factor 4E family
GAR Domain	Glycine-Arginine rich Domain	IGC	Inter chromatin granule clusters
GBF1	Guanine nucleotide exchange factor	IgSF	Immunoglobulin superfamily
GMK	Green Monkey Kidney cell line	IL8	Interleukin 8
GW182	Glycine(G)-tryptophan(W), 128 kD	INF	Interferon receptors
HAV	Hepatitis A virus	INS	<i>cis</i> -acting regulatory element
HCMV	Human cytomegalovirus	IRES	Internal ribosome entry site
HCV	Hepatitis C virus	ISRE	IFN- stimulated response elements
HDV	Hepatitis D virus	ITAF	IRES trans-acting factors
HIV	Human immunodeficiency virus	JEV	Japanese encephalitis virus
hnRNP A1/ hnRNPs	Heterogeneous Nuclear	Kr	kremer bodies

List of Abbreviations

KSHV	Kaposi's sarcoma-associated herpesvirus	Pen Strep	Penicillin streptomycin
La	Lupus autoantigen	PML	Promyelocytic leukemia
LA	Luria Agar	PML NBs	Promyelocytic leukemia nuclear bodies
LB	Luria Broth	POD	PML oncogenic domain
L ^{pro}	Leader protease	pre-VII	Precursor of core protein VII
MCV	Molluscum contagiosum virus	PSF	PTB associated splicing factor
mRNA	Messenger RNA	PSGL-2	P-selectin glycoprotein ligand-2
ncRNA/ lnc-RNA	Long Non codingRNA	PSP1 /	Paraspeckle protein 1
ND10	Nuclear domain 10	PSP2	Paraspeckle protein 2
NE	Nuclear export	PSPC-1	Paraspeckle Component 1
NEAT1	Long ncRNA nuclear- enriched abundant transcript 1	PTB	Polypyrimidine-tract-binding protein
NLP	Nucleoplasmin- like protein	PTDC	Sodium pyrrolidine dithiocarbamate
NLS/NoLS	Nuclear localization signal	PV	Poliovirus
NPCs	Nuclear pore complexes	RGD	Arginine (R)-glycine (G)-aspartate (D) motif
NPM	Nucleophosmin/ B23	RNA	Ribonucleic acid
Nup	Nucleoporins	RNPs	Ribonuclear proteins
P-bodies	Processing bodies	RRM	RNA recognition motif
PABP	poly(A) binding protein	RT	Room temperature
PCBP2	poly (rC) binding protein		
PCR	Polymerase Chain Reaction		

List of Abbreviations

vi

S.G	Stress Granules	TAF-III	Template-activating factor-III
SC35	Splicing component, 35kD	TBP	TATA-box binding protein
SCARB2	Scavenger Receptor Class B member 2	TIA1	T-cell intracellular antigen 1
SF21ASF	Alternate splicing factor or splicing factor 2	TRIM	Tripartite motif
siRNA	Small interfering RNA	TRITC	Tetramethyl-rhodamine
snRNP	small nuclear ribonucleic proteins	Unr	Upstream of N-ras protein
SR	Serine/Arginine-rich proteins	UTR	Untranslated region
ssRNA	single- stranded ribonucleic acid	VSV	Vesicular stomatitis virus
		WT	Wild type

Table of content

Chapter 1	Introduction	1
1.1	Picornaviruses	2
1.1.1	Taxonomy	2
1.1.2	Importance of Picornaviruses	2
1.1.2.1	Enterovirus	4
1.1.2.1.1	Coxsackie virus:	6
1.1.2.2	Parechovirus	6
1.1.2.3	Aphthovirus	7
1.1.2.4	Hepatovirus	8
1.1.3	Structure of particle and genome	8
1.1.3.1	Outline of picornavirus replication	10
1.1.4	Enterovirus replication	12
1.1.4.1	Receptor binding	12
1.1.4.2	Entry	13
1.1.4.3	Un-coating	14
1.1.4.4	Translation	14
1.1.4.5	Polyprotein processing	17
1.1.4.6	Genome replication	18
1.1.4.7	Virus assembly and maturation and cell lysis	19
1.1.5	Viral Non-structural proteins	22
1.1.5.1	2A	22
1.1.5.2	2B	23
1.1.5.3	2C	23
1.1.5.4	3A	24
1.1.5.5	3B	24
1.1.5.6	3C ^{pro} and 3CD ^{pro}	25
1.1.5.7	3D ^{pol}	25
1.2	The effect of viruses on cells	27
1.2.1	The effect on translation	27
1.2.2	The effect on cytoplasmic membranes and secretion	28
1.2.3	The effect on replication complexes	29
1.2.4	The effect on autophagosome	29
1.2.5	The effect on stress granules and P bodies	30
1.2.6	The effect of picornaviruses on the nucleus	31
1.3	Nucleus structures	33
1.3.1	PML bodies	33

1.3.2	Speckles	34
1.3.3	Paraspeckles.....	35
1.4	Nucleolus structures.....	38
1.4.1	Nucleolin.....	38
1.4.2	Fibrillarin	39
1.4.3	B23.....	39
1.5	The effect of the viruses on PML-NB, speckles, paraspeckles, nucleolin, fibrillarin and B23.....	40
1.5.1	The effect of the viruses on PML	40
1.5.2	The effect of viruses on speckles protein SC35.....	41
1.5.3	The effect of the viruses on paraspeckles	43
1.5.4	The effect of viruses on nucleolin	43
1.5.5	The effect of viruses on Fibrillarin	44
1.5.6	The Effect of the viruses on B23	44
1.6	Aims.....	45
Chapter 2 Material and Methods.....		46
2.1	Materials	47
2.1.1	Tissue culture reagent	47
2.1.2	Tissue culture buffers	48
2.1.2.1	Phosphate buffer saline (PBS)	48
2.1.2.2	Mowiol mounting medium	48
2.1.2.3	Carboxy methyl cellulose (CMC) plaque overlay media.....	48
2.1.2.4	Crystal violet stain	48
2.1.3	Virus strains	49
2.1.4	Cell Fixation for microscopy	49
2.1.5	Antibodies.....	50
2.1.6	Plasmid DNA.....	50
2.1.7	Oligonucleotides	50
2.1.8	Polymerase Chain Reaction (PCR) reagents	50
2.1.9	Agarose gel electrophoresis	58
2.1.10	Gel purification.....	58
2.1.11	Ligation.....	58
2.1.12	Competent cells transformation.....	59
2.1.13	DNA isolation from bacteria	60
2.1.14	Restriction enzymes.....	60
2.1.15	Western blot.....	61
2.1.15.1	Separating gel	61
2.1.15.2	Stacking gel.....	61
2.1.15.3	Semi-dry blotting	61
2.1.15.4	Milk solution.....	62
2.1.15.5	3% Blocking	62
2.2	Methods	62

2.2.1	Tissue culture.....	62
2.2.1.1	Cell culture.....	62
2.2.1.2	Cell splitting.....	62
2.2.1.3	DNA transfection.....	63
2.2.1.3.1	Lipofectin transfection method	63
2.2.1.3.2	Xfect transfection method	63
2.2.1.3.3	TurboFect transfection method	64
2.2.1.4	Microscopy	64
2.2.1.4.1	Confocal microscope.....	64
2.2.1.4.2	Wide field microscope.....	65
2.2.1.5	Viral infection and detection of infected cells	66
2.2.1.6	Plaque assay	66
2.2.1.7	Virus propagation	67
2.2.1.8	Cell line storage	67
2.2.2	Molecular methods	68
2.2.2.1	DNA constructs.....	68
2.2.2.2	Polymerase chain reaction (PCR)	68
2.2.2.2.1	Basic PCR	68
2.2.2.2.2	Overlap PCR.....	69
2.2.2.2.3	Colony PCR.....	69
2.2.2.3	Agarose gel electrophoresis	70
2.2.2.4	Gel purification	70
2.2.2.5	Ligation into pGEM-T Easy	73
2.2.2.6	Ligation in EGFP or mCherry vectors	73
2.2.2.7	Transformation of <i>E.coli</i>	73
2.2.2.7.1	Competent cells preparation	73
2.2.2.7.2	Transformation	74
2.2.2.8	Mini prep (QIAGEN).....	74
2.2.2.9	pGEM-T Easy ligation analysis.....	75
2.2.2.10	Double digestion.....	75
2.2.2.11	Midi Prep (Qiagen system).....	76
2.2.2.12	Western Blot	77

Chapter 3 Effect of CAV-9 Infection on the Host Cell Nucleus and Nucleolus Proteins 79

3.1	Introduction.....	80
3.2	Approach.....	81
3.3	EGFP distribution	82
3.4	PML (EGFP-PML) distribution.....	82
3.4.1	EGFP-PML distribution in uninfected cells	82
3.4.2	The effect of CAV-9 infection on EGFP-PML distribution.....	82
3.5	Nucleolin (EGFP-Nucleolin) distribution.....	83

3.5.1	EGFP-nucleolin distribution in uninfected cells.....	83
3.5.2	The effect of CAV-9 infection on nucleolin distribution	83
3.6	Fibrillarin (EGFP-Fibrillarin) distribution.....	84
3.6.1	EGFP-Fibrillarin distribution in uninfected cells	84
3.6.2	The effect of CAV-9 infection on EGFP-fibrillarin distribution.....	84
3.7	B23 (EGFP-B23) distribution.....	89
3.7.1	EGFP-B23 distribution in uninfected cells.....	89
3.7.2	The effect of CAV-9 infection on EGFP-B23 distribution	89
3.8	Paraspeckle (EGFP-PSPC-1) distribution	90
3.8.1	EGFP-PSPC-1 distribution in uninfected cells.....	90
3.8.2	The effect of CAV-9 infection on EGFP-PSPC-1 distribution	90
3.9	Other paraspeckle (EGFP-PSF and EGFP-NONO) distribution	93
3.9.1	EGFP-PSF and EGFP-NONO distribution in uninfected cells	93
3.9.2	The effect of CAV-9 infection on EGFP-PSF and EGFP-NONO distribution	93
3.10	The PSF/NONO and PSPC-1 complex.....	94
3.11	Endogenous paraspeckles	95
3.12	Discussion.....	101

Chapter 4 The Effect of Non Structural Proteins on Nuclear Proteins 108

4.1	Introduction.....	109
4.2	EGFP/mCherry constructs containing 2A and 3C from CAV-9 and HPeV-1	110
4.2.1	Primer design, PCR amplification and validation of the constructs:.....	110
4.3	Approach.....	114
4.4	Transfection of CAV-9 2A and 3C.....	114
4.5	Transfection of HPeV-1 2A and 3C and 3C mutant.....	115
4.6	Cotransfection of CAV-9 and HPeV-1 2A and 3C with nuclear proteins..	121
4.7	The effect of other HPeV-1 non structural protein on paraspeckles:	126
4.8	The effect of other CAV-9 non structural protein on paraspeckles:.....	127
4.9	Discussion.....	131

Chapter 5 Paraspeckle Proteins Mutation and Translocation 137

5.1	Introduction.....	138
5.2	Approach.....	139
5.3	PSPC-1 truncations at predicted 3C ^{pro} cleavage sites.....	139
5.4	PSF phosphorylation and sumoylation	146
5.5	PSF truncations	153

5.6	Cytoplasmic structures which could be the location of DBHS proteins after infection with CAV-9	160
5.6.1	Replication complexes.....	160
5.6.2	Stress granules	161
5.6.3	P body	162
5.6.4	Autophagosome	169
5.7	Discussion.....	175
5.7.1	Protease digestion	175
5.7.2	PSF phosphorylation sites.....	179
5.7.3	PSF deletion mutants	181
5.7.4	Attempts to identify the cytoplasmic granules	184
5.7.5	Conclusion	186
Chapter 6 General discussions		187

Table of figures

Figure 1-1 Picornavirus taxonomy tree.....	3
Figure 1-2 The structure of Coxsackie A9 (CAV-9) virus particle	11
Figure 1-3 Schematic representation of a <i>Enterovirus</i> genome.....	11
Figure 1-4 Diagram of viral Translation	15
Figure 1-5 The different Picornavirus IRES Types structures.....	21
Figure 1-6 The structure of the virus proteases	26
Figure 1-7 A Schematic representation of the PML protein.....	37
Figure 1-8 A Schematic representation of the (SC-35) protein.	37
Figure 1-9 A Schematic representation of the paraspeckle proteins.....	37
Figure 1-10 Schematic diagram of the domain structure of nucleolin.....	42
Figure 1-11 A schematic representation of the fibrillarin protein structure.	42
Figure 1-12 A schematic representation of the B23.1 protein.	42
Figure 2-1 PCR reactions.....	72
Figure 3-1 The effect of CAV-9 on the redistribution of EGFP.....	85
Figure 3-2 The effect of CAV-9 infection on the distribution of EGFP-PML.	86
Figure 3-3 The effect of CAV-9 infection on the distribution of EGFP-Nucleolin.....	87
Figure 3-4 The effect of CAV-9 infection on the distribution of EGFP-Fibrillarin.	88
Figure 3-5 The effect of CAV-9 infection on the distribution of EGFP-B23.....	91
Figure 3-6 The effect of CAV-9 infection on the distribution of EGFP-PSPC-1.....	92
Figure 3-7 The effect of CAV-9 infection on the distribution of EGFP-NONO (time interval).....	96
Figure 3-8 The effect of CAV-9 infection on the distribution of EGFP-PSF (time interval).....	97
Figure 3-9 The effect of 8 hr infection on EGFP-NONO.....	98
Figure 3-10 The effect of 8 hr infection on EGFP-PSF.....	98
Figure 3-11 The effect of CAV-9 on the redistribution of EGFP-NONO/PSF and mCherry PSPC-1 complex.....	99
Figure 3-12 The effect of CAV-9 on the endogenous PSPC-1.....	100
Figure 4-1 Schematic representation of CAV-9 2A and 3C manipulation.....	113
Figure 4-2 Schematic representation of the manipulation of HPeV-1 mCherry 3C.....	113
Figure 4-3 The effect of CAV-9 mCherry 2A and 3C on the cells.....	116

Figure 4-4 The effect of CAV-9 mCherry 2A on the cells.	117
Figure 4-5 The effect of CAV-9 mCherry 3C on the cells.	117
Figure 4-6 The effect of HPeV-1 mCherry 2A and 3C wild type and mutant on the cells.	118
Figure 4-7 The effect of HPeV1 mCherry 2A wild type on the cells.	119
Figure 4-8 The effect of HPeV1 mCherry 3C wild type on the cells.	119
Figure 4-9 The effect of HPeV1 mCherry 3C mutant on the cells.	120
Figure 4-10 The Effect of CAV-9 mCherry 3C on nucleus and nucleolus proteins.....	122
Figure 4-11 The Effect of HPeV-1 mCherry 2A on nucleus and nucleolus proteins.	123
Figure 4-12 The Effect of HPeV-1 mCherry 3C Wild type on nucleus and nucleolus proteins.....	124
Figure 4-13 The Effect of HPeV-1 mCherry 3C mutant on nucleus and nucleolus proteins.....	125
Figure 4-14 The Effect of HPeV-1 non-structural protien on EGFP-PSPC-1 distribution.	128
Figure 4-15 The Effect of HPeV-1 3D on mCherry-PSPC-1 distribution.....	129
Figure 4-16 The Effect of CAV-9 non structural proteins on EGFP-PSPC-1 distribution.	130
Figure 5-1 Weblogo of the sites believed to be cleaved by 3C/3CD in the CAV-9 Griggs polyprotein.	142
Figure 5-2 Schematic diagram for truncated PSPC-1.....	142
Figure 5-3 The distribution of the EGFP-PSPC-1 truncated proteins in uninfected cells.	143
Figure 5-4 The effect of CAV-9 infection on the distribution of EGFP-PSPC-1 fragments.....	144
Figure 5-5 the effect of CAV-9 infection on paraspeckle proteins.....	145
Figure 5-6 A schematic diagram for PSF dephosphorylation and sumoylation.	148
Figure 5-7 The distribution of the EGFP-PSF protein and EGFP-PSF mutations (mock).	149
Figure 5-8 The effect of CAV-9 on the distribution of EGFP-PSF protein and EGFP-PSF mutation.	150
Figure 5-9 The distribution of EGFP-PSF mutations and mCherry PSPC-1 complex (mock).	151
Figure 5-10 The effect of CAV-9 on the localization of EGFP- PSF Mutation and mCherry PSPC-1 complex.....	152
Figure 5-11 A Schematic diagram illustrating the manipulations of the truncated PSF proteins.....	154

Figure 5-12 The effect of CAV-9 on the redistribution of EGFP- PSF Mutation XB....	155
Figure 5-13 The distribution of the EGFP-PSF truncated proteins (mock).....	156
Figure 5-14 The effect of CAV-9 on the distribution of EGFP-PSF truncated protein..	157
Figure 5-15 The effect of CAV-9 on the localization of EGFP- PSF truncated proteins and mCherry PSpC-1 complex.	159
Figure 5-16 The localization of PSpC-1 with the replication complexes (time interval).	164
Figure 5-17 The localization of PSF with the replication complexes (time interval)....	165
Figure 5-18 The localization of NONO with the replication complexes (time interval).	166
Figure 5-19 The effect of CAV-9 infection on the paraspeckles localization into stress granules (G3BP1).....	167
Figure 5-20 The effect of CAV-9 on the colocalization of mCherry-PSpC-1 and stress granules (Time interval).....	168
Figure 5-21 The effect of CAV-9 on the distribution of P body (pT7EGFP-C1HsRCK).	171
Figure 5-22 The effect of CAV-9 on the colocalization of mCherry-PSpC-1 and P body (Time interval).	172
Figure 5-23 The effect of CAV-9 on the localization of EGFP-PSF deletions and P body	173
Figure 5-24 The effect of CAV-9 infection on the distribution of the Autophagosome structures and localization of these structures with EGFP-PSpC-1.....	174
Figure 5-25 A schematic representation of the PSpC-1 wild type sequence and truncated proteins.....	178
Figure 5-26 A schematic representation of the PSF wild type sequence and truncated proteins.....	183

Table of tables

Table 2-1 The antibodies used showing types and sources	51
Table 2-2 All the constructs that were used and their sources.....	52
Table 2-3 Oligonucleotides used.	53
Table 3-1. The normal location of nuclear proteins studied in this thesis, together with the effects of infection by CAV-9.....	107
Table 6-1 A list of some nuclear proteins were affected by RNA virus infection and have an effect on replication.....	192

Chapter 1

Introduction

1.1 Picornaviruses

1.1.1 Taxonomy

Picornaviruses are member of the *Picornaviridae* family that belongs to the Order *Picornavirales* and consists of 31 genera. Picornaviruses infect mainly mammals and birds, although they have also been found recently in fish and amphibians. There are currently 50 species. (Knowles et al., 2012, Adams et al., 2015). The name picornavirus is derived from their structure, as pico means small and RNA is the nucleic acid type (Hunt, 2010). The 31 genera can be divided into 5 subgroups based on sequence identity in the 3CD region. (Figure 1-1).

1.1.2 Importance of Picornaviruses

Picornaviruses are responsible for a wide range of clinical outcomes that affect humans as well as animals. These diseases range from mild and self-limiting to severe and serious conditions that can be life threatening (Oberste et al., 1999). These, include foot and mouth disease (FMD) that is caused by *Aphthovirus*, fever, rash, hand-foot-mouth syndromes, common cold and meningitis caused by *Enterovirus*, Hepatitis A that occurs as a result of infection by *Hepatovirus*, some respiratory illness in horses is due to *Erbovirus*, and Teschen-Talfan disease in pigs caused by *Teschovirus* (Palma et al., 2008).

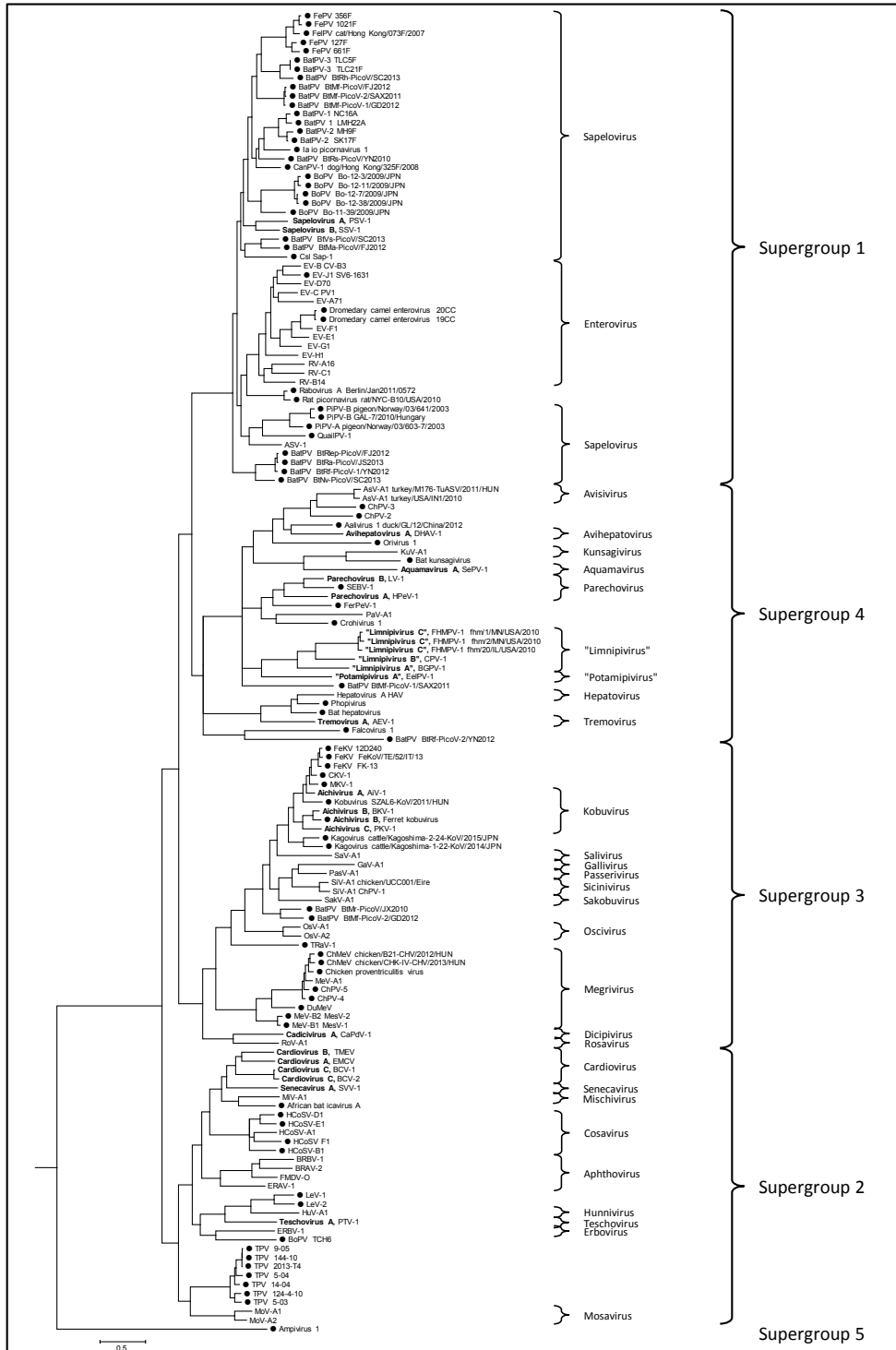


Figure 1-1 Picornavirus taxonomy tree. The genera are divided into 5 subgroups based on the 3CD sequence (Zell, Unpublished). The tree includes all species and unassigned viruses and the species within the 31 genera are marked by brackets. The genera can be grouped into 5 supergroups of more related viruses.

1.1.2.1 Enterovirus

Enteroviruses got their name due to their ability to reproduce initially in the gastrointestinal tract (Longo et al, 2012). This is a large genus and causes human infection varying from mild and asymptomatic to serious and fatal diseases (Hsiung and Wang, 2000). There are over 250 serotypes that infect humans, which means that it is not possible to produce a vaccine against all the different viruses. The genus *Enterovirus* consists of 12 species (*Enterovirus A*, *Enterovirus B*, *Enterovirus C*, *Enterovirus D*, *Enterovirus E*, *Enterovirus F*, *Enterovirus G*, *Enterovirus H*, *Enterovirus J*, *Rhinovirus A*, *Rhinovirus B* and *Rhinovirus C*.) (Adams et al., 2015). Species names are abbreviated EV-A, EV-B etc. Several enteroviruses have been known for many years and newly discovered viruses were originally classified as polioviruses, coxsackie A or B viruses or echoviruses, based on the symptoms of infection in new-born mice. This classification was found not to be useful, as some viruses classified in the same group were later found to be relatively different when sequences were compared (Hyypiä et al., 1992). More recently identified human enteroviruses are named Enterovirus plus a number (68-118), together with a species letter e.g. Enterovirus 71 (EV-A71) which belongs to the species *Enterovirus A* (often the species letter is omitted unless the taxonomy of the virus is being discussed) (Knowles et al, 2011). Members of each species of *Enterovirus* can be responsible for a number of infections, including mild or asymptomatic infection and paralytic poliomyelitis (Murphy and Almond, 1996). There is not a clear distinction between the kind of diseases caused by different species, but of the enteroviruses that often infect humans (*Enterovirus A-D*) paralytic disease can be caused by members of *Enterovirus C*, particularly polioviruses, respiratory illnesses and skin rash (including

hand-foot-and-mouth disease) by members of *Enterovirus A*, aseptic meningitis, myocarditis and pancreatitis by members of *Enterovirus B*, conjunctivitis by members of *Enterovirus D* and respiratory infection, including the common cold, by *Rhinovirus A-C*.

Enterovirus infections are common and are often asymptomatic, but serious illness can occur in a small proportion of cases (Muehlenbachs et al., 2015). For instance, only about 1 % of people infected with poliovirus will show paralytic disease. Poliovirus is still the most important enterovirus and is still present in several countries, even though there has been a global campaign to eradicate the virus for many years (Muehlenbachs et al., 2015). EV-71 is a major problem in the Far East and can cause serious neurological symptoms. Enteroviruses are a major cause of aseptic meningitis in children and echoviruses 30, 6, 16, 13 are the enteroviruses most frequently associated with this condition (Vollbach et al., 2015).

Rhinoviruses are the major cause of the common cold. This is usually thought to be a mild disease but it can cause serious disease in people with existing medical conditions, such as asthma. The common cold is also very important economically and a 2002 study estimated the cost every year in the USA was around \$25 billion, due to absence from work and loss of efficiency (Bramley et al., 2002). Colds are also estimated to be the cause of 30 % of missed school days in Canada (Worrall, 2008). The proportion of common colds that are caused by rhinoviruses is thought to be 30-50 % and so these viruses are very important economically (Mäkelä et al., 1998).

1.1.2.1.1 Coxsackie virus:

In the 1947 there were several outbreaks of poliomyelitis in New York investigated by Dalldorf and Sickles (1948). In particular they were looking for polioviruses that could replicate in mice to facilitate research. They made fecal suspensions from two children suspected to have poliomyelitis and inoculated these into adult and suckling mice but only suckling mice showed paralysis. The damage responsible for limb paralysis was widespread lesions in skeletal muscles, not in the central nervous system as occurs with poliovirus. Further study revealed that the viruses could be distinguished serologically from poliovirus. In 1949 Dalldorf suggested that the new viruses be called Coxsackie viruses, because the first recognized human cases were residents of Coxsackie village in NY (Dalldorf and Gifford 1951).

Coxsackie virus is a picornavirus of the *Enterovirus* genus that was originally classified by clinical manifestations in mice and serology into coxsackie A (23 serotypes) and coxsackie B (6 serotypes) groups (Muckelbauer et al., 1995). Most commonly, the coxsackie virus group A causes the hand -foot- and- mouth disease. Most reported enterovirus encephalitis cases are due to coxsackie viruses types A9, B2 and B5 (Moreau et al., 2011). Coxsackie virus A9 (CAV9) causes a number of other human infections including central nervous system (CNS) infection, myocarditis and wide range of milder illnesses (Williams et al., 2004).

1.1.2.2 Parechovirus

Human parechoviruses (HPeVs) (16 serotypes) circulate commonly in human populations and cause common infections in young children without signs and

symptoms. HPeVs can be responsible for many more serious infections ranging from gastroenteritis and respiratory infections to neurological disease and sepsis-like disease, particularly in new-born babies (Harvala and Simmonds, 2009, Yau et al., 2011). HPeV-3 is usually causes most cases of sepsis-like disease, but HPeV-4 can also be involved (Kolehmainen et al., 2014). *Parechovirus* is comprised of two species, *Parechovirus A* (formerly named *Human parechovirus*) and *Parechovirus B* (formerly named *Ljungan virus*). A new virus, Sebokele virus 1, from rodents may represent a third species in the genus. A fourth virus, ferret parechovirus has recently been described (Smits et al., 2013).

1.1.2.3 Aphthovirus

Aphthovirus is the most important genus in the *Picornaviridae* that infect animal other than humans, as it contains Foot- and-mouth disease virus (FMDV) (Chakraborty et al., 2014). Foot-and-mouth disease was the first disease of mammals to be shown to be caused by a virus, and FMDV was first discovered by Friedrich Loeffler back in 1898. Because it is so important it has been studied extensively. it considered to be one of the highly infectious viral disease amongst cloven-footed animal that cause debilitation, pain and loss of productivity (Chakraborty et al., 2014). The genus *Aphthovirus* consists of four species *Bovine rhinitis A virus*, *Bovine rhinitis B virus*, *Equine rhinitis A virus* and *Foot-and-mouth disease virus*. FMDV also became economically important as in the UK in 2001 the viral infection resulted in slaughtering over 6 million animal which cost over £ 8 billion, it also result in the need of the vaccine that support ‘vaccinate to live’ policy. Vaccine is based on the use of inactivated virus (Porta et al., 2013). Countries like

America, New Zealand, Australia and most of the Europe are free from FMD while it is still endemic in the Africa, most of the South America and several parts of the Asia including India (Chakraborty et al., 2014).

1.1.2.4 Hepatovirus

The genus *Hepatovirus* consists of a single species, *Hepatovirus A* (formerly named *Hepatitis A virus*). A previous member of the genus, avian encephalomyelitis virus, was assigned to a new genus, *Tremovirus* (Adams et al., 2015). HAV was identified more than 35 years ago when it was visualised by immune electronic microscopy. It is responsible for common acute hepatitis in human. In the early 1990s the licence for a safe and very effective vaccine was given after the successful inactivation of the virus (Martin and Lemon, 2006). The vaccine, which is around 95 % effective if two doses are given into a muscle, is recommended for everyone living in areas where there is a significant risk of infection and for travellers to these areas (Ott et al., 2012). Outbreaks of hepatitis A are rare in endemic countries where immunity occurs at an early age, but large epidemics can occur where immunity is low, for example there was an outbreak in Shanghai in 1988, where about 3000,000 people were infected from contaminated sea food (Ott et al., 2012).

1.1.3 Structure of particle and genome

Picornaviruses are very small with a genome consisting of a positive polarity RNA and a capsid that is non enveloped (naked) so does not have a lipid membrane (envelop). The capsid architecture is similar in all genera which is spherical structure of 27 to 30 nm

diameter. The RNA is 6700 nt (*Aquamavirus*) to 9800 nt (*Siclinivirus*) nucleotides long and the icosahedral nucleocapsid symmetry is made up of 60 identical subunits (protomers), each made up of four capsid proteins VP1 through VP4 originate from one protomer known as P1 that is cleaved to give the different capsid components. VP1 components are clustered around the fivefold axes of symmetry while VP2 and 3 alternate around the threefold axes (Figure 1-2) (Tuthill et al., 2010, Smyth and Martin, 2002, Stanway and Hyypiä, 1999). The picornavirus RNA is different from mRNA by having a virus encoded peptide called VPg, that attaches at the 5' whereas mRNA has a methylated cap group at its 5' terminal (Lin et al., 2009b). It also contains a poly (A) tail at the 3' terminal with variable length between 65 and 100 nt, which is genetically encoded and not added post-transcriptionally, unlike cellular mRNA (Hunt, 2010). The 5' region is non coding (5' UTR) followed by an open reading frame encoding a polyprotein that is processed to capsid proteins (VP1-VP4), derived from the P1 precursor and seven nonstructural proteins 2A-C, 3A-D, from P2 and P3 (Figure 1-3) (Hu et al., 2011). The 5' UTR plays an important role in translation, while the structural proteins from the capsid that surrounded the genome, and nonstructural proteins play a major role in virus replication (Harvala et al., 2002). The viral RNA has a large segment at its 5' untranslated region (UTR), about 400 nt in length, which called internal ribosome entry site (IRES). This site is about 200 nt downstream to the 5' end. IRES elements vary from one genus of picornavirus to another but they are functionally similar. The open reading frame is followed by a 3' and a poly A tail (Jang et al., 1989).

1.1.3.1 Outline of picornavirus replication

Picornaviruses have a positive sense, single strand RNA genome with a protein coat that surrounds the genetic material. Infection of a cell starts with an interaction between the virus coat and one or more receptors at the cell surface. This leads to entry, usually in a vesicle that forms from the cell membrane. In the host cell, the capsid releases the genome to act as mRNA in order to create viral proteins. Some proteins are structural and are assemble to make new capsids, while the others are non-structural are involved in viral replication or cell lysis. After the translation, negative sense ssRNA is synthesized from the original genome, and then this is used as a template in order to produce the positive sense ssRNA. Some of the new positive sense ssRNA molecules are also translated to give more protein, while others are packed into the newly assembled capsids. Many picornaviruses are cytolytic, as they cause a lysis of the host cell after replication. As a result, the new virus is released to infect new cells (Broyles and Arnold, 2009).

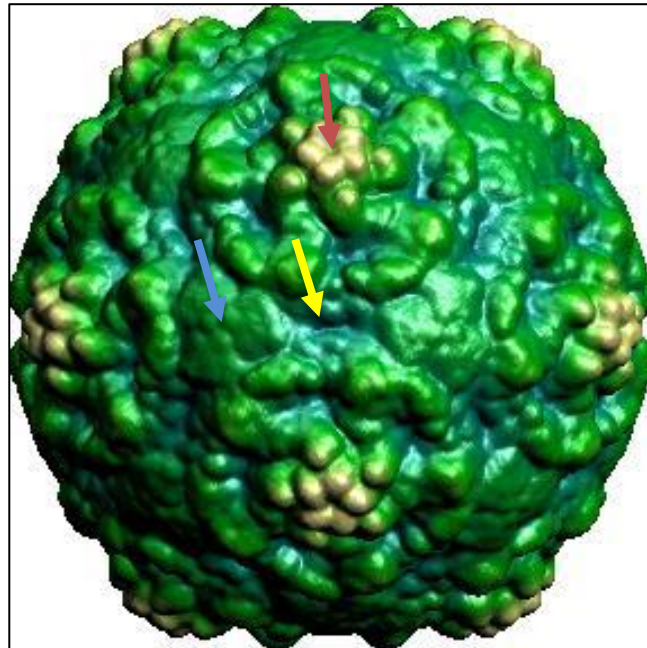


Figure 1-2 The structure of Coxsackie A9 (CAV-9) virus particle determined by X-ray crystallography (<http://www.picornaviridae.com>). The image is colour-coded from blue through yellow to green, representing the distance from the centre of the particle. Valleys are blue and peaks yellow. Red arrow shows the 5 axes fold, the yellow arrow shows the 2 axes fold and the blue arrow shows the 3 axes fold.

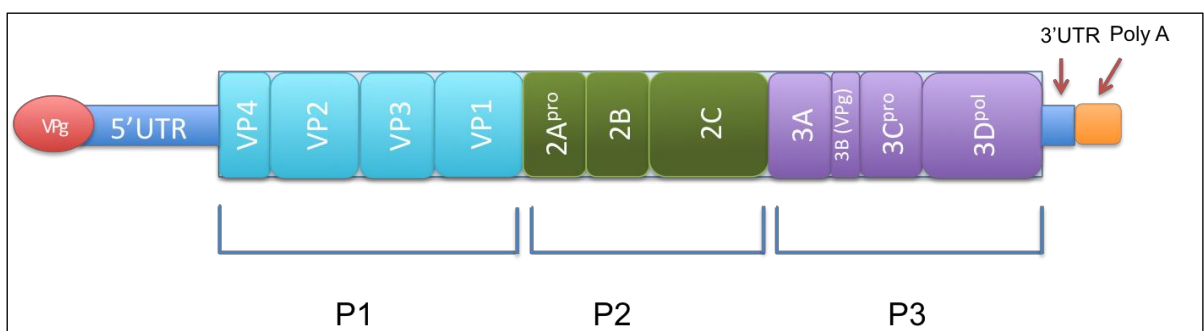


Figure 1-3 Schematic representation of a *Enterovirus* genome showing the coding regions for structural (VP4-VP1) and nonstructural (2A-2C and 3A-3D) proteins, the 5' and 3' untranslated regions (5'UTR; 3'UTR), the poly A tail and the genome-linked protein VPg. 2A (2A^{pro}) is only a protease in some picornaviruses e.g. enteroviruses, while 3C (3C^{pro}) is a protease in all picornaviruses. 3D (3D^{pol}) is the picornavirus polymerase.

1.1.4 Enterovirus replication

As described in the previous section, picornavirus replication involves many steps, which include receptor binding, entry, un-coating, RNA translation, protein processing, genome replication, assembly, maturation and cell lysis (Figure 1-4). There are some differences between different picornaviruses genera and as enteroviruses are the best understood, replication in these viruses will be described mainly.

1.1.4.1 Receptor binding

It has been found that some enterovirus types use cell-surface molecules that belong to the immunoglobulin superfamily (IgSF) as their cellular receptors (Rossmann et al., 2002). These molecules have an amino terminal domain (D1) that interacts with the invading viruses, plus a transmembrane domain and a short cytoplasmic region. Some rhinoviruses and enteroviruses use a canyon-like structure on their surfaces to bind to their receptor this binding initiates the un-coating step. IgSF members such as CAR, ICAM1 and CD155 are used by different picornaviruses. Another important receptor type is the integrins (used by CAV-9, echovirus 9 (E-9) and E-1). CAV-9 and E-9 have an arginine-glycine-aspartic acid (RGD) motif which is located in VP1 (Chang et al., 1989) in a 15 amino acid insertion at the VP1 C- terminus. This binds to integrin $\alpha\beta_6$, an integrin also used by FMDV and several HPeVs (Williams et al., 2004). However, previous studies showed that for CAV-9, there are two different entry routes into the host cell and only one of them depends on the RGD sequence (Hughes et al., 1995). E-1 binds to integrin $\alpha_2\beta_1$ by a non-RGD mechanism. Lack of this integrin gave much lower levels

of viral infection (Marjomäki et al., 2015). Many enteroviruses are using DAF as a receptor (Zocher et al., 2014). Another receptor used by EV71 is SCARB2 located in lysosome and endosome and has N and C terminals cytoplasmic tail (Yamayoshi et al., 2009). The PSGL2 is sialomucin membrane protein expressed on leukocytes that plays an important role in the early infection as EV71 bind to the N terminal of the PSGL2 receptor in order to allow the virus entry (Nishimura et al., 2009). Heparan Sulphate is a wide known receptor that bind to some picornavirus such as echoviruses and foot-and-mouth disease virus, CVB3 (Zautner et al., 2003) and some CAV-9 isolates (McLeish et al., 2012).

1.1.4.2 Entry

After interacting with the receptor on the cell surface, other interactions occur. Receptors are often concentrated in areas of the cell surface such as lipid rafts or clathrin-coated pits (Mercer et al, 2010). These parts of the cell surface are taken into the cell as vesicles, surrounded by proteins like clathrin, caveolin or flotillin containing the virus and some of these vesicles will fuse with endosomes, or other structures, in the cytoplasm (Mercer et al, 2010). Several vesicle types have been defined, based on the proteins surrounding the vesicles and other proteins involved in detaching the vesicle from the cell surface. For CAV-9, lipid rafts seem to be important in entry and entry depends on several proteins including β 2-microglobulin, dynamin, and Arf6 (Triantafilou and Triantafilou, 2003, Heikkilä et al., 2010). It has recently been shown that CAV-9 entry involves multivesicular structures (Huttunen et al., 2014).

1.1.4.3 Un-coating

The step following entry is un-coating. The viral capsid should be stable in order to allow the virus to be transmitted between hosts and to protect the RNA genome, but it must be dissociated in the infected cell to release the genome and this dissociation often starts as a result of interaction with the receptor (Smyth and Martin, 2002). The very first step in the un-coating event is the loss of VP4 and interactions between VP4, which is hydrophobic, and the vesicle membrane may allow a pore to form which allows the RNA to be released from the vesicle into the cytoplasm (Panjwani et al., 2014). The genome and VP4 leave the capsid when a myristate group attached to the N-terminus of VP4 interacts with the host cell membrane. In addition to the loss of VP4, the VP1 N-terminus is moved from its internal position to an external location via a channel in the virus particle. Therefore mutations in VP1 and VP4 can lead to inhibition of the un-coating (Smyth and Martin, 2002). It was believed that the RNA genome was released through this channel, but it now seems likely that during entry the virus particle changes shape and a channel through the coat is formed close to the 2-fold axis to allow the release of the virus (Shingler et al., 2013). It is thought that un-coating can occur at the cell surface or inside a number of different endocytic vesicles (Mercer et al, 2010), for example the plasma membrane for CBV-3 and PV, the cytoplasm for E-12 and the lysosome for PV (Zeichhardt et al., 1985).

1.1.4.4 Translation

Eukaryotic mRNA translation involves several steps (Yu et al., 2011). Several proteins, including eIF4G and eIF4E, assemble at the 5' cap structure on the mRNA to initiate

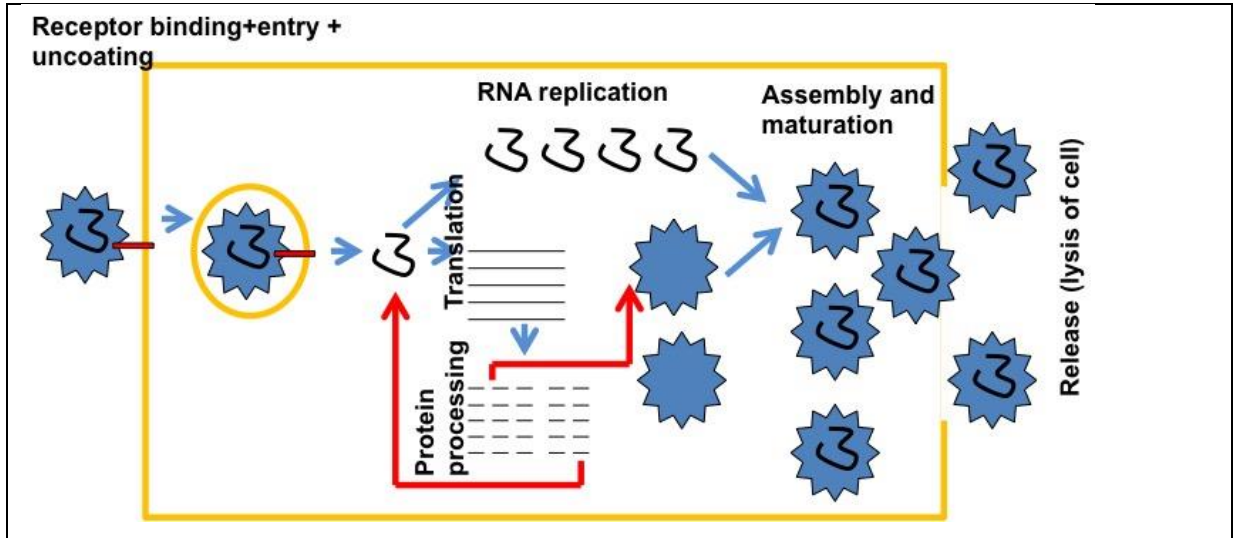


Figure 1-4 Diagram of viral Translation Showing the attachment of a picornavirus to the cell surface through receptors and penetration into the cytoplasm. The viral RNA then translated into polyprotein precursor that proteolytically processed. Viral proteins form replication complexes associated with membrane vesicles where the viral RNA undergoes replication, further translation of viral proteins, viral assembly and release (cell lysis). (Stanway, unpublished).

translation. These recruit the 40S ribosomal subunit which scans along the RNA until it reached the AUG where the 60S subunits is added and the RNA translated. The *Enterovirus* rely on host cell translation machinery (Yu et al., 2011). Thus, they have developed potent mechanisms to compete with host (cap-dependent) translation during infection, such as: the inhibition of cap-dependent translation by inducing the dephosphorylation of eIF4E binding protein; reducing the translation of host mRNA by cleaving the poly-adenosine binding protein (PABP); proteolysis of eIF4G by the enterovirus 2A^{pro} to inhibit the initiation of cap-dependent translation of host mRNA (Grubman and Baxt, 2004). Virus translation occurs by a process that involves the internal ribosome entry site (IRES) and is cap-independent (Pelletier and Sonenberg, 1988). VPg is cleaved from the picornavirus RNA by cellular enzymes before the translation step, so this protein cannot be used to assemble proteins needed for translation. *Picornaviridae* is therefore different from another positive sense RNA virus family the *Caliciviridae* where VPg is involved in translation initiation (Goodfellow, 2011). There is also no cap to recruit these proteins and so picornavirus translation is cap-independent and instead relies on the IRES (Grubman and Baxt, 2004). The difference between cap-dependent and picornavirus IRES-dependent translation is partly based on the way that eIF4G functions. Cleaved eIF4G is not functional in initiation of cap-dependent translation, but still functions in IRES-driven translation initiation (Ehrenfeld and Teterina, 2002). Picornaviruses can be divided into 5 groups on the basis of IRES structure (Figure 1-5). IRES types I-III and V are about 450 nt in length, while IRES type IV is shorter. The picornavirus IRESs require several proteins not usually needed in translation of cell mRNA and these are called ITAFs (IRES transactivating

factors) (Lin et al., 2008). For instance, IRES type I (e.g. *Enterovirus*) binds to the La protein in order to enhance RNA translation and type II (e.g. *Cardiovirus*, *Aphthovirus*, *Parechovirus*, *Erbovirus*) binds to PTB and PCBP2. Type I and type II IRESs are efficient, but the type III IRES (only seen in *Hepatovirus*) has a lower activity. Another feature for its function is that it requires the intact form of eIF4F for its function. It is also inhibited by the La protein that enhances the type I IRES. IRES type IV (e.g. *Teschovirus*, *Tremovirus*, *Sapelovirus*, *Senecavirus*) is very similar in structure to the IRES found in hepatitis C virus, which belongs to a different family of positive sense RNA viruses, *Flaviviridae* (Belsham, 2009, Hellen and de Breyne, 2007). It also lacks some of the features that are common on the other 4 types, such as a polypyrimidine tract. It cannot be inhibited or stimulated by 2A^{pro} unlike other IRES types (Belsham, 2009, Hellen and de Breyne, 2007).

In enteroviruses, the IRES binds to several host proteins (ITAFs) in addition to the usual eIFs (canonical initiation factors) and this plays a major role in specifying the cell type to be infected by the virus (McLeish et al., 2012). The ITAFs act as RNA chaperones to enhance IRES-mediated translation (Ho et al., 2011). Some cellular ITAF are involved in picornaviral IRES-mediated translation such as PTB, La, PCB P1,2, Unr, hnRNP A1, ITAF45, Nucleolin/C23, dsRNA binding protein76:NF45 heterodimer, FBP2 (Lin et al., 2009c).

1.1.4.5 Polyprotein processing

The picornavirus genome encodes a single polyprotein and there is a heavy reliance on processing to produce the individual proteins required (Castelló et al., 2011, Ryan and

Flint, 1997). Processing also generates some intermediate products (precursors) that may also be important e.g. 3CD^{pro}. In enteroviruses the first step of processing is cleavage by 2A^{pro} at its own N-terminus, which separates the capsid protein precursor (P1) from the non-structural precursor (P23) (Toyoda et al., 1986). In some other picornaviruses 2A is not a protease, but close to the P1/P23 boundary an NPGP-motif allows separation of P1 from P23 during translation by an unusual mechanism, and this suggests that this early separation is important (Donnelly et al., 2001). Most, and in some picornaviruses probably all because no other virus protease is known, cleavages in picornaviruses involve 3C^{pro} or 3CD^{pro}. L is a protein found only in some picornaviruses and is located at the N-terminus of the polyprotein. L belongs to different protein types in different picornaviruses, but is a protease (L^{pro}) in *Aphthovirus* and *Erbovirus* and cleaves itself from the polyproteins (Agol and Gmyl, 2010).

1.1.4.6 Genome replication

During RNA replication, the genomic RNA (positive sense) is copied to give several negative sense copies and these are copied to give many more positive sense RNA copies (virus genomes). These steps occur in replication complexes, made by virus proteins from cell membranes. Genome replication involves the protein VPg (product of the 3B gene), which is a protein primer of RNA synthesis, and 3D^{pol}, the virus polymerase. Firstly, Tyr-3 (Y3) of VPg is modified by 3D^{pol} to produce VPg-pUpU. This process known as uridylation (Shen et al., 2008). VPg-pUpU then acts as a primer for the production of antigenomic then genomic RNAs, by base pairing with As in the 3' poly A tail of genomic RNA and 2 As at the 3' end of antigenomic (negative sense) virus RNA.

It was found that a region of the human rhinovirus 14 genome encoding the VP1 protein contains an RNA structure necessary for RNA replication (McKnight and Lemon, 1998). Structures with similar properties were seen in cardioviruses (Lobert et al., 1999) and poliovirus (Goodfellow et al., 2000), then in several other picornaviruses (Steil and Barton, 2009). These structures were named the cre and it was found that the uridylylation of VPg occurs at the cre (Paul et al., 2000). The cre is a stem-loop structure containing an A residue (often part of the sequence CAAAC) in the loop (Al-Sunaidi et al., 2007). This A acts as the template for adding the first pU to VPg and the mechanism involves a slide back step, so that the same A the cre loop structure acts as a template for the addition of the second pU residue (Pathak et al., 2007).

1.1.4.7 Virus assembly and maturation and cell lysis

A new virion (virus particle) is formed by encapsidating the positive polarity viral RNA by capsid proteins in order to complete the replication. The 2C in the replication complex seems to interact with the capsid protein VP3 and this may bring the new RNA and capsid proteins together. The P1 capsid precursor is released from the polyproteins to initiate the assembly of the new virions. This is subsequently folded by the chaperone protein Hsp90 and processed by 3CD in order to release VP0, VP1 and VP3. These capsid proteins assemble to form the protomer, assemble into a pentamer and 12 pentamers assemble to give the empty virus particle, which is then filled with the RNA by an unknown mechanism (Marjomäki et al., 2015). Recently, the structure of Ljungan virus was obtained and the RNA seems to have more fixed position in the virus particle

than in enteroviruses. This may suggest that the assembly pathway is different and each pentamer binds to the RNA before the pentamers assemble (Zhu et al., 2015).

The RNA-induced cleavage of VP0 precursor into capsid proteins VP2 and VP4 is needed to produce the mature infectious virus particles. The mechanism of this cleavage is not known but may be due to amino acids in VP0, including a conserved histidine, together with the virus RNA (Curry et al., 1997). The newly formed virus particle is then released by the host cell lysis (Marjomäki et al., 2015).

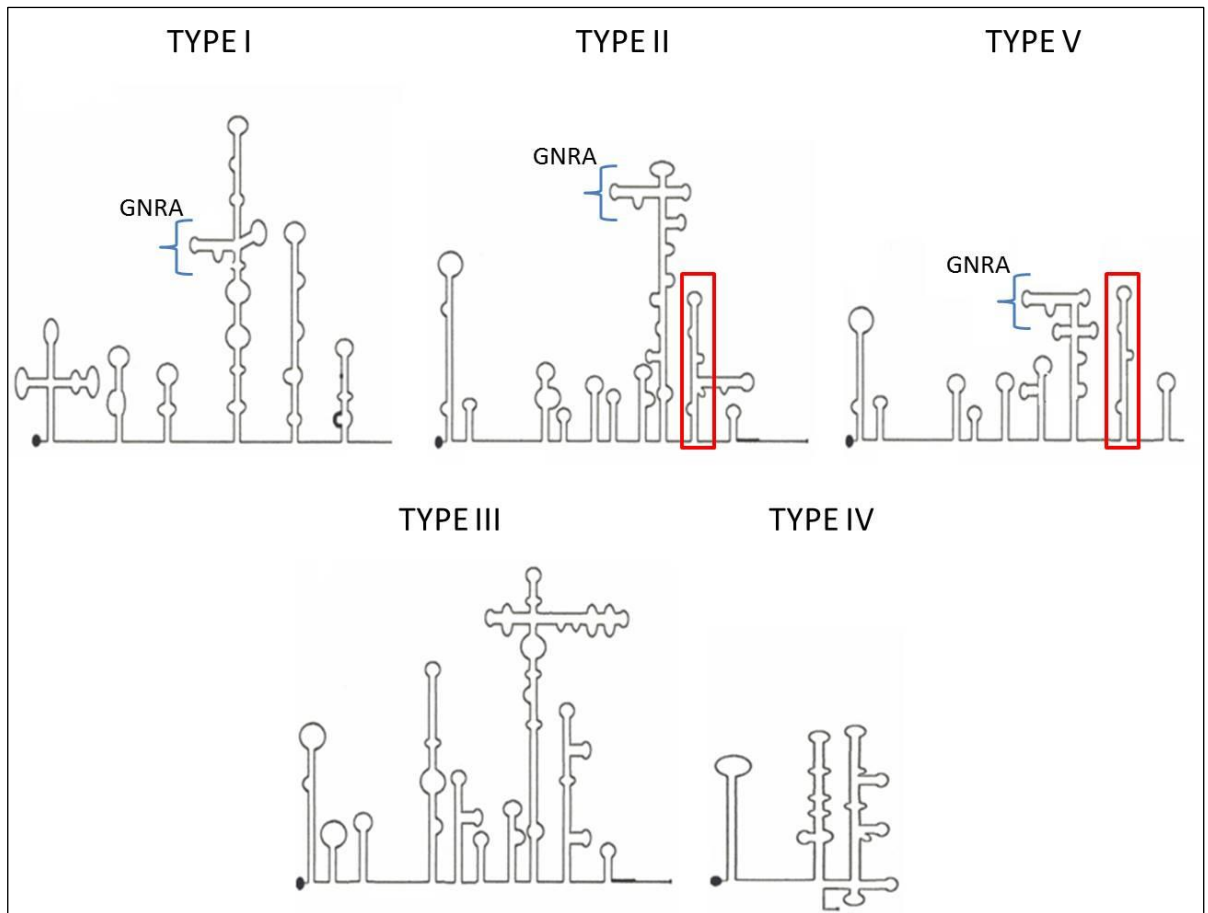


Figure 1-5 The different Picornavirus IRES Types structures (Stanway, unpublished), showing the structures of the 5'UTR in the five different picornavirus IRES types (TYPE I-V). Types I, II and III all have an essential GNRA tetraloop in the largest RNA secondary structure. One of the secondary structures (red box) is similar in structure between types II and V

1.1.5 Viral Non-structural proteins

1.1.5.1 2A

In picornaviruses, proteins are named from their position in the virus polyprotein. Most proteins with the same name have closely-related functions and structures, but L (which only occurs in some picornaviruses) and 2A are very diverse proteins when different picornaviruses are compared (Agol and Gmyl, 2010, Hughes and Stanway, 2000).

In enteroviruses, 2A is a protease (2A^{pro}) that consists of 149 amino acids and belongs to the cysteine protease group. However, it is structurally related to cellular proteins of the chymotrypsin family (Figure 1-6), particularly *S. griseus* proteinase A, which have a serine at the active site (Seipelt et al., 1999). It is autocatalytically processed cleave the virus polyprotein between VP1 C- terminus and 2A N-terminus. It plays an important role in viral replication. The 2A^{pro} has many functions that are essential in virus proliferation. It is known for inducing the cytopathic effect (Castelló et al., 2011). 2A plays an essential role in eIF-4G degradation, which causes an inhibition of cap-dependent translation of cellular mRNAs. The shut off of cellular cap-dependent translation allows the efficient IRES-driven translation of the virus open reading frame (Lu et al., 1995).

In other picornaviruses 2A is not a protease and has different structures and largely unknown function (Agol and Gmyl, 2010, Hughes and Stanway, 2000). Several picornaviruses have a 2A which contains two conserved motifs, an H-box and an NC motif and this type of 2A is related to several human proteins which have the same

motifs (Agol and Gmyl, 2010, Hughes and Stanway, 2000). Several picornaviruses contain an NPGP motif, that is part of a short sequence which performs a ribosome skipping mechanism where a peptide bond is not formed between the amino acids G and P and translation then continues. This means that the virus polyprotein is made in two separate pieces (Donnelly et al., 2001). Some picornaviruses have more than one type of 2A for example Ljungan virus has two and aalivirus A1 has six different 2A sequences (Wang et al., 2014b).

1.1.5.2 2B

2B is a small (97 amino acids in enteroviruses) hydrophobic protein. It is variable among different picornaviruses, but is always contains at least two hydrophobic regions which may interact with membranes (de Jong et al., 2008). It has been reported to inhibit apoptosis, affect intracellular calcium levels and disrupt intracellular protein trafficking (Campanella et al., 2004, de Jong et al., 2008). As part of the precursor 2BC it is believed to cause membrane rearrangement in the cell (van Kuppeveld et al., 1997).

1.1.5.3 2C

The 2C is a nonstructural protein found in the P2 region of the viral genome. 2C and its precursor 2BC migrate to rough ER during the infection in order to form smooth membrane vesicles that colocalize with viral RNA synthesis and are called the replication complex (Sweeney et al., 2010). 2C has ATPase and GTPase, membrane binding and RNA-binding activities (Banerjee and Dasgupta, 2001). 2C and the 2BC precursor are able to shut off protein shuttling between the ER and Golgi and the expression of

proteins on the cell surface. The 2C protein is the largest membrane-binding component of the virus RNA replication complex.

It has 318 amino acids and a predicted amphipathic helix at the N-terminus that allows it to bind to cell membranes. However, the specificity of binding by 2C is still unknown (Sweeney et al., 2010).

1.1.5.4 3A

Like 2B, 3A is a small (89 amino acids in enteroviruses) hydrophobic protein. It forms a homodimer which is needed for virus infectivity (González-Magaldi et al., 2012). In most picornaviruses 3A has a single hydrophobic region close to the C-terminus which interacts with membranes. 3A seems to have several functions such as affecting protein trafficking and membrane permeability (Wessels et al., 2006). As part of the precursor 3AB it has an important role in RNA replication by positioning 3B (VPg) in the replication complex and acting as an RNA chaperone, possibly by binding to and protecting new virus RNA or affecting the structure of the cre (Yang et al., 2015).

1.1.5.5 3B

3B (usually called VPg) is the smallest picornavirus protein (23 amino acids in enteroviruses), except for the short NPGP-containing 2A found in some picornaviruses, which is only 18 amino acids long. VPg was found to be covalently attached to the 5' end of the picornavirus genome and this is due to its role as a protein primer of RNA replication, as described earlier.

1.1.5.6 3C^{pro} and 3CD^{pro}

3C is the main protease (3C^{pro}) in all picornaviruses, as it is responsible for cleaving all of the polyprotein in some picornaviruses and most in the others, including VP2-VP3 and VP3-VP1 in P1, 2A-2B and 2B-2C in P2 and the whole of P3 (Lu et al., 2011). Some of these are performed by the precursor 3CD^{pro}. Like the enterovirus 2A^{pro}, 3C^{pro} is part of an unusual group of cysteine protease which have a serine like protease fold (Malcolm, 1995). Its structure is related closely to chymotrypsin (Figure 1-6) 3C^{pro} is found in the nucleus of infected cells, as the 3CD^{pro} precursor contains the NLS sequence that allows the protein to localise in the nucleus (Lin et al., 2009b). It is involved in shut-off of host cell transcription. It can cleave a number of cellular factors and regulators such as TATA-box binding protein (TBP) and transcription activator p53. It also induces the viral cytopathic effect by cleaving microtubulin, as well as inducing cell apoptosis. It is able to process the cellular PCBPs which involved in IRES-dependent translation (Lin et al., 2009c). It functions as a constituent of the viral replication complex through binding to 5'UTR of the viral RNA genome in the form of the precursor 3CD. It helps the virus to avoid the host antiviral immunity by interaction with or cleavage of several host factors (Lu et al., 2011).

1.1.5.7 3D^{pol}

3D^{pol} is the longest picornavirus protein and the most conserved between different genera. It is the picornavirus polymerase which forms VPgpUpU at the cre and also extends this to make new copies of the virus genome (Kerkvliet et al., 2010).

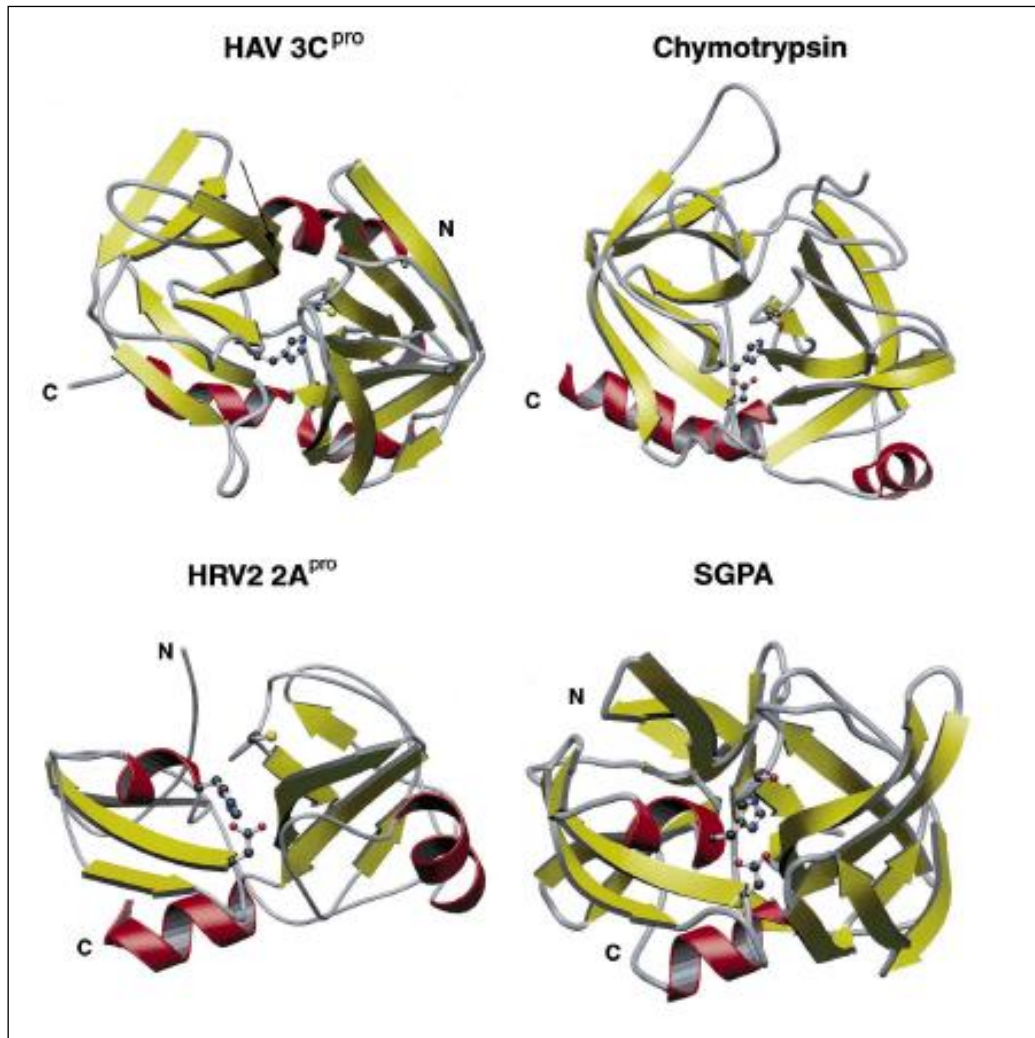


Figure 1-6 The structure of the virus proteases (the example shown is from hepatitis A [HAV]) and 2A^{pro} (the example shown is from human rhinovirus 2 [HRV2]) compared to cellular proteins. 3C^{pro} is most closely related to chymotrypsin, while 2A^{pro} is most closely related to the bacterial protein *S. griseus* proteinase A (SGPA). (taken from Seipelt et al. (1999))

1.2 The effect of viruses on cells

The interaction of viruses with host cells mainly cause death of infected cells. Viruses have the ability to exploit pre-existing cell mechanisms such as apoptosis. Apoptosis is mediated by a number of factors. The final step of apoptosis is characterized by nucleolytic internucleosomal degradation of chromosomal DNA, compaction and fragmentation of chromatin, cellular shrinkage, and cytoplasmic blebbing and fragmentation (Tolskaya et al., 1995).

1.2.1 The effect on translation

The pathological effects as a result of viral infection are often caused by the viral ability to kill host cells directly. The picornavirus non-structural proteins are more conserved than the capsid proteins and their function is preserved across *Picornaviridae* members, which suggests that they play many roles in the interaction with cells (Buenz and Howe, 2006). In enteroviruses, the first phase of viral infection is the cleavage of eIF4G by the viral 2A protease. Enterovirus translation uses the C-terminal fragment of the eIF4G (Goldstaub et al., 2000). However, this cleavage prevents cap-dependent cleavage, which is used to translate most cellular RNAs. Dephosphorelation of the eIF4E- binding proteins (4E-BPs) also occurs in picornavirus-infected cells and correlates with the inhibition of host cell mRNA translation. Picornavirus translation utilizes a mechanism where the ribosomes are recruited to the RNA by an internal ribosome entry site (IRES) This mechanism allows virus RNA translation in cells where cellular mRNA translation has been shut off (Thompson and Sarnow, 2000). The cellular protein poly (rC) binding protein (PCBP2) is also required in enterovirus translation and binds to the stem loop IV

RNA structure of viral IRES. This binding causes an indirect recruitment of ribosomes to the viral RNA. During viral infection, PCBP2 is cleaved by 3C^{pro} or the precursor 3CD^{pro} proteinase, that results in disability of PCB2 to interact with other cellular factors involved in viral translation initiation and ribosome recruitment (Toyoda et al., 2007). This switches off virus RNA translation and switches on RNA replication.

1.2.2 The effect on cytoplasmic membranes and secretion

Several cytopathic effects occur in the infected cells including changes in cell morphology and production of large number of cytoplasmic membrane vesicles (Armer et al., 2008). These vesicles are originally from the endoplasmic reticulum (ER) or from COP II- coated vesicles, which transports proteins to Golgi apparatus. During viral translation, the expression of picornavirus 3A proteins causes swelling to the ER and as a result, inhibits the membrane protein traffic between ER and Golgi apparatus (Moffat et al., 2005). In some viruses, 2C or 2BC are involved in this inhibition (Sweeney et al., 2010). Protein movement depends on COP-I coats and is regulated by the GTPase ADP-ribosylation factor 1 (Arf1) that can be activated by binding to GBF1. It has been found that 3A protein blocks Arf1 by interaction with GBF1, trapping it on membranes, which results in inhibiting the protein movement via COP-I (Wessels et al., 2006).

Virus-induced loss of γ - tubulin from the microtubule organizing centre leads to a lack of tethering of the microtubule, which causes changes in the distribution of microtubule and intermediate filament components. This then changes the structure of the cell (Armer et al., 2008).

1.2.3 The effect on replication complexes

In the replication of most positive sense RNA viruses, enzymatic and non-enzymatic viral proteins play a role in the assembly of membrane vesicles called replication complexes (Denison, 2008). Host cell proteins are also required for the virus replication. The RNA replication complexes are released from the host cell membranes during purification. This destroys the catalytic activity showing that the intracellular membranes are needed to form a functional virus replication complex. During picornavirus infection, the RNA replication occurs in the cytoplasmic vesicles that are derived from the ER while it occurs in mitochondrial membranes during infection with other RNA viruses. Membranes may function to expedite the assembly of replication complexes, to protect/sequester viral RNAs, and also to help segregate the products from templates during replication (Tao and Ye, 2010).

1.2.4 The effect on autophagosome

Autophagosomes play an important role in cellular survival under stress conditions such as viral infection. These organelles involve sequestration of the cytoplasmic proteins and granules in phospholipid membranes vesicles called autophagosomes, which shuttle to the lysosome for degradation. Viruses would use some cellular supply to inactivate the cellular antiviral defence and regulate the cellular processes for viral replication. The autophagy plays an important role during viral infection, they can act as intrinsic immune defence against viruses by forming xenophagosome which are then targeted for degradation instead of the autophagosomes. In addition, autophagy gene may limit viral replication (Kudchodkar and Levine, 2009). Interestingly, some viruses such as vesicular

stomatitis virus (VSV) are invading the cellular autophagosome for their replication. Other viruses such as HSV-1, BHV-1, HCMV, KSHV, HVS and MCV are able to develop counteracting mechanism to avoid degradation by autophagosomes and suppress the organelles. While some DNA viruses activate the autophagy pathways to enhance their replication. Enteroviruses such as PV and CVB4 induce autophagosome in order to provide cell membrane for RNA replication (Tang et al., 2012).

1.2.5 The effect on stress granules and P bodies

Host mRNAs which shuttling between translation and non-translation. The RNA which not being translated are organised in cytoplasmic granules for RNA known as stress granules (SG) and processing bodies (P-bodies). These play an important role in host mRNA inhibition and degradation, particularly in response to cell stresses, and thus potentially affect viral RNA. During infection, viruses interact with SG and P-bodies to control viral replication and cellular antiviral responses, although hosts cell start producing SG soon after the viral infection starts (Reineke and Lloyd, 2013). Different viruses can be grouped according to how they interact with SG and P-bodies. PV triggers the formation of SG at early stage of replication, but then manipulate the SG produced. Other viruses such as HSV and influenza virus can effectively repress SG formation throughout infection. PV 3C^{pro} cleaves the protein G3BP (a key protein for SG formation), which inhibits the co-localization of ribosome subunits and mRNA in SG, which results in aggregation of TIA1 protein (Lloyd, 2012). FMDV also trigger the formation of SG but as a result of cleaving G3BP by L^{pro} (Polacek et al., 2014).

The interaction between viruses and P-bodies is poorly understood. RNA viruses may have to regulate host RNA processes within RNA granules such as P-bodies to prevent viral RNA degradation. Some interaction between viruses and P-bodies may also occur due to gene expression being closely linked to these structures. During viral infection, viruses are able to repress P-bodies and cause relocation of P-bodies components for RNA replication. Depletion of P-bodies proteins such as GW182 (key protein for the P-bodies) causes a reduction in viral RNA (Reineke and Lloyd, 2013). Picornavirus infection also causes disruption to the cytoplasmic (P bodies) (Dougherty et al., 2011) for example, enterovirus infection causes a complete disruption of P-bodies foci during the mid stage of viral replication (Reineke and Lloyd, 2013).

1.2.6 The effect of picornaviruses on the nucleus

Most DNA viruses replicate inside the nucleus because the eukaryotic nucleus provides all the components and the perfect environment for DNA replication, transcription, and RNA-processing. For most RNA viruses, all essential replication, translation, and RNA synthesis processes occur in the host cell cytoplasm and can take place in nuclei-free cytoplasts or cytoplasmic extracts (Porter et al, 2006). However, in order to proceed efficiently with their reproduction, these viruses require non-essential materials that occur in the nucleus to optimise their infectious cycle. The nuclear pore complexes (NPCs) allow the transportation of proteins between the cytoplasm and nucleus, and they span the nuclear envelope (NE) (Porter et al, 2006). So enteroviruses disrupt this transportation by disrupting NPCs, which causes accumulation of nuclear proteins in the cytoplasm, due to an increase of nuclear protein efflux. Nup proteins are key components

of the NPC and enteroviruses manipulate the nucleus/cytoplasm shuttle pathway during viral infection by changing Nup proteins. This is caused by the proteolytic protein 2A^{pro} which causes degradation of Nups (Bardina et al, 2009). The NPC found in human cells contains over 30 different Nup proteins, of which several (e.g. Nup62, Nup98, and Nup153 for rhinoviruses) can be cleaved by 2A^{pro} (Watters and Palmenberg, 2011) and inhibition of Nup cleavage reduces viral RNA replication which result in reduction of the production of viral protein (Flather and Semler, 2015). Cardioviruses also disrupt the function of the NPC and allow nuclear proteins out of the nucleus. However, this is due to hyperphosphorylation of Nups, caused by the L protein, not protease cleavage (Porter and Palmenberg, 2009).

It has been observed that some picornaviruses proteins are detected in the host cell nuclei (Porter et al, 2006). 2A and 3C proteases target different histones and nuclear transcription factors. 2A protein interacts with a ribosome precursor in order to cause alteration in the translation control of the host cell nuclei (Porter et al, 2006). Other nuclear changes occur in response to picornavirus infections. Picornavirus infection triggers translocation of a number of nuclear proteins into the cytoplasm in order to stimulate viral replication and relocalization (Lidsky et al, 2006). Viral replication is enhanced when the nuclear polypyrimidine tract binding protein (PTB) which redistributes to the cytoplasm. Virus induced changes also cause the cells to be unable to mount a viable interferon-dependent anti-viral response to infection (Porter et al, 2006).

1.3 Nucleus structures

There are number of sub-nuclear bodies within the mammalian cell nucleus, including nucleoli, splicing speckles, paraspeckles, cajal bodies, and PML bodies. These bodies are known to interact with many nuclear proteins. However, any disruption in nuclear proteins organization may result in defect in cell functions (Fox et al., 2002).

1.3.1 PML bodies

Generally all mammalian cells have promyelocytic leukemia (PML) nuclear bodies (PML-NBs) in their nucleus (Dellaire and Bazett- Jones, 2004) also known as PML oncogenic domain (POD), nuclear domain 10 (ND10), or kremer bodies (Kr). Approximately, there are 5-30 bodies per nucleus, with a variable diameter ranging between 0.2 and 1 μm . These structures are associated with the nuclear matrix (Grande et al., 1996). These particles play a major role in cell differentiation and cell growth (Ching et al., 2005). Moreover, these nuclear bodies are also associated with basic cellular functions including, transcriptional regulation, viral infection, DNA repair and apoptosis (Reichelt et al., 2011). The direct contact of chromatin thread and RNA with the surface of the bodies might help to stabilize nuclear body structure (Brand et al., 2010). Disruptions of the PML gene are seen in acute promyelocytic leukemia (APL) and was identified as a chromosomal translocation (Grande et al., 1996). PML-NBs are dynamic structures that release protein, mediate their post translation modifications and promote specific nuclear events in response to cellular stress (Bernardi and Pandolfi, 2007). The significant protein of PML-NBs is the promyleocytic leukemia gene (PML) product as PML-negative cells are unable to form nuclear bodies and other PML-NB components

show dispersed nuclear disruption (Brand et al., 2010). This protein belongs to the TRIM protein super family that contains TRI partite Motifs that have a C3HC4 zinc ring finger (Figure 1-7). PML mediates INF- regulated cellular functions including growth and tumour suppressor activities and induces a block in the G1 phase of the cell cycle (Yang et al., 2004).

1.3.2 Speckles

Speckles are subcellular structures that are also known as inter-chromatin granule clusters (IGC). These nuclear domains are enriched in pre-mRNA splicing factors and are located in the inter chromatin regions of the nucleoplasm of mammalian cells. These clusters are irregular punctate structures that vary in shape and size. Speckles are dynamic structures and their protein and RNA protein can easily exchange between nucleoplasm and other nuclear locations including the active translocation site (Lamond and Spector, 2003, Spector and Lamond, 2011). Nuclear speckles are rich in RNA splicing factors including SC35, SF21ASF. These structures act as storage, assembly or modification domains for splicing factors, and recruit splicing factors to active transcription sites constituting nascent polymerase II transcript- containing perichromatin fibrils (Inoue et al., 2008). Some studies found that speckles usually form in regions that contain little or no DNA throughout the nucleoplasm. They may have a functional relationship with gene expression as they are located close to highly active transcription sites (Lamond and Spector, 2003). ASF/SF2 and SC35 belong to a highly conserved family of nuclear proteins called SR proteins which play a crucial role in splicing of pre-mRNA and influence selection of alternative splice sites. These proteins are required for

the early step in spliceosome assembly. Previous studies showed that a high concentration of SR proteins is able to circumvent the need for U1 snRNP in *in vitro* splicing. They are characterized by a C-terminal region rich in arginine-serine dipeptide repeats (RS region) and one or more N-terminally located RNP-type RNA recognition motifs (RRM) (Figure 1-8) (Tackel and Manley, 1995).

1.3.3 Paraspeckles

Paraspeckles are sub-nuclear structures that were discovered relatively recently, when a nuclear protein was found localized to nucleoplasmic foci which did not overlap with any known subnuclear markers. These foci were called paraspeckles as they were found in the interchromatin space close to speckles (Bond and Fox, 2009). These structures are RNA-protein structures that are formed between long non-protein-coding RNA species and DBHS members (Drosophila Behavior Human Splicing) family (Fox and Lamond, 2010). Paraspeckles plays a major role in the regulation of gene expression through retention of RNA in the nucleus. RNA nuclear retention is involved in several nuclear and cellular processes such as viral infection, stress response and circadian rhythm maintenance. They are also involved in reprogramming cell differentiation by altering the key protein expression by RNA nuclear retention (Fox and Lamond, 2010). Paraspeckles also contain long ncRNA nuclear- enriched abundant transcript 1 (NEAT1) (Morimoto and Boerkoel, 2013). NEAT1 plays an architectural role in the formation and localization of paraspeckles proteins. The knock down of NEAT1 by siRNA leads to absence and depletion in the number of paraspeckle while the over expression of NEAT1 increase the number of paraspeckles (Nakagawa and Hirose, 2012).

When paraspeckles were analyzed proteomically three proteins were originally characterised. These were non.POU (Pit1/oct1/UNC-86) domain contain octamer binding (NONO/ P54NRB) , paraspeckle protein 1 (PSP1), paraspeckle protein 2 (PSP2) (Morimoto and Boerkoel, 2013). Other paraspeckle proteins are defined by their co-localization in foci with these DBHS members of P54 NRB/ NONO or PSF /SFPQ/PSP-2 (Bond and Fox, 2009). DBHS members can be found in the nucleoplasm, nuclear caps and paraspeckles (Yarosh et al., 2015). They can be homo or heterodimers and compose of two major regions; N-terminal RNP type RNA recognition motifs and a C-terminal coiled-coil domain (Figure 1-9) (Bond and Fox, 2009). In addition, PSF contain additional domain that not found in NONO or P54 NRB (Yarosh et al., 2015). The knock down of NONO or SFPQ by RNAi leads to the loss of paraspeckles, while P54 NRB is less critical for paraspeckle formation (Morimoto and Boerkoel, 2013). PSF/SFPQ is a nuclear protein that plays an important role in range of RNA biogenesis processing from basic splicing to nuclear export and transcription (Heyd and Lynch, 2010). The PSF is a PTB associated protein as it got its name from as a PTB associated splicing factor (PSF) as it was firstly identified as a required protein for pre-mRNA splicing which interact with splicing regulated by the PTB proteins (Yarosh et al., 2015). Recent study identified another 35 paraspeckle proteins including RNA binding proteins, hnRNPs that binds to RNA pol II transcripts (Morimoto and Boerkoel, 2013).

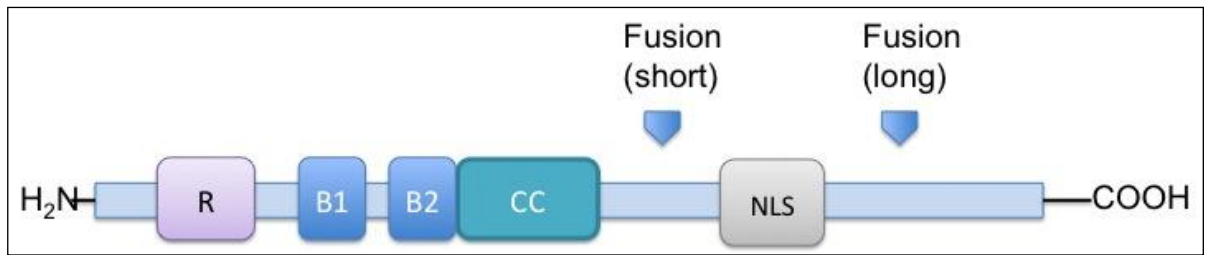


Figure 1-7 A Schematic representation of the PML protein. R: RING finger domain, B: B-boxes, CC: coiled-coil domain, NLS: nuclear localization signal. Based on the genomic breakpoint in the PML gene, either a short (PM/RAR-alpha-B) or long (PML/RAR-alpha-A) isoform is generated. Drawn from information given in the PML Genecard (<http://www.genecards.org/cgi-bin/carddisp.pl?gene=PML>)

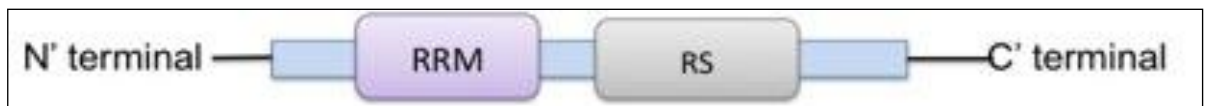


Figure 1-8 A Schematic representation of the (SC-35) protein. It contains one or two N terminal RNA recognition motifs (RRM) and a C-terminal domain that is rich in alternating serine and arginine residues (RS) domain. Drawn from information given in the SF2 Genecard (<http://www.genecards.org/cgi-bin/carddisp.pl?gene=SRSF1>)

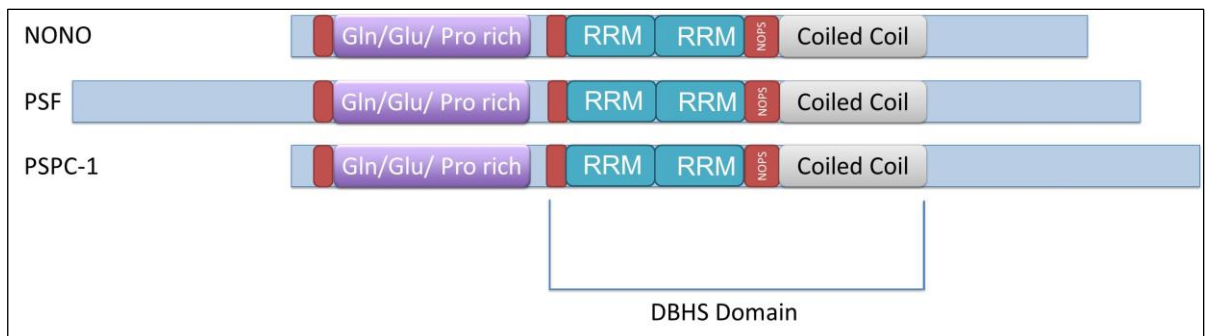


Figure 1-9 A Schematic representation of the paraspeckle proteins. It shows the domain structures of paraspeckle-localized DBHS proteins. The two major regions are Gln/Glu Pro rich domain, RNP type RNA recognition motifs (RRM) and a C-terminal coiled-coil domain. Redrawn from (Fox and Lamond, 2010).

1.4 Nucleolus structures

Nucleolus is nuclear subdomain that assembles ribosomal subunits. It has become clear that they play a role in RNA related function such as RNA processing and assembly of ribonuclear proteins (RNPs). The active nucleoli contain at least two ultrastructures component, the nuclear dense fibrillar component and granular component which contain mature pre-ribosomal compartments. In addition, some nucleoli contain a fibrillar centre (Shaw and Brown, 2012, Olson and Dundr, 2010)

1.4.1 Nucleolin

Nucleolin is one of the distinct nuclear proteins, which, plays a crucial role in ribosome biogenesis (Ghisolfi-Nieto et al., 1996). It may also be involved in other cellular processes as is also found in the cytoplasm and on the cell membrane. It was originally called C23 because of its properties on a two dimensional gel (Ginisty et al., 1999). It is associated with intranuclear chromatin and pre-ribosomal particles (Lapeyre et al., 1987). Nucleolin is also required for the transcription by RNA polymerase I, assembly of ribosome, proliferation of the cell and cell cycle (Cong et al., 2012). Nucleolin protein activates the cellular apoptotic process by regulating the fundamental proteins such as Bcl-2, P53 and retinoblastoma protein (Rb). It also leads to cancer cell transformation by binding to tumour suppressor retinoblastoma protein and the expression of nucleolin is enhanced in tumour cells (Destouches et al., 2011). It has a number of key domains (Figure 1-10).

1.4.2 Fibrillarin

Fibrillarin is found in the fibrillar region of the nucleolus (de Silva et al., 2012) and it is a conserved nucleolus protein that is involved in ribosome biogenesis including pre-mRNA processing and methylation, it plays a crucial role in viral infection as it binds to viral RNPs. It is also plays a structural and functional role in rRNA- containing dense fibrillar and fibrillar centre regions of the nucleolus (Ochs et al., 1985). It contains several domains. It has 320 amino acids (Rakitina et al., 2011). The N-terminal domain is formed by a GAR domain that contains the NLS sequence, which facilitates the migration of fibrillarin into nucleoli. The RNA binding domain binds to RNA (ribonuclear protein) in order to localize the fibrillarin in nucleoli. The protein C terminal region contains a short α - helical domain (Figure 1-11) (Barygina et al., 2010).

1.4.3 B23

B23/nucleophosmin (NPM) is also called nuclear protein NO 38 or numartin is a multi functional nuclear protein that plays an important role in cells growth and proliferation (Okuwaki, 2008). B23 is associated with nuclear ribonucleoprotein structures and binds single stranded nucleic acids. It also colocalizes with ribosomal subunit proteins in the cytoplasm, nucleus and nucleolus. The absence of B23 leads to the inhibition of the nuclear export of ribosomal subunits that reduce the availability of cytoplasmic polysomes which decrease the synthesis of proteins. This also leads to a cellular proliferation block (Maggi et al., 2008). B23 exists in two isoforms designated as B23.1 and B23.2, 294 and 259 amino acid respectively which differ only in their carboxyl-terminal short sequences and they both are highly acidic. The B23.1 carboxyl domain is

essential in RNA-binding activity. The N-terminal 257 residues of the two isoforms are identical. The crystal structure of *Xenopus* nucleoplasmin-core, *Drosophila* nucleoplasmin-like protein (NLP) shows that the two pentameric rings form a decamer associated in a head-to-head form. This decamer act as chaperone and binds with core histone to form a large complex (Figure 1-12) (Lee et al., 2007). It is also involve in many diverse cellular processes such as ribosome biogenesis, centrosome duplication, cancer and apoptosis. B23 localization and mobility within cells is highly regulated by phosphorylation events (Ramos- Echazábal et al., 2012).

1.5 The effect of the viruses on PML-NB, speckles, paraspeckles, nucleolin, fibrillarin and B23

Infection by viruses, particularly DNA viruses, has been shown to affect several nuclear structures.

1.5.1 The effect of the viruses on PML

There are number of studies suggesting that the interaction between viral genomes and PML-NBs happens that associate with host factors plays an important role in the early stages of virus infections (Everett, 2001). Certain changes in the appearance, distribution or composition of PML-NBs as a result of viral infection. The viruses may require either all PML-NBs compartments or some of them for their replication. PML- NBs are modified in different ways during viral infection (Leppard and Dimmock, 2004). Some virus proteins interact with CK2 and USP7 in order to increase the phosphorylation of

PML proteins. This triggers PML polyubiquitination and degradation (Frappier, 2010). In herpes viruses, inhibition of viral-gene expression by INF is blocked by virus protein ICPO which disrupts PML- NBs during viral infection by inducing proteasome-dependent degradation of both PML and SP100 (Gu and Roizman, 2009). Poliovirus infection stimulates PML phosphorylation by the extracellular signal regulated kinase pathway, increases PML SUMOylation, and induces its movement from the nucleoplasm to the nuclear matrix (Pampin et al., 2006). Infection by picornaviruses leads to a decrease in PML protein levels, which is carried out by 3C protease. At an early stage of the infection, viruses induce PML transfer from the nucleoplasm to the nuclear matrix, which leads to an increase in PML-NBs size. This process causes PML degradation occurring in a proteasome and SUMO-dependent manner but does not involve the SUMO-interacting motif of PML (El Mchichi et al., 2010).

1.5.2 The effect of viruses on speckles protein SC35

It had been found that viruses cause inhibition to host cell splicing, and redistribution of SC35. In herpes viruses, ICP27 protein is involved in changes of snRNPs distribution. The C-terminus region of ICP27 is required for the splicing inhibition and is also involved in ICP27 and SC35 redistribution. During the infection, the level of splicing target RNA remains constant (Sandri-goldin et al., 1995). Viral proteins accumulate in the speckles, which cause rounding and morphological changes of the domain that interfere with the normal function. The interaction between the viral protein and speckles may reflect a recruitment function to promote viral gene expression (Schneider et al., 2009).



Figure 1-10 Schematic diagram of the domain structure of nucleolin. It includes, RNA binding domain; RBD1, RBD2, RBD3 and RBD4 and the C-terminal GAR domain. Drawn from information given in the nucleolin (C23) Genecard <http://www.genecards.org/cgi-bin/carddisp.pl?gene=NCL&keywords=Nucleolin>

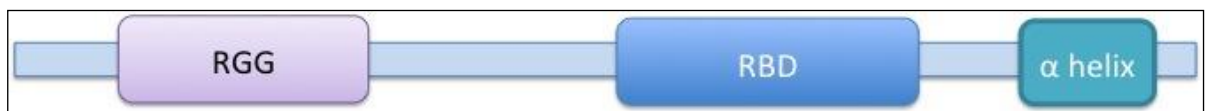


Figure 1-11 A schematic representation of the fibrillar protein structure. The RGG box, the RNA binding domain (RBD), and the α helix are indicated. Drawn from information given in the fibrillar Genecard (<http://www.genecards.org/cgi-bin/carddisp.pl?gene=FBL&keywords=fibrillar>)

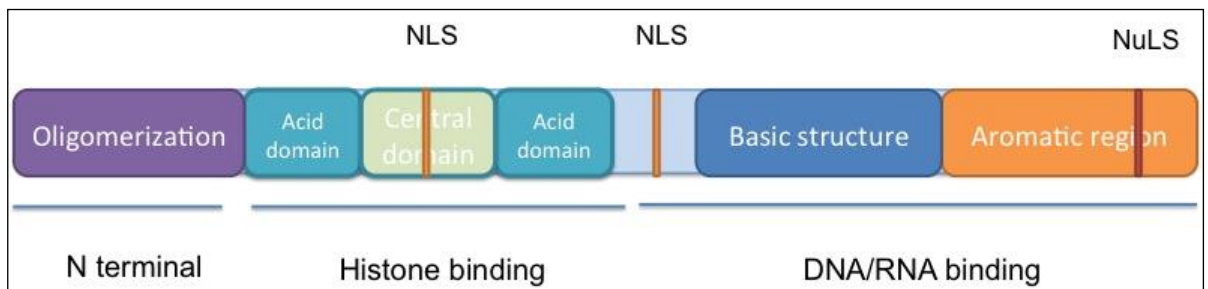


Figure 1-12 A schematic representation of the B23.1 protein. The N-terminal region includes a non-polar region involved in oligomerisation and one or more acidic domains rich in aspartic and glutamic acid residues. These are followed by two acidic stretches that are important for binding to histones. The central portion is required for ribonuclease activity, together with the C-terminal domain, which contains basic regions followed by an aromatic stretch. In addition, B23 includes a nuclear-localization signal (NLS) and a nuclear-export signal (NES). Drawn from information given in the B23 Genecard (<http://www.genecards.org/cgi-bin/carddisp.pl?gene=NPM1>)

1.5.3 The effect of the viruses on paraspeckles

It has been found that PSF plays an important role in regulation of some viruses replication such as HIV, HDV and influenza virus. PSF interacts with HIV- encoded rev, as siRNA causes a depletion of PSF resulting in decrease of HIV unspliced viral RNA which leads to decrease of viral production. PSF can also decrease the expression of HIV rev dependent transcription by binding to the viral mRNA through cis-acting regulatory element (INS) (Yarosh et al., 2015). Influenza virus requires PSF for RNA multiplication and replication. siRNA knock down of PSF cause decrease in viral production and reduce or delay the viral gene expression as well as decrease the viral transcription (Yarosh et al., 2015) PSF also interact with stem loop domain of HDV RNA in order to disrupt host cell processing (Yarosh et al., 2015).

1.5.4 The effect of viruses on nucleolin

Some studies have shown that viral particles bind to nucleolin and dramatically relocalize it from nucleoli to the cytoplasm, due to the relocalization ability of nucleolin between nucleolus, nucleus and cytoplasm, which is important for RNA virus replication. This localization could cause ribosome biogenesis alteration in the host cell that enhances virus protein expression (Masiuk, 2008). Herpes infection causes a wide redistribution of nucleolin throughout the nucleus of HSV-1 infected cells with the involvement of UL₂₄ protein in this nuclear modification. The UL₂₄ N-terminal is the main cause of nucleolin distribution in the absence of other viral protein (Bertrand et al., 2010). Nucleolin plays a functional role in the early stage of the poliovirus life cycle that effects virus replication. Immunofluorescence analysis demonstrated a nucleocytoplasmic relocalization of

nucleolin, which induce the inhibition of translation and cellular transcription (Waggoner and Sarnow, 1998). The C-terminus of Adenovirus protein V also cause a redistribution of nucleolin to cytoplasm (Matthews, 2001).

1.5.5 The effect of viruses on Fibrillarin

During infection with the herpes virus HSV-1, fibrillarin is redistribution throughout the nucleoli as small spots, some of which also colocalize with centromeres. This relocalization can be grouped into UL₂₄ –independent and UL₂₄ –dependent events (Lymberopoulos and Pearson, 2010). In human influenza H3N2 virus, the NS1 protein interacts with nuclear proteins such as fibrillarin. This direct interaction causes colocalization with fibrillarin in the nucleolus (Melén et al., 2012).

1.5.6 The Effect of the viruses on B23

It has been found that nucleophosmin/ B23 has a potential role as a chaperone for viral chromatin assembly. It acts as template-activating factor-III (TAF-III) which stimulate adenovirus DNA replication when it interacts with viral core protein V and the precursor of core protein VII (pre-VII) at the late phase of infection (Samad et al., 2007). The depletion of B23 increases the association of cellular histones and viral DNA with viral core protein (Samad *et al*, 2012). B23 also plays an important role in intracellular localization of core protein and replication of Japanese encephalitis virus (JEV). During viral infection, B23 translocates from nucleoli to cytoplasm. The cytoplasmic B23 colocalized with the core protein of wild type JEV (Tsuda et al., 2006). The 2A viral protein of encephalomyocarditis virus is associated with B23. This association helps to

traffic 2A into nucleoli by the putative nuclear localization signal (NoLS) (Aminev et al., 2003). Recent studies suggested that B23 is also playing a role as a chaperone in the assembly of core protein into the viral core (Samad et al., 2012).

1.6 Aims

There is growing evidence that although picornaviruses replicate in the nucleus they redistribute and use some nuclear proteins during infection. Most work has been done on a few picornaviruses and it is important to extend the range of viruses that have been studied to find how common these changes are, to assess if they could be the basis for new antiviral drugs. In addition, the effect of picornavirus infection on only a limited number of nuclear proteins have been studied.

The aim of the project was to:

Investigate the effect of infection by coxsackievirus A9 (CAV-9), as a representative of the medically important *Enterovirus B* species of picornaviruses, on a panel of nuclear proteins to identify any that are redistributed from their normal location and understand the molecular basis of the effect and how it may enhance virus replication.

Chapter 2

Material and Methods

2.1 Materials

The sources of the materials used are shown in the following sections. All solutions were made with deionised water purified using the Purite system.

2.1.1 Tissue culture reagent

Dulbecco's Modified Eagle's Medium (DMEM) (Sigma-Aldrich).

Fetal Bovine Serum (FBS) (Lonza or Sigma-Aldrich).

Gentamicin (Sigma-Aldrich).

Penicillin streptomycin (Pen Strep) (Sigma-Aldrich).

Non-essential amino acid (Sigma-Aldrich).

OPTIMEM GlutMax™-1 1X (Invitrogen).

Trypsin-EDTA 10X (Fisher).

Lipofectin transfection reaction (Life technology).

Xfect transfection reagent (Clontech).

TurboFect transfection reagent (Thermo Scientific)

Hoechst 33342, Trihydrochloride Trihydrate (Invitrogen).

Vectashield hard set, antifade mounting media with DAPI (H-1500, Vector laboratories).

2.1.2 Tissue culture buffers

2.1.2.1 Phosphate buffer saline (PBS)

Each 1 tablet of PBS (Fisher) was dissolved in 100 ml of water then autoclaved to make 1X PBS.

2.1.2.2 Mowiol mounting medium

In a 50 ml Falcon tube 6 g of glycerol was added to 2.4 g mowiol (CalBiochem) and stirred to mix. Then 6 ml of water was added and incubated at room temperature (RT) for 2 hr. 12 ml of 2 M Tris buffer (pH 8.5) was added and incubated in a water bath at 50-60 °C for 10 min until the mowiol dissolved, then the sample was centrifuged at 5800 g for 15 min in order to remove non-dissolved solid. The media was aliquotted into a 1.5 ml Eppendorf tube and stored at -20 °C.

2.1.2.3 Carboxy methyl cellulose (CMC) plaque overlay media

2 g of agarose and 2 g of CMC (sigma-Aldrich) were added to 100 ml of water then it was autoclaved.

2.1.2.4 Crystal violet stain

0.5 g of crystal violet dye was dissolved in 495 ml of water and 5 ml of absolute ethanol.

2.1.3 Virus strains

CAV-9 Griggs was the main virus used in this study and the sample used was obtained from the cDNA clone pCAV-9 and propagated on GMK cells (Hughes et al., 1995). HPeV-1 Harris was obtained from the cDNA clone pHPeV-1 and propagated on HT29 cells (Nateri et al., 2000).

2.1.4 Cell Fixation for microscopy

Cell fixation using 4 % Formalin

1 ml of 40 % formaldehyde (Fisher Chemicals) added to 10 ml 1X PBS.

Cell washing using glycine solution

0.3754 g of glycine (Fisher) was added to 50 ml 1X PBS to make a 100 mM solution.

Cell permeablization

125 µl of Triton X100 (Sigma-Aldrich) was added to 50 ml of 1X PBS to make a 0.25 % solution.

Cell Blocking (0.05 % Tween 20, 1 % BSA, 2 % serum)

0.1 g BSA (Bovine serum albumin) (Fraction V, Sigma), 200 µl of FBS and 50 µl of Tween 20 (Sigma-Aldrich) were added to 10 ml of 1X PBS.

Antibody diluent

0.1 g BSA and 50 µl of Tween 20 were added to 10 ml 1X PBS.

2.1.5 Antibodies

The different antibodies used are summarised in Table 2-1.

2.1.6 Plasmid DNA

The DNA constructs used are shown in Table 2-2.

2.1.7 Oligonucleotides

All the sequences of oligonucleotides used in order to make DNA constructs are shown in Table 2-3. Oligonucleotides were made by Fisher and supplied as a dry powder. They were dissolved in water to give a 100 μ M solution.

2.1.8 Polymerase Chain Reaction (PCR) reagents

Pfu DNA Polymerase (Fermentas)

10X Pfu buffer was provided and contained 20 mM Tris-HCl (pH 8.2), 1 mM DTT, 0.1 mM EDTA, 100 KCl, 0.1 % (v/v) nonidet P40, 0.1 % (v/v) Tween 20 and 50 % (v/v) glycerol.

Taq DNA Polymerase (Fermentas)

10X Taq buffer was provided and contained 20 mM Tris-HCl (pH 8.2), 1 mM DTT, 0.1 mM EDTA, 100 KCl, 0.5 % m(v/v) nonidet P40, 0.1 % (v/v) tween 20 and 50% (v/v) glycerol.

dNTP Mix 10 mM each (Fermentas)

Nuclease free water (Thermo Scientific)

Table 2-1 The antibodies used showing types and sources

Antibody	Clone Type	Company
Alexa fluor 555-labelled	Goat anti mouse IgG (secondary)	Life technology
Alexa fluor 568-labelled	Goat anti rabbit IgG (secondary)	Life technology
Alexa fluor 488-labelled	Goat anti-rabbit IgG (secondary)	Life technology
Anti-G3BP (ab 56574)	Mouse monoclonal IgG1 (primary)	Abcam
Anti-coxsackievirus A9 (mab 947)	Mouse monoclonal IgG2b (primary)	Millipore
Anti-PSPC1	Rabbit polyclonal (primary)	Sigma Aldrich
Anti-PSF (H-80)	Rabbit polyclonal (primary)	Santa Cruz
Anti -B23	Mouse monoclonal IgG1 (primary)	Sigma Aldrich
Anti-PTBP-2	Rabbit polyclonal (primary)	Santa Cruz
Anti-GW182	Rabbit polyclonal (primary)	Sigma Aldrich
Anti-dsRNA (J2)	Mouse monoclonal IgG2 (primary)	Scicons

Table 2-2 All the constructs that were used and their sources

Construct	Source
EGFP-PSF	Professor B.K. Felber
EYFP-PSPC-1	Professor A.I. Lamond
EGFP-NONO (NRB54)	Professor B.K. Felber
EGFP-PML	Professor M. Vihinen-Ranta
EGFP-Nuclolin	Professor J. Hiscox
EGFP-Fibrillarin	Professor J. Hiscox
EGFP-B23	Professor J. Hiscox
ERFP-LC3	Professor J.L. Iovanna
TP53INP1-EGFP	Professor J.L. Iovanna
pT7EGFP-C1HsTNRC6A (GW182, P body)	Dr. E. Izaurralde's (Addgene)
pT7EGFP-C1HsRCK (DDX6, P body)	Dr. E. Izaurralde's (Addgene)
pEGFP-N1HDAC6 (HDAC6, Stress granule)	Dr. Tso-Pang Yao (Addgene)

Table 2-3 Oligonucleotides used. Yellow highlights indicate restriction enzyme sites and red highlights show the site of mutations.

Oligonucleotide	Description	Sequence (5' to 3')	Enzymes
OL 2006	2A CAV-9 Forward	TCT CGA GCT GGT GCC TTC GGA CAA CAA TCC GGG GCC GT	<i>XhoI</i>
OL 2007	2A CAV-9 Reverse	AGG ATC CTT ACT GCT CCA TAG CGT CAT CCT CTA ACC A	<i>BamHI</i>
OL 2008	3C CAV-9 Forward	ACT CGA GCT GGT CCC GCA TTT GAA TTC GCC GTT GCA ATG	<i>XhoI</i>
OL 2009	3C CAV-9 Reverse	AGG ATC CTT ATT GTT CAT CAT TGA AGT AGT GCT TGA GAA G	<i>BamHI</i>
OL 2063	HPeV-1 3C Forward	CTC GAG CTC GGG AGT T CA AAA ATG AAG CTC	<i>XhoI</i>
OL 2064	HPeV-1 3C Reverse	GGA TCC TTA TTG ATC AGA CAT GTC ATT TTT A	<i>BamHI</i>
OL 2133	HPeV-1 3C mutant with S Forward	GTT AAA TCT TGC AAA GGA ATG TCC GGT GGC CTA CTT ATT TCA	
OL 2134	HPeV-1 3C mutant with S reverse	TGA AAT AAG TAG GCC ACC GGA CAT TCC TTT GCA AGA TTT AAC	

Oligonucleotide	Description	Sequence (5' to 3')	Enzymes
OL 2086	HPeV-1 3C mutant with A Forward	GTT AAA TCT TGC AAA GGA ATG GCT GGT GGC CTA CTT ATT TCA AAA GT	
OL 2087	HPeV-1 3C mutant with A Reverse	ACT TTT GAA ATA AGT AGG CCA CCAGCC ATT CCT TTG CAA GAT TTA AC	
OL 1637	EGFP Forward (for sequencing)	CTG GAG TAC AAC TAC AAC AGC CA	
OL 2167	PSF Forward	TCT CGA GCT TCT CGG GAT CGG TTC CGG AGT CGT	<i>XhoI</i>
OL 2168	PSF Reverse	TGT CGA CTA AAA TCG GGG TTT TTT GTT TGG GCC TTC	<i>Sall</i>
OL 2169	P54 NRB (NONO) Forward	GAA GCT TCG CAG AGT AAT AAA ACT TTT AAC TTG GAG AAG CA	<i>HindIII</i>
OL 2170	P54 NRB (NONO) Reverse	AGG ATC CTA GTA TCG GCG ACG TTT GTT TGG GGC A	<i>BamHI</i>
OL 2177	PSPC-1 Forward	GAA GCT TCG ATG TTA AGA GGA AAC CTG AAG CAA GTG	<i>HindIII</i>

Oligonucleotide	Description	Sequence (5' to 3')	Enzymes
OL 2178	PSPC-1 Reverse Fragment-1	TGG ATC CTA CTG AGA AAA TGC TTG CTC TAG CAG	<i>BamHI</i>
OL 2179	PSPC-1 Reverse fragment-2	TGG ATC CTA TTG GTT ACC AGC AGG GGC TGG GCT	<i>BamHI</i>
OL 2182	PSPC-1 (for sequencing)	AGG CAA GAT CTA ATG AGG CGT CAA G	
OL 2228	PSF WT Forward	TCT CGA GCT TCT CGG GAT CGG TTC CGG AGT CGT GGC GGT	<i>XhoI</i>
OL 2235	PSF WT Reverse	TCA TGG GTG TAT CAT CCA GTT CGG CT	
OL 2226	PSF Y to E Forward	AGG CCT GGA GAG AAA ACT GAG ACA CAG CGA TGT CGG T	
OL 2227	PSF Y to E Reverse	ACC GAC ATC GCT GTG TCT CAG TTT TCT CTC C AG GCC T	
OL 2224	PSF Y to F Forward	AGG CCT GGA GAG AAA ACT TTC ACA CAG CGA TGT CGG T	

Oligonucleotide	Description	Sequence (5' to 3')	Enzymes
OL 2225	PSF Y to F Reverse	ACC GAC ATC GCT GTG TGA AAG TTT TCT CTC CAG GCC T	
OL 2233	PSF S to A Forward	TCT CGA GCT TCT CGG GAT CGG TTC CGG GCT CGT GGC GGT	
OL 2234	PSF S to E Forward	TCT CGA GCT TCT CGG GAT CGG TTC CGG GAG CGT GGC GGT	
OL 2240	PSF S to A (for sequencing)	CTG GAG GCT GGT GGT GCG CTG CCT ACT	
OL 2241	PSF Y to F (for sequencing)	TGC CGC CTT TGG GAC CAC CCG GA	
OL 2250	PSF Deletion-1 (XX) Forward	TCG AGC TGG CAA AGG ATT CGG ATT TAT TAA GCT TGA AT	<i>XhoI</i>
OL 2251	PSF Deletion-1 (XX) Reverse	CTA GAT TCA AGC TTA ATA AAT CCG AAT CCT TTG CCA GC	<i>XbaI</i>
OL 2252	PSF Deletion-2 For ward (XB)	CTA GAG CTT TGG CTG AAA TTG CCA AAG CCG AAC TGG	<i>XbaI</i>

Oligonucleotide	Description	Sequence (5' to 3')	Enzymes
OL 2253	PSF Deletion-2 Reverse (XB)	GAT CCC AGT TCG GCT TTG GCA ATT TCA GCC AAA GCT	<i>BamHI</i>
OL 2254	Truncated PSF Forward (for sequencing)	GTT GGG AAT CTA CCT GCT GAT ATC ACG GAG	
OL 2255	Truncated PSF Reverse 1	AGG ATC CAG GAA GAC CAT CTT CAT CAT CTA GTT G	<i>BamHI</i>
OL 2256	Truncated PSF Reverse 2	AGG ATC CAC CCA TTC GCA TGT CTC TTT CCC GT	<i>BamHI</i>
OL 2257	Sumoylation mutant PSF Reverse	CAA AGC TCT AGA TTC AAG GGC AAT AAA TCC GAA TCC T	

2.1.9 Agarose gel electrophoresis

Agarose (Fisher Scientific)

50X ELFO buffer

242 g Tris base was added to 100 ml EDTA solution (0.5 M pH 8.8), adjusted to pH 7.7 with glacial acetic acid and made up to 1 L with water.

1X ELFO

100 ml of 50X ELFO was added to 4900 ml water.

5X clear loading dye

5X ELFO, 50 % (v/v) glycerol

SafeView nucleic acid stain (NBS Biological)

1 kb DNA ladder (Fermentas)

10 µl 1 kb ladder (1 µg/ml) was added to 10 µl 6X loading buffer and the volume was made up to 60 µl with water.

2.1.10 Gel purification

QIAquick Gel Extraction Kit (QIAGEN)

2.1.11 Ligation

T4 DNA ligase supplied with 10X ligase buffer (400 mM Tris-HCl (pH 7.8), 100 mM MgCl₂, 100 mM DTT, 5 mM ATP) (Fermentas).

pGEM-T easy vector kit (Promega):

The high copy number pGEM®-T Easy Vector contains T7 and SP6 RNA polymerase promoters flanking a multiple cloning region within the alpha-peptide coding region of the enzyme beta-galactosidase. Insertional inactivation of the alpha-peptide allows recombinant clones to be directly identified by blue/white screening on indicator plates. The linearised vector has a single T added to each 3' end to allow cloning of PCR fragments generated by or treated with Taq polymerase, which adds a non-templated A nucleotide to each 3' end of the product. pfu polymerase was used for most PCR reactions as it has proof-reading activity. As pfu does not add the non-templated A, the PCR product was treated with Taq polymerase for 15 minutes at 72 °C to allow the pGEM®-T Easy Vector to be used. The vector was provided with 2X Rapid Ligation Buffer (60mM Tris-HCl (pH 7.8), 20mM MgCl₂, 20mM DTT, 2mM ATP 10% polyethylene glycol (MW8000, ACS Grade).

2.1.12 Competent cells transformation

Escherichia coli (*E.coli*) top 10 strain was used for cloning DNA.

Genotype F⁻ mcrA Δ(mrr-hsdRMS-mcrBC) Φ80lacZΔM15 ΔlacX74 recA1 araD139 Δ(ara leu) 7697 galU galK rpsL (Str^R) endA1 nupG

Luria Broth (LB)

10 g of sodium chloride (NaCl) was added to 10 g tryptone and 5 g of yeast extract, water was added to make up a volume of 1 L and the solution was adjusted to pH 7.0 with 5 N NaOH. The mixture was autoclaved.

Luria Agar (LA)

15 g of agar was added to 10 g of sodium chloride (NaCl), 10 g of tryptone and 5 g of yeast extract in 1 L of water after the solution had been adjusted to pH 7.0 The mixture was autoclaved.

Blue and white colony selection plates

A solidified LA was melted and left at RT to cool down to approximately 37 °C. 100 µl of IPTG (100 mM) was added to 100 ml LA with 100 µl of 100 mg/ml ampicillin and 20 µl Xgal (2 % solution). The mixture was poured into 100 mm Petri dishes (~25 ml/plate) and allowed to solidify.

2.1.13 DNA isolation from bacteria

QIAprep Spin Miniprep Kit (QIAGEN)

HiSpeed Plasmid Midi Kit (QIAGEN)

2.1.14 Restriction enzymes

The following enzymes were used:

EcoRI (Invitrogen)

BamHI (Invitrogen)

HindIII (Invitrogen)

XbaI (Invitrogen)

XhoI (Invitrogen)

Sall (Invitrogen)

the buffer recommended by the supplier was used in each case.

2.1.15 Western blot

2.1.15.1 Separating gel

20 ml of Acrylamide solution (30% solution) was mixed with 9.2 ml of water, 10 ml of 1.5 M TRIS (pH 8.8), 400 μ l of 10% SDS, 400 μ l of 10% APS and 16 μ l TEMED. The prepared plate was then filled with 8 ml of the mixture and the liquid covered with isopropanol. The gel was then left for 30 min to be polymerised.

2.1.15.2 Stacking gel

In a 50 ml tube, 5.7 ml of water was added and mixed with 1.25 ml of Acrylamide solution (30% solution), 1.89 ml of 0.5 M TRIS (pH 8.8), 90 μ l of 10% SDS, 90 μ l of 10% APS and 9 μ l of TEMED. The isopropanol was removed from the plate and the gel was washed with water to remove the remaining isopropanol. The stacking gel was then poured on the top of the 15% acrylamide gel and a 1.5 mm comb was inserted.

2.1.15.3 Semi-dry blotting

4 trays were labelled as Anode I, Anode II, Cathod and membrane. 6 pieces of Whatman paper were cut at the dimensions 10 cm x 7 cm. 2 pieces for Anode I, 1 piece for Anode II, and 3 for the cathode tray. A Western blotting membrane was cut into 9 cm x 6 cm (1/gel) and activated by methanol. The trays were then filled with anode and cathode

solutions to soak the paper. The gel was washed with water to remove excess SDS. The paper from Anode I was rolled over it to remove air bubbles, then same to Anode II. The gel was then gently placed on the top of the paper.

2.1.15.4 Milk solution

1.5 g of milk + 50 ml TBST buffer

2.1.15.5 3% Blocking

0.3 g of BSA + 10 ml TBST. 3 ml of the blocking mixture + 6 µl antibody.

2.2 Methods

2.2.1 Tissue culture

2.2.1.1 Cell culture

Green Monkey Kidney (GMK) cells were used for most experiments and were provided by Dr. Merja Roivainen. Cells were grown on 25 cm² flasks in a growth medium consisting of DMEM supplemented with 10% FBS, 0.2 % Gentamycin or Pen Strep and 1 % Non- essential amino acid in a humidified incubator at 37 ° C.

2.2.1.2 Cell splitting

GMK cell monolayers were washed twice with 1X PBS after removing the media. They were then incubated with Trypsin 1X (Sigma-Aldrich, 100 µl) on a rocking plate at room temperature until the cells detached (3-5 min). The cells were re-suspended by adding

fresh medium (20 ml) and 5 ml aliquots were dispensed into new flasks to give a splitting ratio of 1:4. The cells were split every 3-4 days. Cells were also split in the same way into 6 well tissue culture plates, where each well contained a sterile, glass cover-slip. The cells were dispensed at 2 ml per well and incubated over-night.

2.2.1.3 DNA transfection

Three transfection methods were applied in this study.

2.2.1.3.1 Lipofectin transfection method

5 μ l of Lipofectin (Invitrogen) was incubated with 100 μ l Optimum GlutMaxTM-1 1X in tube A for 1 hr at RT. 5 μ l (1-5 μ g) of DNA (or 5 μ l of both DNAs in co-localization experiments) were placed in tube B, together with 100 μ l optimum GlutMaxTM-1 1X for 1 hr at RT. Both tubes were mixed together and incubated for 20 min at RT. Cells were washed twice with Optimum GlutMaxTM-1 1X then 800 μ l of the optimum GlutMaxTM-1 1X was added to the tubes. The mixture was added to the cell line and incubated for 24 hrs at 37 °C. Then, the medium was replaced with 2 ml of fresh growth medium for 24 hrs at 37 °C. After 24 hrs, cells were either infected with the virus or washed twice with 1X PBS and the nucleus stained with Hoechst 33342 and mounted on the slides using Mowiol mounting medium.

2.2.1.3.2 Xfect transfection method

5 μ l of DNA (as described above) was added into 95 μ l of the buffer provided. 1.5 μ l of polymer were added into 98.5 μ l of the buffer. Both mixtures were combined and incubated for 10 min at RT. Then, 1 ml of the cell culture media was removed and the

mixture was added to the cell culture and incubated for 4 hr at 37 °C. Then, the liquid was removed and 2 ml of DMEM was added and incubated for a maximum 48 hrs at 37 °C. Cells were stained with 0.5 µl Hoechst 33342 per 1 ml of warm DMEM and incubated at 37 °C for 20 min. Cells were washed twice with 1X PBS and cover slips were mounted on the slides using Mowiol mounting medium.

2.2.1.3.3 TurboFect transfection method

In 6 wells plate of 2 ml media in each plate and 50-70 % of confluent cells, 1 µg of DNA was diluted in 100 µl of Optimem GlutMax™-1 1X. 2 µl of TurboFect was added to the diluted DNA and the solution was mixed thoroughly by pipetting. The mixture was incubated for 15-20 min at R.T. Mixture was added to the plate was rocked gently to evenly distribute the mixture. Plate was then incubated for 24-48 hr at 37 °C. Cells were then fixed and examined by microscope.

2.2.1.4 Microscopy

Cells were examined with a BX41 microscope, wild field microscope or confocal microscope, using a 60x oil immersion magnification using red (TRITC), green (FITC) and blue (DAPI) filters/channels.

2.2.1.4.1 Confocal microscope

A Nikon A1si confocal microscope was used with a plan-apochromatic VC1.4 N.A. 60x magnifying oil-immersion objective. Software used for image acquisition; NIS-Elements AR 4.13.01(Build 916). Images were acquired in four channels, using one-way sequential line scans. DAPI was excited at 400 nm with laser power 7.2 arbitrary units,

and its emission collected at 450/50 nm with a PMT gain of 118. GFP was excited at 488 nm with laser power 5.8, its emission collected at 525/50 nm with a PMT gain of 90. mCherry signal was excited at 560 nm with laser power 3.2, and collected at 595/50 nm with a PMT gain of 121. Scan speed was $\frac{1}{4}$ frames/s (galvano scanner). The pinhole size was 47.5 μm , approximating 1.2 times the Airy disk size of the 1.4 N.A. objective at 525 nm. Scanner zoom was centred on the optical axis and set to a lateral magnification of 60 nm/pixel. Axial step size was 105 nm, with 80-100 image planes per z-stack. Identical settings were used for all acquired datasets, Following Nyquist–Shannon reconstruction theorem (Nyquist, 1928, Shannon, 1949) with a pixel size of 60 nm.

2.2.1.4.2 Wide field microscope

A Nikon A1 plus wide field microscope was used with a plan-apochromatic VC1.4 N.A. 60x magnifying oil-immersion objective. Software used for image acquisition; NIS-Elements AR 4.13.01(Build 916) using camera Andor Luca-R DL-626. Images were acquired in four channels, using one-way sequential line scans. DAPI was excited at 398.7 nm with laser power 13.0 arbitrary units, and its emission collected at 450/50 nm with a PMT gain of 118. GFP was excited at 488 nm with laser power 6.8, its emission collected at 525/50 nm with a PMT gain of 90. mCherry signal was excited at 560.5 nm with laser power 3.2, and collected at 595/50 nm with a PMT gain of 121. Scan speed was $\frac{1}{4}$ frames/s (galvano scanner). The pinhole size was 47.8 μm , approximating 0.25 times the Airy disk size of the 1.4 N.A. objectives at 525 nm. Scanner zoom was centred on the optical axis and set to a lateral magnification of 60 nm/pixel. Axial step size was 105 nm, with 80-100 image planes per z-stack. Identical settings were used for all

acquired datasets, Following Nyquist–Shannon reconstruction theorem (Nyquist, 1928, Shannon, 1949) with a pixel size of 60 nm.

2.2.1.5 Viral infection and detection of infected cells

In order to study the effect of the virus on the nucleus or nucleolus, 100 μ l (10^6 pfu) of the virus (CAV-9 Griggs strain or HPeV-1 Harris) was added to 500 μ l of DMEM and applied to the cells. Cells were incubated at RT on a rocking plate for 30-45 min then incubated in a 37 °C in a humidified incubator for (1, 2, 3, 4, 6 or 8 hrs). Then, cells were fixed with 1 ml of 4 % formalin for 20-30 min on a rocking plate at RT, then washed with 1X PBS/100mM Glycine for 5 min. Cells were permeabilized with 1X PBS/0.25% Triton X 100, washed twice with 1X PBS and blocked with 1X PBS containing 1% BSA and 0.05% Tween 20. Fixed and permeabilized cells were incubated overnight in the dark at 4 °C with diluted mouse anti coxsackie virus A9 labeled primary antibody at 1:112 in PBS/1% BSA or ds RNA antibody (Scicons) labelled primary antibody at 1:500 μ g/ml in PBS/1% BSA. Cells were washed with 1X PBS for 10 min and incubated with diluted Alexa Fluor 555 goat anti-mouse secondary antibody at 1:500 μ g/ml in PBS/1% BSA for 2 hrs in the dark at 4 °C. Cells were washed for 10 min with PBS and coverslips were mounted using Vectashield hard set, antifade mounting media with DAPI.

2.2.1.6 Plaque assay

In order to determine virus concentrations, plaque assays were performed. From a confluent flask of the cell line, the old media was removed and 1 ml of fresh media was added. 100 μ l of a diluted virus (10^2 , 10^3 , 10^4 , 10^5 dilutions) was added to the flask and

incubated for 30-45 min at RT on a rocking plate. A 1:3 mixture of agarose/CMC to growth medium mixture was prepared by melting the agarose/CMC in a microwave, adding to medium and keeping at 56 °C to prevent setting. 3ml of the mixture was added to each flask and incubated in a humidified incubator at 37 °C for 2-3 days or until the plaques formed. The overlay was removed and cells were washed with 1X PBS before being stained with 0.1 % crystal violet in 1 % ethanol for 5 min.

2.2.1.7 Virus propagation

The old media from flasks containing confluent cells was removed and replaced with 900 µl of fresh growth media. 100 µl of the virus was added to the flask and incubated at RT for 45-60 min on a rocking plate, then 4 ml of fresh growth media was added and incubated at 37 °C for 3-4 days or until CPE was observed. Then, the infected cells were frozen at -20 °C and thawed at RT three times. The infected cell lysate was aliquotted into 1.5 ml eppendorf tubes and stored at -80 °C.

2.2.1.8 Cell line storage

A confluent cell line flask was washed twice with PBS. 200-300 µl of Trypsin 1X was added and incubated for 3-5 min on a rocking plate. 1 ml of FBS was added to the flask and mixed gently. 1 ml of that mixture was placed in a cryo tube and 111 µl of DMSO was added. The tube was placed in an insulated container to ensure slow freezing and placed at -80°C.

In order to recover the stored cells, one tube was thawed quickly at 37 °C. 1 ml of the tube was taken and 4 ml of fresh growth media was added and incubated at 37 °C for 24

hr. When the cells were confluent the media was replaced with fresh growth media. Then the cells were split into 1:2 or 1:3 once, before being treated as normal.

2.2.2 Molecular methods

2.2.2.1 DNA constructs

In order to make the required DNA constructs encoding the viral non-structural proteins or cellular proteins, fused to EGFP or mCherry, the virus genomic sequence of CAV-9 Griggs or HPeV-1 Harris was extracted from the database, via the Picornavirus Home Page (<http://www.picornaviridae.com/>), and the mRNA sequence encoding cellular proteins was extracted using the NCBI site (<http://www.ncbi.nlm.nih.gov/>). The sequences were analysed using the program webcutter 2 (<http://rna.lundberg.gu.se/cutter2/>) to choose restriction enzyme sites present in the polylinker of the vector (pEGFP-C1 or mCherry-C1) that are not present in the DNA to be inserted. These, and any nucleotides needed to keep the correct frame, were added to the 5' end of oligonucleotides designed to amplify the required coding region by PCR. The oligonucleotides were synthesized commercially by Fisher on a 50 nmole scale and were dissolved in water to a concentration of 100 μ M.

2.2.2.2 Polymerase chain reaction (PCR)

2.2.2.2.1 Basic PCR

To amplify the desired DNA sequence PCR was performed in a 50 μ l total reaction volume. 5 μ l of 10X buffer (containing MgSO₄), 1 μ l of 10 mM dNTP, 1 μ l of sample

DNA or cDNA (10 ng), 1 μ l of each forward and reversed primers (100 pmoles), 1 μ l of pfu DNA polymerase and 40 μ l of nuclease free H₂O were combined. The typical PCR conditions are shown in Figure 2.1. Where DNA amplified using pfu polymerase was going to be ligated into pGEM-T Easy, 1 μ l of Taq polymerase was added after the PCR reaction and the sample was incubated at 70 °C for 15 min, to add an A residue to each end of the DNA. The typical PCR conditions are shown in Figure 2-1.

2.2.2.2.2 Overlap PCR

Overlap PCR was used for mutagenesis. This gives the products PCR1, using an internal reverse mutagenesis primer and a forward primer, and PCR2, using an internal forward mutagenesis primer and a reverse primer. PCR1 and PCR2 overlap, as the mutagenesis primers cover the same region, and a joining PCR is performed on the purified PCR1 and PCR2 products using the external forward and reverse primers. The typical PCR conditions are shown in Figure 2-1.

2.2.2.2.3 Colony PCR

Colony PCR was used for examining the ligation and if the plasmid inserted from *E.coli* colonies. Colony PCR was performed in a 50 μ l total reaction volume. 5 μ l of 10X buffer (containing MgSO₄), 1 μ l of 10 mM dNTP, 1 μ l of each forward and reversed primers (100 pmoles), 1 μ l of Taq DNA polymerase and 41 μ l of nuclease free H₂O were combined with a small amount of colony by a sterile tooth pick or a fine yellow pipette tip and the mixture was mixed well by pipetting. The typical PCR conditions are shown in Figure 2-1.

2.2.2.3 Agarose gel electrophoresis

Agarose gel electrophoresis was used to analyse or purify DNA samples, usually using a 1 % agarose gel. This was made by mixing 0.5 g of agarose with 50 ml 1X ELFO buffer and heating in a microwave for 2 min until the agarose dissolved. It was allowed to cool down at RT to about 37 °C and 5 µl of Safeview (NBS biological) was added, before the mixture was poured into a mould with either a small or large comb to form wells in the gel. When the gel was set, for an analytical gel 5-10 µl of the DNA was mixed with 1/5th the volume of 5X loading dye and loaded into a small well. 5 µl of 1 kb ladder was added to the first well of each row as a size marker. For DNA purification, 45-50 µl DNA samples were used and after adding loading buffer (1/5th volume) the samples were loaded into larger wells. The electrophoresis was carried out at 100-150 V (corresponding to ~ 100 mA) for 10-20 min. The gel was then visualised under blue light and images were taken using gel documentation (ingenius 3) system software (gene sense sys version 1.3.9.0, data base version 1.72).

2.2.2.4 Gel purification

The DNA was observed under a blue light (Syngene) and the desired band was cut from the gel using a clean scalpel blade. DNA isolation was done using a Qiagen DNA band isolation kit. The DNA slice was incubated with QG buffer (300 µl per 100 mg of gel) and incubated for 10-15 min at 50 °C with regular vortexing until the gel slice dissolved completely. 1 gel volume of iso-propanol was then added and the sample mix was transferred into a QIAquick spin column in a 2 ml collection tube. The sample was centrifuged for 1 min at 16000 x g to allow the DNA to bind to the column. The flow-

through was discarded and 500 μ l of QG buffer was added to the column and centrifuged for 1 min. The flow-through was discarded and the column was washed with 750 μ l of PE buffer, then centrifuged for 1 min. The flow-through was discarded and the column was centrifuged for 1 min to get rid of remaining ethanol present in the PE buffer. The column was then placed into a 1.5 ml eppendorf tube and 50 μ l of EB buffer was added to the centre of the column to elute the DNA by centrifuging for 1 min. 5 μ l of the purified DNA was analysed using an agarose gel and the purified DNA concentration was also measured using the nano drop system (ND-1000 spectrophotometer).

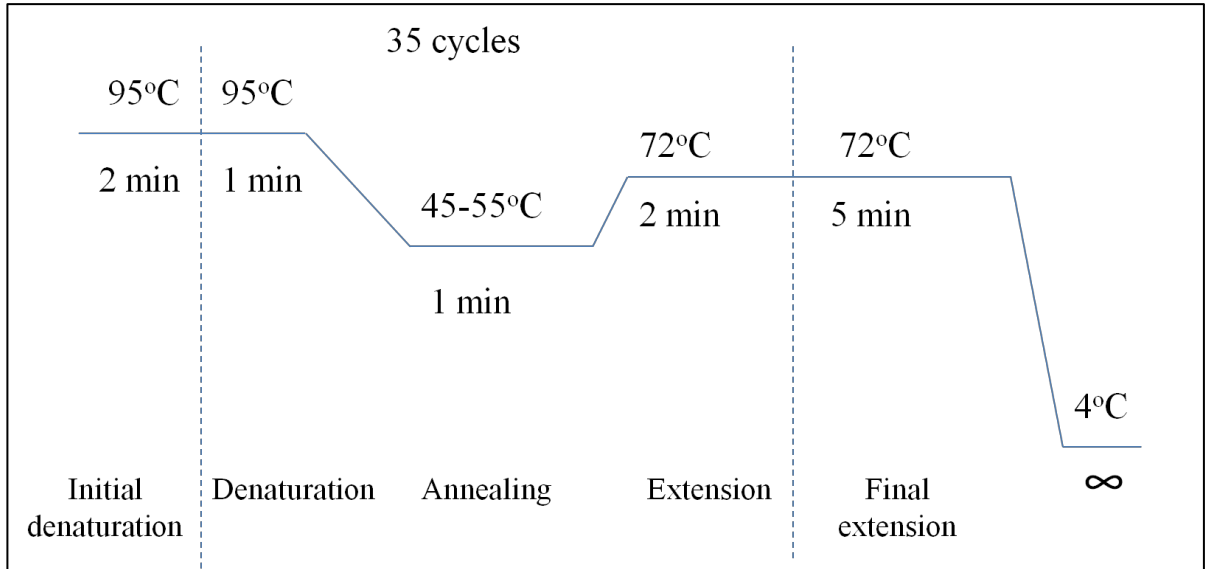


Figure 2-1 PCR reactions. Starting at 95 °C to activate the polymerase enzyme followed by 35 cycles of denaturation at 95 °C to separates two strands DNA, annealing at 45-55 °C, where the primers bind to specific areas of the target gene, and DNA polymerase, extension at 72 °C. A final extension at 72 °C confirms that strand synthesis has been completed, before the reaction is stopped by cooling to 4 °C. The annealing temperature depends on the melting temperature of the primers and the length of the 72 °C extension may vary based on the length of the amplified DNA fragment. pfu polymerase requires a time of 2 min per 1000 bases amplified.

2.2.2.5 Ligation into pGEM-T Easy

The components provided by the manufacturer of the pGEM-T Easy kit (Promega) were used. 2 μ l of the purified DNA was added to 1 μ l pGEM-T Easy vector, with 1 μ l of T4 ligase, 5 μ l of 2X rapid T4 DNA ligase buffer and 1 μ l of nuclease free H₂O to make up a volume of 10 μ l. The mixture was incubated for 1 hr at RT or overnight at 4 °C.

2.2.2.6 Ligation in EGFP or mCherry vectors

Using 4-15 μ l of purified DNA was added to 2 μ l 10X T4 buffer, 1 μ l T4 enzyme, 2 μ l vector and nuclease free water to make up a volume of 20 μ l. The mixture was incubated for 10 min at RT or overnight at 4 °C.

2.2.2.7 Transformation of *E.coli*

2.2.2.7.1 Competent cells preparation

A single colony of *E. coli* XL1-blue was selected and inoculated into 10 ml LB and incubated in a shaker at 37 °C overnight set at 250 rpm. 200 μ l of the culture was transferred to 10 ml LB media and incubated for 3-4 hrs at 37 °C in a shaker set at 250 rpm. The culture was centrifuged at 2750x g for 10 min at 4 °C and the pellet was suspended with 5 ml cold 0.1 M CaCl₂ and incubated in ice for 30 min. The cells were centrifuged at 2750x g for 10 min at 4 °C and the pellet was suspended with 500 μ l cold 0.1 M CaCl₂ and incubated in ice for 60 min in order to obtain ready to use competent cells.

2.2.2.7.2 Transformation

100 μ l of competent cells was added to 5 μ l of ligated DNA and incubated in ice for 30 min. After the incubation time a heat shock was performed by incubating the sample mixture at 42 °C for 2 min, then in ice for 1 min in order to allow the competent cells to take up the ligated DNA. 250 μ l of LB was added the sample and incubated in a shaker for 1 hr at 37 °C at 250 rpm. 150 μ l of the mixture was spread onto a petri dish containing LB agar and 100 μ g/ml ampicillin or 50 μ g/ml kanamycin. For blue/white selection plates also included IPTG and 20 X-gal. Plates were incubated overnight at 37 °C. After the incubation time the petri dishes were incubated in a fridge for 2 hr and at RT for 2 hr in order to get definite white and blue colonies. White colonies were streaked onto an LB plate then the same toothpick was placed into 10 ml LB containing 100 μ g/ml ampicillin and incubated for 24 hrs at 37 °C in a shaker at 250 rpm. For pEGFP or mCherry transformations several colonies were picked and usually screened by colony PCR before positive colonies were picked into LB.

2.2.2.8 Mini prep (QIAgen)

The cells were harvested by centrifuging 1-5 ml of an overnight LB culture containing transformed bacteria colonies and incubated ON at 6000x g for 10 min at RT. The supernatant was discarded and the pellet was re suspended in 250 μ l of P1 buffer and transferred to an eppendorf tube. 250 μ l of P2 buffer was added and mixed thoroughly by inverting the tube. 350 μ l of N3 buffer was added and the mixture was centrifuged for 10 min at 15000 x g. The supernatant was placed onto a QIAprep spin column by pipetting, then centrifuged for 1 min. The supernatant in the collection tube was discarded and the

spin column was replaced onto the collection tube and washed with 750 µl PE buffer. The spin column was centrifuged for 1 min and the flow through was discarded and an additional 1 min centrifugation was performed to get rid of the ethanol residue. The spin column was then placed onto a 1.5 ml eppendorf tube and the DNA was eluted with 50µl EB buffer by centrifuging for 1 min. Purified DNA was analysed by agarose gel electrophoresis and the concentration was measured using the nano drop system.

2.2.2.9 pGEM-T Easy ligation analysis

In order to check the ligation into pGEM-T Easy, a double digestion using *EcoRI* restriction enzyme was performed. 5 µl of purified DNA was added to 1 µl *EcoRI*, 1 µl 1x *EcoRI* buffer and 3 µl nuclease-free H₂O to make up a volume of 10 µl. The mixture was incubated at 37 °C in a water bath for 1 hr. 2 µl of 10X clear loading dye was added to the mixture and it was ran on a 1% agarose gel electrophoresis as described in 2.2.2.3. The gel was visualised under blue light (Syngene) to check the DNA bands and if the expected result was obtained 10 µl of the purified DNA was sent to be sequenced commercially (Source Bioscience Life Science).

2.2.2.10 Double digestion

To obtain DNA fragments for ligating into EGFP or mCherry vectors double digestion was performed. 5 µl of the purified DNA was added to 2 µl of both restriction enzymes, 5 µl of 10X buffer and 36 µl of nuclease free H₂O. The buffer used was selected by comparing charts to fine a buffer where both enzymes work efficiently. The mixture was incubated for 1-2 hr at 37 °C in a water bath. 2 µl of 10X clear loading dye was added to

the mixture and separated by 1% agarose gel electrophoresis as described in section 2.2.2.3 The gel was visualised under blue light to check the DNA bands. The desired band at the correct size was cut with a clean scalpel and purified as described in 2.2.2.4.

2.2.2.11 Midi Prep (Qiagen system)

When the sequencing results validated the plasmid DNA, a colony from the streak plate was picked and incubated in 10 ml LB with a selective antibiotic and incubated for 6 hr at 37 °C in a shaker at 250 rpm. Then 200 µl of the selective antibiotic was added to 200 ml LB and the growth mixture was transferred to the 200 ml LB and incubated overnight at 37 °C in a shaker at 250 rpm. The growth culture was then centrifuged for 15 min at 4 °C and 6000x g. The bacterial pellet was then resuspended in 6 ml P1 buffer. 6 ml of P2 buffer was added and mixed by inverting 4-6 times and incubated for 5 min at RT. The pellet was then lysed in 6 ml of chilled P3 buffer. The lysate was then poured into a prepared QIAfilter Cartridge and incubated at RT for 10 min. During the incubation time, the HiSpeed Midi Tip was equilibrated with 4 ml QBT buffer. The cell lysate was then filtered into the equilibrated filter by gravity flow. The QIAGEN-tip was then washed with 20 ml QC buffer. The filter tip was then placed on a clean bottle and the DNA was eluted with 5 ml QF buffer. The DNA was then precipitated by adding 3.5 ml isopropanol and incubated for 5 min at RT. A 20 ml syringe was prepared by removing the plunger and attaching the QIAprecipitator onto the outlet nozzle. The eluted mixture was then transferred into the syringe and the plunger was inserted with a constant pressure to filter the DNA. The QIAprecipitator was removed and the plunger pulled out, then the QIAprecipitator was re-attached and 2 ml of 70 % ethanol was added in order to wash the

DNA. The membrane was dried by pressing air through the QIAprecipitator using constant pressure, this step was repeated 3 times. A 5 ml syringe was prepared and the QIAprecipitator was attached onto the outlet nozzle and 1 ml of buffer TE was added and the DNA was elute into the collection tube using constant pressure. The QIAprecipitator was removed and the plunger was pulled out then the QIAprecipitator was reattached and the eluate was transferred to the 5 ml syringe and eluted for the second time into the same collection tube. The DNA was then aliquotted (200 µl aliquots) into 5 1.5 ml tubes.

2.2.2.12 Western Blot

Cells were grown in 2 wells of a 6 well plate 24 hr prior to infection. Cells were then infected with CAV-9 for 0, 2, 8 hr in duplicate (0 hr was the mock to use as control). Cells were then harvested. In an eppendorf tube, the media from the well were collected and cells were washed with 200 µl of BPS X1 and transferred to the tube. 200 µl of trypsin was added to the well in order to detach the cells and incubated for 3 min and moved the tube. Cells were then washed with the mixture to make sure that all the cells were harvested. Cells were then collected in the eppendorf tube and centrifuged for 10 min. Cells were then resuspended in 250 µl of lysate buffer and incubated for 20 min in ice, then centrifuged for 10 min at 4°C. The supernatant was removed and kept at -20 °C until needed.

Protein determination was performed using the Pierce BCA protein assay kit (Thermo Fisher scientific) as described by the manufacturer. 50 µg of the protein was added to 10 µl loading buffer and boiled for 5 min, cooled in ice for 5 min then spun for 1 min. 1.5 of the marker (Lonza) was loaded into the prepared gel (section 2.1.15.1 and 2.1.15.2).

Samples were also loaded and the gel was run using Bio Rad Power PAC 300 at 80 V for 30 min then increased to 130 V for 1 hr.

The membrane was semi-dry blotted as described in (2.1.15.3) then transfer was done for 40 min using a Biometra standard Power Pack P25, on constant A at 0.06 Amp, and 8W, limiting the voltage at 20V. Then the membrane was washed with panacea (red stain) then the membrane was transferred to the milk solution for blocking. It was shaken for 1 – 1.5 hr then washed with TBST buffer and incubate with primary anti body (anti PSPC-1 or anti PSF) overnight. The membrane was washed with TBST buffer 3 times before being incubated with the secondary antibody (Horse reddish peroxidase) (1 hr incubation). The membrane was then rinsed with TBST buffer, then milk for 15 – 20 min on the shaker. The images were then taken by Fusion FX Vilber Lourmat using Fusion software. After the viral infection and the cell lysis the western blot work was carried out by Andrea Moher and her team.

Chapter 3

**Effect of CAV-9 Infection on the Host
Cell Nucleus and Nucleolus Proteins**

3.1 Introduction

Many viruses, particularly DNA viruses, access and manipulate the nucleus for replication (Cohen et al., 2011). It is becoming clear that infection by other viruses can affect the nucleus, even when virus replication is confined to the cytoplasm. Transcription factors may be cleaved by virus proteases, some viruses change the permeability of the nuclear membrane by affecting the nuclear pore complex and the nucleoli are modified in some cases (Castelló et al., 2011, Park et al., 2008, Rawlinson and Moseley, 2015).

The nucleus has a number of small domains such as (PML-NBs), nuclear speckles and paraspeckles, while nucleoli are much larger than these structures. PML-NBs are nuclear substructures found in most mammalian cells and regulate functions such as DNA replication, transcription and epigenetic silencing (Jeanne et al., 2010). PML-NBs (named after the key protein PML) play an important role in innate immunity during viral infection, as they are able to increase transcription when interferon I and II (IFNs) bind IFN- stimulated response elements (ISRE) and IFN-activation site (GAS) elements on PML (Nardella et al., 2011). Paraspeckles are small sub-nuclear structures that are associated with the long non-coding RNA NEAT-1 (Naganuma et al., 2012). These bodies act as regulators of gene expression in cells by nuclear retention of RNA. Paraspeckles contain many proteins that play an important role in RNA processing and transcription. The key protein of paraspeckles is PSF/SFPQ (Bond and Fox, 2009). PSF, together with P54NRB (NONO), is responsible for paraspeckle formation and maintenance. Depletion of these proteins leads to paraspeckle disorganisation (Nakagawa

and Hirose, 2012). Nucleolin, fibrillarin and B23 are proteins largely found in the nucleoli and are involved in ribosome biogenesis and signalling pathways (Destouches et al., 2011, Ghisolfi-Nieto et al., 1996).

It has been previously found that infection with human parechovirus (*Parechovirus* genus of *Picornaviridae*) redistributes the paraspeckle protein PSPC-1 and the nucleolar protein B23 (Mutabagani, 2012). This study has investigated if this is a general feature of picornaviruses by investigating coxsackievirus A9 (CAV-9), a member of a different and genetically distant picornavirus genus (*Enterovirus*), in order to examine if this may be an important feature of picornavirus infection.

3.2 Approach

A number of DNA constructs were obtained which encode fusions of the nuclear protein under test fused to EGFP (Table 2-2). GMK cells on glass coverslips were transfected with the constructs. 24 hr post transfection, cells were fixed with 4% formalin for 30 min on a rocking table then washed with 1X PBS containing glycine. Nuclei were stained with DAPI included in the hard-set mounting media. The images were taken by confocal microscopy using a Nikon A1 si confocal microscope.

To test the effect of infection, after infection cells were fixed, permeabilised and blocked, then a primary mouse monoclonal antibody against CAV-9 and goat anti-mouse IgG (labeled with Alexa 555) secondary antibody were used to identify infected cells. Cells were then mounted on a glass slide using DAPI hard set mounting media. Slides were then visualized using a Nikon A1 si confocal microscope.

3.3 EGFP distribution

To ensure that any apparent effect of infection on the nuclear proteins was not due to over-expression or the presence of EGFP, initially pEGFP-C1 was transfected into GMK cells, after infection (8hr) EGFP fluorescence was detected and it can be seen that there is no significant difference between the EGFP signal distribution in infected and non infected cells (Figure 3-1).

3.4 PML (EGFP-PML) distribution

3.4.1 EGFP-PML distribution in uninfected cells

In order to study the distribution of PML, pEGFP-PML was transfected. The fluorescence images show the expected distribution of PML (Jul-Larsen et al., 2010), as the protein showed a punctate distribution with many spots throughout the nucleus (Figure 3-2). In some cells the stain was much more intense, but still punctate in the nucleus (data not shown).

3.4.2 The effect of CAV-9 infection on EGFP-PML distribution

In order to examine the effect of CAV-9 on PML distribution, GMK cells were transfected with pEGFP-PML then infected with CAV-9 virus. In this experiment and most experiments looking at other nuclear proteins, the results from 6 and 8 hr time point are shown. A more complete time series (2, 4, 6 and 8 hr) was examined in some cases, but it is difficult to detect virus infected cells at earlier time points and preliminary work

showed that cells became rounded and detached at later time points (data not shown). The result showed that there was no clear change in the distribution of EGFP-PML in the infected cells after 6 or 8 hr (Figure 3-2). However, the EGFP-PML protein has only a small number of spots in the nucleus after 8 hr of infection, which is the same result that was shown during 6 hr infections. In both cases, the number is less than seen in the uninfected cells.

3.5 Nucleolin (EGFP-Nucleolin) distribution

3.5.1 EGFP-nucleolin distribution in uninfected cells

In order to study the distribution of nucleolin, GMK cells were transfected with pEGFP-Nucleolin. The fluorescence shows the expected distribution of nucleolin (Dambara et al., 2007, Emmott and Hiscox, 2009) as the protein showed slight diffusion in the nucleus with a strong signal accumulated in 2-3 irregular structures (Figure 3-3). These structures are presumably nucleoli as they correspond to areas in the nucleus which are not stained with DAPI.

3.5.2 The effect of CAV-9 infection on nucleolin distribution

In order to examine the effect of CAV-9 infection on nucleolin, GMK cells were transfected with pEGFP-Nucleolin then infected with CAV-9 virus for 6 and 8 hr. Results showed that the EGFP-Nucleolin has no clear change in distribution after 6 hr of infection, although some of the nucleolar detail seems to be lost. After 8 hr of infection

there is more diffusion into the nuclear matrix and also some into the nucleoplasm, but most remains in the nucleolus (Figure 3-3).

3.6 Fibrillarin (EGFP-Fibrillarin) distribution

3.6.1 EGFP-Fibrillarin distribution in uninfected cells

In order to study the structure of fibrillarin, GMK cells were transfected with pEGFP-Fibrillarin. The fluorescence shows the expected distribution of fibrillarin (Emmott and Hiscox, 2009), as it accumulated in the nucleolus (Figure 3-4), but in some cells the EGFP-Fibrillarin is also distributed throughout the nucleus, with some fluorescence in the cytoplasm.

3.6.2 The effect of CAV-9 infection on EGFP-fibrillarin distribution

In order to examine the effect of CAV-9 on fibrillarin, GMK cells were transfected with pEGFP-Fibrillarin, then infected with CAV-9 virus for 6 and 8 hr. After 6 and 8 hr of infection the results showed that there is no change to the nucleolar distribution, as the EGFP-fibrillarin protein is concentrated in the nucleolus in 2-3 spots (Figure 3-4). Uninfected cells in the fields have a very similar distribution of EGFP-Fibrillarin to the infected cells.

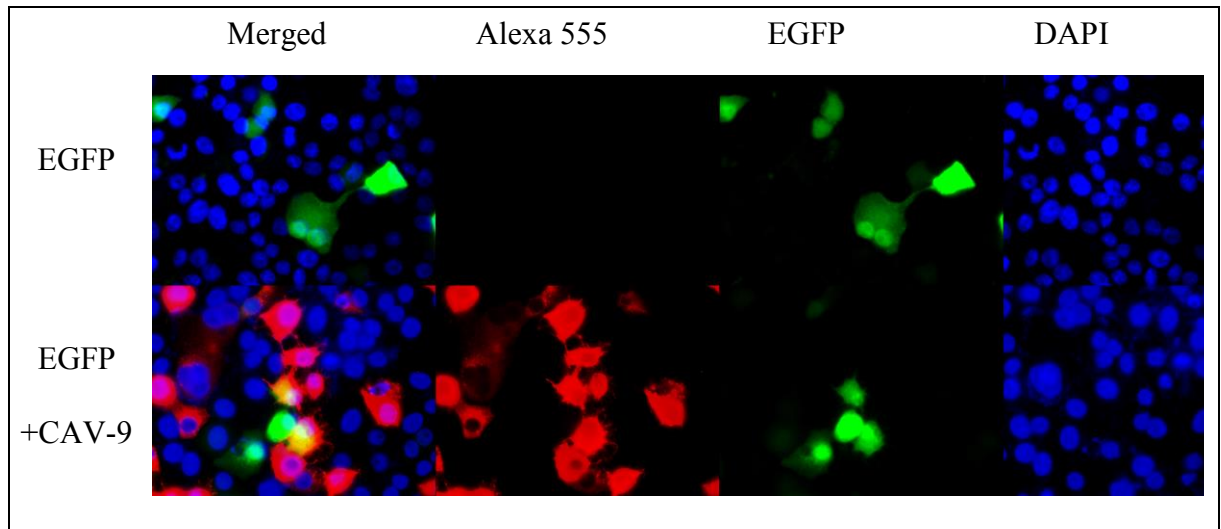


Figure 3-1 The effect of CAV-9 on the redistribution of EGFP. GMK cells were grown on coverslip and transfected with EGFP using lipofectin. Cells were then infected with CAV-9 for 8 hr. Nuclei were stained with DAPI in the mounting medium before being visualized using a Nikon A1 si confocal fluorescence microscope. Nuclei were observed using DAPI (blue), EGFP using the EGFP channel (green) and infected cells in the Alexa 555 channel (red).

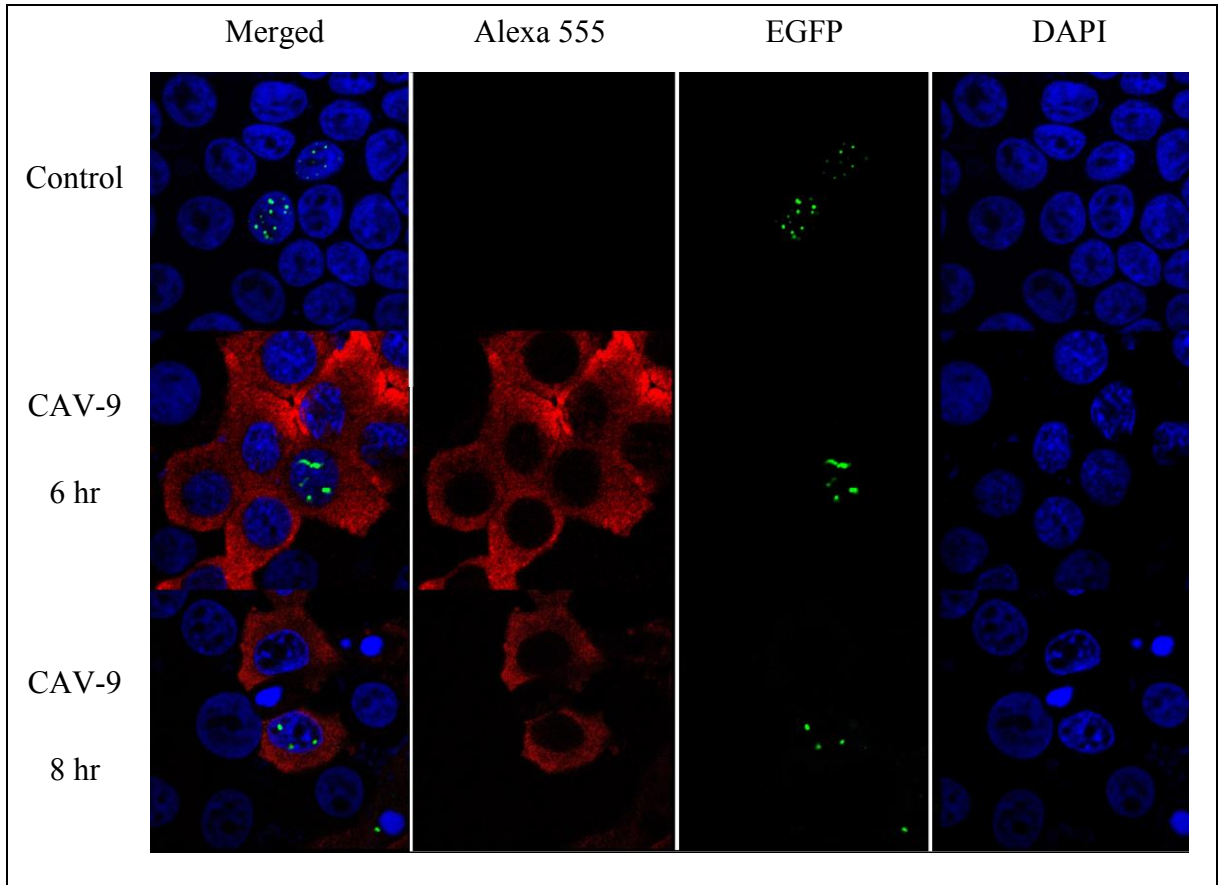


Figure 3-2 The effect of CAV-9 infection on the distribution of EGFP-PML. GMK cells were grown on coverslips and transfected with pEGFP-PML using Lipofectin. Cells were then either left uninfected (Control) or infected with CAV-9 for 6 and 8 hr, before being stained with CAV-9 primary/goat anti-mouse IgG secondary antibody labelled with Alexafluor 555. Nuclei were stained with DAPI in the mounting medium. Images were visualized using a Nikon A1 si confocal microscope. Nuclei were observed using the DAPI channel (blue), EGFP-PML in the EGFP channel (green) and infected cells in the Alexa 555 channel (red).

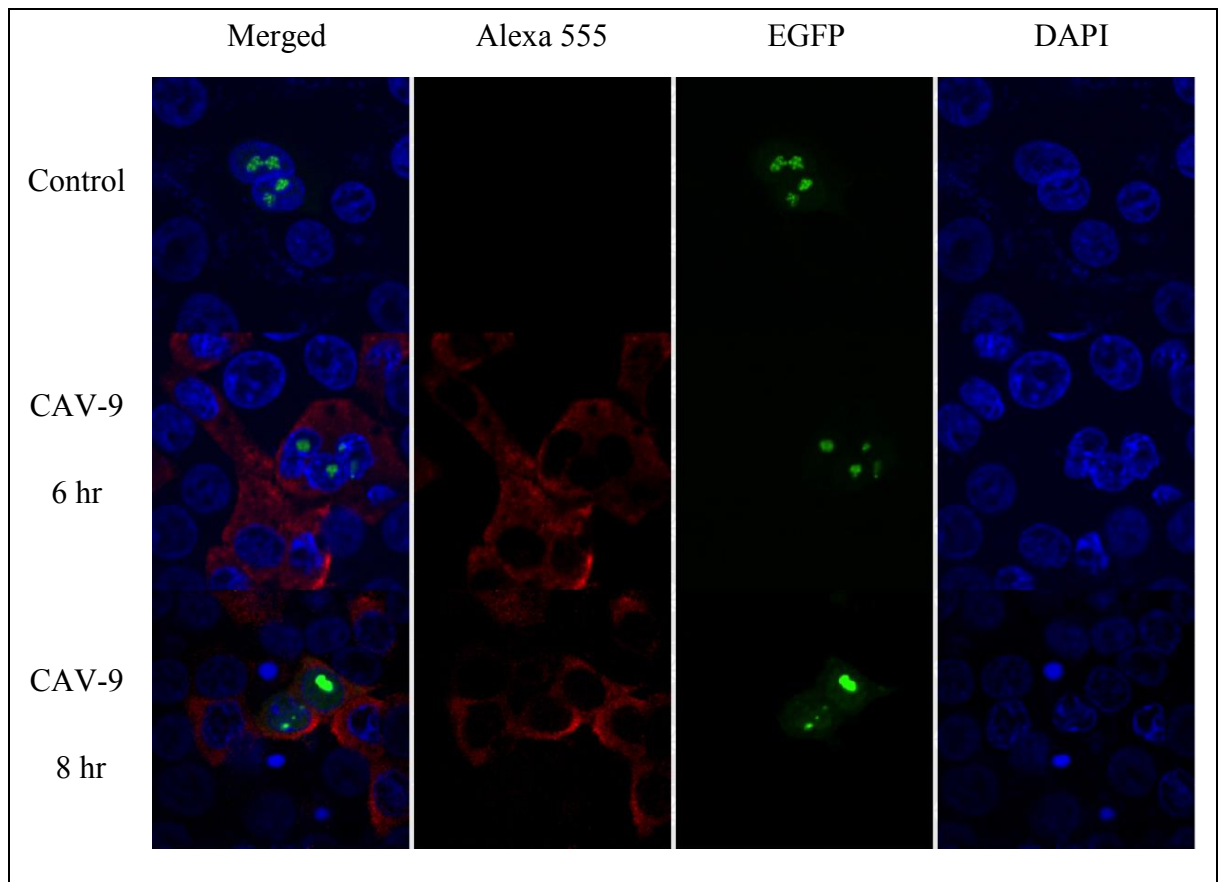


Figure 3-3 The effect of CAV-9 infection on the distribution of EGFP-Nucleolin. GMK cells were grown on coverslips and transfected with pEGFP-Nucleolin using Lipofectin. Cells were then either left uninfected (Control) or infected with CAV-9 for 6 and 8 hr, before being stained with CAV-9 primary/goat anti-mouse IgG secondary antibody labelled with Alexafluor 555. Nuclei were stained with DAPI in the mounting medium. Images were visualized using a Nikon A1 si confocal microscope. Nuclei were observed using the DAPI channel (blue), EGFP-Nucleolin in the EGFP channel (green) and infected cells in the Alexa 555 channel (red).

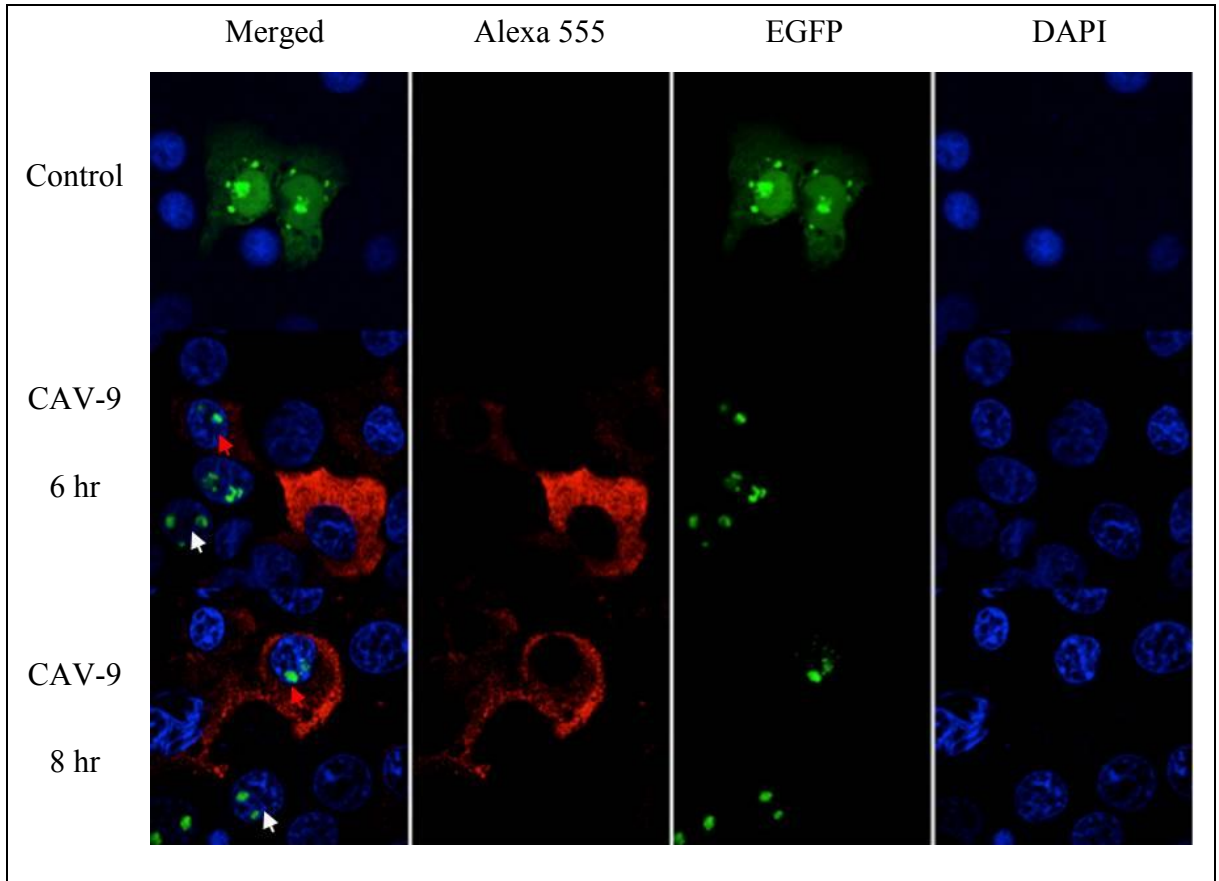


Figure 3-4 The effect of CAV-9 infection on the distribution of EGFP-Fibrillarin. GMK cells were grown on coverslips and transfected with pEGFP-Fibrillarin using Lipofectin. Cells were then either left uninfected (Control) or infected with CAV-9 for 6 and 8 hr, before being stained with CAV-9 primary/goat anti-mouse IgG secondary antibody labelled with Alexafluor 555. Nuclei were stained with DAPI in the mounting medium. Images were visualized using a Nikon A1 si confocal microscope. Nuclei were observed using the DAPI channel (blue), EGFP-Fibrillarin in the EGFP channel (green) and infected cells in the Alexa 555 channel (red). The scale bars represent 20 μ m. In the CAV-9 infected samples, (white arrows) is similar to in infected cells (red arrows).

3.7 B23 (EGFP-B23) distribution

3.7.1 EGFP-B23 distribution in uninfected cells

In order to study the structure of B23 and the distribution of its proteins, GMK cells were transfected with pEGFP-B23. The images were taken using a BX41 fluorescence microscope 24 hr post transfection. The fluorescence shows the expected distribution of B23 (Emmott and Hiscox, 2009), as the protein showed a strong nucleolus signal (Figure 3-5).

3.7.2 The effect of CAV-9 infection on EGFP-B23 distribution

In order to examine the effect of CAV-9 on B23 GMK cells were transfected with pEGFP- B23 then infected with CAV-9 virus for 6 and 8 hr. Slide was then visualized using a BX41 fluorescence microscope. No cells that were both infected and transfected could be found after 6 hr of infection. At the 8 hr of infection, EGFP-B23 did not show any obvious change in its distribution, as the protein was diffused in the nucleus with 1-2 very bright spots corresponding to nucleoli (Figure 3-5).

3.8 Paraspeckle (EGFP-PSPC-1) distribution

3.8.1 EGFP-PSPC-1 distribution in uninfected cells

In order to study the structure of paraspeckles in GMK cells and the distribution of one paraspeckle protein, PSPC-1, GMK cells were transfected with pEGFP-PSPC-1. The images were taken by the fluorescence microscope BX41 24 hr post transfection. The fluorescence show the expected distribution of PSPC-1 (Fox et al., 2002) as the protein showed a punctate structure in the nucleus (Figure 3-6).

3.8.2 The effect of CAV-9 infection on EGFP-PSPC-1 distribution

In order to examine the effect of CAV-9 infection on paraspeckles, GMK cells were transfected with pEGFP-PSPC-1 then infected with CAV-9 virus for 6 and 8 hr. The fluorescence images show changes in the distribution of the EGFP-PSPC-1 after both 6 and 8 hr of infection. A huge redistribution of the protein was observed, as the protein was mainly located in bright spots in the cytoplasm (Figure 3-6).

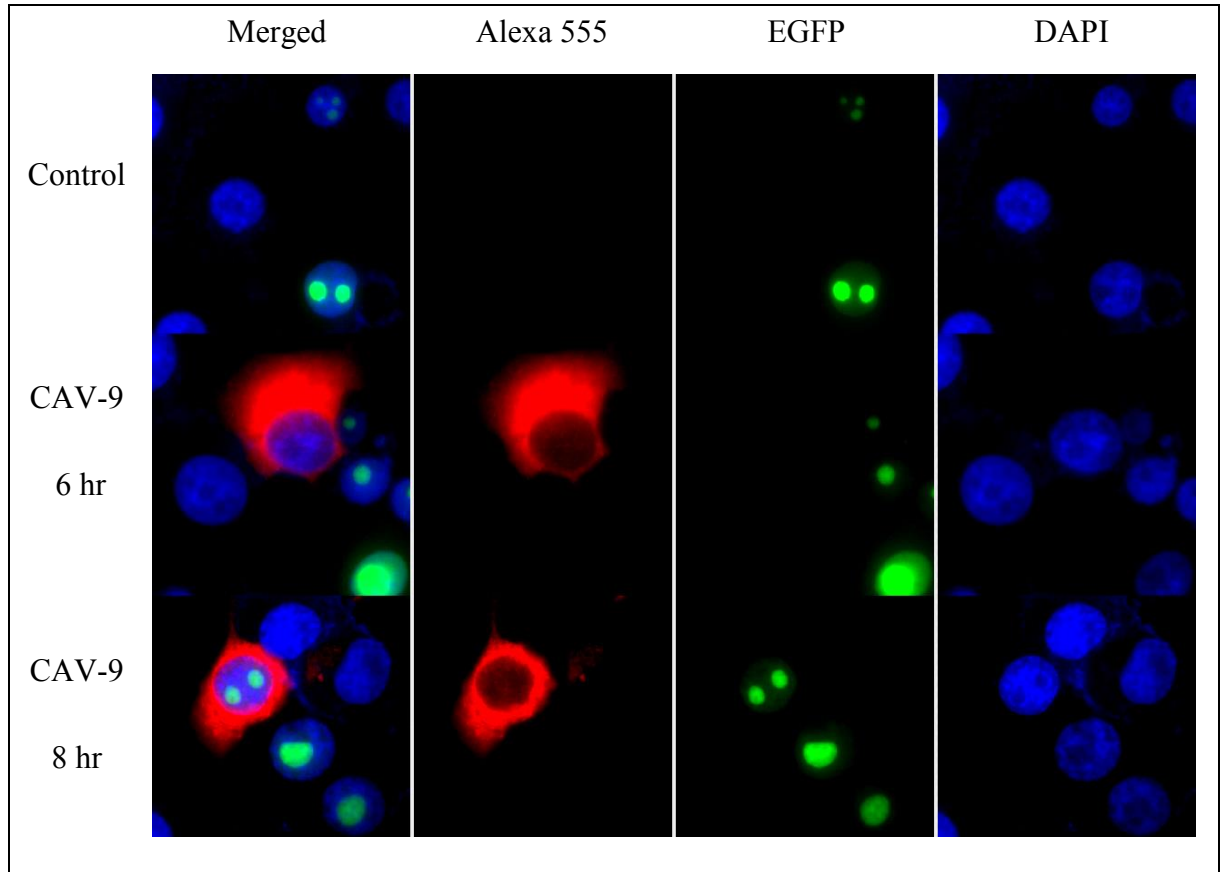


Figure 3-5 The effect of CAV-9 infection on the distribution of EGFP-B23. GMK cells were grown on coverslips and transfected with pEGFP-B23 using Lipofectin. Cells were then either left uninfected (Control) or infected with CAV-9 for 6 and 8 hr, before being stained with CAV-9 primary/goat anti-mouse IgG secondary antibody labelled with Alexafluor 555. Nuclei were stained with DAPI in the mounting medium. Images were visualized using a Nikon A1 si confocal microscope. Nuclei were observed using the DAPI channel (blue), EGFP-B32 in the EGFP channel (green) and infected cells in the Alexa 555 channel (red).

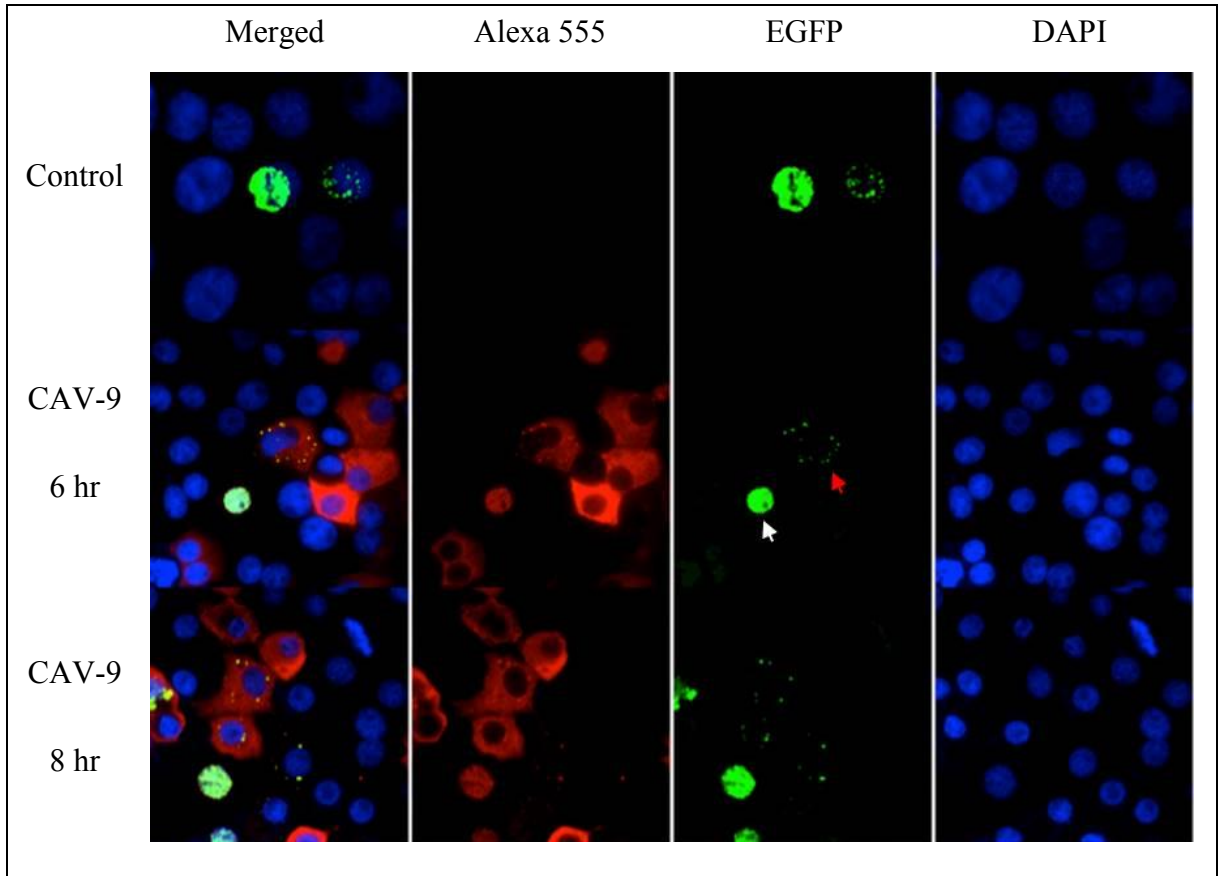


Figure 3-6 The effect of CAV-9 infection on the distribution of EGFP-PSPC-1. GMK cells were grown on coverslips and transfected with pEGFP-PSPC-1 using Lipofectin. Cells were then either left uninfected (Control) or infected with CAV-9 for 6 and 8 hr, before being stained with CAV-9 primary/goat anti-mouse IgG secondary antibody labelled with Alexafluor 555. Nuclei were stained with DAPI in the mounting medium. Images were visualized using a BX41 fluorescence microscope. Nuclei were observed using the DAPI channel (blue), EGFP-PSPC-1 in the EGFP channel (green) and infected cells in the Alexa 555 channel (red). In the CAV-9 infected samples, the distribution in uninfected cells (white arrows) is very different to infected cells (red arrows).

3.9 Other paraspeckle (EGFP-PSF and EGFP-NONO) distribution

3.9.1 EGFP-PSF and EGFP-NONO distribution in uninfected cells

In order to examine whether the protein (PSPC-1) changing distribution due to CAV-9 infection is a general feature for paraspeckle proteins or seen only for PSPC-1, two other paraspeckle proteins were examined (NONO/P54 NRB and PSF). GMK cells were grown on coverslips 24 hr prior to transfection. Cells were then transfected with pEGFP-NONO and pEGFP-PSF. The images were taken using a BX41 fluorescence microscope 48 hr post transfection (Figure 3-7 and Figure 3-8). For EGFP-NONO (Figure 3-7), the expected paraspeckle distribution was seen (Zolotukhin et al., 2003), as the protein showed a punctate structure throughout the nucleus. For EGFP-PSF, there was a more diffuse nuclear localization (Figure 3-8).

3.9.2 The effect of CAV-9 infection on EGFP-PSF and EGFP-NONO distribution

GMK cells were grown on coverslips for 24 hr prior to transfection then transfected with pEGFP fusion contain (NONO/P54 NRB or PSF). 48hr post transfection, cells were infected with CAV-9 and at different time intervals (2, 4, 6 and 8 hr). Cells were then visualized with a BX41 fluorescence microscope.

It is difficult to identify infected cells after 2 hr as there is not enough virus protein present to detect with the antibodies. For EGFP-NONO, some cells showed a more

diffuse nuclear localization which may be the result of infection (Figure 3-7). The EGFP-NONO showed a slight change after 4 hr of infection, with more diffuse nuclear distribution and a small amount of the protein in the cytoplasm with a small number of speckles. After 6 and 8 hr, there was more relocalization out of the nucleus to cytoplasmic spots.

For EGFP-PSF, there was no obvious change in the distribution after 2 hr of infection (Figure 3-8). Unfortunately, there were no cells that were found to be both transfected/infected after 4 hr (data not shown). After 6 and 8 hr of infection EGFP-PSF had mainly left the nucleus and redistributed in the cytoplasm with a large number of punctate structures.

EGFP-NONO and EGFP-PSF were also examined after 8 hr of infection using a Nikon wide field A 1 plus microscope in order to show a more detailed image (Figure 3-9 and Figure 3-10). Both EGFP-PSF and EGFP-NONO disappeared from the nucleus and completely redistributed in the cytoplasm showing a large number of the punctate structures throughout the cytoplasm.

3.10 The PSF/NONO and PSpC-1 complex

It is known that PSF, NONO and PSpC-1 interact together (Gao et al., 2014). In order to examine these paraspeckle proteins to find if they are translocated similarly after 8 hr of CAV-9 infection, cotransfection/infection experiments were performed on the paraspeckle proteins. A pmCherry fusion of PSpC-1 was made by cutting pEGFP-PSpC-1 with the restriction enzymes *EcoRI* and *BamHI* to remove the PSpC-1 sequence, which

was then ligated into pmCherry. GMK cells were grown on coverslips for 24 hr then cotransfected with pmCherry-PSPC-1 and pEGFP-NONO or pEGFP-PSF. Cells were then infected with CAV-9 for 8 hr then fixed with formalin. Slides were then visualized with a Nikon A1 si confocal microscope (Figure 3-11). Infected cells were identified on the basis of the characteristic relocalization of PSPC-1. Results of both EGFP-NONO and EGFP-PSF showed that both proteins perfectly colocalized with mCherry-PSPC-1 in the cytoplasm (Figure 3-11). This shows that all three paraspeckle proteins are relocalised to the same cytoplasmic compartment during CAV-9 infection.

3.11 Endogenous paraspeckles

In order to examine if the paraspeckle protein redistribution due to CAV-9 is a genuine feature for paraspeckle proteins, not an artefact of the EGFP/mCherry fusions or over-expression of the proteins, an experiment on endogenous paraspeckles was conducted. GMK cells were grown on a coverslip for 24hr. Cells were infected with CAV-9 for 8 hr then fixed with formalin and permeabilised then blocked, a specific antibody for PSPC-1 was applied then a goat anti rabbit antibody was used as a secondary antibody. Cells were then mounted with mounting media containing DAPI in order to stain the nucleus. Cells were then visualized with Nikon A1 si confocal microscope. The result shows that the endogenous protein gave the expect distribution of paraspeckles as the non infected cells gave the punctate structure in the nucleus while the protein in the infected cells showed redistribution to the cytoplasm with some brighter spots in the cytoplasm (Figure 3-12).

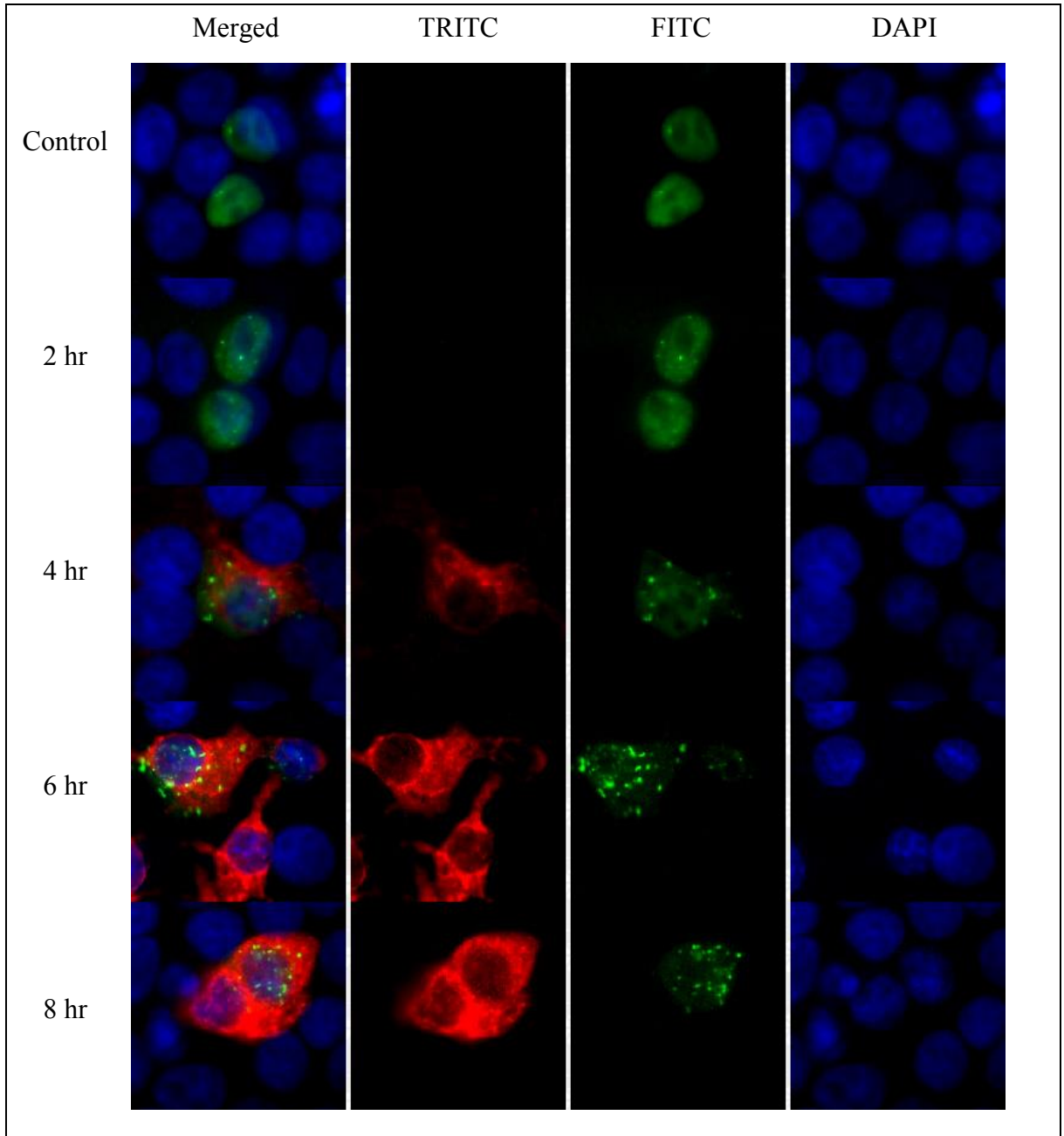


Figure 3-7 The effect of CAV-9 infection on the distribution of EGFP-NONO (time interval). GMK cells were grown on coverslips and transfected with pEGFP-NONO using Lipofectin. Cells were then either left uninfected (Control) or infected with CAV-9 for 2, 4, 6 and 8 hr, before being stained with CAV-9 primary/goat anti-mouse IgG secondary antibody labelled with Alexafluor 555. Nuclei were stained with DAPI in the mounting medium. Images were visualized using a BX41 fluorescence microscope. Nuclei were observed using the DAPI channel (blue), EGFP-NONO in the EGFP channel (green) and infected cells in the Alexa 555 channel (red).

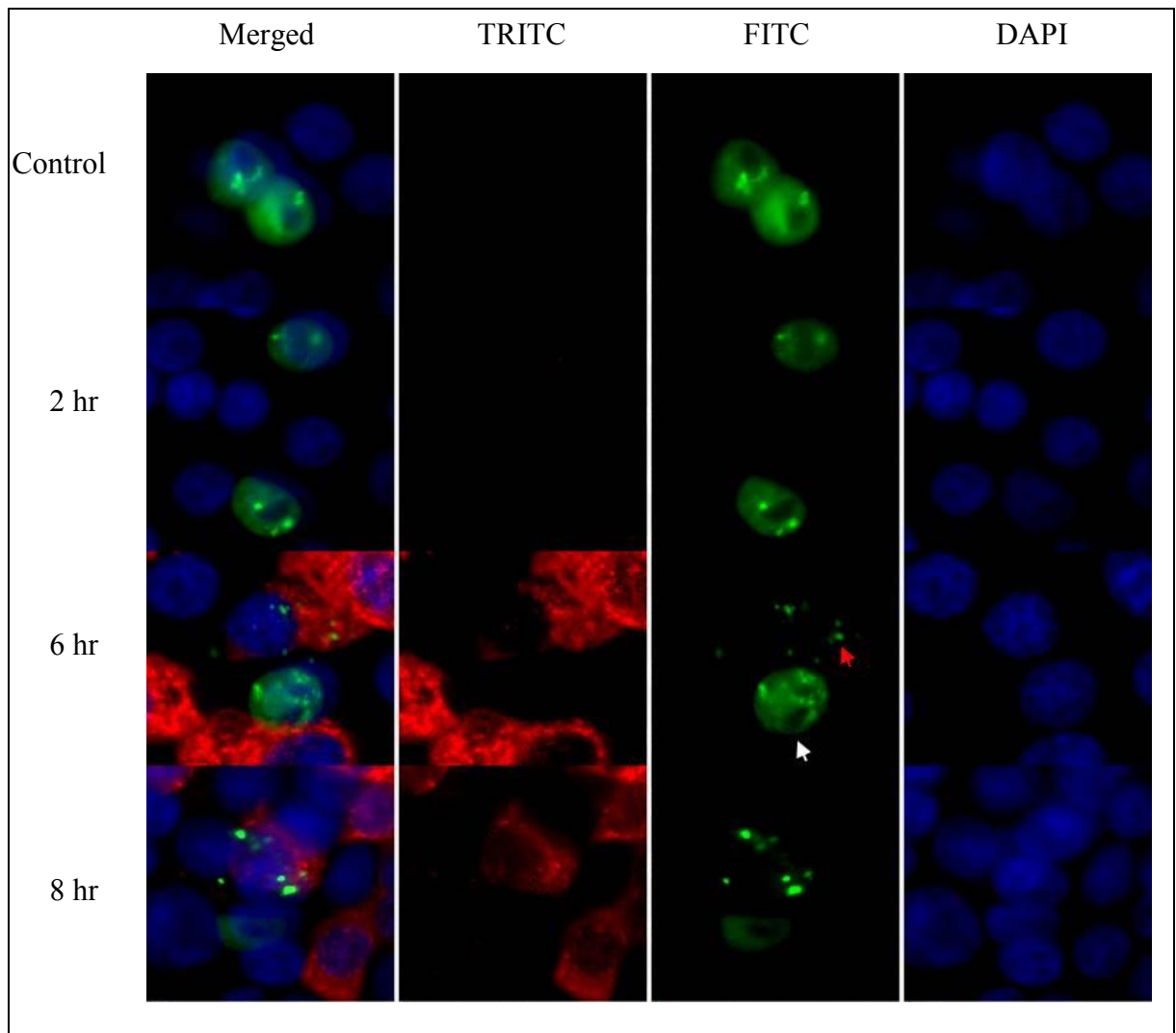


Figure 3-8 The effect of CAV-9 infection on the distribution of EGFP-PSF (time interval). GMK cells were grown on coverslips and transfected with pEGFP-PSF using Lipofectin. Cells were then either left uninfected (Control) or infected with CAV-9 for 2, 6 and 8 hr, before being stained with CAV-9 primary/goat anti-mouse IgG secondary antibody labelled with Alexafluor 555. Nuclei were stained with DAPI in the mounting medium. Images were visualized using a BX41 fluorescence microscope. Nuclei were observed using the DAPI channel (blue), EGFP-PSF in the EGFP channel (green) and infected cells in the Alexa 555 channel (red). In the CAV-9 infected samples, the distribution in uninfected cells (white arrows) is very different to infected cells (red arrows).

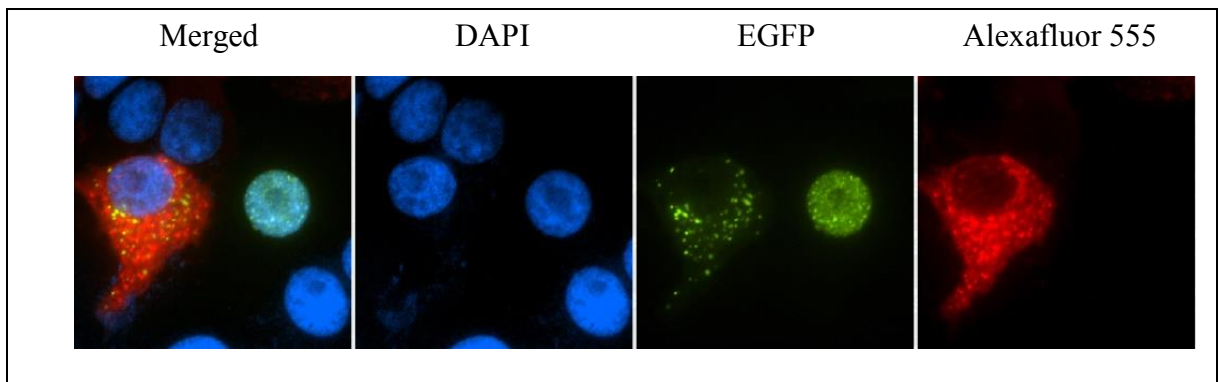


Figure 3-9 The effect of 8 hr infection on EGFP-NONO. GMK cells were grown on coverslip and transfected with EGFP-NONO using lipofectin. Cells were then infected with CAV-9 for 8 hr before being stained with CAV-9 primary/goat anti-mouse IgG secondary antibody labelled with Alexafluor 555. Nuclei were stained with DAPI in the mounting medium. Images were visualized using a Nikon A1 si confocal microscope. Nuclei were observed using the DAPI channel (blue), EGFP-NONO in the EGFP channel (green) and infected cells in the Alexa 555 channel (red).

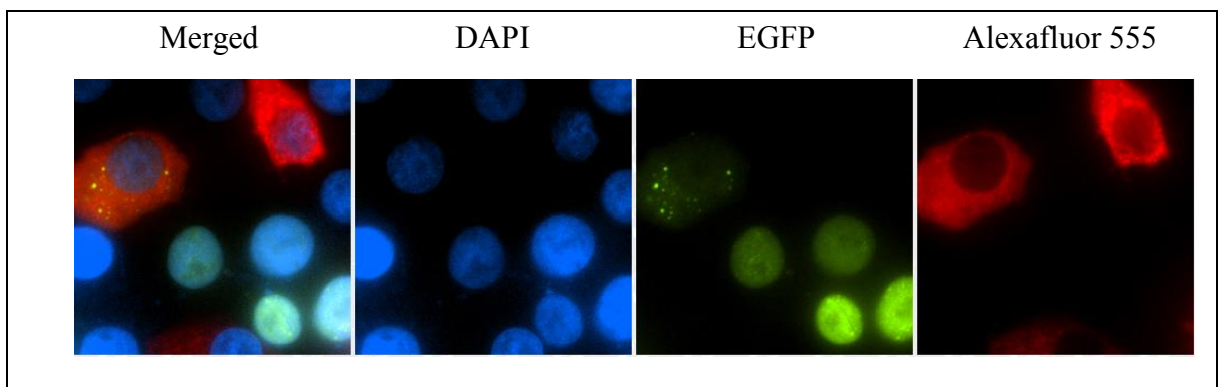


Figure 3-10 The effect of 8 hr infection on EGFP-PSF. GMK cells were grown on coverslip and transfected with EGFP-PSF using lipofectin. cells were grown on coverslips and transfected with EGFP-PSF. Cells were then infected with CAV-9 for 8 hr. Nuclei were stained with DAPI and infected cells with CAV-9 primary/goat anti-mouse IgG secondary antibody labelled with Alexafluor 555, before being visualized using a Nikon A1 plus wide field fluorescence microscope. Nuclei were observed using the DAPI channel (blue), EGFP-PSF using the EGFP channel (green) and infected cells in the Alexa 555 channel (red).

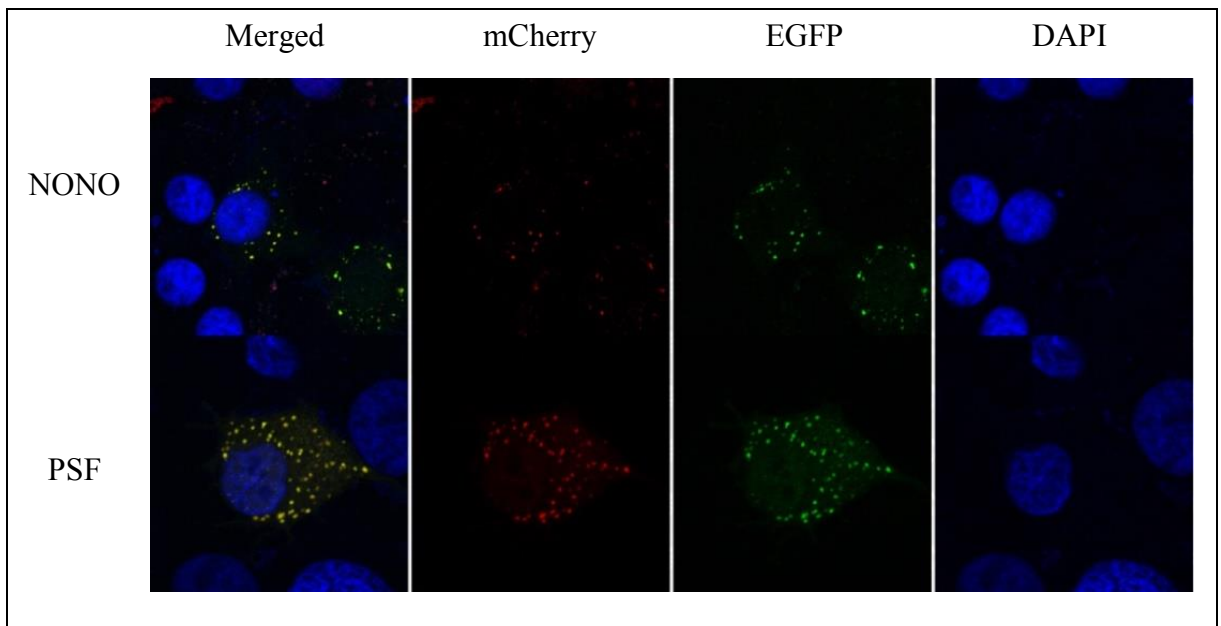


Figure 3-11 The effect of CAV-9 on the redistribution of EGFP-NONO/PSF and mCherry PSpC-1 complex. GMK cells were grown on coverslip and cotransfected with EGFP-PSF/or NONO and mCherry PSpC-1 using lipofectin. Cells were then infected with CAV-9 for 8 hr. Nuclei were stained with DAPI in the mounting medium before being visualized using a Nikon A1 si confocal fluorescence microscope. Nuclei were observed using DAPI (blue), EGFP-NONO/PSF using the EGFP channel (green) and mCherry-PSpC-1 using the mCherry channel (red).

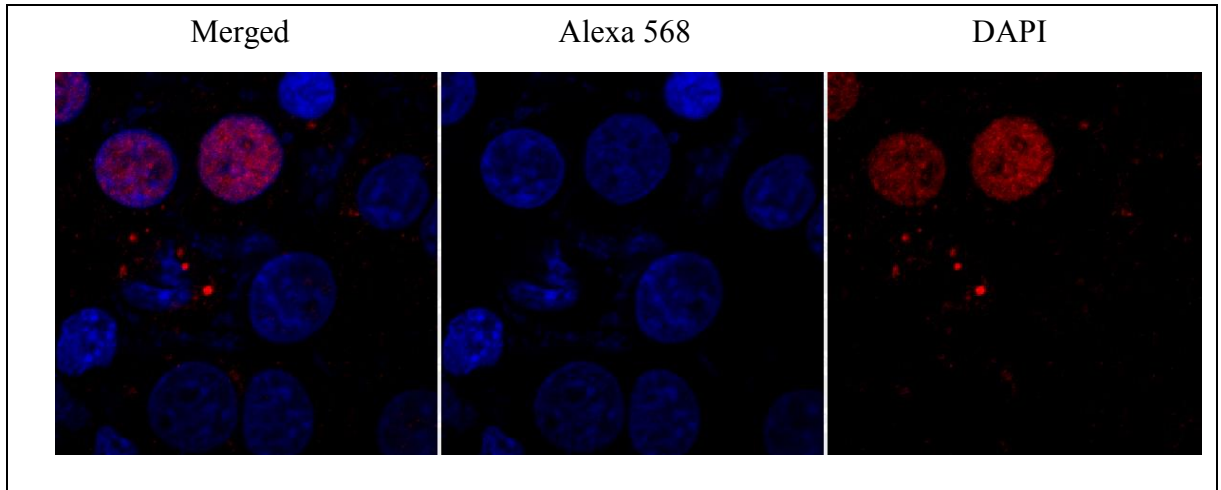


Figure 3-12 The effect of CAV-9 on the endogenous PSPC-1. GMK cells were grown on coverslip then infected with CAV-9 for 8 hr. Cells were then fixed and labelled with PSPC-1 antibody and Alexa fluor 568 as secondary antibody. Nuclei were then stained with DAPI and visualized using a Nikon A1 si confocal fluorescence microscope. Nuclei were observed using DAPI (blue),Alexa fluor 568 (red channel).

3.12 Discussion

Picornavirus infection causes several changes to the host cell by the interaction between viral proteins and cellular proteins. These cause alteration in host cells synthetic, signaling and secretory mechanisms, and improve viral replication (Younessi et al., 2012). There is growing evidence showing that picornaviruses cause disruption in nuclear/cytoplasmic shuttling by inhibiting nuclear pore functions which results in relocalization of nuclear proteins into the cytoplasm (Younessi et al., 2012). In addition, virus proteases may remove the nuclear localization signals (NLS) of nuclear proteins and this causes relocalisation to the cytoplasm (Haugwitz, 2002). Some studies showed that La is located in the nucleus but during PV infection, the protein redistributed in the cytoplasm in the presence of 3C^{pro} in infected cells, which suggested that 3C^{pro} remove the NLS from the La C-terminus. La binds to the IRES of PV, CVB3 and hepatitis A virus and stimulates viral translation (Lin et al., 2009c). Another protein that is altered by picornavirus infection is PTB. PTB is a member of the nuclear RNP (hnRNP) family which normally shuttle between nucleus and cytoplasm. During infection with PV PTB stimulates viral IRES-dependent translation (Chase and Semler, 2012), although it has also been reported that cleavage by poliovirus 3C^{pro} causes redistribution of PTB to the cytoplasm and inhibits IRES-dependent translation (Back et al., 2002). To investigate whether the distribution of other nuclear proteins may be affected by virus infection, we studied several proteins (PML, nucleolin, fibrillarin, B23, PSPC-1, NONO and PSF) by using EGFP/mCherry fusions and infecting cells with CAV-9.

PML, found in PML NBs, is a protein that is found to be affected by infection with

several DNA viruses (Everett, 2001). Nucleolin, fibrillarin and B23 are found in different part in the nucleolus and these structures have been found to be involved or modified during infection by several viruses (Emmott and Hiscox, 2009). Nuclear paraspeckles are less well-understood, but there is recent evidence that these structures, or proteins/NEAT-1 located in these structures, are important in host-virus interactions in the case of HIV-1 infections (Copeland et al., 2013, Zhang et al., 2013). The effect of CAV-9 infection on the distribution of these proteins is summarised in Table 3-1.

EGFP-PML was completely localized in the nucleus in most cells and displayed a predominantly nucleoplasmic pattern with several dots (Figure 3-2). The sub-nuclear distribution of PML was then examined during CAV-9 infection. There was no clear difference, but the result show a reduced number of nuclear spots in the EGFP-PML distribution (Figure 3-2). Previous studies showed that poliovirus infection affects PML phosphorylation and causes alteration in PML body localization and transfer from the nucleoplasm to the nuclear matrix (Pampin et al., 2006). Another study examined the effect of encephalomyocarditis virus (EMCV) infection on PML bodies and found that EMCV infection increase PML body size, which leads to a decrease in PML protein expression (El Mchichi et al., 2010). This seems to be related to SUMOylation of PML. It was also found that the absence of PML results in an increase of EMCV replication, while the presence of PML inhibited virus replication. The results suggest that CAV-9, as PV and EMCV do, may manipulate PML to enhance virus replication.

Poliovirus infection results in redistribution of nucleolin from the nucleus to the cytoplasm (Yu et al., 2005). Nucleolin binds to the IRES after the relocalization and this

stimulates IRES-dependent translation (Maramorosch et al., 2011 2001). Nucleolin also interacts with the poliovirus 3' UTR in order to be involved in synthesis of negative strand RNA (Zakaryan and Stamminger, 2011). It also stimulates translation in FMDV (Foot-and-Mouth-Disease virus) by interacting with the 5'UTR and stimulating the IRES (Pacheco and Salas, 2010). Other RNA binding proteins can bind to the picornavirus 5'UTR and have a negative effect on virus replication. Some studies showed that AUF1 acts as restricting factor during enterovirus infection. It is relocalised from the nucleus to the cytoplasm by the virus protease 2A^{pro} and binds to the virus 5'UTR causing inhibition of translation, but this is overcome by 3C^{pro}/3CD^{pro} cleavage of AUF1 (Cathcart et al., 2013). AUF1 is also relocalised from the nucleus to the cytoplasm during EMCV infection. Unlike enterovirus infection, AUF1 is not cleaved by EMCV 3C^{pro}/3CD^{pro}, which suggests that it does not inhibit infection of all picornaviruses, but could act as selective restricting factor targeting enterovirus (Cathcart and Semler, 2014). hn(RNP) A1 is redistributed to the cytoplasm during infection. It is a trans acting factor that binds to the EV71 5' UTR and regulates the IRES-dependant translation (Lin et al., 2009a). As a large change in nucleolin distribution has been previously for PV it was seen surprising that the changes seen in CAV-9-infected cells were relatively minor. There was loss in the nucleolar details and some movement to the nuclear matrix plus a small amount to the cytoplasm (Figure 3.2) when infected with CAV-9. This may suggest that nucleolin may not play an important role in CAV-9 replication.

In contrast to nucleolin, there was no effect of CAV-9 infection on either fibrillarin or B23 (Figure 3-4 and Figure 3-5). It has been found that EMCV 2A enters the host cell

nucleus due to colocalisation with B23, which acts as a nuclear shuttling chaperone protein (Castelló et al., 2011). EMCV 2A contains a short motif (KRVRPFRLP), which seems to act as an NLS as well as facilitating the colocalisation with B23. It has been suggested that 2A may target the nucleolus to alter ribosomal biogenesis in some way, promoting viral IRES-dependent translation and/or 2A inclusion within ribosomes. The EMCV 3BCD precursor also associates with B23 and enters the nucleolar compartment through the presence of an NLS in the 3D (Flather and Semler, 2015). The EMCV 2A is a different type of protein from any found in enteroviruses, and so these interactions seen between EMCV and B23 may not occur in infections by CAV-9 and other enteroviruses (Hughes and Stanway, 2000). It has also been found that not all nucleus proteins are redistributed during PV infection, for instance fibrillarin and SC35 (Castelló et al., 2011).

It was previously observed that the PSPC-1 is redistributed by human parechovirus (HPeV) infection, but not proteins associated with other NBs such as PML or the nuclear speckle protein SC35 (Mutabagani, 2012). This redistribution was within the nucleus. It was interesting that CAV-9 also causes a redistribution of PSPC-1, although this redistribution is much more radical as it involves the relocalisation to intense foci in the cytoplasm (Figure 3-6). PSPC-1 is a member of the DBHS family of proteins along with PSF and NONO and these proteins are key components of the paraspeckles (Passon et al., 2012). Both PSF and NONO are also redistributed into the same cytoplasmic structures as PSPC-1, as seen in the colocalisation experiment (Figure 3-11). This redistribution was also shown to occur to endogenous PSPC-1 in infected cells (Figure 3-12) and so is a real effect, rather than being due to the over expressed EGFP and mCherry fusion

proteins. It has been known that PSF plays an important role in cellular processes, but it was also been reported that PSF plays a key role in regulating RNA virus replication. PSF protein (and the PSF/NONO dimer) is important in HIV-1 replication and accelerates the production of viral transcripts, while the knockdown of the protein causes a decrease in unspliced viral RNA (Zolotukhin et al., 2003). PSF is also required for multiplication and replication of the influenza viral RNA and the depletion of PSF by siRNA causes a delay in virus gene expression and decrease in viral transcription (Yarosh et al., 2015).

Recently, a high throughput screen of proteins which bind to the poliovirus 5' UTR was performed and identified both NONO and PSF (Lenarcic et al., 2013). NONO was studied in detail and it was found that NONO directly binds to PV RNA in order to enhance virus amplification. NONO was knocked down at an early stage of infection and the results showed a great reduction in the virus titre (10-30 fold decrease). It was concluded that absence of this host cell factor caused a delay in viral production. It was also found that NONO had no effect on PV translation, but the knockdown of the protein triggered a 10 fold decrease in positive strand RNA and a 2 fold decrease in minus strand RNA, which suggests that it is involved in RNA replication. This would suggest that the cytoplasmic spots seen after CAV-9 infection are related to RNA replication and this will be investigated in Chapter 5.

Picornaviruses are cytoplasmic replicating viruses, but several host proteins used by these viruses are nuclear or cycle between the nucleus and cytoplasm. PV infections cause a disruption in nuclear-cytoplasmic pathway by degrading several nucleoporins

which result in relocalization of nuclear host protein to cytoplasm (Lenaric *et al.*, 2013). Cleavage of some proteins is another mechanism that changes distribution. Of the proteins studied, CAV-9 infection had the clearest effect on the paraspeckle proteins. As there has been little work on these proteins in relation to picornavirus infection, they were studied in more detail as described in chapters 4 and 5.

Table 3-1. The normal location of nuclear proteins studied in this thesis, together with the effects of infection by CAV-9

Protein	Structure	Change
PML	PML NBs	Reduced number of nuclear spots
Nucleolin	Fibrillar centre	Loss of details and some movement to nuclear matrix with small amount in the cytoplasm
Fibrillarin	Dense fibrillar component	No change
B23	NPM1/Nucleophosmin (granular component)	No change
PSPC-1 PSF NONO	Paraspeckles	Relocalization to bright cytoplasmic spots

Chapter 4
The Effect of Non Structural Proteins
on Nuclear Proteins

4.1 Introduction

Proteolytic cleavage of the picornavirus polyprotein, to give precursors and the final virus proteins, is essential for virus replication (Castelló et al., 2011, Lin et al., 2009b). Most of the picornavirus proteins are homologous in structure and function when the same protein is compared between genera. However, there is more diversity in the 2A protein (Agol and Gmyl, 2010, Hughes and Stanway, 2000). The 2A protein of §It is also believed that parechoviruses are different from enteroviruses by not shutting off the synthesis of host cell protein during infection (Chang, 2015, Stanway et al., 1994). In contrast, the enterovirus 2A ($2A^{\text{pro}}$) is a cysteine protease that starts the processing of the virus precursor polyprotein by cleaving between the VP1 C-terminus and 2A N-terminus (Toyoda et al., 1986). $2A^{\text{pro}}$ also makes several changes to the cell such as interfering with nuclear traffic and hijacking the transcription machinery. $2A^{\text{pro}}$ also shuts off the host cap-dependant translation, by cleaving eIF4GI/II, in order to avoid competition for synthesis of the viral polyprotein (Wu et al., 2013). The proteolytic protein 3C ($3C^{\text{pro}}$ /3CD precursor) is the main protease in all picornaviruses (Ryan and Flint, 1997) as it cleaves the other junction sites within the polyprotein, including, 2A-2B and 2B-2C in P2 and the whole of P3. As part of the precursor $3CD^{\text{pro}}$ it also cleaves the junctions between VP2-VP3 and VP3-VP1 in P1 (Ypma-Wong et al., 1988). $3C^{\text{pro}}$ helps to shut off host translation by cleaving eIF4AI and also by cleaving poly (A) binding protein (PABP) (Lin et al., 2009b). It has been found that 3C induces apoptosis in neuronal cells and blocks type I interferon (IFN) responses to antiviral activities (Lei et al., 2010). $3C^{\text{pro}}$ has a unique structure among proteases, as it has a cysteine at the active site but

chymotrypsin-like serine protease structure (May Wang and Chen, 2007, Ryan and Flint, 1997). It includes the classic motif GXCG (GXSG is seen in most other members of this protease family) and C-H-D/E catalytic triad (Wang et al., 2014a). As the virus proteases 2A^{pro} and 3C^{pro} interfere with several different events in the virus-infected cell, 2A^{pro} and 3C^{pro} of the enterovirus CAV-9, and 3C^{pro}, as well as 2A (not a protease), from HPeV1 were investigated to see if they are involved in changes to the nuclear protein distributions seen in Chapter 3.

4.2 EGFP/mCherry constructs containing 2A and 3C from CAV-9 and HPeV-1

4.2.1 Primer design, PCR amplification and validation of the constructs:

Primers specific to the sequences encoding the N-terminal and C-terminal regions of 2A and 3C of CAV-9 Griggs cDNA were designed (Table 2-3). The 2A forward primer (OL 2006), 29 nucleotides long, recognises position 3345-3373 from the CAV-9 DNA sequence and the restriction site sequence for *XhoI* was added to the primer, as well as 2 nucleotides after the restriction site to keep the frame when ligated into both pEGFP and pmCherry vectors. In order to design the 2A reverse primer (OL 2007), 27 nucleotides were chosen from position 3768-3794 from the CAV-9 DNA. A stop codon was added, plus the restriction site for *BamHI*. Then the sequence was reversed using the reverse complement tool (http://www.bioinformatics.org/sms/rev_comp.html). These primers were then used in the PCR reaction (2.2.2.2.1). The same procedure was followed in

order to make CAV-9 3C primers (OL 2008 and OL 2009). The forward sequence was chosen from the position 5412-5441 and the reverse sequence was chosen from the position 5931-5960. For both the 2A and 3C constructs, the Web Cutter tool (<http://rna.lundberg.gu.se/cutter2/>) was used in order to choose the restriction enzyme sites added to the primers, to ensure that these sites do not occur in the virus cDNA. PCR was performed using pfu polymerase, followed by Taq-treatment to add A residues to the 3' ends of the PCR products. PCR gave the expected bands and these were cloned into pGEMT-Easy. A DNA fragment was cut from the pGEMT-Easy clones using enzymes *XhoI* and *BamHI*, and then ligated into pEGFP-C1 or pmCherry-C1 cut with the same enzymes (Figure 4-1). The final constructs were confirmed by sequencing and found to have the correct sequence, with no unexpected mutations (Appendix 1).

Primers specific to N-terminal and C-terminal areas of the 3C encoding region of HPeV-1 cDNA were designed (Table 2-3) using the HPeV-1 DNA sequence. In order to design HPeV-1 3C primer (OL 2063) a 22 nucleotide base were chosen from the position 5243-5264 from the HPeV-1 DNA sequence and restriction site for *XhoI* sequence was added to the primer as well as 2 nucleotide bases (CT) were added after the restriction site to keep the frame when ligated in pmCherry vector. In order to design the reverse primer (OL 2064) a 24 nucleotide bases were chosen from the position 5821-5842 from the HPeV-1 DNA. Then the sequence was reversed using reverse complement tool (http://www.bioinformatics.org/sms/rev_comp.html). Restriction site nucleotide sequence for *BamHI* was added plus a stop codon to keep the frame. The PCR was performed as illustrated in section (2.2.2.2.1). PCR gave the expected bands and these

were cloned into pGEMT-Easy. Few steps were carried out in order to construct mCherry fusion containing HPeV-1 3C (Figure 4-2). The final constructs were confirmed by sequencing and found to have the correct sequence, with no unexpected mutations (Appendix 2).

In addition to the HPeV-1 pmCherry-3C construct, a mutant form containing a mutation C to A mutation in the active site, made by Lisa Nicol, was also used.

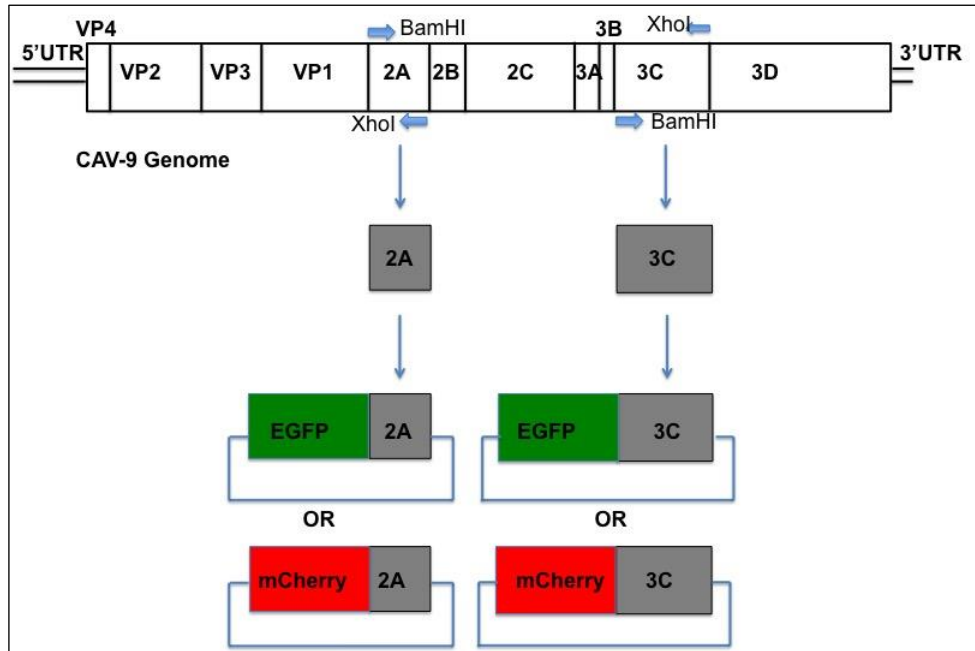


Figure 4-1 Schematic representation of CAV-9 2A and 3C manipulation. It shows how the CAV-9 Griggs fusion protein constructs (pEGFP-2A, pEGFP-3C, pmCherry-2A and pmCherry-3C) were generated.

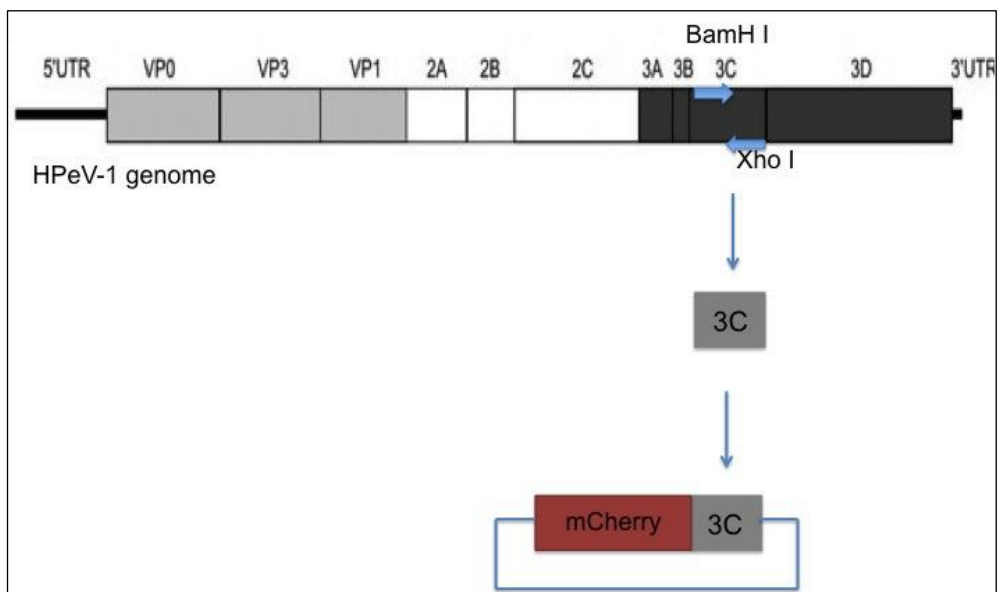


Figure 4-2 Schematic representation of the manipulation of HPeV-1 mCherry 3C. It shows how the fusion protein (mCherry-3C) isolated from the HPeV-1 Harris strain used for transfection

4.3 Approach

The 2A and 3C constructs were used together with the nuclear protein constructs which were studied in the work described in Chapter 3. GMK cells were grown on glass cover slips were co-transfected with different combinations of the protease and nuclear protein constructs. Cells were fixed with 4% formalin for 30 min on a rocking table then washed with 1X PBS containing glycine. Nuclei were stained with DAPI included in the hard-set mounting media. The images were taken by confocal microscopy using a Nikon A1 si confocal microscope. In some cases a BX41 fluorescence microscope was used to examine the slides.

4.4 Transfection of CAV-9 2A and 3C

In order to examine the effect of pEGFP and pmCherry fusions containing CAV-9 2A and 3C, these were transfected into GMK cells using lipofectin and cells were imaged 15 hr post-transfection. After the pEGFP/pmCherry 2A fusion was transfected into the GMK cells no fluorescence was seen (Figure 4-3). Several experiments were performed to observe the fluorescence at different time post-transfection but no fluorescence was observed. The cells were then treated with Sodium Pyrrolidine DithioCarbamate (PTDC) at 100 μ M or 50 μ M. The drug is known to bind to zinc and can inhibit enterovirus replication by inactivating 2A (Krenn et al., 2005). However, the drug caused cell toxicity (data are not shown). When GMK cells were transfected with CAV-9 pmCherry 2A using TurboFect, a few fluorescent cells were seen at 48 hr post-transfection. As shown in Figure 4-4, in some cells the fluorescence of mCherry-2A was distributed

throughout the cell nucleus and in others the protein seems to have caused degradation to the cell nucleus. pEGFP/pmCherry-3C gave few transfected cells (Figure 4-3). Expression of the protein again seemed to cause major change to the nucleus (Figure 4-5)

4.5 Transfection of HPeV-1 2A and 3C and 3C mutant

In order to study the effect of HPeV-1 2A and 3C, GMK cells were transfected with pmCherry fusions containing 2A and 3C. Results from cells transfected with pmCherry-3C show that the transfected nuclei are compressed, suggesting that HPeV-3C has an apoptotic effect (Figure 4-6). In order to study the possible apoptotic effect of HPeV-1 3C further, a protease negative mutant (with a cysteine to alanine change in the active site) was used. This had no obvious effect on the nuclei of transfected cells. Results were initially visualized with a BX41 fluorescent microscope (Figure 4-6). Slides were then visualized with a Nikon A1 si confocal microscope to obtain more detailed images. HPeV-1 mCherry-2A showed a fluorescence signal throughout the cytoplasm and nucleus with no obvious changes to the structure of the nucleus (Figure 4-7). The results also showed that the fluorescence of mCherry-3C was distributed in the cytoplasm of the cells, mainly in spots near the nucleus (Figure 4-8). The 3C mutant distribution was unlike the wild type. It was found throughout the cytoplasm, possibly associated with membranes or cytoskeleton. There was no significant change to the cell nucleus which suggests that the effect on the nucleus caused by the wild type 3C is due to the protease activity of 3C (Figure 4-9).

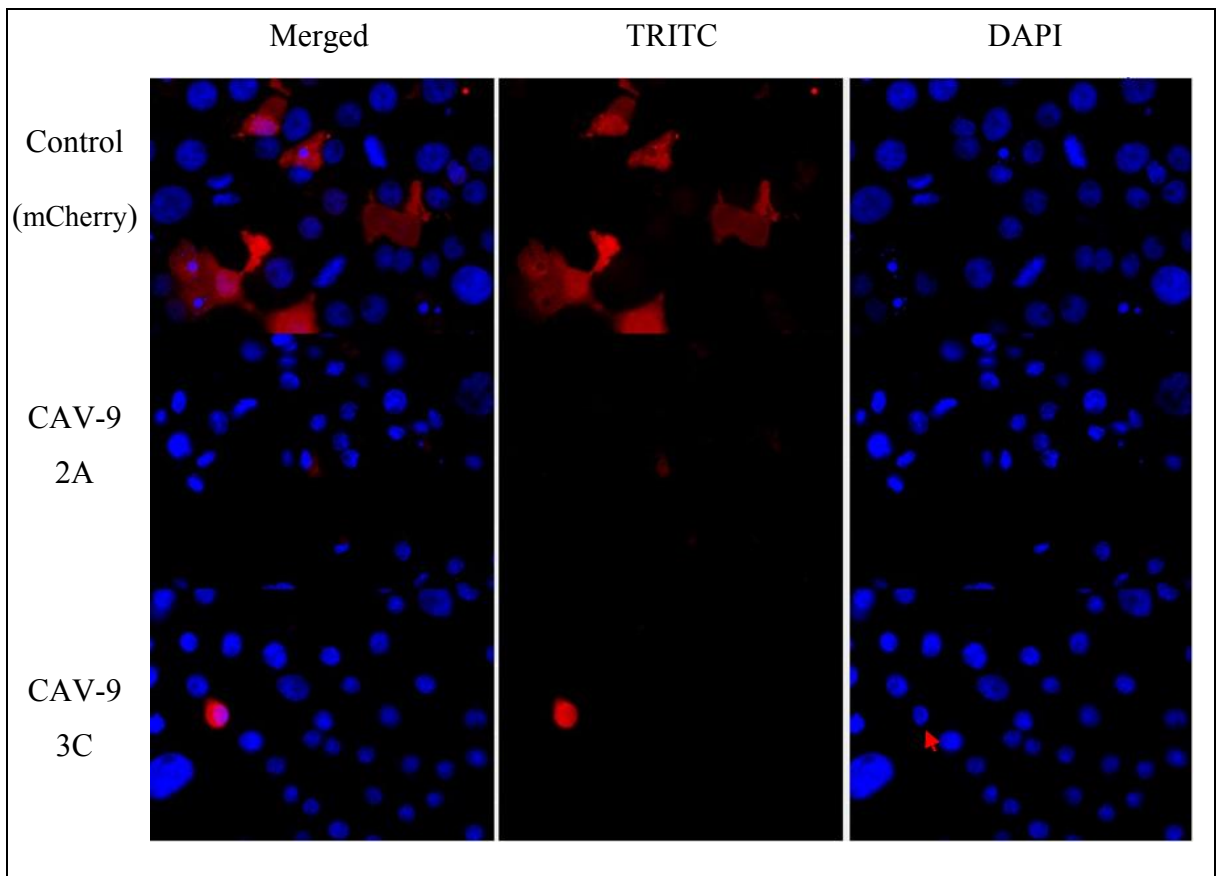


Figure 4-3 The effect of CAV-9 mCherry 2A and 3C on the cells. GMK cells were grown on cover slips and transfected with the mCherry fusion containing CAV-9 2A and 3C using lipofectin. 15 hr post transfection nuclei were stained with DAPI in the mounting medium. Images were visualized using a BX41 fluorescent microscope. Nuclei were observed in the blue channel (DAPI), and mCherry fusions in the red channel (TRITC). The nuclear morphology of transfected cells is different than in non transfected cells (red arrow).

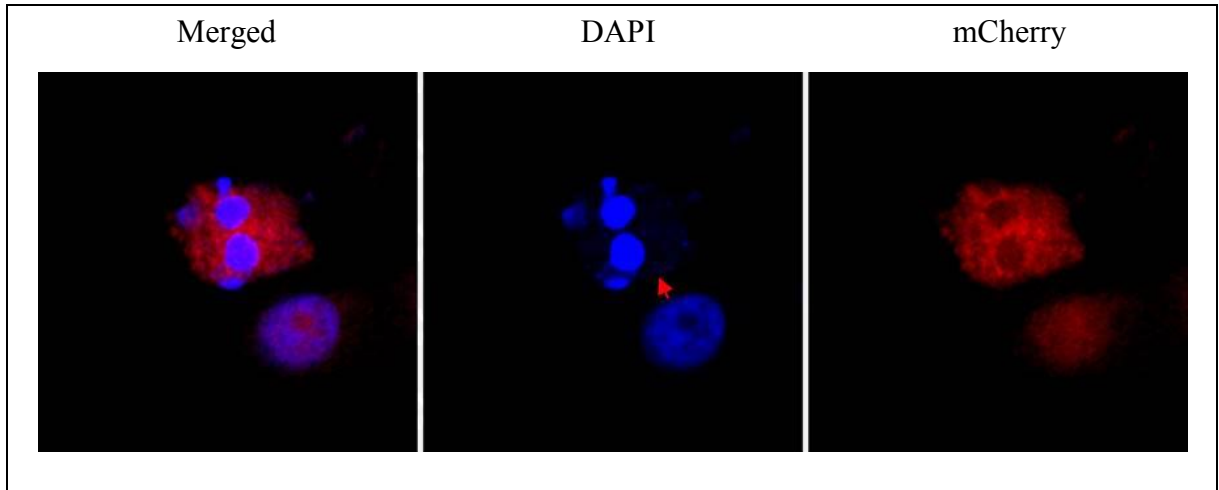


Figure 4-4 The effect of CAV-9 mCherry 2A on the cells. GMK cells were grown on cover slips and transfected with the pmCherry fusion containing CAV-9 2A using TurboFect. 48 hr post transfection nuclei were stained with DAPI in the mounting medium. Images were visualized using a Nikon A1si confocal microscope. Nuclei were observed in the blue channel (DAPI), and red channel (mCherry). The nuclear morphology of transfected cells is different than in non transfected cells (red arrow).

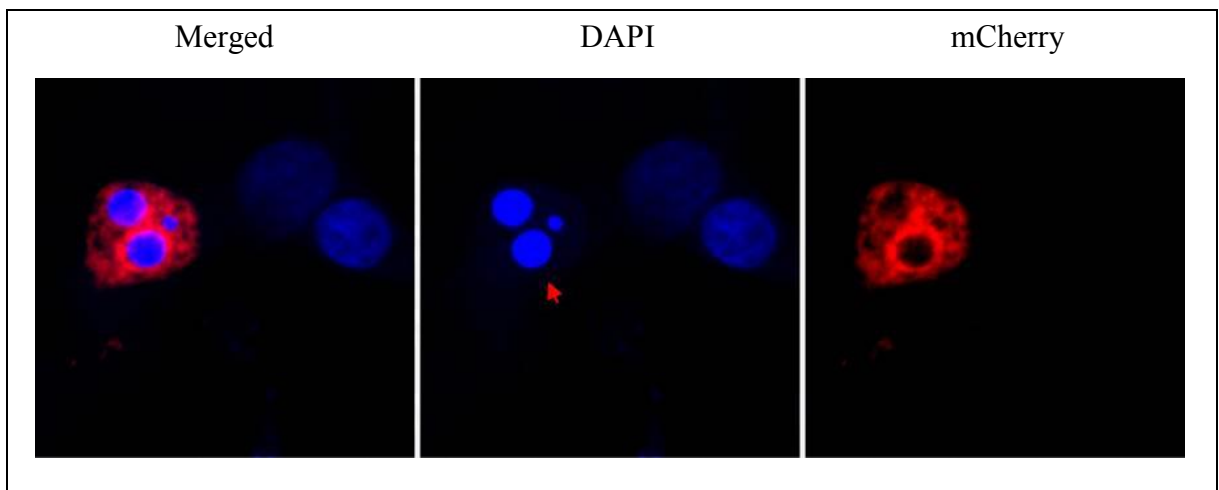


Figure 4-5 The effect of CAV-9 mCherry 3C on the cells. GMK cells were grown on cover slips and transfected with the pmCherry fusion containing CAV-9 3C using TurboFect. 48 hr post transfection nuclei were stained with DAPI in the mounting medium. Images were visualized using a Nikon A1si confocal microscope. Nuclei were observed in the blue channel (DAPI), and red channel (mCherry). The nuclear morphology of transfected cells is different than in non transfected cells (red arrow).

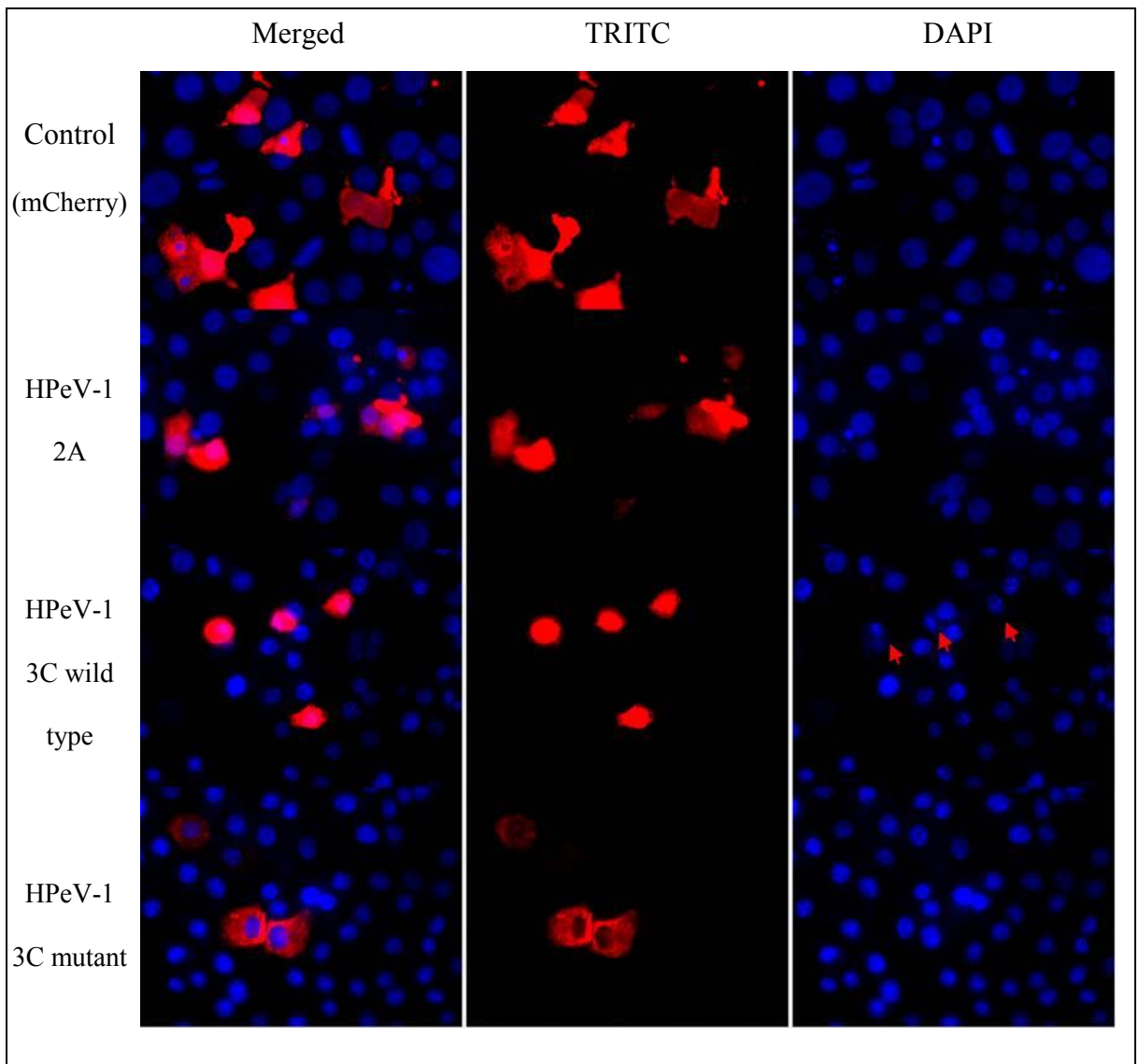


Figure 4-6 The effect of HPeV-1 mCherry 2A and 3C wild type and mutant on the cells. GMK cells were grown on cover slips and transfected with the pmCherry fusion containing HPeV-1 2A, 3CW and 3CM using lipofectin. 15 hr post transfection nuclei were stained with DAPI in the mounting medium. Images were visualized using a BX41 fluorescent microscope. Nuclei were observed in the blue channel (DAPI), and red channel (mCherry). The nuclear morphology of transfected cells is different than in non transfected cells (red arrows).

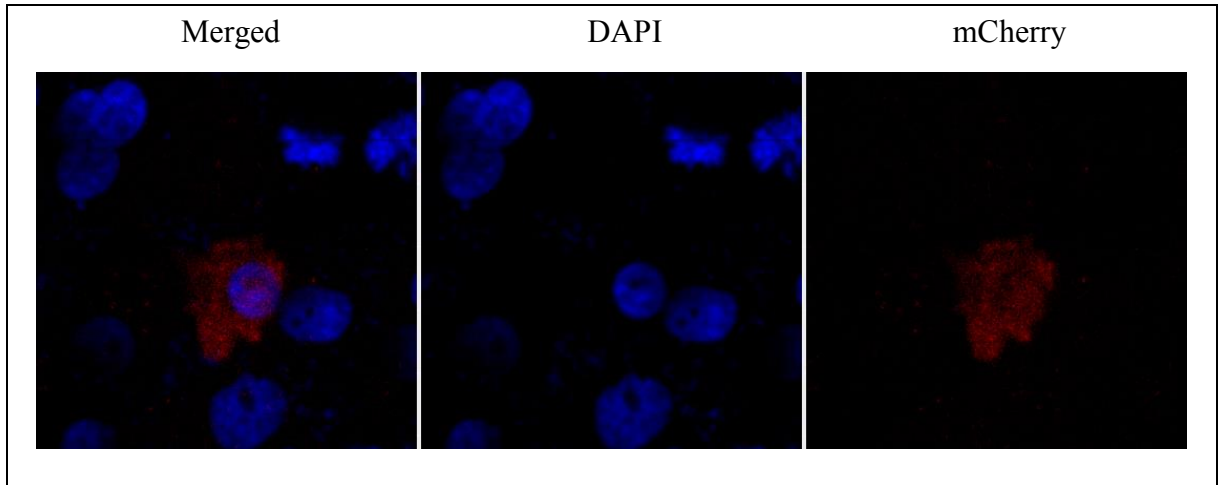


Figure 4-7 The effect of HPeV1 mCherry 2A wild type on the cells. GMK cells were grown on cover slips and transfected with the pmCherry fusion containing HPeV1 2A using TurboFect. 48 hr post transfection nuclei were stained with DAPI in the mounting medium. Images were visualized using a Nikon A1si confocal microscope. Nuclei were observed in the blue channel (DAPI), and red channel (mCherry).

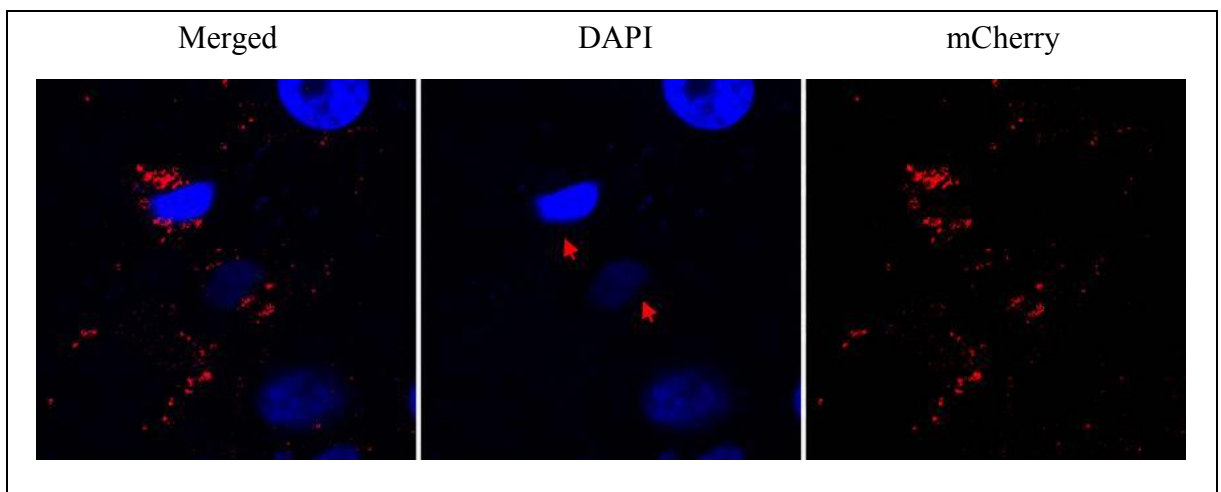


Figure 4-8 The effect of HPeV1 mCherry 3C wild type on the cells. GMK cells were grown on cover slips and transfected with the pmCherry fusion containing HPeV1 3C using TurboFect. 48 hr post transfection nuclei were stained with DAPI in the mounting medium. Images were visualized using a Nikon A1si confocal microscope. Nuclei were observed in the blue channel (DAPI), and red channel (mCherry). The nuclear morphology of transfected cells is different than in non transfected cells (red arrows).

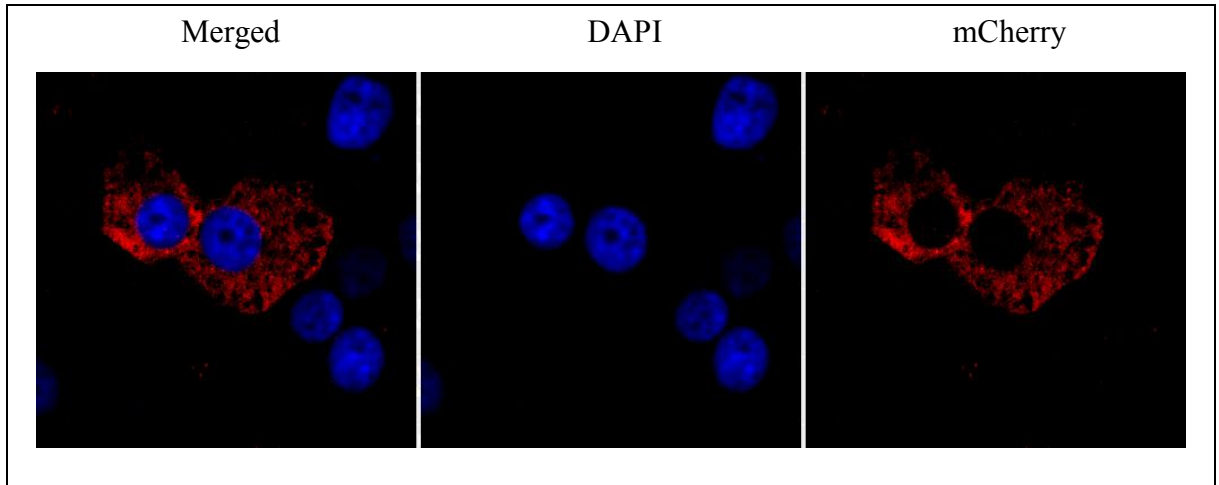


Figure 4-9 The effect of HPeV1 mCherry 3C mutant on the cells. GMK cells were grown on cover slips and transfected with the pmCherry fusion containing HPeV1 3C mutant using TurboFect. 48 hr post transfection nuclei were stained with DAPI in the mounting medium. Images were visualized using a Nikon A1si confocal microscope. Nuclei were observed in the blue channel (DAPI), and red channel (mCherry).

4.6 Cotransfection of CAV-9 and HPeV-1 2A and 3C with nuclear proteins

In order to study the effect of the virus on nuclear and nucleolar proteins, CAV-9 and HPeV-1 2A and 3C pmCherry fusion were cotransfected into GMK cells with pEGFP fusion containing (PSPC-1, PML, Nucleolin, Fibrillarin and B23). GMK cells were transfected with pmCherry 3C or 2A and pEGFP (PSPC-1, PML, Nucleolin, Fibrillarin and B23). Images were taken with Nikon A1 si confocal microscopy in 24hr post transfection.

For CAV-9 2A (time interval) no fluorescent cells were observed, and so the effect of this protein could not be studied (data not shown). There is no huge effect of CVA-9 3C on the distribution of any of the nuclear and nucleolar proteins (Figure 4-10). All remained within the nucleus.

HPeV-1 mCherry-2A also had little effect on the EGFP-B23, EGFP-PSPC-1, EGFP-PML, EGFP-Nucleolin or EGFP-Fibrillarin distributions (Figure 4-11). Finally, HPeV-3C was analysed. The results shown that both HPeV-1 mCherry-3C wild type and HPeV-1 mCherry-3C mutant have no effect on the distribution of most of the nuclear and nucleolus proteins (Figure 4-12 and Figure 4-13). However, EGFP-Nucleolin was redistributed throughout the cell in cells transfected with the wild type 3C construct. Surprisingly, the mCherry-3C mutant caused a huge redistribution of PML to the cytoplasm and also had some effect on fibrillarin. Cells transfected with mCherry-3C wild type show some changes in nucleus morphology.

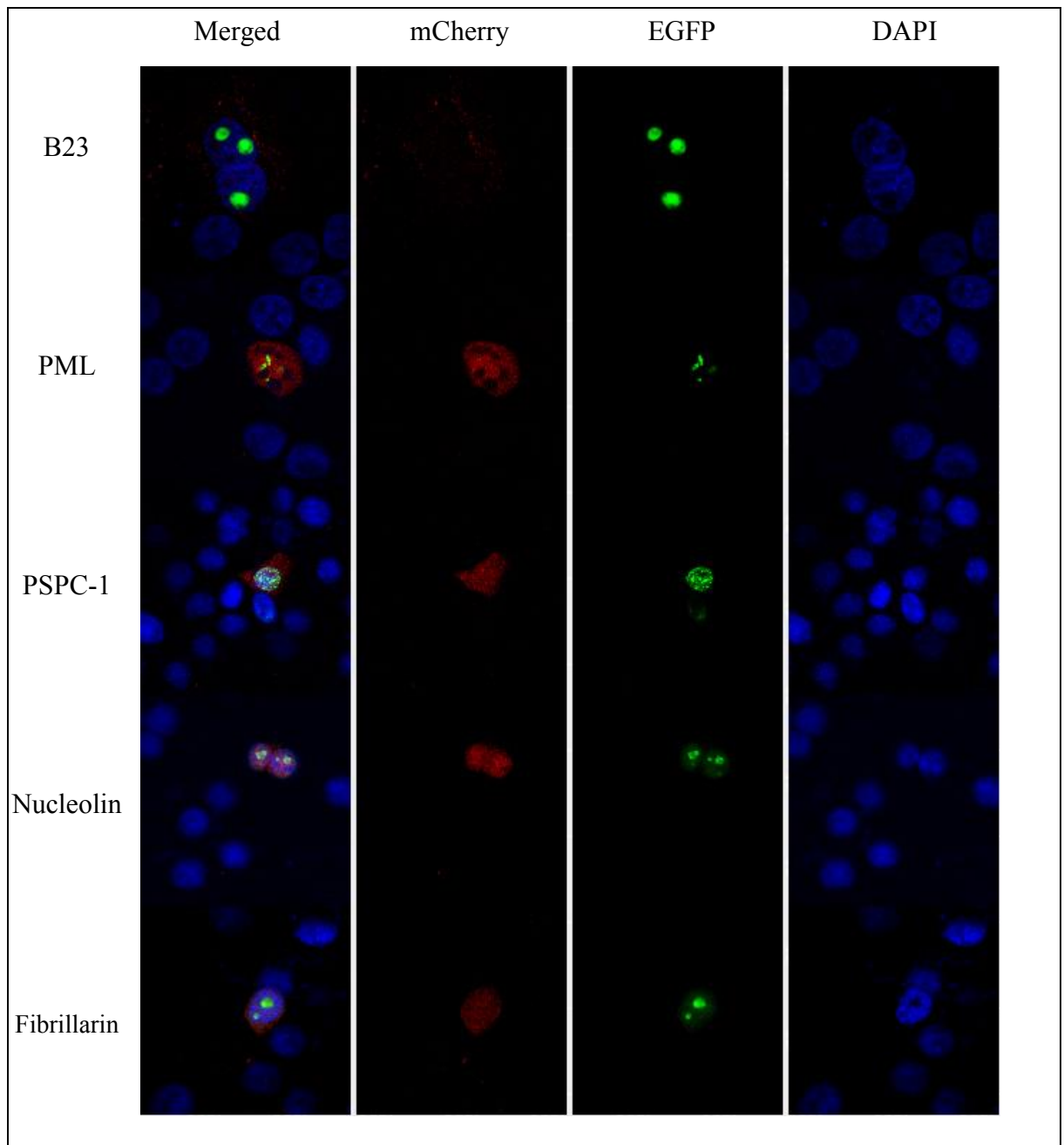


Figure 4-10 The Effect of CAV-9 mCherry 3C on nucleus and nucleolus proteins. GMK cells were grown on coverslips and cotransfected with DNA constructs fusions pEGFP containing (B23, PML, PSCP-1, Nucleolin and fibrillarin) and pmCherry fusion containing CAV-9 3C using TurboFect. 24 hr post transfection nuclei were stained with DAPI in the mounting medium. Images were visualized using a Nikon A1si confocal microscope. Nuclei were observed in the blue channel (DAPI), green channel (EGFP) and red channel (mCherry). The scale bars represent 20 μ m. Reading from the top the rows show EGFP-B23, EGFP-PML, EGFP-PSCP-1, EGFP-Nucleolin then EGFP-fibrillarin

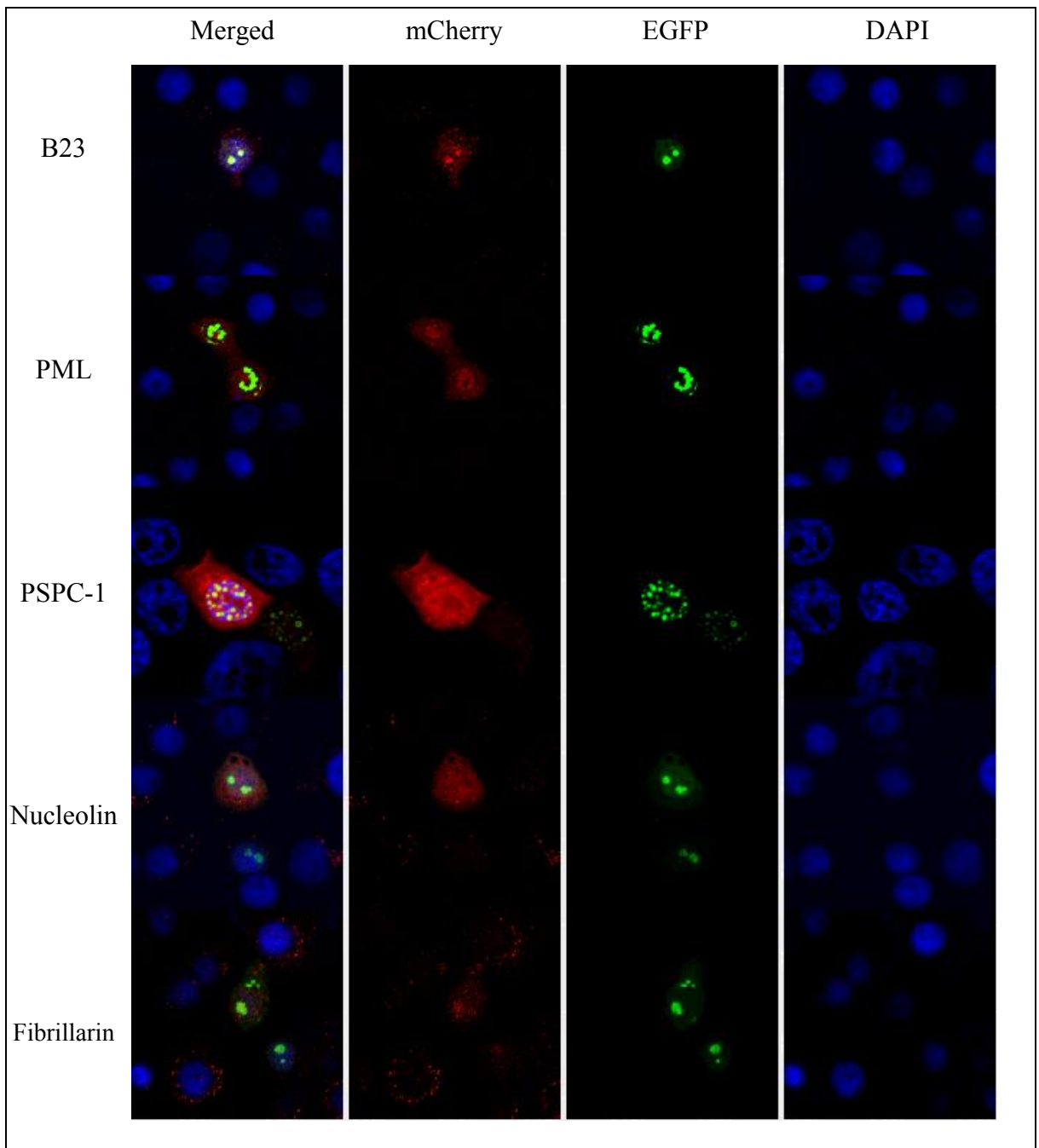


Figure 4-11 The Effect of HPeV-1 mCherry 2A on nucleus and nucleolus proteins. GMK cells were grown on coverslips and cotransfected with DNA constructs fusions pEGFP containing (B23, PML, PSPC-1, Nucleolin and fibrillarin) and pmCherry fusion containing HPeV-1 2A using TurboFect. 24 hr post transfection nuclei were stained with DAPI in the mounting medium. Images were visualized using a Nikon A1si confocal microscope. Nuclei were observed in the blue channel (DAPI), green channel (EGFP) and red channel (mCherry).

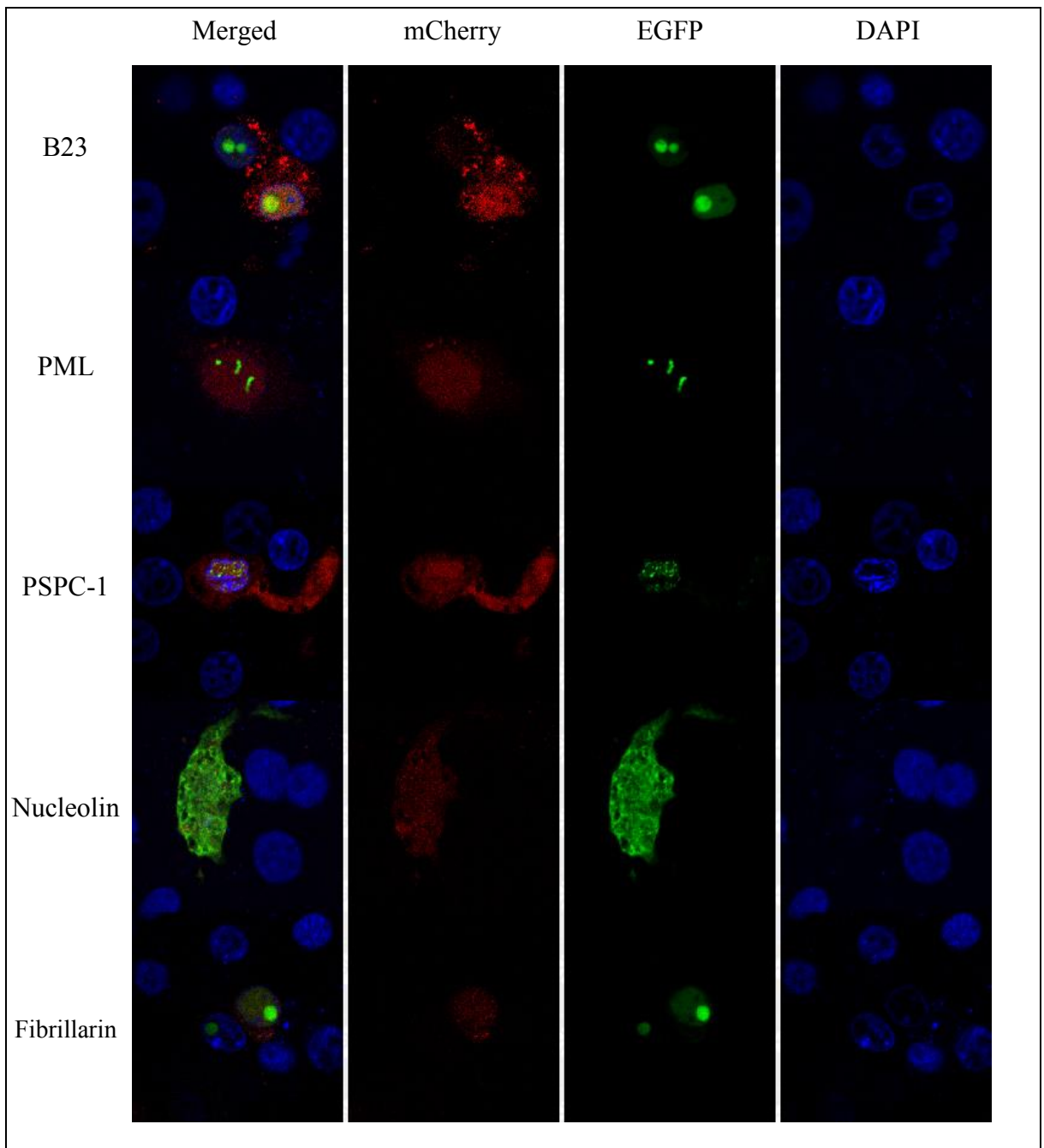


Figure 4-12 The Effect of HPeV-1 mCherry 3C Wild type on nucleus and nucleolus proteins. GMK cells were grown on coverslips and cotransfected with DNA constructs fusions pEGFP containing (B23, PML, PSPC-1, Nucleolin and fibrillarin) and pmCherry fusion containing HPeV-1 3C wild type using Turbofect. 24 hr post transfection nuclei were stained with DAPI in the mounting medium. Images were visualized using a Nikon A1si confocal microscope. Nuclei were observed in the blue channel (DAPI), green channel (EGFP) and red channel (mCherry).

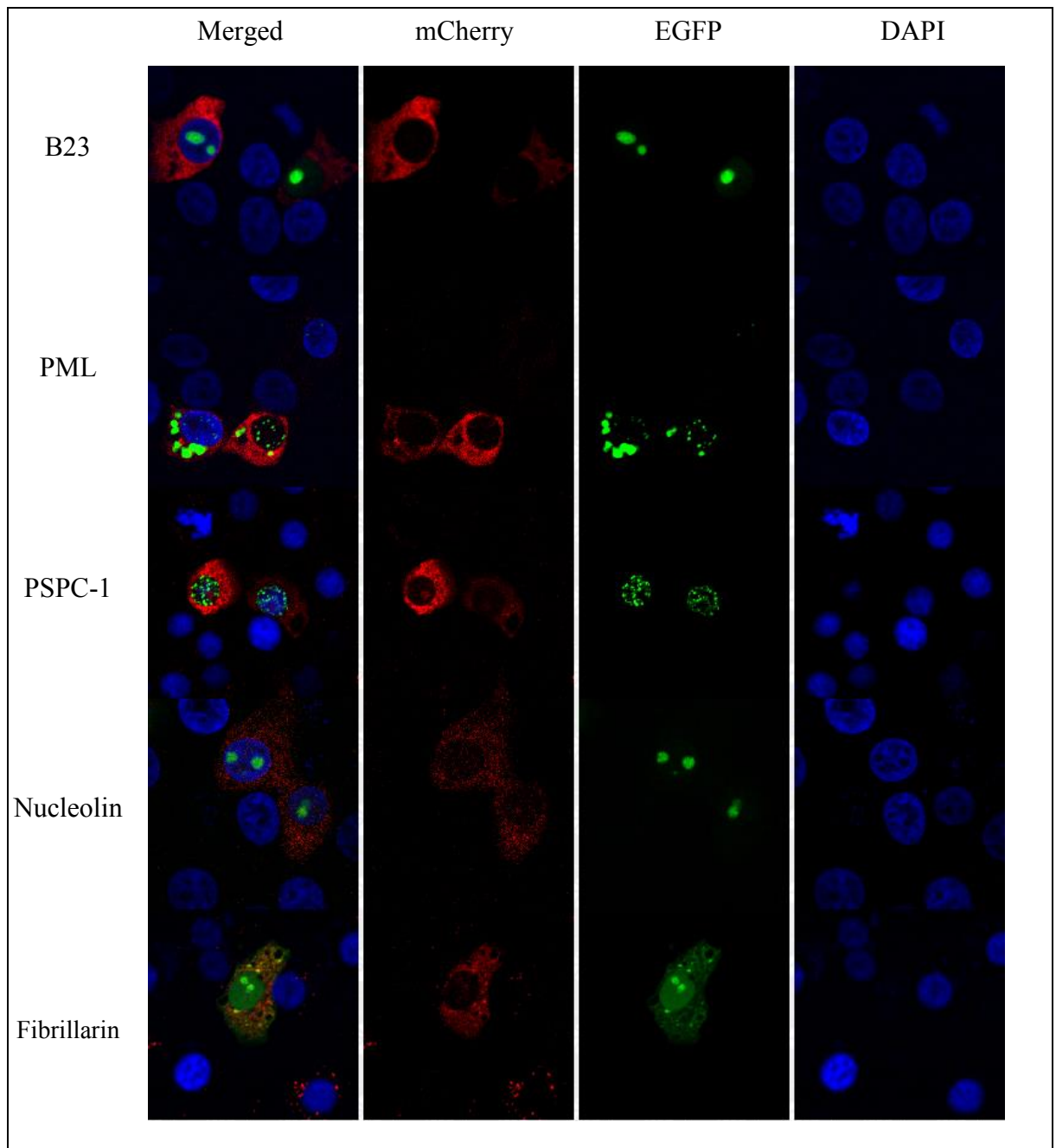


Figure 4-13 The Effect of HPeV-1 mCherry 3C mutant on nucleus and nucleolus proteins. GMK cells were grown on coverslips and cotransfected with DNA constructs fusions pEGFP containing (B23, PML, PSPC-1, Nucleolin and fibrillarin) and pmCherry fusion containing HPeV-1 3C mutant using TurboFect. 24 hr post transfection nuclei were stained with DAPI in the mounting medium. Images were visualized using a Nikon A1si confocal microscope. Nuclei were observed in the blue channel (DAPI), green channel (EGFP) and red channel (mCherry).

4.7 The effect of other HPeV-1 non structural protein on paraspeckles:

The proteins most affected by infection with CAV-9 were the paraspeckle proteins PSPC-1, NONO and PSF (chapter 3). None of the 2A or 3C constructs tested caused the same redistribution of PSPC-1 seen in infected cells. Different virus non-structural protein constructs were therefore cotransfected with pEGFP-PSPC-1.

GMK cells were co transfected with pmCherry constructs encoding HPeV-1 2B, 2C, 3A together with pEGFP-PSPC-1 and images were visualised with a BX41 fluorescent microscope (Figure 4-14). The results shown that HPeV-1 mCherry-2B changed the distribution of EGFP-PSPC-1. The EGFP-PSPC-1 was redistributed into two clusters in the nucleus, with smaller punctate structures diffused throughout the nucleus. These clusters corresponded with areas of the nucleus not stained with DAPI, presumably nucleoli. HPeV-1 mCherry 2C and 3A caused some redistribution of EGFP-PSPC-1 into clusters, but this was less clear than mCherry-2B.

For 3D only an EGFP-3D construct was available and this was used with mCherry-PSPC-1 (Figure 4-15). Results showed that there is no obvious change in the PSPC-1 protein distribution and the protein is still in the nucleus.

4.8 The effect of other CAV-9 non structural protein on paraspeckles:

The same experiment was done with several CAV-9 non-structural protein constructs (Figure 4-16). There was no huge change in the EGFP-PSPC-1 when cotransfected with CAV-9 2BC, but the protein was redistributed in the nucleus when cotransfected with CAV-9 2C as the protein was diffused throughout the nucleus with few small punctate structures. EGFP-PSPC-1 was redistributed in the nucleus into two clusters when cotransfected with CAV-9 pmCherry-3A. The distribution is very similar to that seen when HPeV-1 pmCherry-2B was used (Figure 4-14)

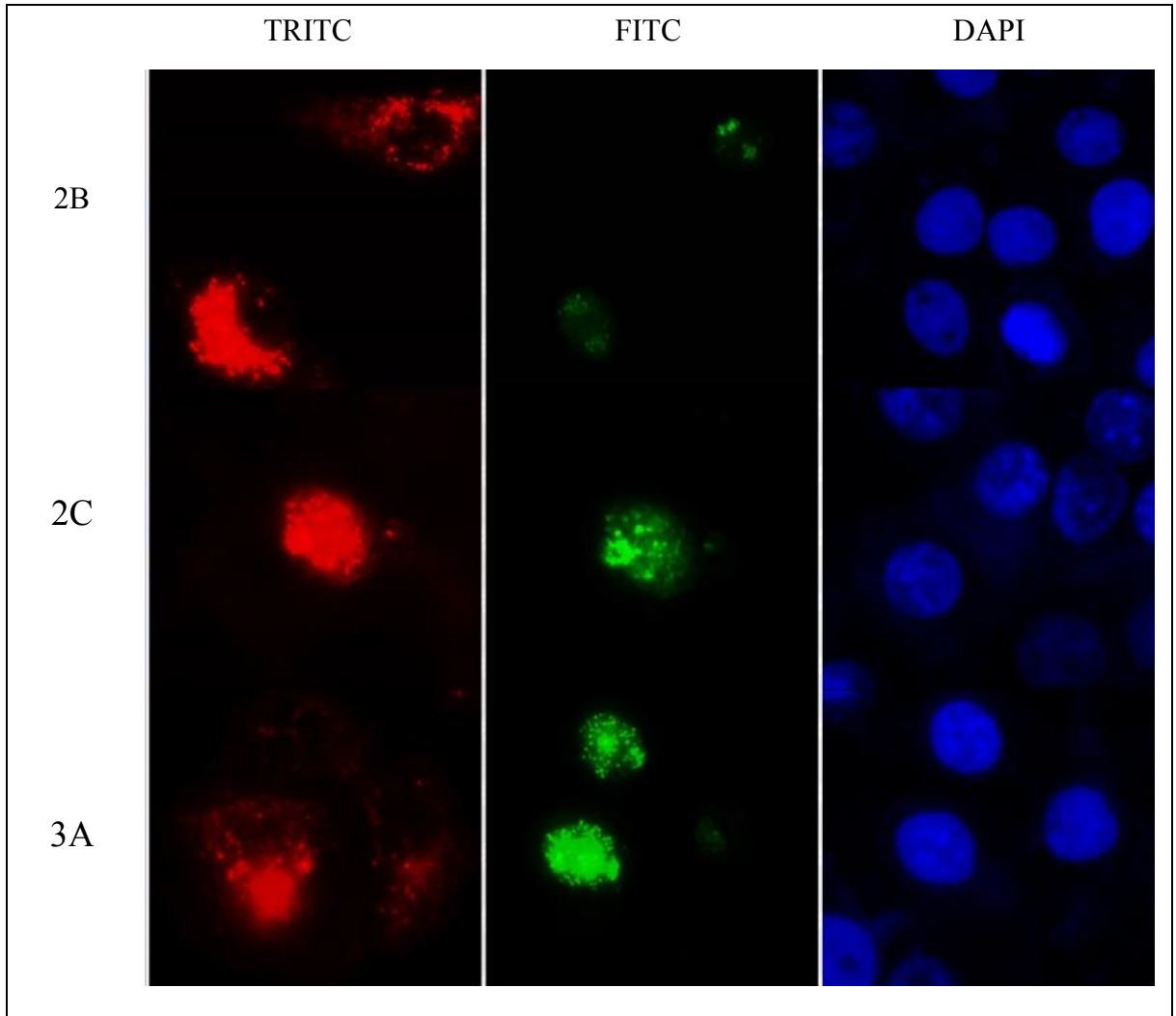


Figure 4-14 The Effect of HPeV-1 non-structural protein on EGFP-PSPC-1 distribution. GMK cells were grown on coverslips and cotransfected with HPeV-1 non-structural proteins fusions in pmCherry containing (2B, 2C and 3A) and pEGFP fusion containing PSPC-1 using lipofectin. 15 hr post transfection nuclei were stained with DAPI in the mounting medium. Images were visualized using a BX41 fluorescent microscope. Nuclei were observed in the DAPI filter, EGFP-PSPC-1 in FITC filter and mCherry (2B, 2C and 2A) in TRITC filter.

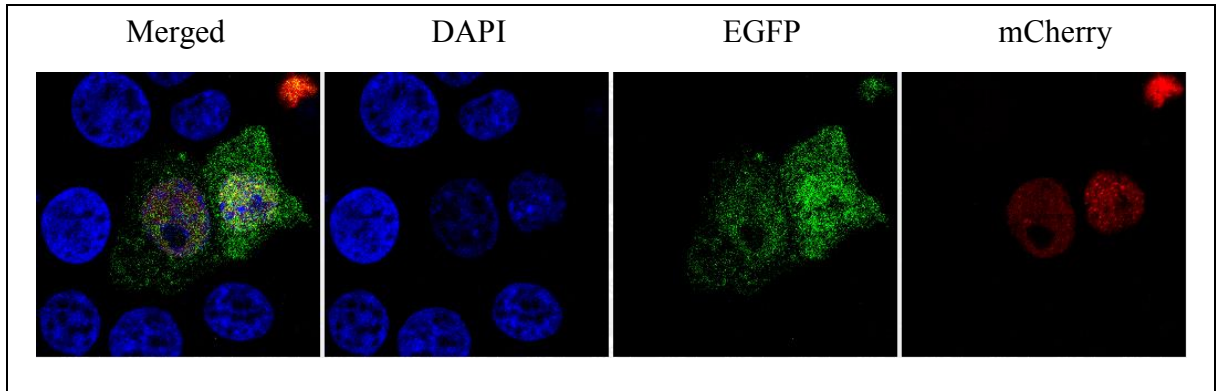


Figure 4-15 The Effect of HPeV-1 3D on mCherry-PSPC-1 distribution. GMK cells were grown on coverslips and cotransfected with HPeV-1 pEGFP 3D and pmCherry-PSPC-1 using lipofectin. 15 hr post transfection nuclei were stained with DAPI in the mounting medium. Images were visualized using a Nikon A1 si confocal microscope. Nuclei were observed in the blue channel (DAPI), green channel (EGFP) and red channel (mCherry).

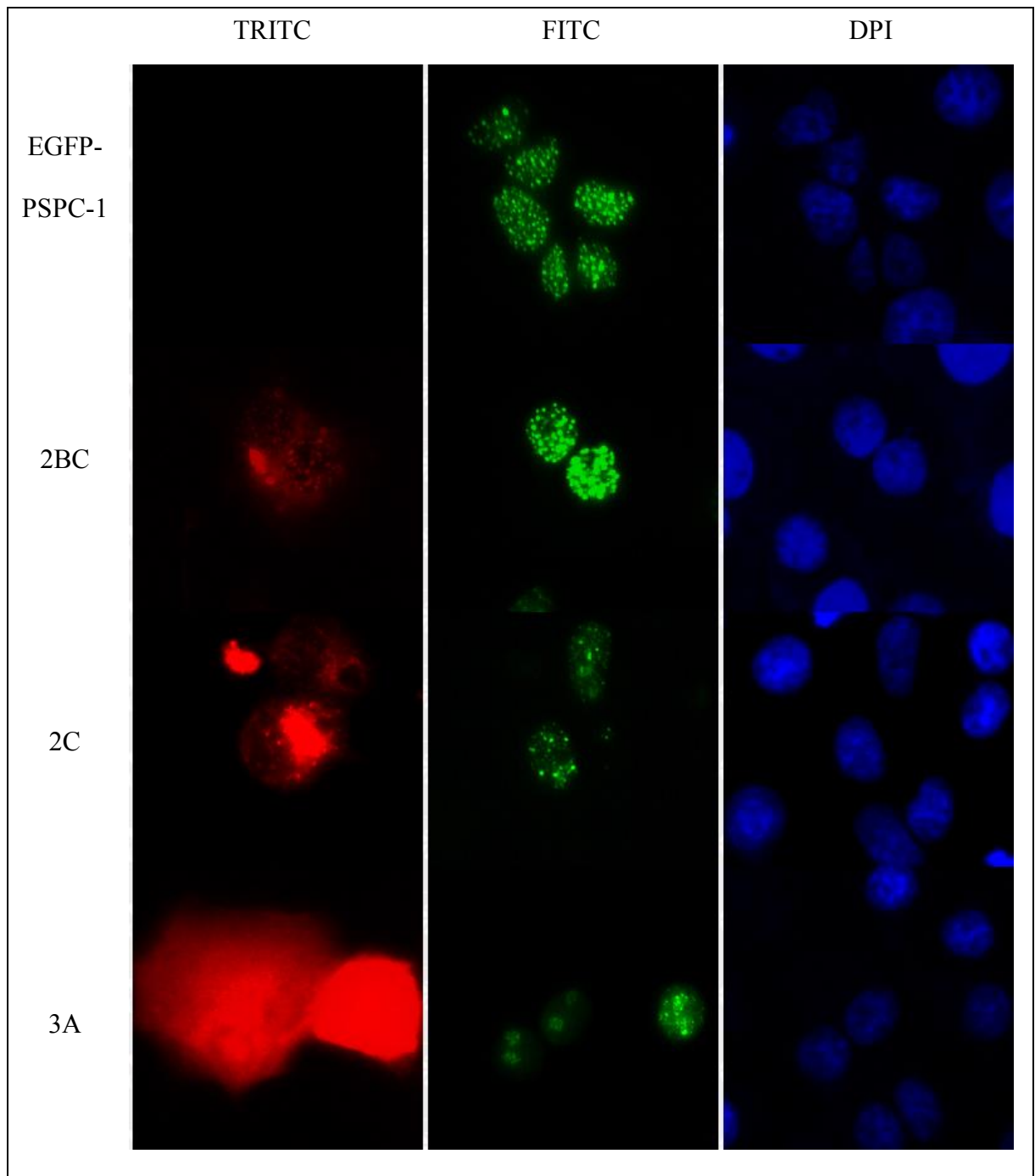


Figure 4-16 The Effect of CAV-9 non structural proteins on EGFP-PSPC-1 distribution. GMK cells were grown on cover slip then co transfected, using lipofectin, with the DNA construct of EGFP-PSPC-1 and mCherry CAV-9 2BC, 2C and 3A After 48 hr nucleus were stained by Hoechst, cells were mounted using Mowoil mounting medium and were visualized using a BX41 microscope. Nuclei were observed using a blue (DAPI) filter, EGFP-PSPC-1 using a green (FITC) filter and mCherry CAV-9 (2BC, 2C and 3A) using red (TRITC) filter.

4.9 Discussion

To investigate whether the redistribution of nuclear proteins, particularly paraspeckle proteins, caused by CAV-9 infection (chapter 3) is due to the effect of the proteases 3C^{pro} and 2A^{pro}, EGFP/mCherry fusion constructs of these proteins were produced for cotransfections (Figure 4-1). The same proteins from HPeV-1 were also studied (Figure 4-2). It was found that CAV-9 3C^{pro} and 2A^{pro}, and HPeV-1 3C^{pro} caused nuclear degradation, as the nuclei in transfected cells appeared to be more compressed or fragmented than those in non-transfected cells (Figure 4-3 to Figure 4-9). This degradation could be due to the toxic effect of over-expressing these proteolytic enzymes, which leads to apoptosis. It has been found that PV 2A^{pro} expression causes apoptotic cell death as does the expression of EV71 2A^{pro} (Kuo et al., 2002). As we found for CAV-9 2A^{pro}, expression of GFP-2A in transfected cells led to condensed or fragmented nuclei. The authors concluded that these findings indicated that enterovirus 2A^{pro} plays an important role in eliciting the apoptotic features seen when cells are infected. It is known that 2A^{pro} cleaves host cells proteins such as eIF4G1 which plays a key role in cap dependent translation and it has been proposed that the shut off of cap-dependent translation is a major phase of apoptosis that leads to rapid cell death (Kuo et al., 2002). As CAV-9 is an enterovirus, it is likely that its 2A^{pro} has a similar effect and that is the why we observed the nuclear changes in the few transfected cells that could be found (Figure 4-4). It is also likely that more transfected cells were not seen as these were killed by the expressed 2A^{pro}.

It has also been shown that other viral proteins can contribute to apoptosis, such as 3C^{pro} of many enteroviruses, including PV 3C^{pro} that activates the caspase which results in killing of cells by apoptosis, and CVB-3 3C^{pro} that also induces cell death by activating caspases (Barco et al., 2000, Carthy et al., 1998). A previous study by Li et al. (2002) demonstrated that EV71 3C^{pro} proteolytic activity is also involved in caspase dependent apoptosis. The authors also altered two amino acids of the catalytic triad by changing the C146 and H39 to G. The mutant 3C did not only lose the protease activity, but the apoptosis-inducing effect was also lost. When cells were transfected with EV71 3C a number of alteration in cellular morphology were observed when cells were transfected with wild type 3C, whereas there was no change observed when cells were transfected with the mutant 3C (Li et al., 2002). These findings give clear evidence that the enterovirus 3C^{pro} plays a major role in inducing cell apoptosis. CAV-9 is closely related to CBV-3 as they belong to the same species (Enterovirus B) and it is likely the CAV-9 3C^{pro} will have a similar effect on cells (Figure 4-5).

The HPeV-1 3C^{pro} has not been studied previously and since this belongs to a different picornavirus genus (*Parechovirus*) from the *Enterovirus* genus where most work has been done, it could have a different effect. However, in our work when GMK cells were transfected with HPeV-1 mCherry-3C, the results again showed some damaged nuclei in transfected cells (Figure 4-6 and Figure 4-8). To investigate this further, a mutant version of HPeV-1 mCherry-3C was constructed by changing the cysteine of the active site motif (GXCG) to alanine. There were no significant changes to the nuclei in cells transfected with the mCherry-3C mutant, unlike the wild type construct (Figure 4-6 and Figure 4-9).

Although apoptosis was not studied directly, this finding probably means that HPeV-1 3C^{pro} has an apoptotic effect on cells particles due to its protease activity, while the mutant 3C lost the apoptotic effect as it has not protease activity.

The HPeV-1 2A is not a protease and its function is not yet known (Hughes and Stanway, 2000). It had no clear effect on the nucleus in transfected cells (Figure 4-7) and so probably does not cause apoptosis.

The constructs were made to investigate if virus proteases are involved in the relocalization of proteins seen during virus infection (Chapter 3). There was no similar effect of the expression of protease proteins on the nuclear and nucleolus proteins as seen in the infected cells. CAV-9 infection causes a major change in paraspeckle proteins distribution by translocating the proteins from the nucleus to the cytoplasm. In cells transfected with CAV-9 3C^{pro}, the PSPC-1 was still in the damaged nucleus (Figure 4-10) and it can be concluded that the 3C^{pro} itself may not be able to cause the relocalization of the protein.

On the other hand, CAV-9 2A^{pro} did not give visual results as no cotransfected cells could be found. So, it is still possible that the relocalization could be due to this protein. Attempts to inhibit the 2A^{pro} activity to allow enough expression of the nuclear protein for detection, by treating it with the drug PTDC, were unsuccessful. Studies showed that the PTDC is an antiviral compound that inhibits the replication of some enteroviruses and influenza virus. The drug did not interfere with the receptor binding or internalization by receptor mediated endocytosis, but it inhibits the viral polyprotein processing which results in inhibition of viral replication (Krenn et al., 2005). The drug is

metal binding compound and a number of viral processes, particularly 2A^{pro} activity in enteroviruses, are influenced by various metal binding function of PTDC as part of the antiviral effects. Another attempt to reduce the expression of CAV-9 2A^{pro} was also tried by using dilutions of the CAV-9 2A^{pro} constructs, but again no results were obtained. It may be useful to use an inducible system, e.g. Tet on/Tet off and turn on the 2A^{pro} expression after enough of the EGFP/nuclear protein fusions has been produced.

There was no effect seen of the expression of HPeV-1 2A on EGFP/nuclear protein fusions (Figure 4-11). For HPeV-1 3C there was a large change to nucleolin distribution (Figure 4-12). A previous study (Mutabagani, 2012) showed that HPeV-1 virus infection caused a redistribution of PSpC-1 in the nucleus. This was much less clear than the redistribution out of the nucleus caused by CAV-9 infection. There was some change to PSpC-1 distribution within the nucleus caused by expression of HPeV1 mCherry-3C (Figure 4-12), but as transfected cells had damaged nuclei it is not clear if 3C expression is a specific cause of PSpC-1 relocalization.

Surprisingly, HPeV-1 3C mutant caused a translocation of EGFP-PML from the nucleus to the cytoplasm (Figure 4-13). The PML gene is located on chromosome 15 and consists of 9 exons (Carracedo et al., 2011, Salomoni and Bellodi, 2007). The NLS which is located in exon 6 of PML isoforms restricts the majority of PML localization to the nucleus. However, PML transcripts undergo a number of alternative splicings which gives several nuclear and cytoplasmic isoforms. The NES located in exon 9 of the C terminal of PML1 allows the protein to shuttle between the nucleus and cytoplasm. It has been suggested that the expression of PML isoform 1 may correlate with the

transformation status of the cell, while PML isoform VII lacks the NLS and is mainly cytoplasmic PML (Carracedo et al., 2011, Salomoni and Bellodi, 2007). This suggested that the relocalization of the PML could be due to changes in splicing, as the mutant has no protease activity and so should not be able to cleave PML.

Mutant mCherry-3C showed a localization in the cytoplasm, unlike the wild type proteolytic protein, which mainly distributed in the nucleus (Figure 4-9 and Figure 4-13). As these fusion proteins are both small enough to diffuse into the nucleus, the mutant either has a definite cytoplasmic localization e.g. bound to membranes or the cytoskeleton, or contains a NES. The distribution of the mutant 3C suggests that it is localized in structures in the cytoplasm, rather than being evenly distributed in a soluble form. It may be that 3C has other functions in the infected cells as well as protease activity. It might be useful to perform co-immunoprecipitation followed by mass spectrometry, using the mutant 3C, in order to identify the proteins that 3C binds to, which might help in studying the other function of the protein.

It is known that PML, as well as being a mainly nuclear protein involved in transcription, is a regulator of apoptosis and can be found in the endoplasmic reticulum and mitochondria-associated membranes in stressed cells (Giorgi et al., 2010). Over expression of the mutant 3C or binding to cellular proteins could cause stress and lead to the change in PML distribution from the nucleus to the cytoplasm.

As there was no clear effect of the 2A and 3C fusion constructs on PSPC-1 distribution, the effects of fusions of other non-structural proteins from both CAV-9 and HPeV-1 were analysed (Figure 4-14 - Figure 4-16). None gave the same changes as seen when

cells are infected with CAV-9, but some of the proteins had an unexpected effect on PSpC-1 distribution. CAV-9 2B and HPeV-1 3A fusions caused the PSpC-1 to relocalise within the nucleus, to structures which were probably nucleoli. The distribution of PSpC-1 and also NONO within the nucleus is cell cycle dependent and during telophase these proteins are present in peri-nucleolar caps (Fox et al., 2005). These are structures around the edge of the nucleoli and PSpC-1/NONO are also found in these structures when transcription is prevented. The paraspeckle protein PSF is redistributed to spots near to the nucleoli when cells are blocked at G1/S, possibly due to phosphorylation allowing binding to different protein partners (Shav-Tal et al., 2001). It is possible that expression of CAV-9 2B and HPeV-1 3A may lead to a cell cycle block and this would be an interesting area for study in the future.

Chapter 5
Paraspeckle Proteins Mutation and
Translocation

5.1 Introduction

The only clear effect of CAV-9 infection on nuclear proteins seen in the work described in Chapter 3 was on several nuclear paraspeckle proteins. Paraspeckles are found in close proximity to nuclear speckles as a variable number of foci enriched in characteristic RNA binding proteins (Naganuma et al., 2012). The 3 paraspeckle proteins studied in Chapter 3 (PSPC-1, NONO/p54nrb and SFPQ/PSF) belong to the *Drosophila melanogaster* behaviour and human splicing (DBHS) protein family and are believed to be the key proteins involved in paraspeckle formation (Fox and Lamond, 2010). All these DBHS proteins are localised mainly in the nucleus and bind to RNA and DNA and it has been found that they are involved in number of nucleus process such as transcriptional regulation, RNA processing and DNA repair (Fox and Lamond, 2010). It also has been found that an abundant long noncoding RNA (lnc-RNA), the nuclear paraspeckles assembly transcript 1 (NEAT1), is localised to paraspeckles and forms an essential structural component (Hirose *et al.*, 2014). PSF and NONO bind directly to NEAT-1 and PSPC-1, NONO and PSF also interact with one another (Gao et al., 2014).

There is little information on the effect of virus infection on nuclear paraspeckles, but it has been suggested that viral (herpes simplex virus and influenza virus) infection or poly I:C treatment induces NEAT-1 expression, and this lnc-RNA then binds to PSF and causes the relocation of the protein within the nucleus, from the IL8 promoter to the paraspeckles, in order to activate the IL8 antiviral factor (Imamura *et al.*, 2014). HIV-1 infection is enhanced by paraspeckles (Zhang et al., 2013). There are no reports of DBHS proteins being relocated to cytoplasmic structures similar to those seen following CAV-9

infection, but phosphorylation and sumoylation has been associated with changes in distribution within the nucleus and from the nucleus to the cytoplasm (Wilson and Anderson, 2009). Virus infection induces or manipulates structures such as stress granules, P-bodies and autophagosomes, and replication of positive sense RNA viruses, including picornaviruses, requires the generation of replication complexes (Reineke and Lloyd, 2013, Chiramel et al., 2013, den Boon et al., 2010).

The aim of the work described in this chapter is the definition of regions of the DBHS proteins needed for relocalisation during CAV-9 infection and the identification of the cytoplasmic structures where the proteins are found in infected cells.

5.2 Approach

A number of DNA constructs were obtained which encode fusions of the paraspeckle proteins under test fused to EGFP/EYFP/mCherry (Table 2-2). Cells were co-transfected with DNA constructs which encode marker proteins of cellular structures fused to EGFP/EYFP/ERFP (Table 2-2) and were examined by confocal microscopy. Some cell proteins were identified using antibodies (Table 2-1).

5.3 PSPC-1 truncations at predicted 3C^{pro} cleavage sites

Although no clear effect of virus proteases on the location of DBHS proteins was shown in Chapter 4, as picornavirus proteases have been shown to be involved in the relocalisation of other nuclear proteins, we examined the effect of truncating one of the DBHS proteins (PSPC-1) at possible virus protease recognition sites (Cathcart et al.,

2013). A weblogo of the 3C^{pro}/3CD^{pro} cleavage sites predicted for CAV-9 Griggs is shown in Figure 5-1. It can be seen that there is a strong preference for the sequence AXXQ↓G (cleavage between Q and G). The PSPC-1 sequence was scanned to identify if this sequence occurs and the motif was found at position 413-417 (AGNQ↓G) and partially at position 175-179 (AFSQ↓F). Two truncated PSPC-1 mutants were produced, each truncated at one of these sites. Primers OL2177, OL2178 and OL2179 (Table 2-3) were designed and PCR was performed using PSPC-1 as DNA template. PCR products were then purified and ligated into pGEM-T easy vector. After sequence confirmation, the inserted were ligated into pEGFP-C1 in order to obtain pEGFP-PSPC-1 fragment 1 (contains PSPC positions 1-178) and pEGFP-PSPC-1 fragment 2 (PSPC-1 positions 1-416) (Figure 5-2).

GMK cells were transfected with these fusion constructs. Cells were then fixed and nuclei were stained with DAPI included in mounting media. Slides were then visualized with a BX41 fluorescent microscope. The results (Figure 5-3) showed that EGFP-PSPC-1 fragment 1 protein distribution was different from the EGFP-PSPC-1 wild type distribution in non-infected cells. It was more similar to the distribution of EYFP protein used as a control, as the fluorescent was throughout the nucleus and the cytoplasm. EGFP-PSPC-1 fragment 2 showed a typical paraspeckles distribution, as the protein was distributed in the nucleus showing the speckled structures with only a small amount of protein in the cytoplasm.

In another experiment, 24 hours after transfection cells were infected with CAV-9 for 8 hr then fixed, immunostained and mounted on glass slides (Figure 5-4). Results were visualized with a Nikon A1plus wide field microscope. No cells were found to be both

infected and transfected with EGFP-PSPC-1 fragment-1. In infected cells EGFP-PSPC-1 fragment 2 was mainly redistributed into the cytoplasm in punctate structures. The relocalisation was similar to that seen for EGFP-PSPC-1.

If cleavage of EGFP-PSPC-1 is enough to relocalise the protein to the cytoplasmic structures, it would be expected that one of the truncated proteins would be found in these structures in uninfected cells. This was not seen, and so possibly the predicted cleavage sites are not correct or the cytoplasmic structures are only present in infected cells. EGFP-PSPC-1 fragment 2 behaves similarly to the wild type protein, which suggests that the region deleted is not necessary for paraspeckle localization or for the redistribution in infected cells. EFPF-PSPC-1 fragment 1 contains much less of the full PSPC-1 and nuclear/paraspeckle distribution is completely lost. No infected/transfected cells could be found and so it is not known if there is enough of the protein to allow it to distribute into the cytoplasmic structures.

In order to find if there is any proteolytic cleavage of PSPC-1 or PSF during infection, a Western blot was performed. GMK cells were infected for 0, 2 and 8 hr with CAV-9, protein extracts were made, and equal amounts of protein were analysed run on an acrylamide gel and blotted (protein determination and western blot was performed by Andrea Moher and her team). The results show that there is an up-regulation of both proteins after 2 hours, but the levels decrease after 8 hours (Figure 5-5).

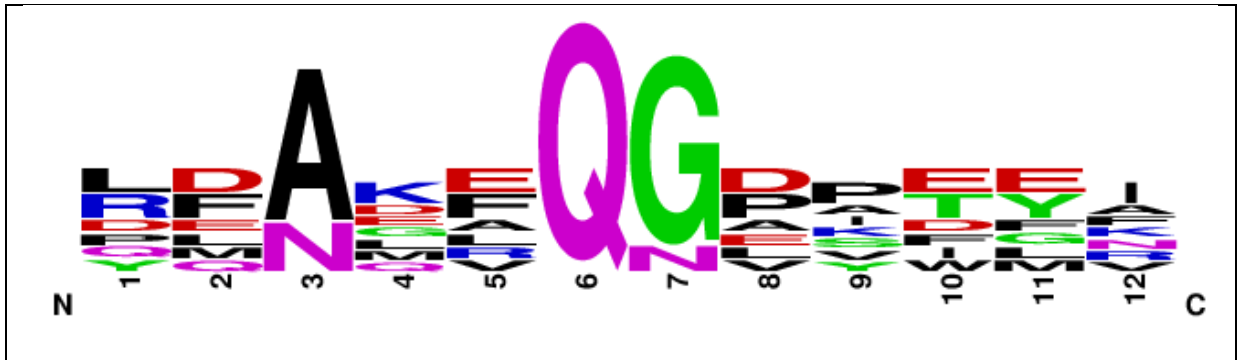


Figure 5-1 Weblogo of the sites believed to be cleaved by 3C/3CD in the CAV-9 Griggs polyprotein.(Chang et al., 1989). 6 amino acids (positions 1-12) N-terminal (N) or C-terminal (C) of the predicted cleavage site (marked with an arrow) are shown and the size of the letter is proportional to the number of times that amino acid occurs at the position shown. The weblogo was created using the on-line tool at the University of Berkley (<http://weblogo.berkeley.edu/logo.cgi>).

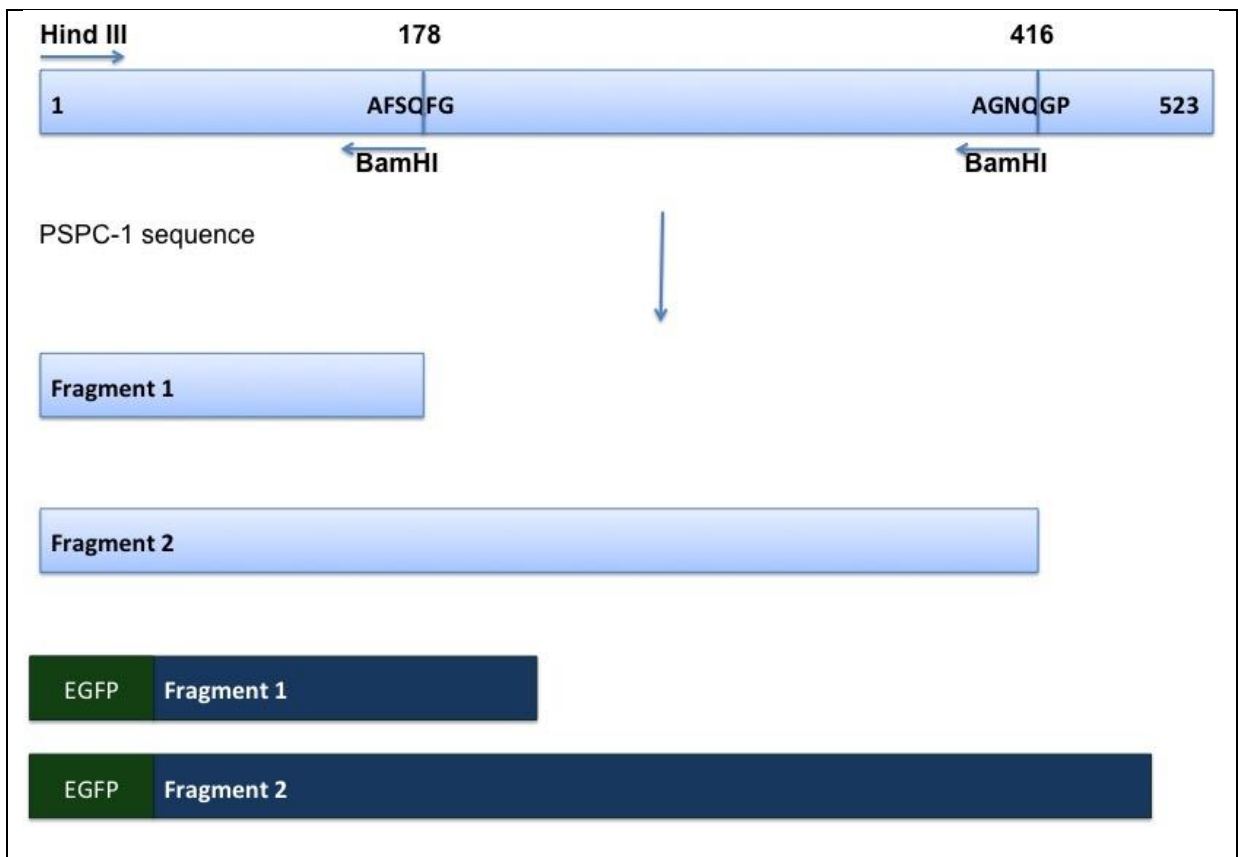


Figure 5-2 Schematic diagram for truncated PSpC-1.Illustrating the PCR truncations of the region encoding PSpC-1 protein at the predicted 3C^{pro}/3CD^{pro} cleavage sites. The structures of the EGFP fusion proteins are also shown.

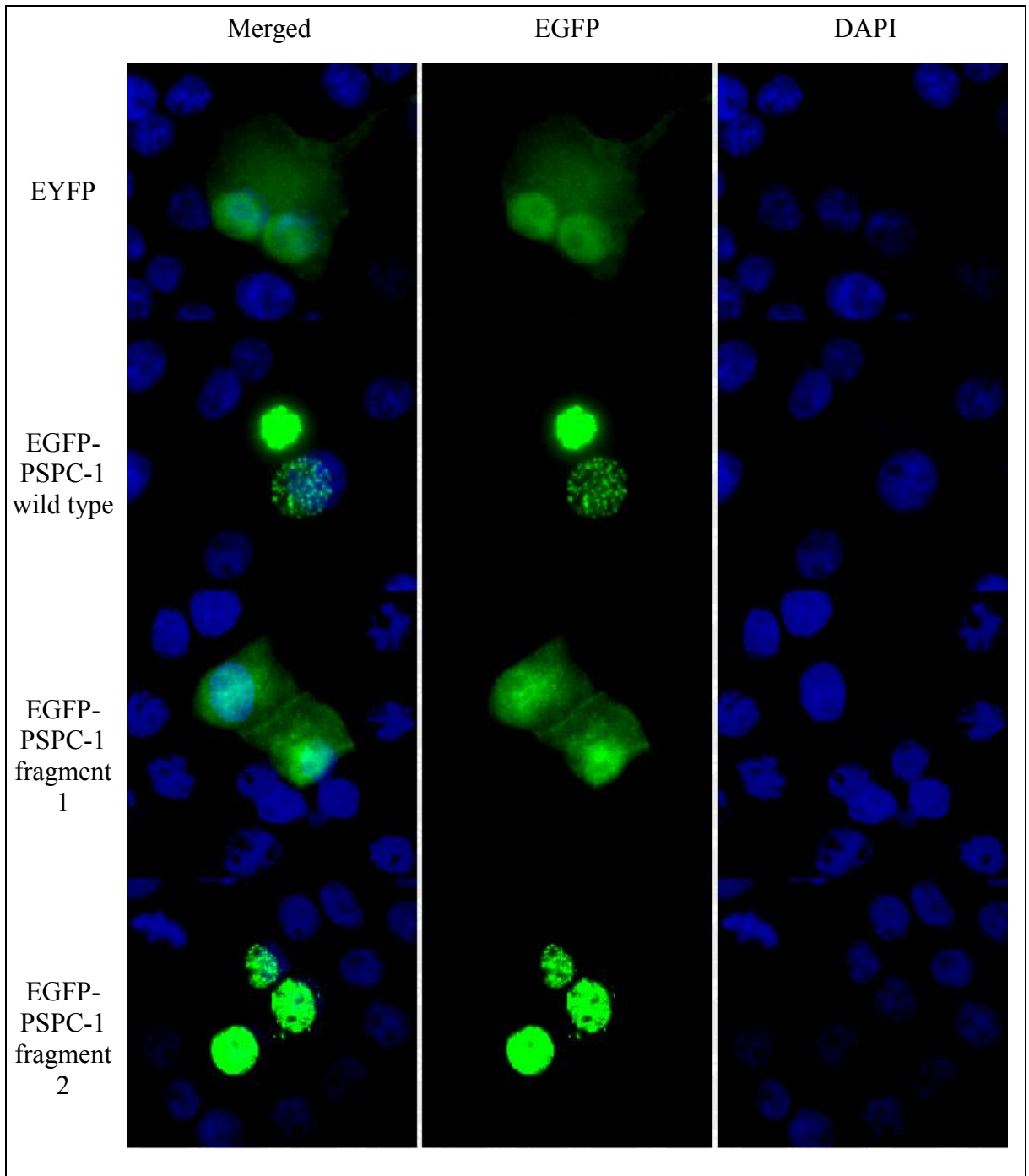


Figure 5-3 The distribution of the EGFP-PSPC-1 truncated proteins in uninfected cells. GMK cells were grown on coverslips and transfected with pEYFP, pEGFP-PSPC-1, pEGFP-PSPC-1 fragment 1 or pEGFP-PSPC-1 fragment 2 using lipofectin. Cells were fixed and nuclei were stained with DAPI before being visualized with a BX41 fluorescent microscope. Nuclei were observed using a DAPI filter, expression of EYFP, EGFP-PSPC-1 and EGFP-fragments were visualized with a FITC filter.

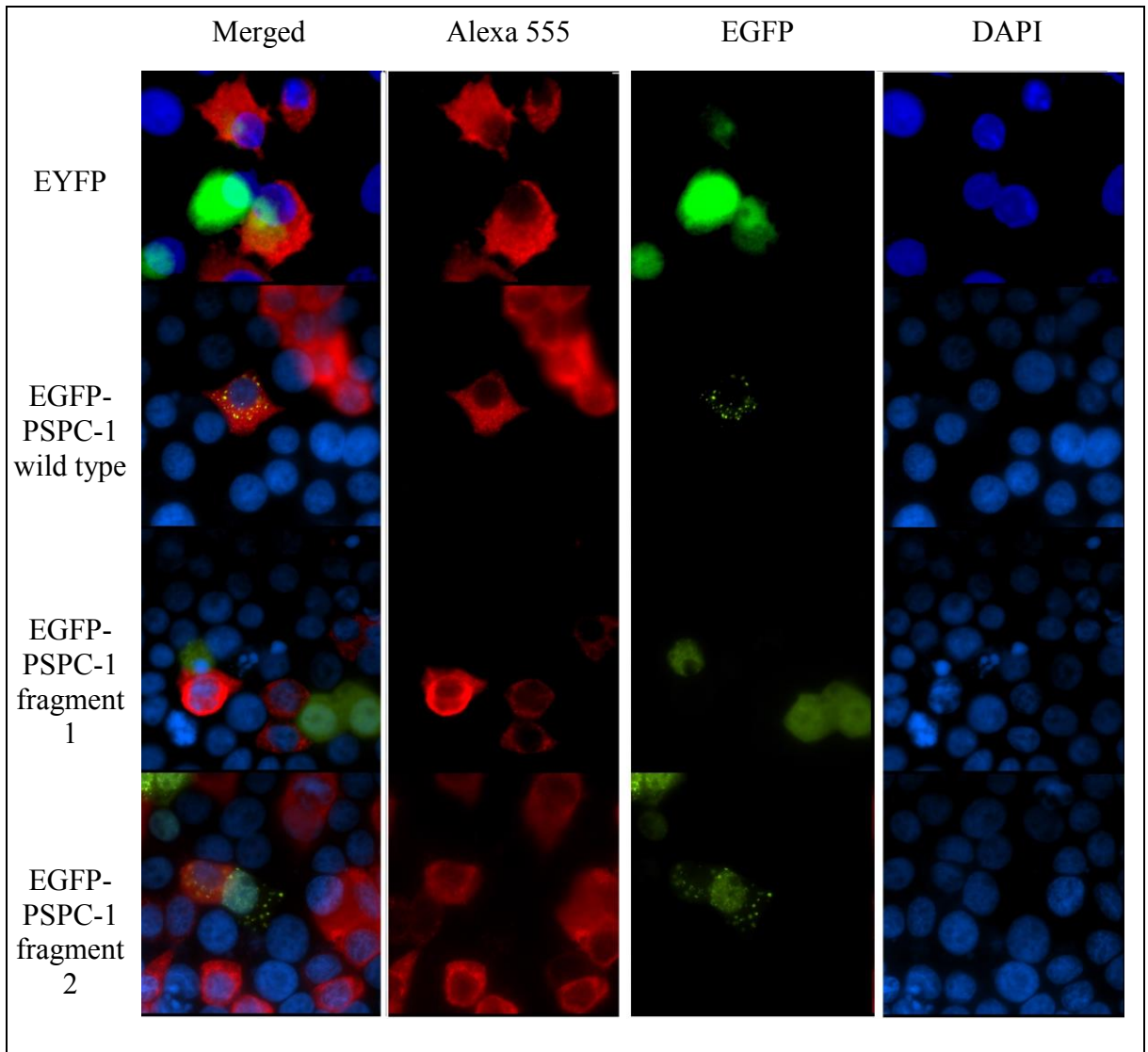


Figure 5-4 The effect of CAV-9 infection on the distribution of EGFP-PSPC-1 fragments. GMK cells were grown on coverslip and transfected with pEYFP, pEGFP-PSPC-1, pEGFP-PSPC-1 fragment 1 or pEGFP-PSPC-1 fragment 2 using lipofectin. Cells were then infected with CAV-9 for 8 hr. Nuclei were stained with DAPI before being visualized using a Nikon A1 plus Wide field microscope. Nuclei were observed using DAPI (blue channel), expression of EGFP-PSPC-1 (green channel) and infected cells identified using anti-CAV-9 antibody and secondary antibody labelled with Alexa 555 (red channel). No transfected and infected cells could be found for pEGFP-PSPC-1 fragment 1.

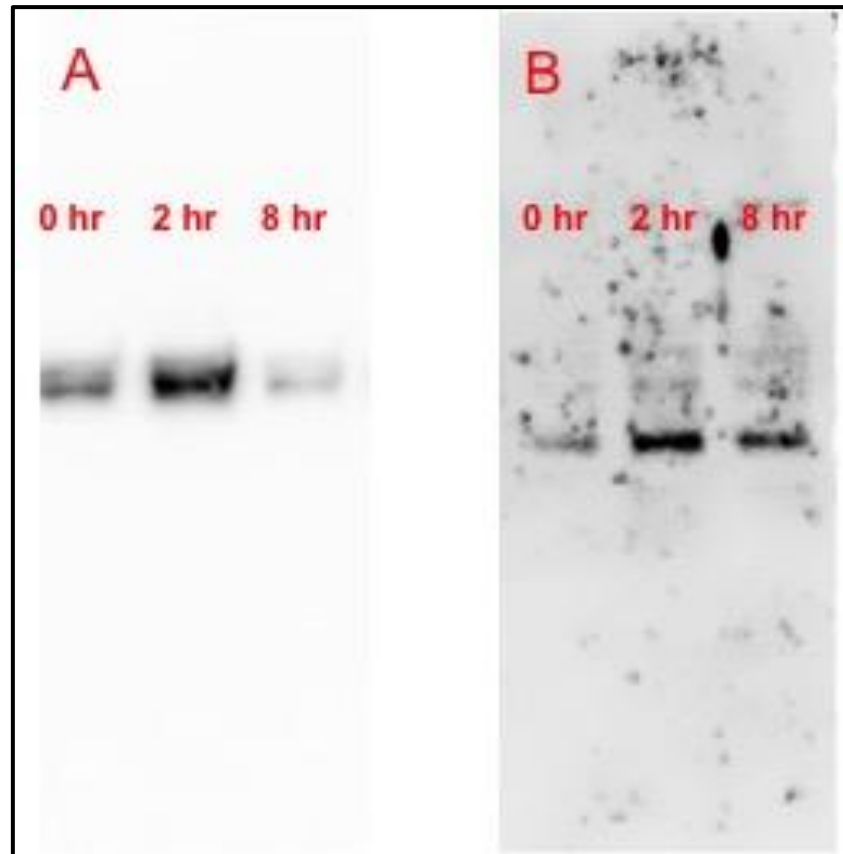


Figure 5-5 the effect of CAV-9 infection on paraspeckle proteins. Western blot was performed on the endogenous PSPC-1 and PSF. GMK cells were infected for 0, 2 and 8 hr. Cells were lysed and a protein extract was made. The protein concentration was determined and equal amounts were loaded onto the gel. After separation the membrane was blotted and protein were detected by using specific primary antibody (anti PSPC-1, anti PSF) and secondary antibody A PSPC-1 B PSF

5.4 PSF phosphorylation and sumoylation

In order to examine whether the translocation of the EGFP-PSF protein after infection is caused by phosphorylation or sumoylation, a number of mutations to the PSF protein that prevent phosphorylation or sumoylation were constructed. The primer OL 2233 was designed in order to make the mutant S8A, OL 2224 to make Y293F and OL 2257 to construct a K338A mutant which cannot be sumoylated. PSF DNA was used as DNA template to perform PCR with the help of DMSO in order to improve the amplification of a GC rich region. In the case of Y293F, an overlap PCR was conducted as the mutation is not located near to useful restriction enzyme site. S8 is located close to the N-terminus of the protein and K338 is located near to a unique XbaI site, so single PCR reactions using mutated primers could be done. PCR products were purified and ligated into pGEM-T easy vector. The ligated DNA was then transformed into *E. coli*, and after confirming the sequence of the clones produced, DNA was cut with *XbaI* and *XhoI* (as there is a unique site in pEGFP-C1) and ligated into pEGFP-PSF cut with the same enzymes, giving pEGFP-PSF S8A, pEGFP-PSF Y293F and pEGFP-PSF sumo K338A (Figure 5-6).

GMK cells were transfected with the pEGFP-PSF mutation constructs. 24 hr post transfection cells were infected or mock-infected with CAV-9 for 8 hr. Cells were then fixed, permeabilised, blocked and immunostained then mounted on glass slides using hard set mounting media containing DAPI then visualized by Nikon A1si confocal microscope.

The results showed that in mock-infected cells EGFP-PSF S8A was diffused throughout the nucleus with a smaller number of speckled structures than seen in the wild type (Figure 5-7). It was completely redistributed into the cytoplasm after 8 hr of infection, giving a pattern similar to the wild type protein (Figure 5-8). EGFP-PSF Y293F had a punctate distribution in the nucleus, with some a relocation in the cytoplasm as speckled structures. The protein was completely redistributed in the cytoplasm after 8 hr of infection with CAV-9. EGFP-PSF Sumo was distributed as punctate with some diffusion in the nucleus, with some diffuse signal in the cytoplasm. After infection the protein was redistributed to cytoplasmic speckles (Figure 5-7 and Figure 5-8).

The results showed that the mutations possibly had some effect on protein distribution in the nucleus, but none on the redistribution after infection. In order to study this more, GMK cells were cotransfected with mCherry-PSPC-1 and EGFP PSF mutants. In all cases the mCherry-PSPC-1 and EGFP mutants colocalised in both mock-infected and infected cells after 8 hr infection (Figure 5-9 and Figure 5-10). In mock-infected cells, the S8A and Y293F mutants had a punctate distribution, while the Sumo mutant was more diffuse. After 8 hr infection all the mutants and mCherry-PSPC-1 were in granules in the cytoplasm (Figure 5-9 and Figure 5-10). The results confirmed that the mutations do not affect the movement to these granules.

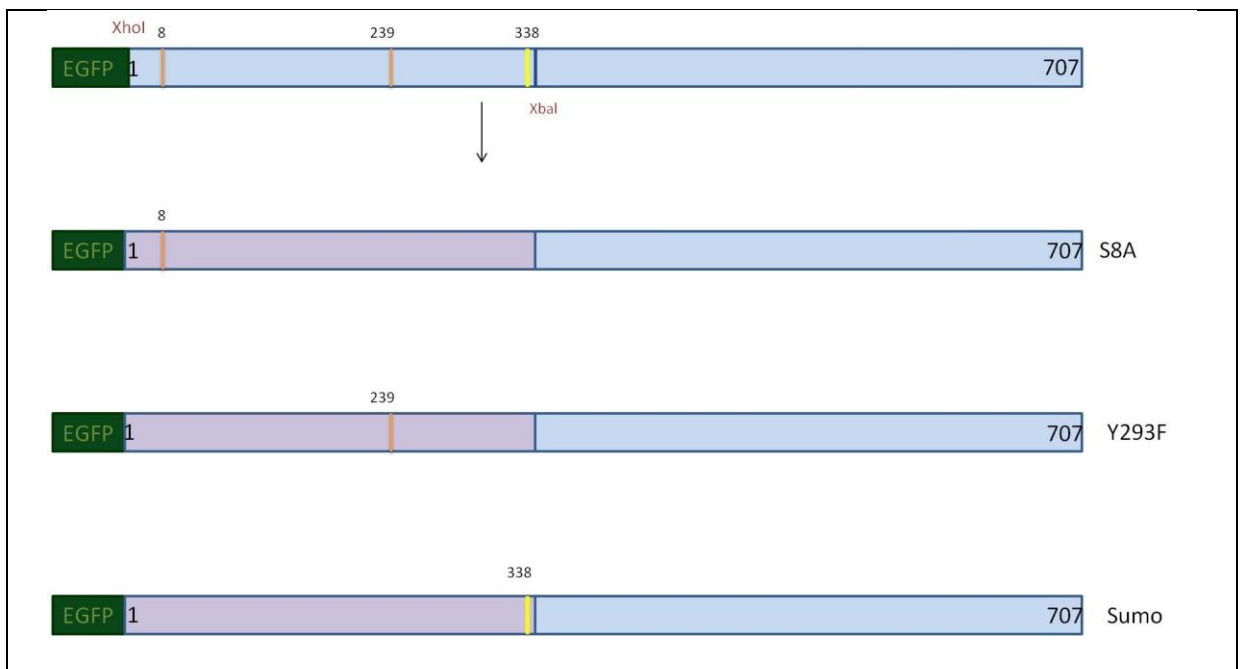


Figure 5-6 A schematic diagram for PSF dephosphorylation and sumoylation. Illustrating the PSF protein mutagenesis that makes protein dephosphorylation and sumoylation.

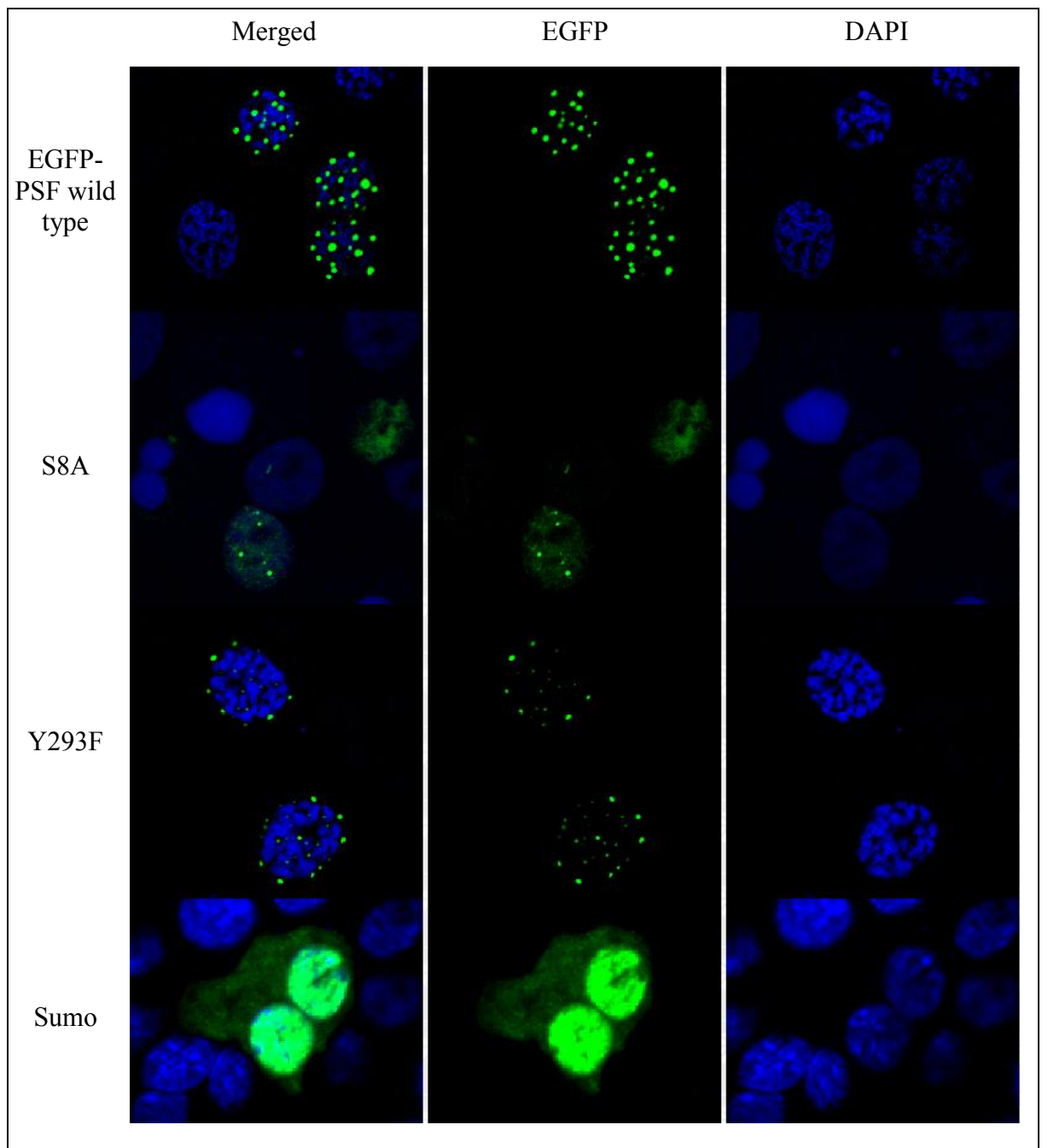


Figure 5-7 The distribution of the EGFP-PSF protein and EGFP-PSF mutations (mock). GMK cells were grown on the coverslips and transfected with pEGFP-PSF, pEGFP-PSF S8A, pEGFP-PSF Y293F, EGFP-PSF Sumo using lipofectin. Cells were fixed and nuclei were stained with DAPI being visualized using a Nikon A1si confocal microscope. Nuclei were observed using DAPI (blue channel), expression of EGFP-PSF and EGFP truncated (green).

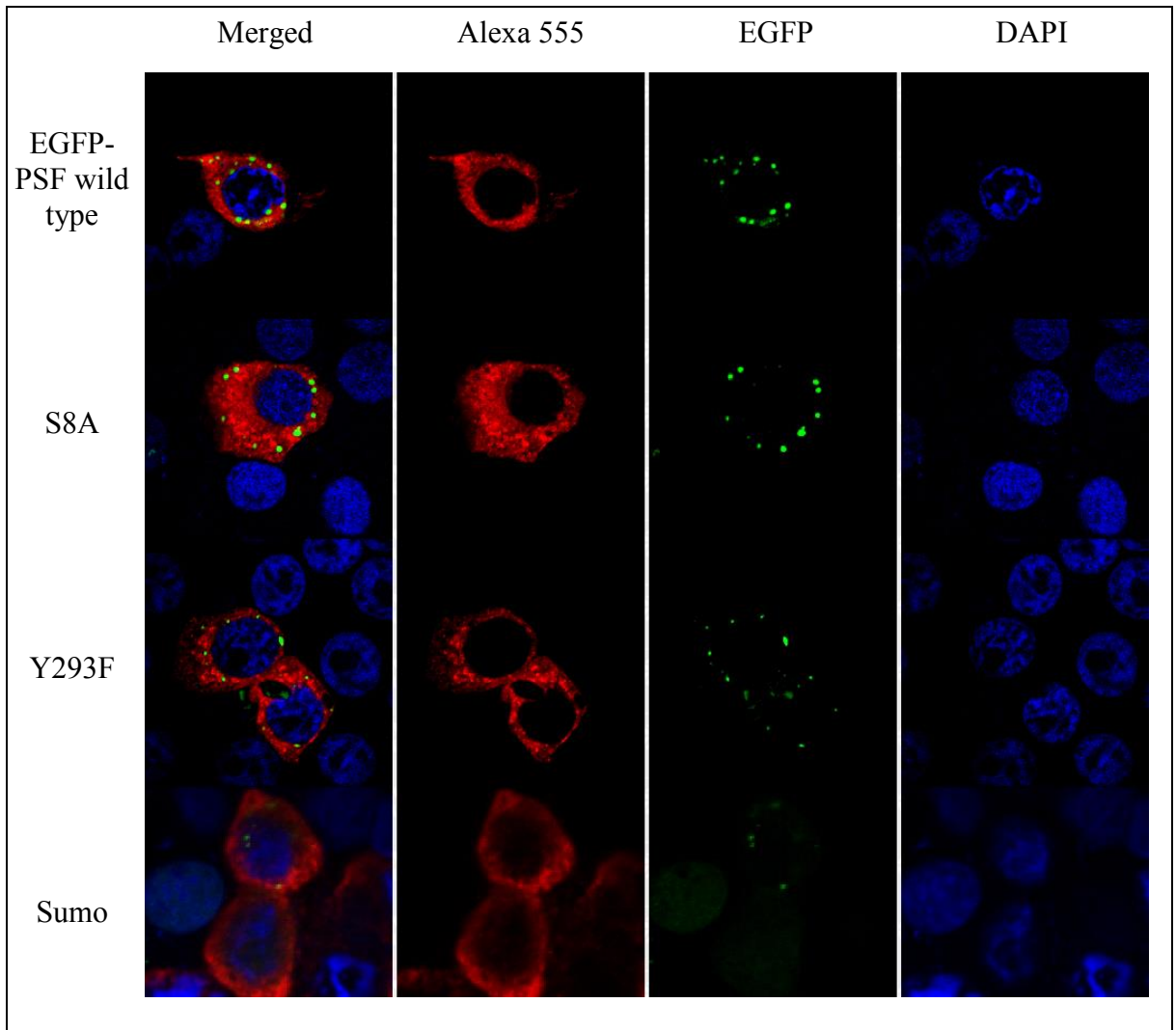


Figure 5-8 The effect of CAV-9 on the distribution of EGFP-PSF protein and EGFP-PSF mutation. GMK cells were grown on coverslip and transfected with pEGFP-PSF, pEGFP-PSF S8A, pEGFP-PSF Y293F, pEGFP-PSF Sumo using lipofectin. Cells were then infected with CAV-9 for 8 hr. Nuclei were stained with DAPI being visualized using a Nikon A1si confocal microscope. Nuclei were observed using DAPI (blue channel), expression of EGFP-PSF (green channel), and infected cells identified using anti-CAV-9 antibody and secondary antibody labelled with Alexa 555 (red channel).

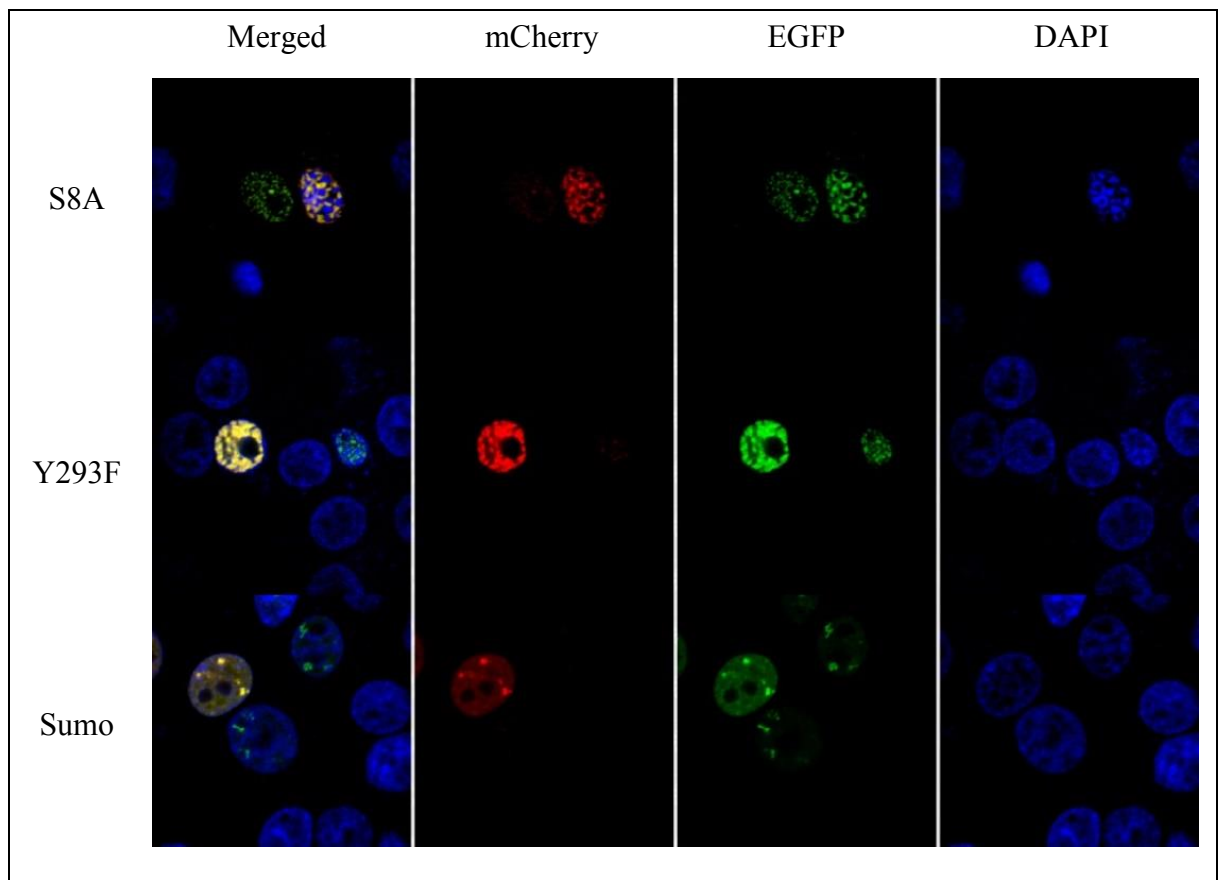


Figure 5-9 The distribution of EGFP-PSF mutations and mCherry PSpC-1 complex (mock). GMK cells were grown on coverslip and cotransfected with pEGFP-PSF mutation and pmCherry PSpC-1 using lipofectin. Nuclei were stained with DAPI being visualized using a Nikon A1si confocal microscope. Nuclei were observed using DAPI (blue channel), expression of EGFP- PSF Mutation (green channel), and expression of mCherry-PSpC-1 (red channel).

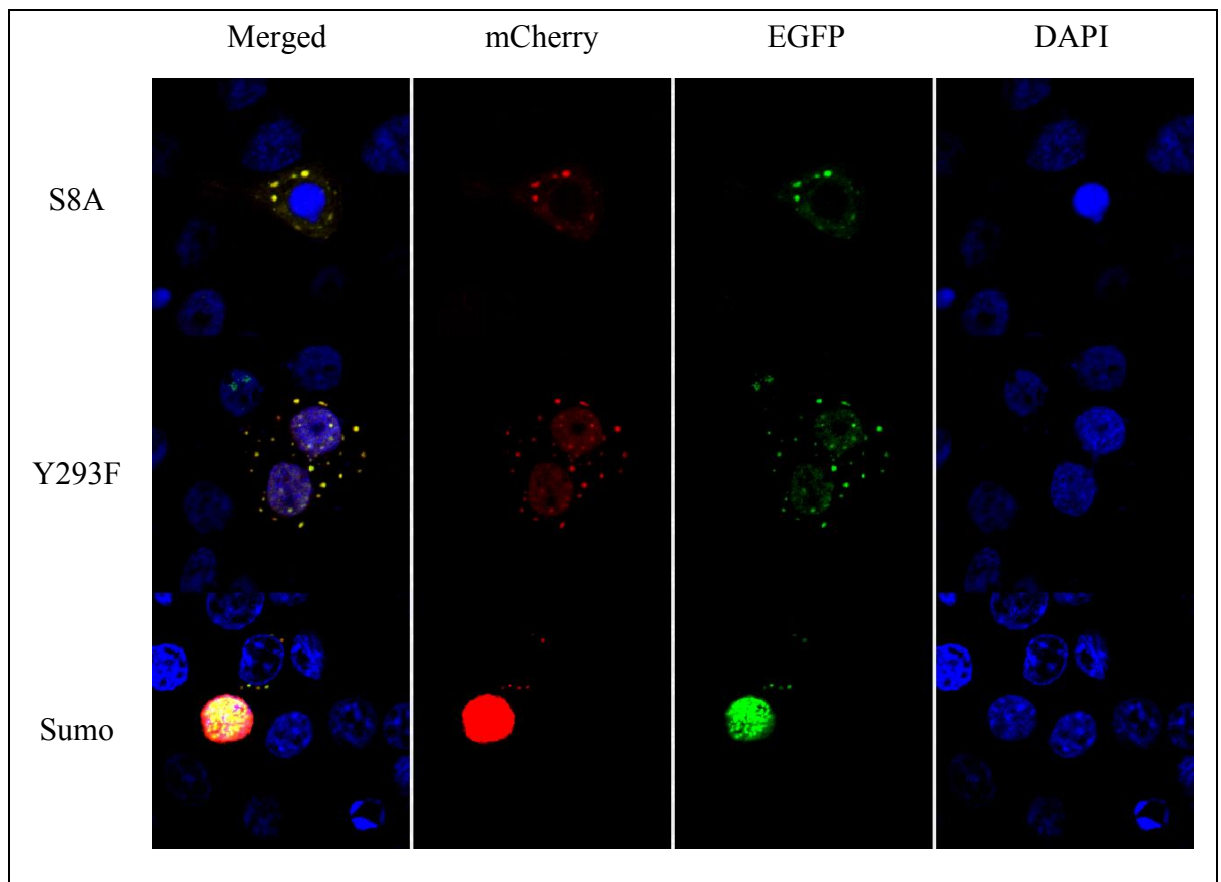


Figure 5-10 The effect of CAV-9 on the localization of EGFP- PSF Mutation and mCherry PSpC-1 complex. GMK cells were grown on coverslip and cotransfected with pEGFP-PSF mutation and pmCherry PSpC-1 using lipofectin. Cells were then infected with CAV-9 for 8 hr. Nuclei were stained with DAPI being visualized using a Nikon A1si confocal microscope. Nuclei were observed using DAPI (blue channel), expression of EGFP-PSF Mutation (green channel), and expression of mCherry-PSpC-1 (red channel).

5.5 PSF truncations

In order to study which part of the PSF is responsible for the protein redistribution, constructs were made to truncate the PSF into smaller pieces. pEGFP-PSF was cut with *Bam*HI (in the vector at the 3' end of the PSF) and XbaI (internal site). Oligonucleotides OL 2252 and OL 2253 were annealed to give a linker with *Bam*HI and XbaI ends, that was ligated to the cut pEGFP-PSF to give the mutant pEGFP-PSF XB (Figure 5-11). This was transfected into GMK cells which were either mock-infected or infected for 8 hours. The cells were visualized with a Nikon A1 plus wide field microscope. The results showed that the EGFP-PSF XB was distributed throughout the cell in mock-infected cells and there was no movement to the cytoplasm in infected cells (Figure 5-12).

Another two different truncation constructs were produced (Figure 5-11). These were D1, which includes amino acid positions 1-452, and D2, which includes positions 1-606. PCR was performed with OL 2254 and OL 2255 or OL 2256 primers and the fragments were ligated into pGEM-T easy and their sequence was checked. The PSF DNA was then cut from the vector with XbaI and *Bam*HI and ligated into pEGFP-PSF cut with same restriction enzymes, in order to make pEGFP-PSF D1 and pEGFP-PSF D2 (Figure 5-11). When transfected and the cells visualized with BX41 microscope, EGFP-PSF D1 was diffuse in the both the nucleus and the cytoplasm. EGFP-PSF D2 was present in the nucleus and diffuse, but there were several punctate structures in the cell cytoplasm with a large number of spots (Figure 5-13). No cell could be found both infected/transfected with EGFP-PSF D1. Infected EGFP-PSF D2 was completely redistributed in the cytoplasm into typical spots similar to the wild type (Figure 5-14).

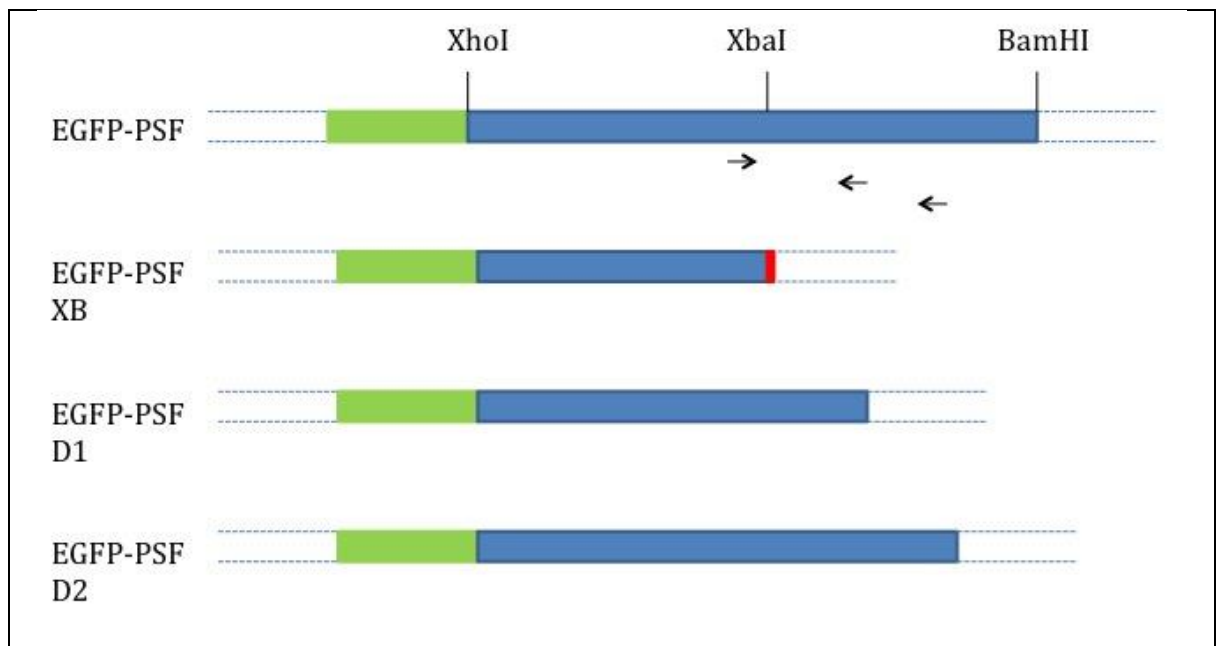


Figure 5-11 A Schematic diagram illustrating the manipulations of the truncated PSF proteins. The green box indicates EGFP, the blue box is PSF DNA and the red box is a short annealed oligonucleotide pair which gives *XbaI* and *BamHI* overlap.

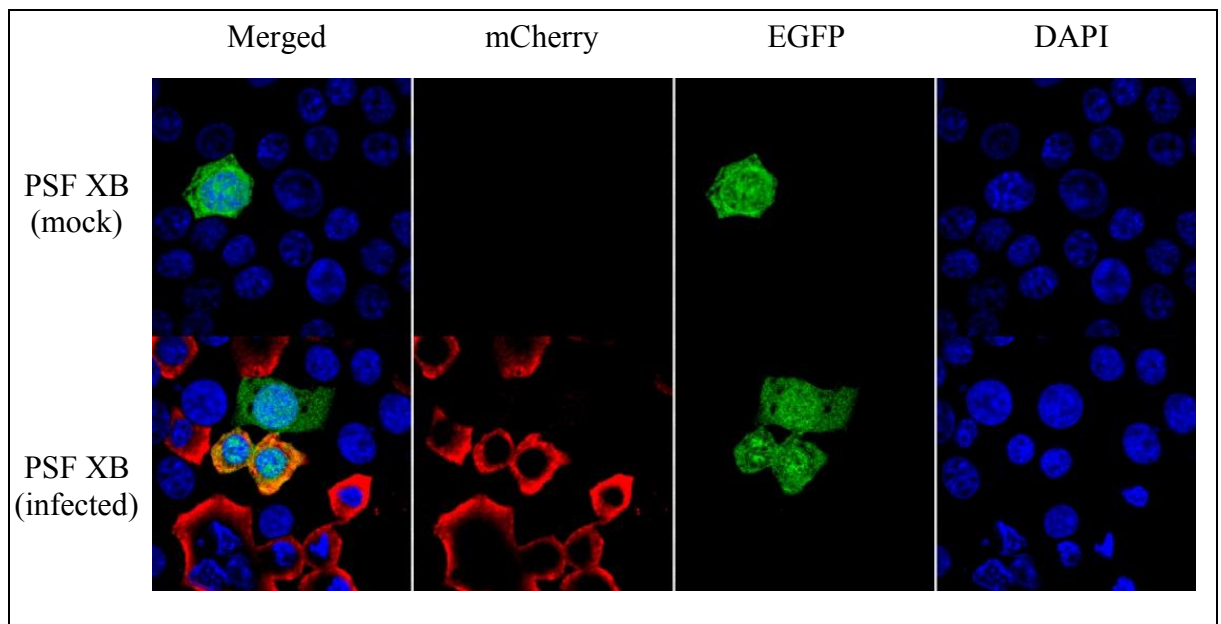


Figure 5-12 The effect of CAV-9 on the redistribution of EGFP- PSF Mutation XB. GMK cells were grown on coverslip and transfected with pEGFP-PSF XB using lipofectin. Cells were then infected with CAV-9 for 8 hr. Nuclei were stained with DAPI being visualized using Nikon A1si confocal microscope. Nuclei were observed using DAPI (blue channel), expression of EGFP- PSF Mutation (green channel), and infected cells identified using anti-CAV-9 antibody and secondary antibody labelled with Alexa 555 (red channel).

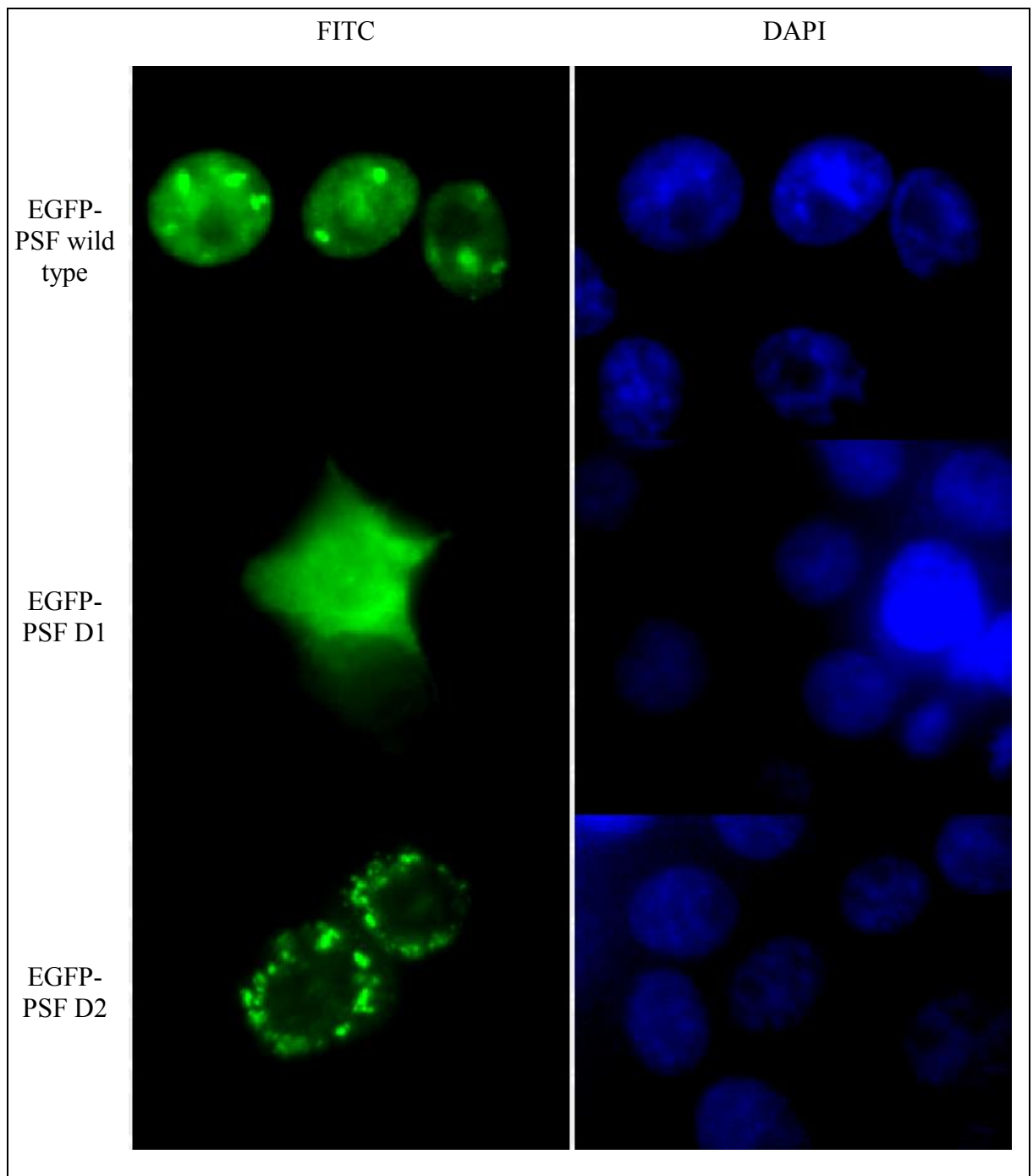


Figure 5-13 The distribution of the EGFP-PSF truncated proteins (mock). GMK cells were grown on the coverslips and transfected with pEGFP-PSF, pEGFP-PSF D1, pEGFP-PSF D2. Cells were fixed and nuclei were stained with DAPI being visualized with BX 41 fluorescent microscope. Nuclei were observed with DAPI filter, EGFP-PSF and EGFP-PSF deletions were visualized with FITC filter.

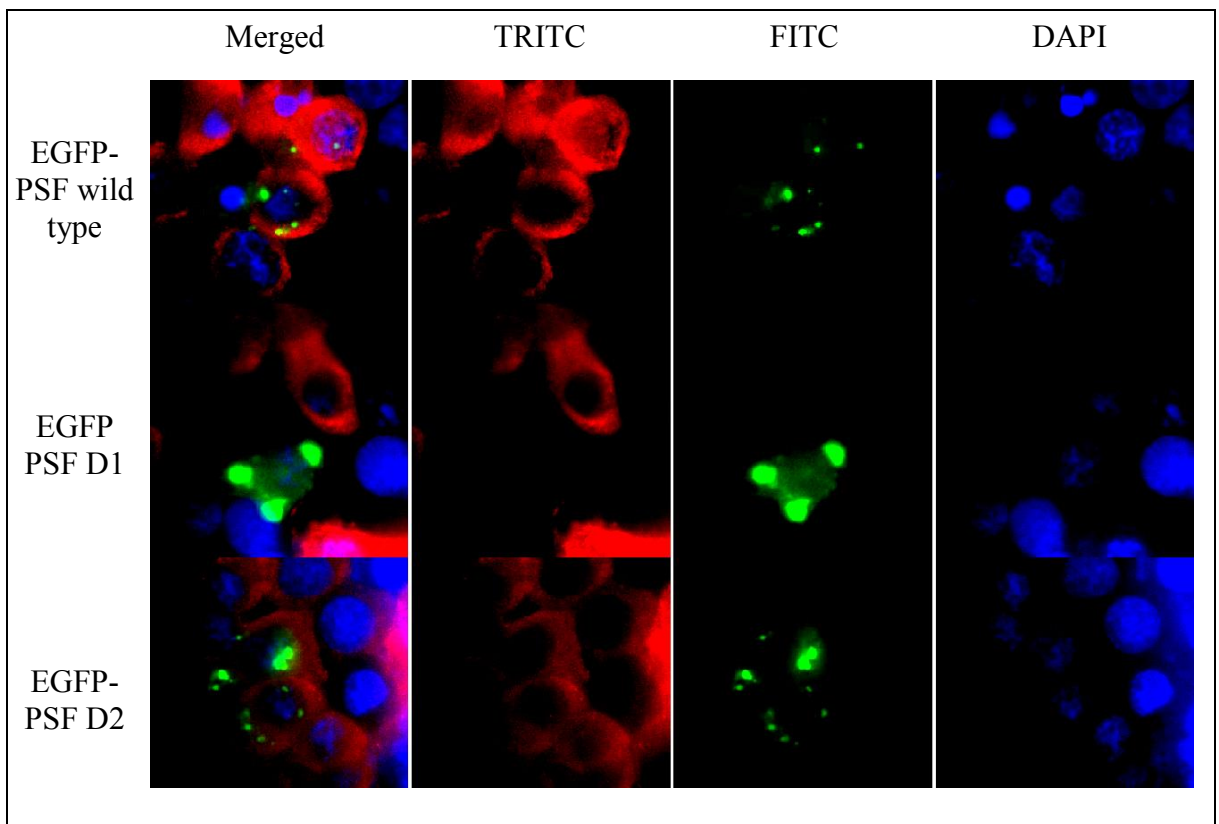


Figure 5-14 The effect of CAV-9 on the distribution of EGFP-PSF truncated protein. GMK cells were grown on the coverslips and transfected with pEGFP-PSF, pEGFP-PSF D1, pEGFP-PSF D2 using lipofectin. Cells were infected with CAV-9 for 8 hr and nuclei were stained with DAPI being visualized with a BX41 fluorescent microscope. Nuclei were observed with DAPI filter, EGFP-PSF, EGFP-PSF deletions were visualized with FITC filter and and infected cells identified using anti-CAV-9 antibody and secondary antibody labelled with Alexa 555 with TRITC filter.

To find if the patterns seen in Figure 5-13 and Figure 5-14 were the same or different from wild type protein, GMK cells were cotransfected with pmCherry-PSPC-1 and pEGFP mutant fusions (pEGFP-PSF D1 and pEGFP-PSF D2). Cells were also infected with CAV-9 for 8 hr or mock-infected then visualized with a Nikon A1si confocal microscope. Infected cells were identified by the typical relocalisation of mCherry-PSPC-1. There was no colocalization between EGFP-PSF D1 and mCherry-PSPC-1 in either mock infected or 8 hr infected cells (Figure 5-15). The EGFP-PSF D1 protein was distributed throughout the nucleus and cytoplasm, while mCherry-PSPC-1 distributed in the nucleus in speckled structures. EGFP-PSF D2 mainly colocalized with mCherry-PSPC-1 in the nucleus, with a minor relocation of EGFP-PSF D2 in the cytoplasm in the mock infection cell. No mCherry-PSPC-1 was seen in the cytoplasm. Both EGFP-PSF D2 and mCherry PSPC-1 were found in the cytoplasm and colocalized after 8 hr of infection (Figure 5-15).

The results suggest that the sequences deleted in the pEGFP-PSF XB and pEGFP-PSF D1 constructs are needed for both paraspeckle localization and movement to the cytoplasmic granules.

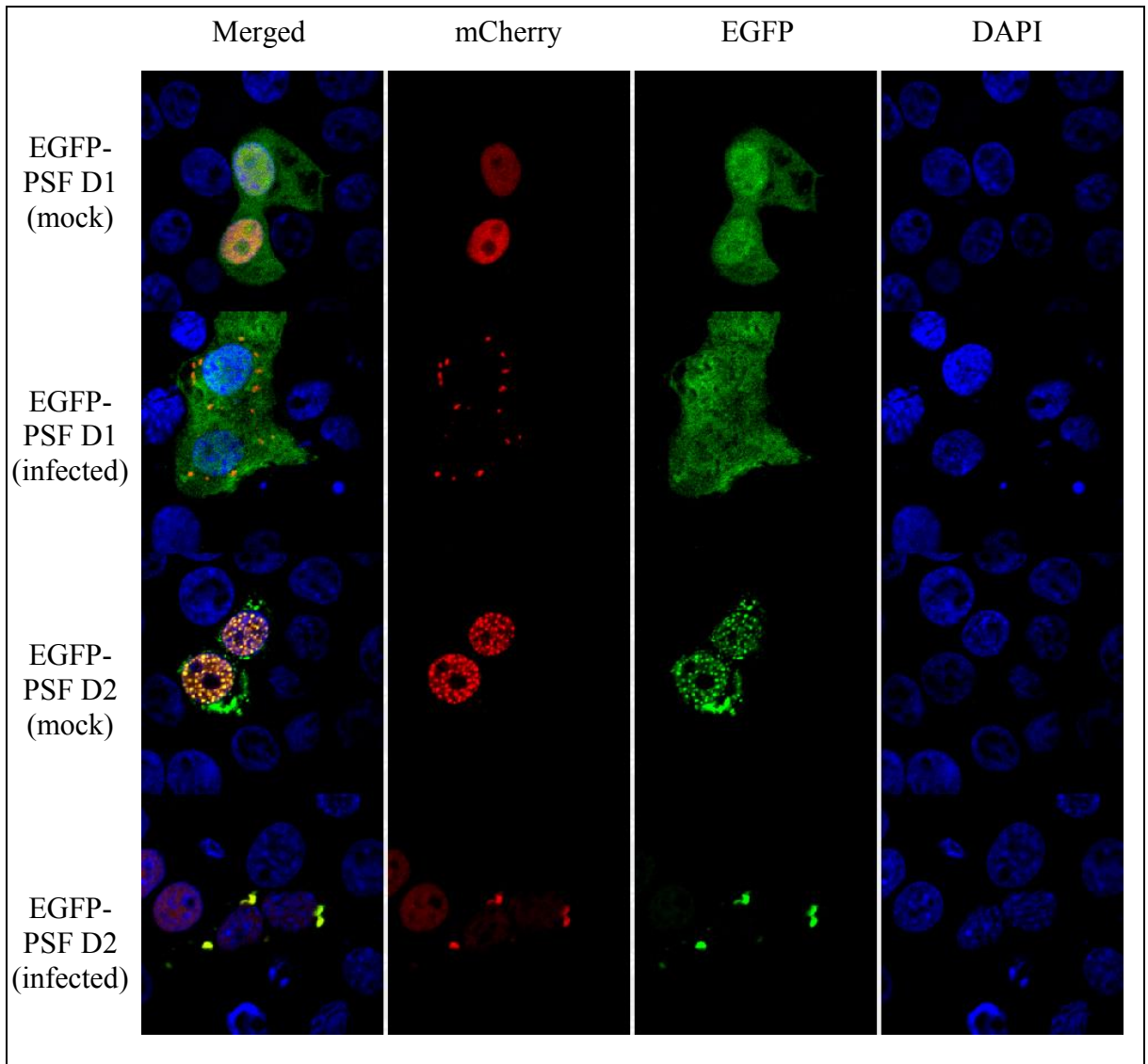


Figure 5-15 The effect of CAV-9 on the localization of EGFP- PSF truncated proteins and mCherry PSpC-1 complex. GMK cells were grown on coverslip and cotransfected with pEGFP-PSF truncations and pmCherry PSpC-1 using lipofectin. Cells were then infected with CAV-9 for 8 hr. Nuclei were stained with DAPI being visualized using a Nikon A1 si confocal fluorescent microscopy. Nuclei were observed using DAPI (blue channel), expression of EGFP- PSF deletions using (green channel), expression of mCherry-PSpC-1 (red channel).

5.6 Cytoplasmic structures which could be the location of DBHS proteins after infection with CAV-9

In order to investigate further the translocation of the DBHS proteins PSF, PSCP-1 and NONO into cytoplasmic granules after CAV-9 infection and to identify what these granules are, a number of cytoplasmic candidates were examined.

5.6.1 Replication complexes

GMK cells were transfected with pEGFP (PSCP-1, PSF and NONO). 24 hr post transfection cells were infected with CAV-9 for different time intervals (2, 4, 6 and 8 hr). Cells were then fixed, permeabilised, blocked and immunostained with primary antibody for replication complexes (Anti-dsRNA monoclonal) and alexafluor 555 (goat anti mouse) as secondary antibody. Nuclei were stained with DAPI in mounting media and visualized with a Nikon A1si confocal microscope. In the EGFP-PSCP-1 experiment few infected cells were identified after 2 hr, presumably because not enough replication complexes were formed early in replication. EGFP-PSCP-1 had the expected distribution in the nucleus with the usual speckled structures through the nucleus. EGFP-PSCP-1 was redistributed in the cytoplasm after 4 hr infection with no colocalization with the replication complexes that were also distributed in the cytoplasm. Similarly, after 6 and 7 hr of infection EGFP-PSCP-1 redistributed completely in the cytoplasm with colocalization with the replication complexes (Figure 5-16). In the EGFP-PSF experiment, it was hard to find cells that were both infected and transfected at 2 and 4 hr after infection. After 6 and 8 hr of infection, the protein started to redistributed in the

cytoplasm with no obvious colocalization with the replication complexes (Figure 5-17). There was no change in the EGFP-NONO protein distribution after 2 hr of infection. EGFP-NONO showed a slight redistribution to the cytoplasm after 4 hr of infection but no colocalization was spotted. After 6 and 8 hr of infection, EGFP-NONO showed a complete redistribution from the nucleus to cytoplasm but also no colocalization was shown with replication complexes (Figure 5-18).

5.6.2 Stress granules

GMK cells were grown on coverslips and transfected with pEGFP-PSPC-1, pEGFP-PSF D1 or pEGFP-PSF D2 then infected with CAV-9 for 8 hr. Cells were then fixed and immunostained with a monoclonal primary antibody specific for the stress granule protein G3BP and goat anti-mouse antibody as secondary antibody (Alexafluor 555). Cells were visualized with a Nikon A1si confocal microscope. Results showed that there is no clear colocalization of the EGFP-PSPC-1 into stress granules, as in the infected cells the anti-G3BP does not have the punctate stress granule distribution that was observed in the non-infected cells. For the pEGFP-PSF D1 experiment, the stress granule stain was not punctate and was in the cytoplasm, as was the EGFP signal, but there was no clear co-localization. There was no obvious colocalisation between EGFP-PSF D2 and stress granules (Figure 5-19). HDAC6 has been reported to be a critical component of stress granules (Kwon et al., 2007). GMK cells were therefore cotransfected with the construct pEGFP-N1HDAC6 and pmCherry PSPC-1. 24 hr post transfection cells were infected with CAV-9 for 2, 4, 6 and 8 hr then fixed and coverslips mounted on glass slides using mounting media including DAPI. Slides were then visualized with Nikon

A1si confocal microscope. In non-infected cells the EGFP-NHDAC6 was distributed through the cellular cytoplasm with a lack of the punctate structures seen using G3BP (Figure 5-20). There was no clear difference in the distribution in the stress granule marker in infected cells at any time after infection and no colocalization with mCherry-PSPC-1 cytoplasmic granules (Figure 5-20).

5.6.3 P body

GMK cells were grown on coverslips and three samples were transfected with pT7EGFP-C1HsRCK, as HsRCK [Homo sapiens] RCK (DDX6) is reported to be a P-body marker (Tritschler et al., 2009). One sample was cotransfected with pmCherry-PSPC-1 then infected with CAV-9 for 6 hr and one was just infected with CAV-9 for 6 hr. Cells were then fixed and the infected pT7EGFP-C1HsRCK sample was immunostained for CAV-9. Results showed that in the non-infected cells EGFP-C1HsRCK was distributed in the cytoplasm with clear punctate structures, which probably correspond to P-bodies, and a more diffused background. After 6 hr of infection, in cells positive for anti-CAV-9 staining the cytoplasmic spots had mostly disappeared and as well as being in the cytoplasm EGFP-C1HsRCK was in the nucleus. In cells cotransfected with pmCherry-PSPC-1 and identified as infected due to the relocalisation of the pmCherry signal, there was no colocalisation between mCherry PSPC-1 and EGFP-C1HsRCK (Figure 5-21).

GMK cells were also cotransfected with pT7EGFP-C1HsRCK and pmCherry PSPC-1 then 24 hr post-transfection cells were infected with CAV-9 for the time intervals 2, 4 and 6 hr, then fixed and coverslips mounted on glass slides using mounting media including DAPI. Slides were then visualized with a Nikon A1 plus wide field

microscope. In non-infected cells the P-body protein fused to EGFP was distributed through the cellular cytoplasm with a punctate structures (Figure 5-22). No colocalization between mCherry PSPC-1 and the P-body marker was observed through the infection time intervals (Figure 5-22).

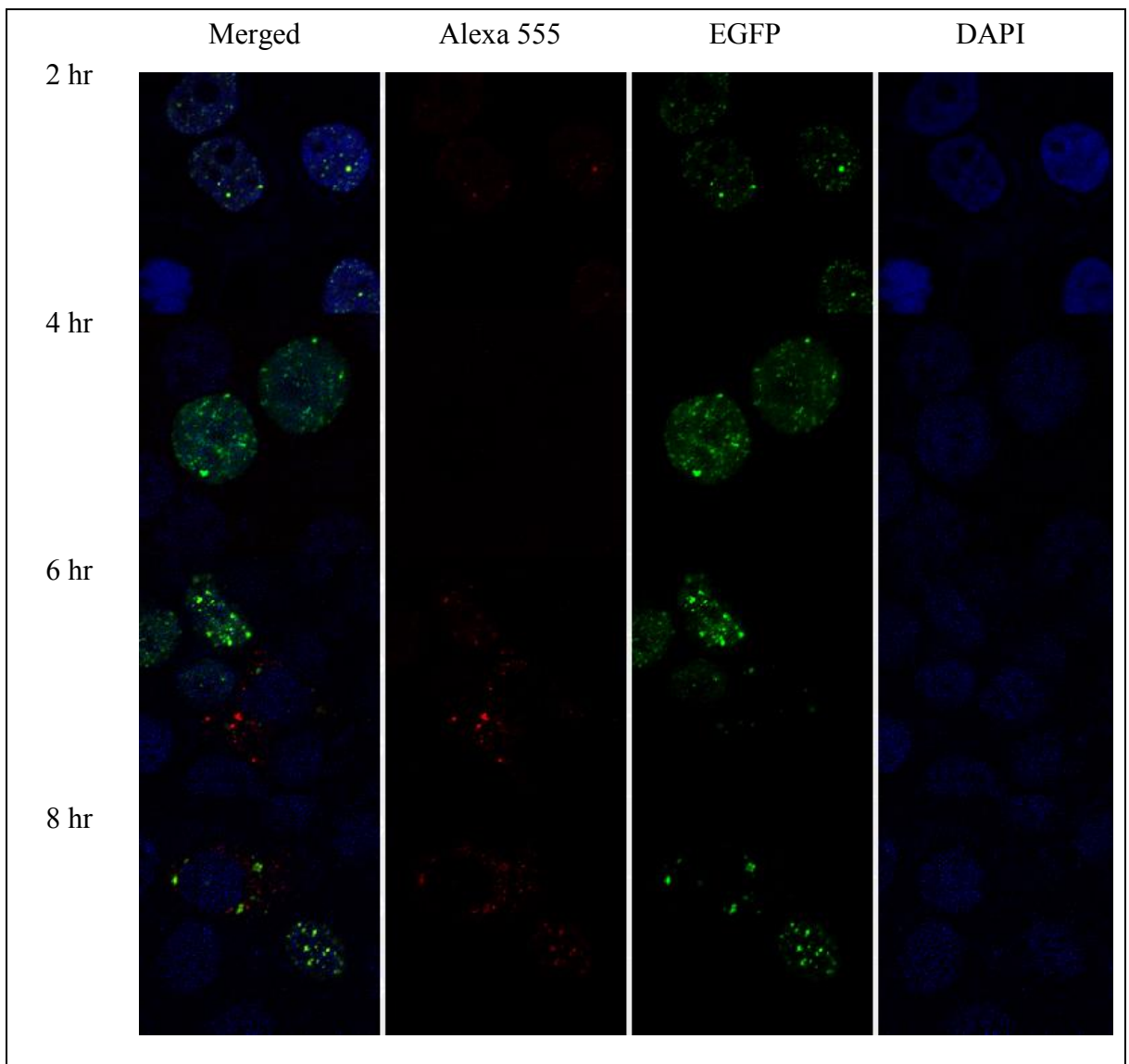


Figure 5-16 The localization of PSPC-1 with the replication complexes (time interval). GMK cells were grown on coverslip and transfected with pEGFP-PSPC-1 using lipofection. Cells were then infected with CAV-9 for 2, 4, 6 and 8 hr. Nuclei were stained with DAPI being visualized using a Nikon A1si confocal microscope. Nuclei were observed using DAPI (blue channel), expression of EGFP- PSPC-1 (green channel), and infected cells identified using anti-dsRNA antibody and secondary antibody labelled with Alexa 555 (red channel).

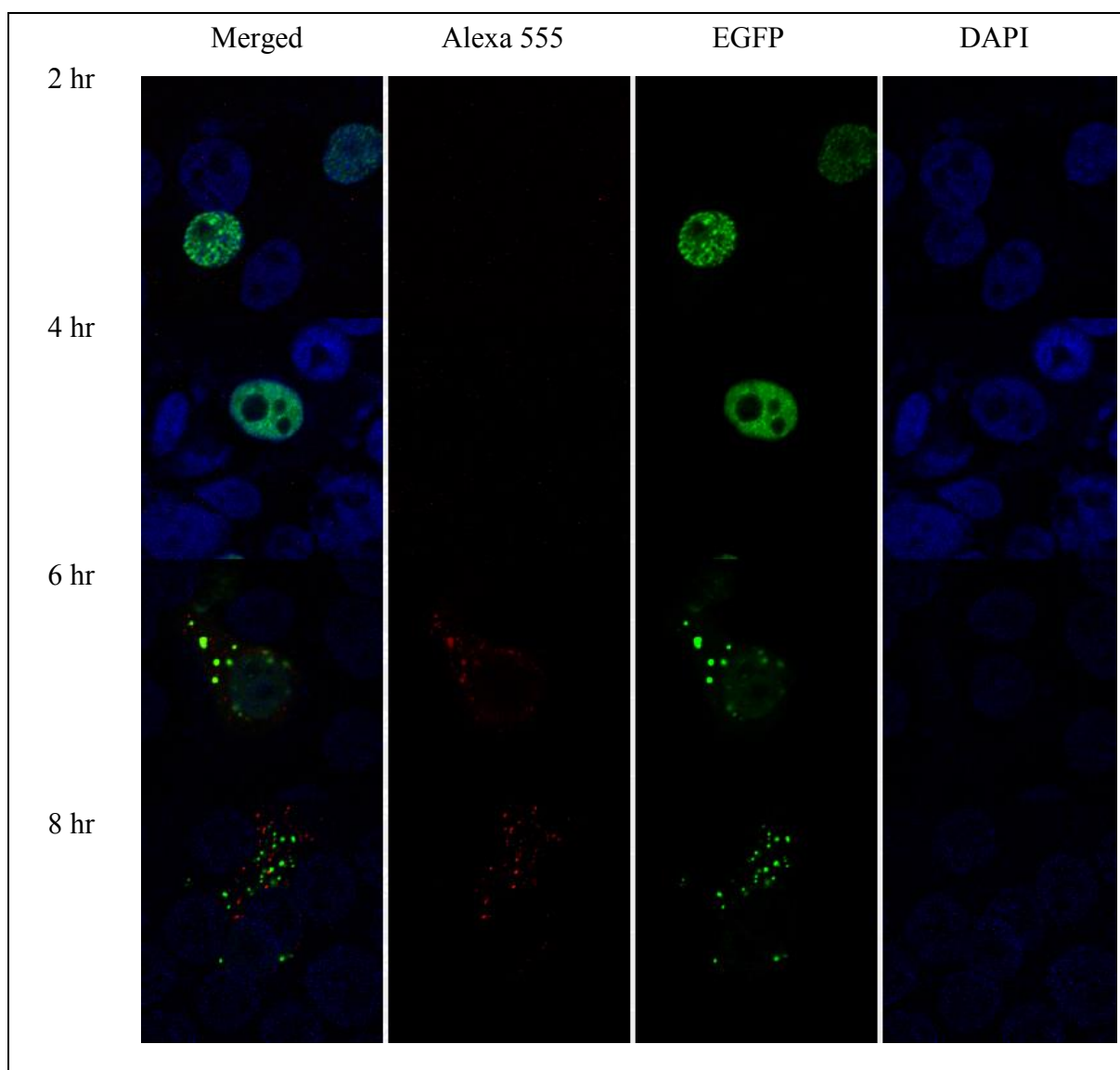


Figure 5-17 The localization of PSF with the replication complexes (time interval). GMK cells were grown on coverslip and transfected with pEGFP-PSF using lipofection. Cells were then infected with CAV-9 for 2, 4, 6 and 8 hr. Nuclei were stained with DAPI being visualized using a Nikon A1si confocal microscope. Nuclei were observed using DAPI (blue channel), expression of EGFP- PSF (green channel), and infected cells identified using anti-dsRNA antibody and secondary antibody labelled with Alexa 555 (red channel).

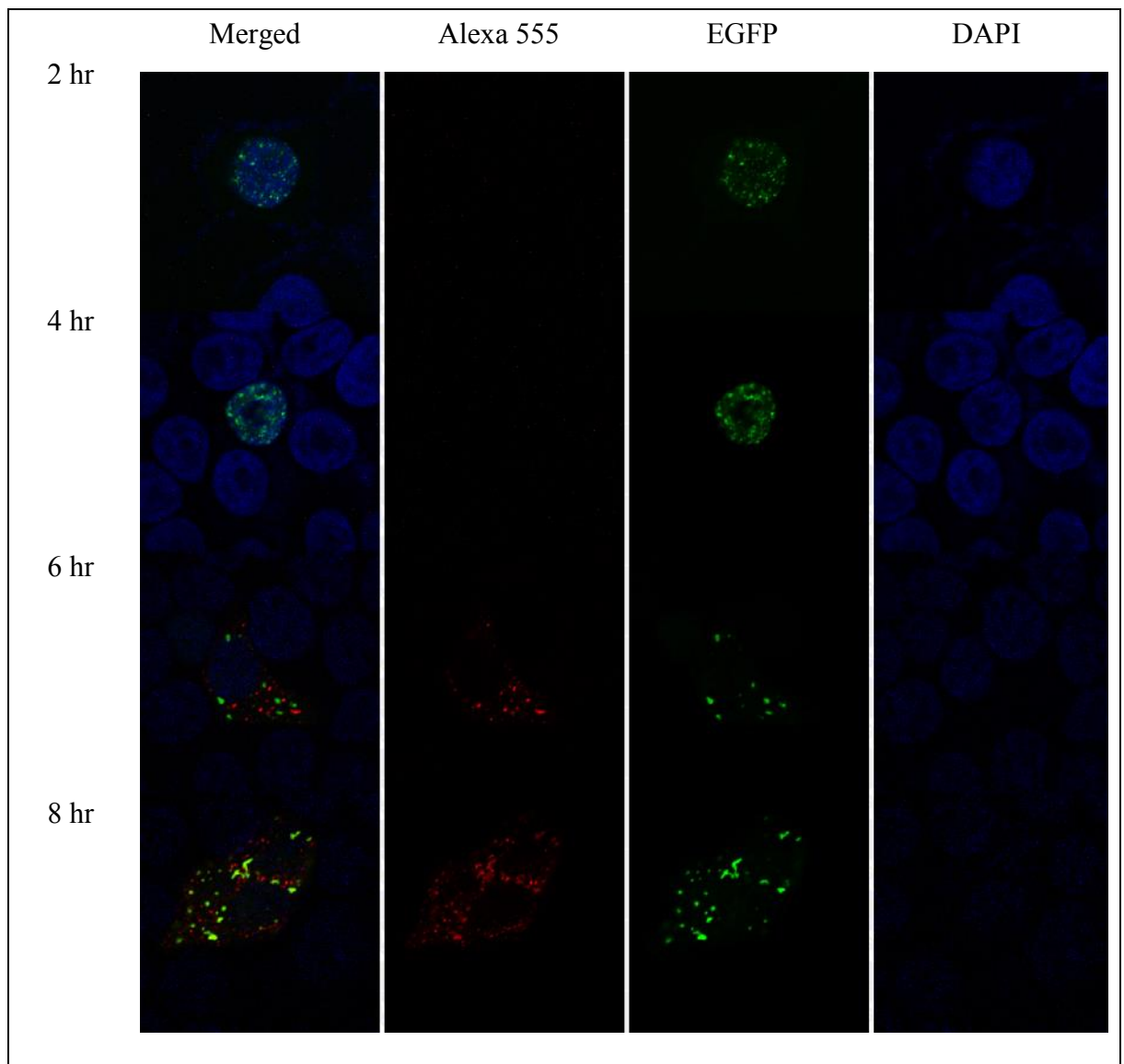


Figure 5-18 The localization of NONO with the replication complexes (time interval). GMK cells were grown on coverslip and transfected with pEGFP-NONO using lipofection. Cells were then infected with CAV-9 for 2, 4, 6 and 8 hr. Nuclei were stained with DAPI being visualized using a Nikon A1si confocal microscope. Nuclei were observed using DAPI (blue channel), expression of EGFP- NONO (green channel), and infected cells identified using anti-dsRNA antibody and secondary antibody labelled with Alexa 555 (red channel).

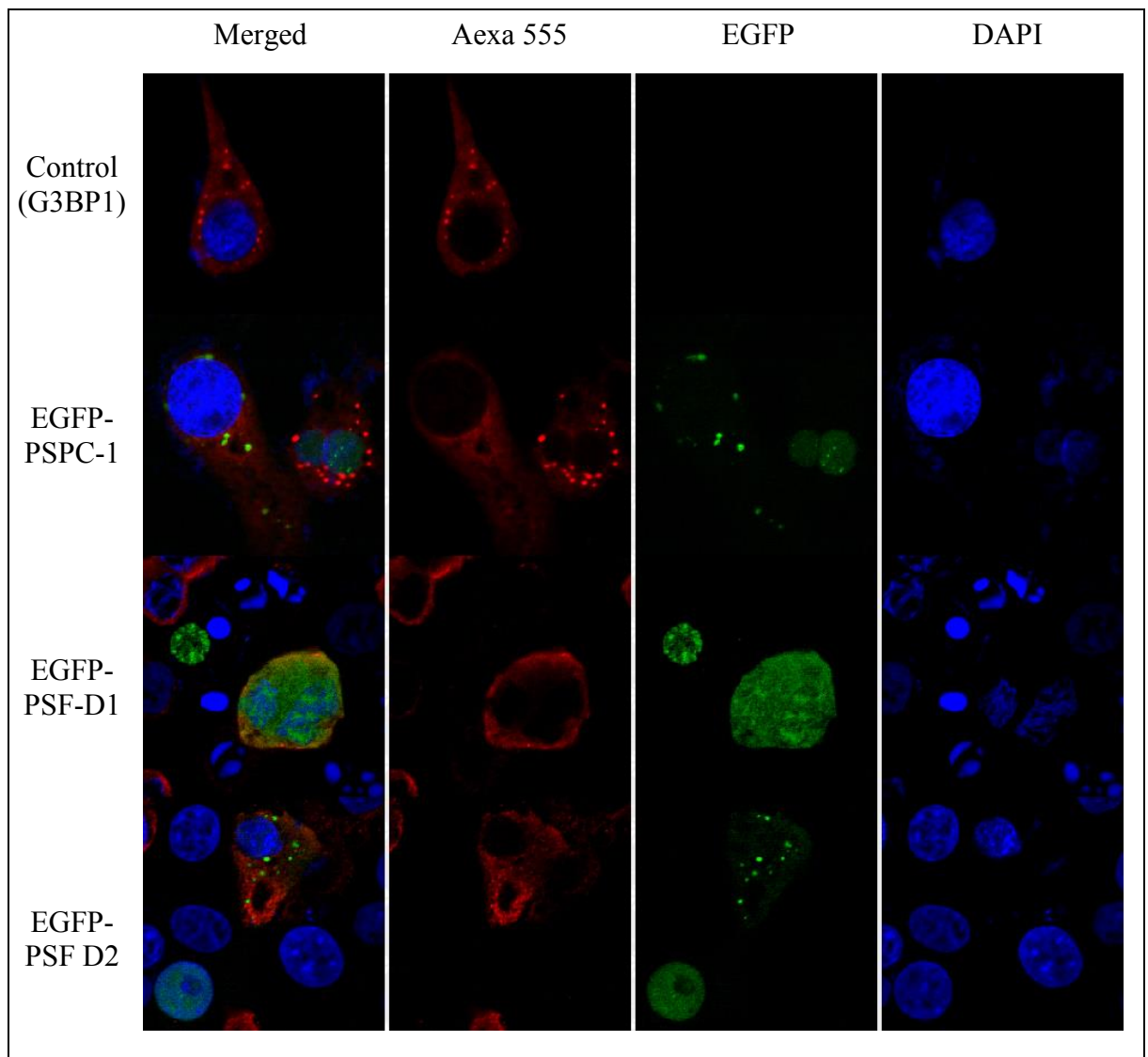


Figure 5-19 The effect of CAV-9 infection on the paraspeckles localization into stress granules (G3BP1). GMK cells were grown on coverslip and transfected with pEGFP-PSPC-1 or pEGFP-PSF deletions using lipofectin. Cells were then infected with CAV-9 for 8 hr. Nuclei were stained with DAPI being visualized using a Nikon A1si confocal microscope. Nuclei were observed using DAPI (blue channel), expression of EGFP- paraspeckles using (green channel), stress granules identified using anti-G3BP1 antibody and secondary antibody labelled with Alexa 555 (red).

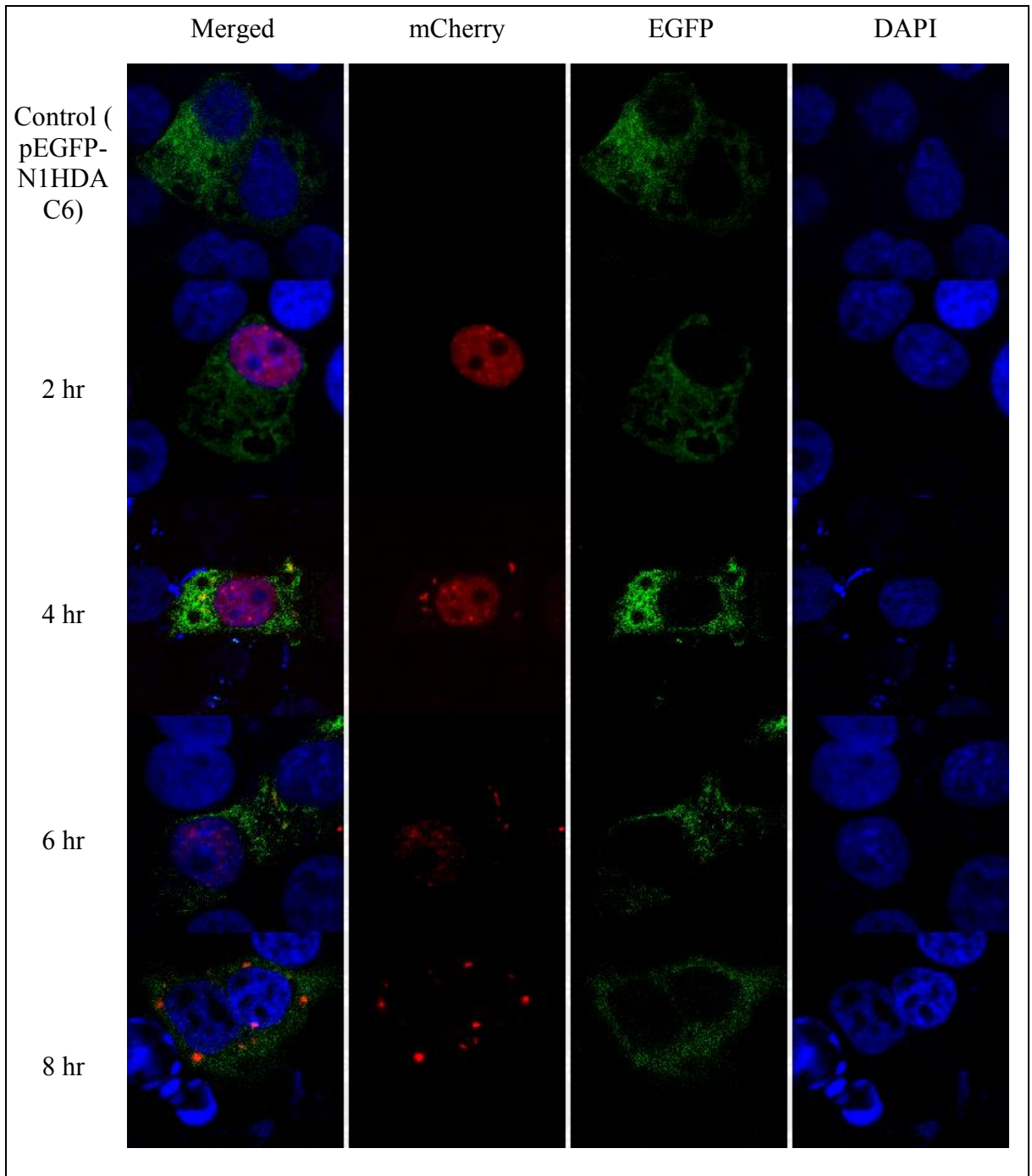


Figure 5-20 The effect of CAV-9 on the colocalization of mCherry-PSPC-1 and stress granules (Time interval). GMK cells were grown on coverslip and cotransfected with pEGFP-N1HDAC6 and pmCherry PSPC-1 using lipofectin. Cells were then infected with CAV-9 for 2, 4, 6 and 8 hr. Nuclei were stained with DAPI being visualized using a Nikon A1si confocal microscope. Nuclei were observed using DAPI (blue channel), the expression of pEGFP-N1HDAC6 using EGFP (green channel), the expression of mCherry PSPC-1 using mCherry (red channel).

GMK cells were also grown on coverslips and transfected with pEGFP-PSF D1 or pEGFP-PSF D2, then infected with CAV-9 for 8 hr. Cells were then fixed and immunostained with a polyclonal primary antibody specific for the P-body protein GW182 and goat anti-rabbit antibody as secondary antibody (Alexa fluor 568). Coverslips were then mounted on glass slides with mounting media including DAPI in order to stain the nuclei and visualized with a Nikon A1si confocal microscope (Figure 5-23). The GW182 distribution was punctate but not as clear as that seen using the pT7EGFP-C1HsRCK construct. There was little change in the cells shown to be infected due to the relocalisation of the EGFP-PSF D2 and no colocalisation between EGFP-PSF D2 and GW182. Infected cells cannot be identified in the EGFP-PSF D1 sample as this protein is not relocalised.

Overall, the results show that P-bodies are disrupted in CAV-9 infections, based on the EGFP-C1HsRCK experiment and there is no colocalisation between P-bodies and the PSPC-1 cytoplasmic granules in infected cells.

5.6.4 Autophagosome

LC3 is a well-known marker for autophagosomes (Cherra et al., 2010) while TP53INP1 is also located in autophagosomes (Seillier et al., 2012). Constructs encoding these proteins were used to find if the DBHS protein cytoplasmic granules were related to autophagosomes. GMK cells were grown on coverslips and transfected with pERFP-LC3 or TP53INP1-pEGFP. Some cells were co-transfected with pERFP-LC3 or pEGFP-PSPC-1 and infected, in order to study the localization while other were co-transfected with pERFP-LC3 and TP53INP1-pEGFP in order to study whether the autophagosome

proteins are distributed similarly or not. 24 hr post transfection cells were infected with CAV-9 for 8 hr or mock infected and fixed then immunostained. Then nuclei were stained with DAPI included in the hard-set mounting and cells were observed with a BX41 fluorescent microscope. The ERFP-LC3 in non-infected cells was distributed more in the nucleus than the cytoplasm, showing some distinctive speckled structures in the cytoplasm, while the ERFP-LC3 in infected cells was also diffused more in the nucleus with a small number of fine speckled structure in the cytoplasm (Figure 5-24). Non-infected TP53INP1-EGFP showed speckled structures in the cytoplasm with more distribution in the nucleus, while it is more diffused in the nucleus and the cytoplasm of the infected cells (Figure 5-24). The two autophagosome markers colocalised. In the cells cotransfected with pEGFP-PSPC-1 and pERFP-LC3, infected cells could be identified from the EGFP-PSPC-1 cytoplasmic granules which are seen in infected cells. In the infected cells there was some possible colocalisation between these PSPC-1 granules and ERFP-LC3 spots, but they did not perfectly colocalise (Figure 5-24).

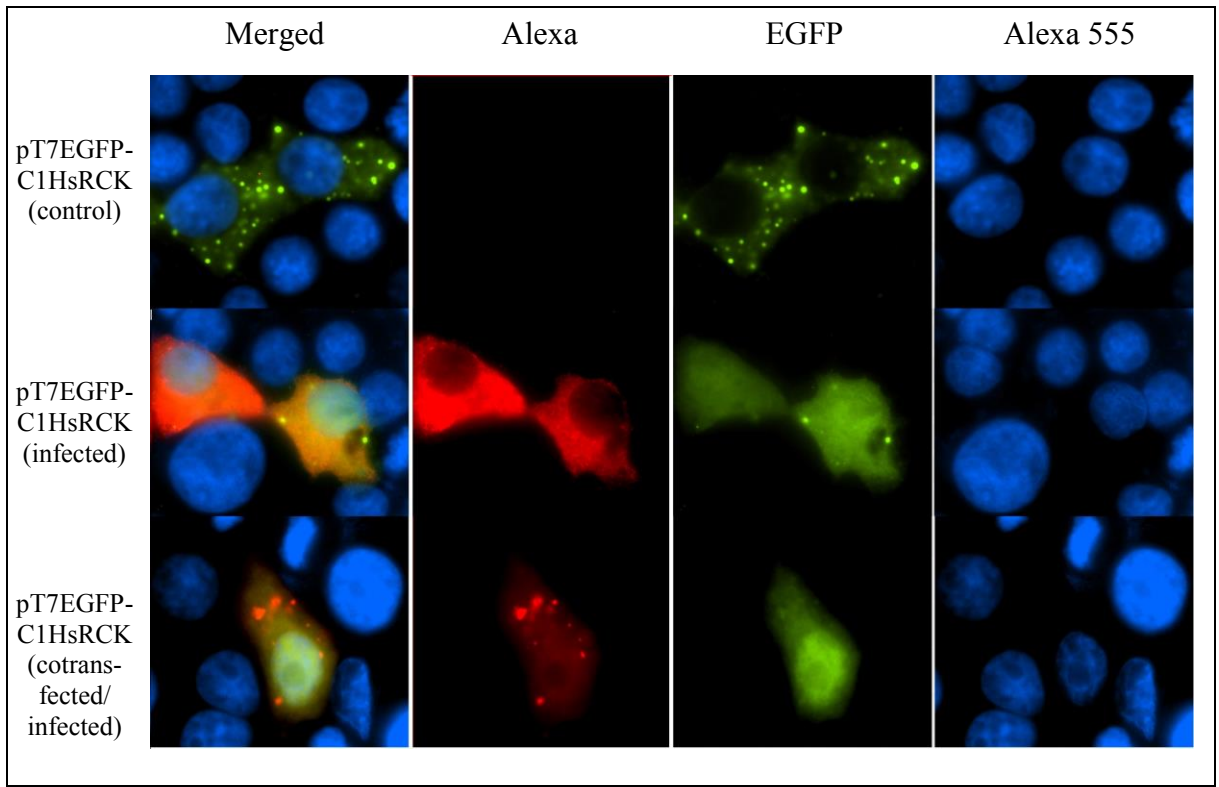


Figure 5-21 The effect of CAV-9 on the distribution of P body (pT7EGFP-C1HsRCK).

GMK cells were grown on coverslip and transfected with pT7EGFP-C1HsRCK, or cotransfected with pT7EGFP-C1HsRCK and pmCherry P5PC-1 using lipofectin. Cells were then infected with CAV-9 for 8 hr. Nuclei were stained with DAPI being visualized using a Nikon A1 plus wide field microscope. Nuclei were observed using DAPI (blue channel), expression of pT7EGFP- C1HsRCK (green channel), and infected cells identified using anti-CAV-9 antibody and secondary antibody labelled with Alexa 555 (red), or expression of mCherry P5PC-1 (mCherry).

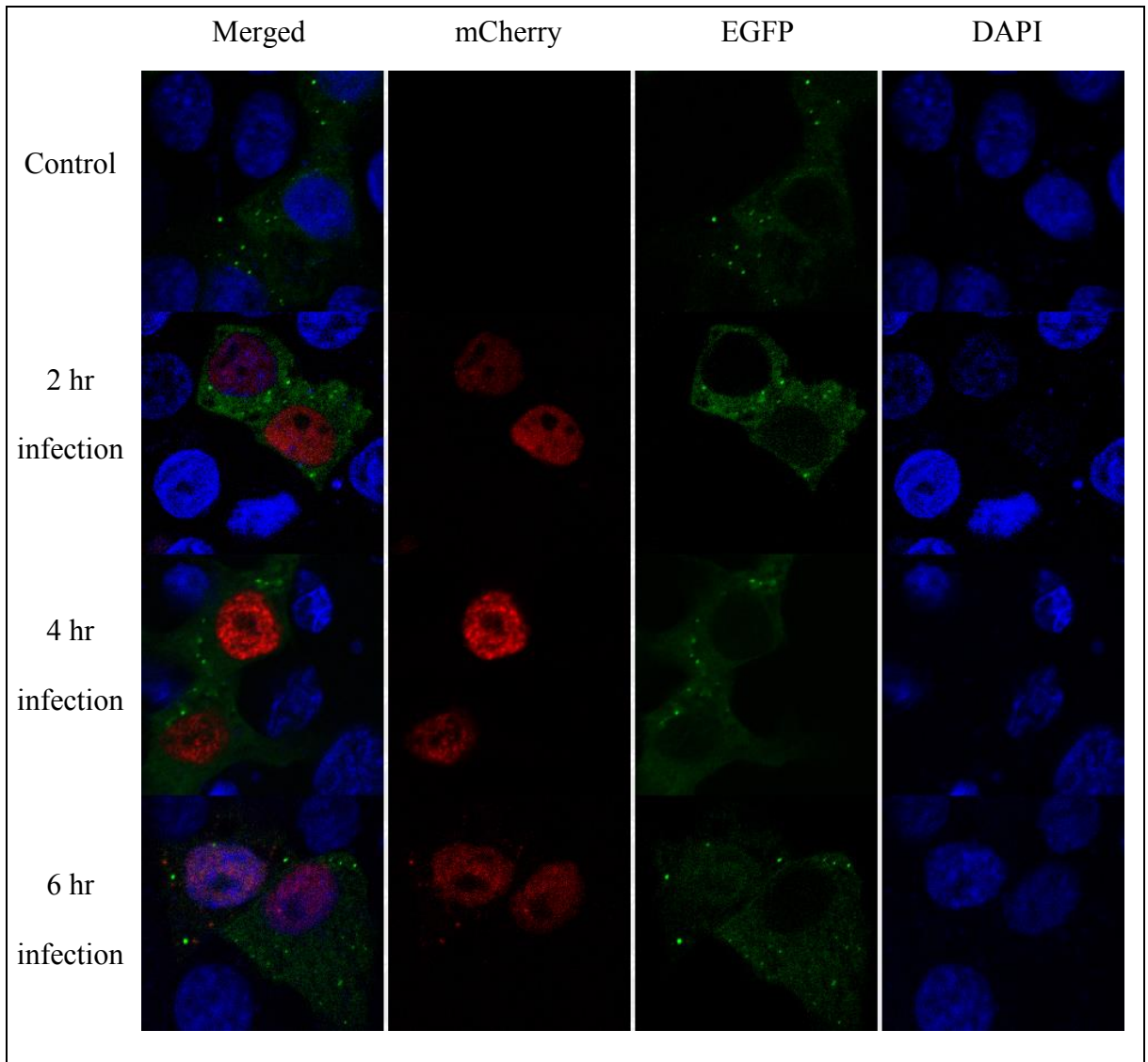


Figure 5-22 The effect of CAV-9 on the colocalization of mCherry-PSPC-1 and P body (Time interval). GMK cells were grown on coverslip and cotransfected with pT7EGFP-C1HsRCK and pmCherry PSCP-1 using lipofectin. Cells were then infected with CAV-9 for 2, 4 and 6 hr. Nuclei were stained with DAPI being visualized using a Nikon A1 plus wide field microscope. Nuclei were observed using DAPI (blue channel), the expression of pT7EGFP-C1HsRCK using EGFP (green channel), the expression of mCherry PSPC-1 using mCherry (red channel).

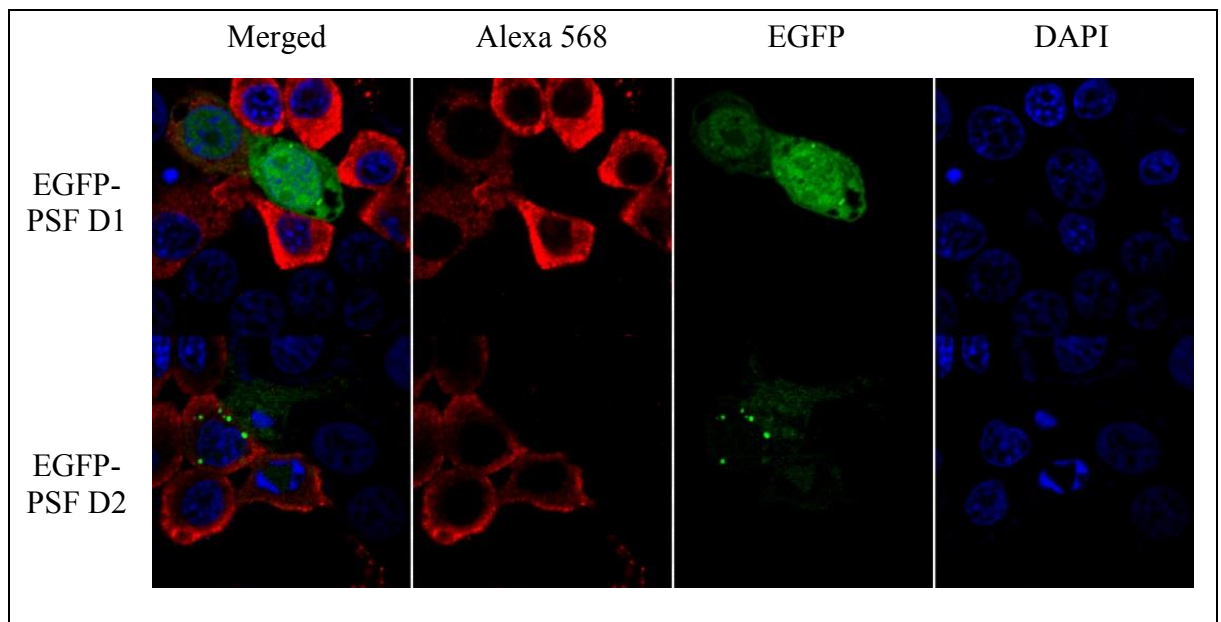


Figure 5-23 The effect of CAV-9 on the localization of EGFP-PSF deletions and P body. GMK cells were grown on coverslip and transfected with pEGFP-PSF deletions using lipofectin. Cells were then infected with CAV-9 8 hr. Nuclei were stained with DAPI being visualized using a Nikon A1si confocal microscope. Nuclei were observed using DAPI (blue channel), EGFP- PSF deletions using (green channel), and P body identified using anti-GW182 antibody and secondary antibody labelled with Alexa 568 (red).

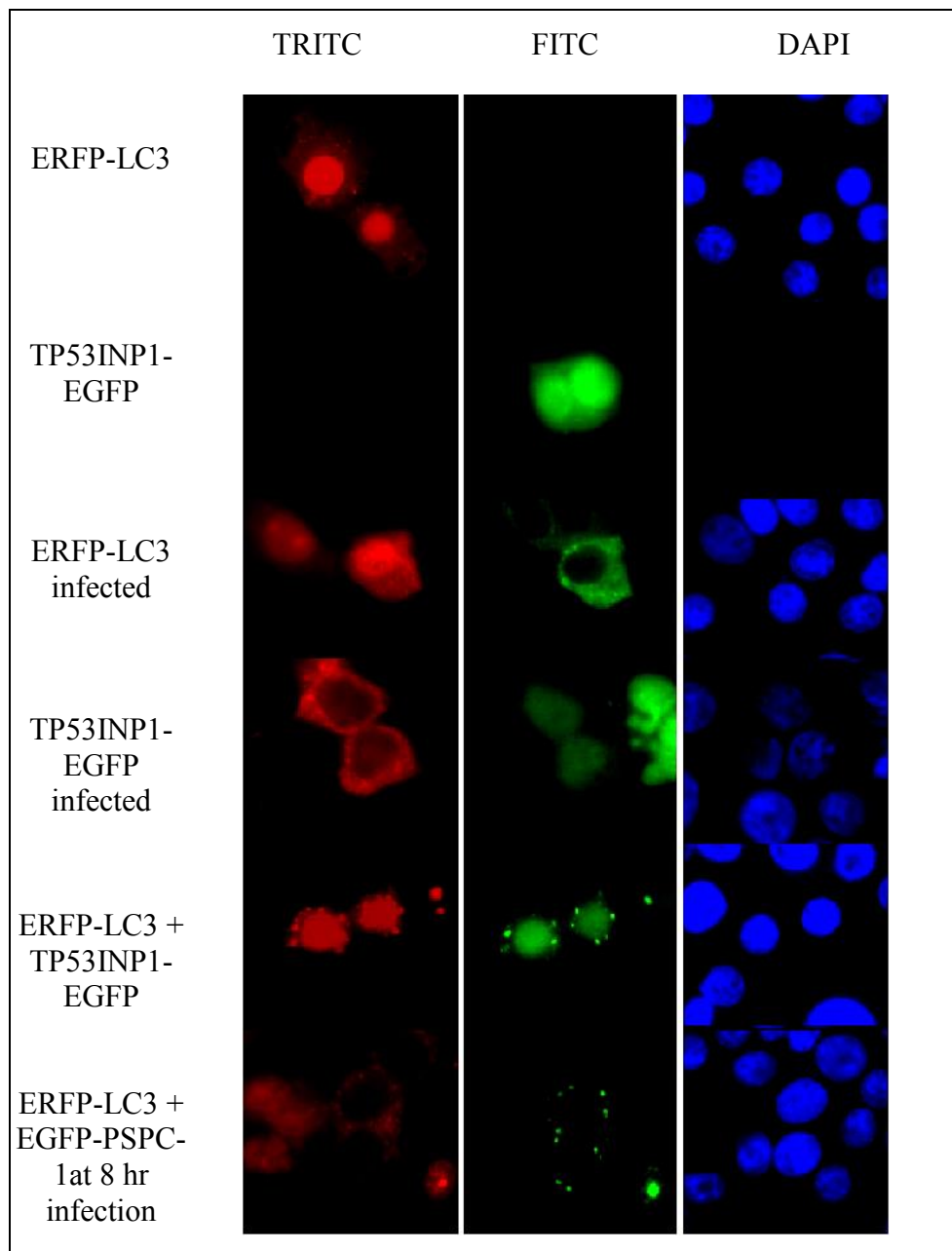


Figure 5-24 The effect of CAV-9 infection on the distribution of the Autophagosome structures and localization of these structures with EGFP-PSPC-1. GMK cells were grown on coverslip and transfected with pERFP-LC3/ TP53INP1-pEGFP. Cotransfected with pERFP-LC3 and pEGFP-PSPC-1 using lipofectin. Cells were then infected with CAV-9 for 8 hr. Nuclei were stained with DAPI being visualized using a BX41 fluorescent microscope. Nuclei were observed using DAPI filter (blue), expression of TP53INP1-EGFP / EGFP-PSPC-1 or Alexa 488 using FITC filter (green), ETRFP-LC3/ Alexafluor 555 with TRITC filter (red).

5.7 Discussion

This chapter describes work done to find the basis of the movement of the DBHS proteins PSF, PSPC-1 and NONO to cytoplasmic granules and to find if the cytoplasmic granules are the same as any known cellular structures.

5.7.1 Protease digestion

It has been found that some cellular proteins are cleaved by picornavirus proteases during infection and this inactivates the proteins or causes redistribution in the cell (Castelló et al., 2011). One of these proteins is eIF4G and Gradi et al. (2003) studied the cleavage site of the enterovirus 2A^{pro} on the human eIF4G, to find that the rhinovirus 2A cleaves the eIF4G protein at the sequence LSTR↓GPP, after position 681. The 2A^{pro} of enterovirus and rhinovirus was analysed previously by making a sequence logo from 22 unique 2A^{pro} cleavage sites. The weblogo showed that the site R↓G is one of the 2A^{pro} possible cleavage sites in these viruses (Blom et al., 1996). This analysis also shows that a 2A^{pro} cleavage site has the sequence (V,I,L)X(S/T) X↓G. Other previous studies observed that the rabbit eIF5B is cleaved proteolytically during enterovirus infection by the CVB3 3C^{pro} at VVEQ↓G and it was remarked that it is expected to be at the same position (sequence VMEQ↓G) in human eIF5B (de Breyne et al., 2008).

In this study we examined the predicted cleavage sites of the 2A^{pro} and 3C^{pro} of CAV-9 Griggs on the PSPC-1, in order to study the possible effect of these proteins on paraspeckle localization. No possible 2A cleavage sites were found in the PSPC-1 protein (data not shown). A weblogo analysis (Figure 5-1) showed that 3C^{pro} cleavage

sites in CAV-9 have the preferred sequence AXXQ↓G. A similar sequence was found at two positions in the PSCP-1 sequence and two deletion mutants were made that end at positions 178 (fragment 1) and 416 (fragment 2) (Figure 5-2). We found that in uninfected cells EGFP-PSCP-1 fragment 1 had an EGFP-like distribution, in the cell nucleus and cytoplasm, while EGFP-PSCP-1 fragment 2 had an unaffected distribution which was the same as EGFP-PSCP-1 (Figure 5-3). This suggested that 3C^{pro} cleavage sites are not likely to be involved in the relocalization, as could be expected that one of these deletion mutant proteins would be located in to cytoplasmic granules if 3C^{pro} cleavage was needed for the relocalisation. In infected cells (Figure 5-4) EGFP-PSCP-1 fragment 1 showed no relocalisation to the cytoplasmic granules, which suggest that the deleted part of the protein is needed for this relocalisation. EGFP-PSCP-1 fragment 2 was relocalised, showing that the part of the protein deleted is not needed for the relocalisation.

Little is known about PSCP-1 localization to the cytoplasm, but both RRM domains play an important role in the DBHS localization to paraspeckles (Passon et al., 2012). In fragment 1 part of RRM2 and all the coiled coil were deleted, while in fragment 2 both RRM domains and coiled coil domains are present in the deleted protein (Figure 5-25). The NLS domain, which is located at the C-terminus of the protein, is lost in both deletions. (Fox et al., 2005) studied the importance of these motifs for PSCP-1 localization by manipulating series of truncated and mutated forms of EYFP-PSCP1. They found that the deletion of N-terminal, C-terminal or both terminals did not affect the localization of the protein to paraspeckles. Then they removed one or both RRM motifs and coiled coil domain, and they found that the mutant that has both RRM2 and

coiled coil was able to localize to the paraspeckles. These findings suggesting that the RRM2 and coiled coil domains together are important for the localization. The coiled coil domain and most of RRM2 are lost in the fragment 1 deletion (diffuse distribution), but are both present in the fragment 2 deletion (paraspeckle distribution in uninfected cells, cytoplasmic granules in infected cells) (Figure 5-25). This may suggest that the domains needed for the cytoplasmic granule localization in infected cells are the same as those needed for paraspeckle localization.

In order to find if there is any proteolytic cleavage of PSpC-1 or PSF during infection, a Western blot was performed. There is no evidence of cleavage as there are no smaller bands seen. Western blot analysis is consistent with the idea that there is not a cleavage at a specific point by either 2A^{pro} or 3C^{pro} as no smaller products are produced in infected cells (Figure 5-5). Interestingly, PSF and PSpC-1 seem to be up-regulated early in infection and the levels decrease later in infection. This should be studied further to find if this is a cell response to overcome the virus infection or is induced by the virus to make its replication more efficient.

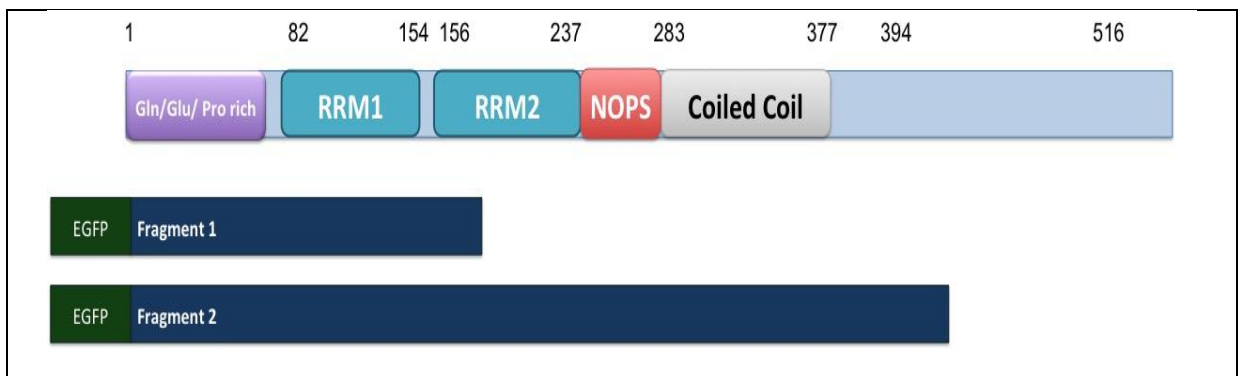


Figure 5-25 A schematic representation of the PSPC-1 wild type sequence and truncated proteins. The PSPC-1 domains are the N terminal Gln/Glu/Pro-rich domain, two RRM domains (1,2), a coiled coil domain, a NOPS region and a C-terminal domain that include the NLS. The two deletion mutants (fragment 1 and fragment 2) are aligned with the PSPC-1 sequence.

5.7.2 PSF phosphorylation sites

It has been found that the phosphorylation of PSF by BRK causes a relocation of the protein to the cytoplasm. A proteomic analysis of BRK found PSF as a BRK-interacting protein and also a substrate for BRK, which interacts with the PSF polyproline-rich motif at the N terminus, and a tyrosine at the C-terminus, which is then phosphorylated by the kinase. This phosphorylation causes the relocalization of PSF into the cytoplasm (Lukong et al., 2009). These findings suggested that phosphorylation of PSF during CAV-9 infection could be the main cause of the translocation to cytoplasmic granules during infection. Relocalization of some splicing factors within the nucleus is also believed to be due to phosphorylation, in this case of SR domains close to the C-terminus. Although PSF does not have SR domain, it shares some features with SR proteins (Shav-Tal et al., 2001). Another study carried out a proteomic analysis on MAP kinase to identify the binding proteins. MAP kinase is involved in cellular translation, as it interacts with cap-binding initiation factor complex. They identified PSF, together with NONO, as interacting proteins and PSF is phosphorylated at two sites by the MAP kinase (S8 and S283) (Buxadé et al., 2008). Galiotta et al. (2007) used a proteomic approach to identify anaplastic lymphoma kinase binding proteins and they found that PSF was interacting with the kinase, dependent on the active domain of the kinase. It was also found that PSF was phosphorylated at one site (tyrosine 293) and was delocalized to the cytoplasm, while when the PSF expressed alone it was distributed in the nucleus.

In this study we made mutagenesis dephosphorylation of the PSF at S8 and Y293, in order to examine the effect of the phosphorylation on the paraspeckle relocalisation to the

cytoplasm during CAV-9 infection (Figure 5-8). Results showed that both PSF S8A and Y293F were distributed into the cytoplasm similarly to the wild type in infected cells, although there were some differences in distribution in uninfected cells (Figure 5-7). It might be concluded that neither is important in localization to the cytoplasmic granules, but several other PSF sites are known to be phosphorylated and one of these could be important. Another possibility is to do a study by making mimic phosphorylation constructs of PSF.

It has been found that sumoylation promote PSF transcriptional repression properties (Vethantham. and Manley, 2009). PSF and NONO were also identified as putative SUMO targets. It has also been found that SUMO-3 plays a major role in nuclear localization of other nuclear proteins, such as PML protein, and is needed for its localization into PML-NBs. The knockdown of SUMO-3 caused a decrease in the number of PML-NBs (Fu et al., 2005). We constructed a mutant of PSF that cannot be sumoylated. In uninfected cells this was diffuse in the nucleus, but was relocated to cytoplasmic granules as normal PSF (Figure 5-7-Figure 5-8).

To confirm the distribution of PSF mutants, we attempted to do colocalization with mCherry-PSPC-1. This seemed to change the distribution of the phosphorylation mutants in uninfected cells to be more like the normal PSF distribution and the mutants colocalized with the mCherry-PSPC-1 (Figure 5-9) The sumoylation mutant was still diffuse in the nucleus and mCherry-PSPC-1 has a similar distribution. Probably, the analysis is complicated by the fact that PSPC-1 and PSF interact and so some of the effects of the mutation may be overcome by the presence of large amount of wild type PSPC-1. In infected cells, all the mutants seemed to localize to the same cytoplasmic

granules containing PSPC-1 (Figure 5-10), which suggests that the mutations are not affecting the relocalization, although again the fact that PSPC-1 and PSF interact may complicate the results.

5.7.3 PSF deletion mutants

PSF protein contains a Gln/Glu/Pro-rich region, two RRM domains, a coiled coil domain, NOPS region and two NLSs at the C-terminal end (Figure 5-26). It has been found that the loss of RRM2 results in a diffuse PSF accumulation in the nucleus, which suggested that RRM2 is required for subnuclear localization. However, PSF is more likely to localize to speckles through RRM1 (Dye and Patton, 2001). The localization of three truncations of EGFP-PSF was analysed after transfection into GMK cells (Figures Figure 5-12-Figure 5-14). A PSF construct lacking the C-terminal half of the protein (PSF XB) was completely diffused in the nucleus and cytoplasm (Figure 5-12). Infection with CAV-9 did not change the localization. This suggests that sequences needed for both paraspeckle and cytoplasmic granule localization are present in the deleted region. The same results were obtained from the construct lacking just part of the NOPS region, the coiled coil domain and the C-terminal domain (Figure 5-13). The deletion of this part of the protein, which contains an the NLS, is probably the reason for the mutant being present in the cytoplasm (Figure 5-13) A recent study by (Lee et al., 2015) made a truncated EYFP-PSF construct, PSF276-555, which contain both RRM motifs and coiled coil domain and found there is no localization to the paraspeckles. They identified, from the structure of the protein, a further region, up to position 598, which allows PSF to

form polymers and this polymerization domain is required for PSF localization. They also found that amino acids 1-275 are not important for paraspeckle localization.

In our work, another deletion construct, EGFP-PSF D2, was made by adding sequences up to position 606, including the rest of the coiled coil domain and the polymerization domain shown to be important by (Lee et al., 2015). The results show an improvement in the paraspeckle localization in uninfected cells, but there seems to a lot of the mutant present in the cytoplasm with a punctate distribution. Cytoplasmic granules were seen in infected cells. These finding are partially consistent with the (Lee et al., 2015) data. Attempts to colocalize with mCherry-PSPC-1 did not change the EGFP-PSF D1 distribution. However, EGFP-PSF D2 had a more typical appearance, with more protein seen punctate in the nucleus, but with still some present in the cytoplasm in uninfected cells. There was good colocalisation into cytoplasmic granules in infected cells (Figure 5-15).

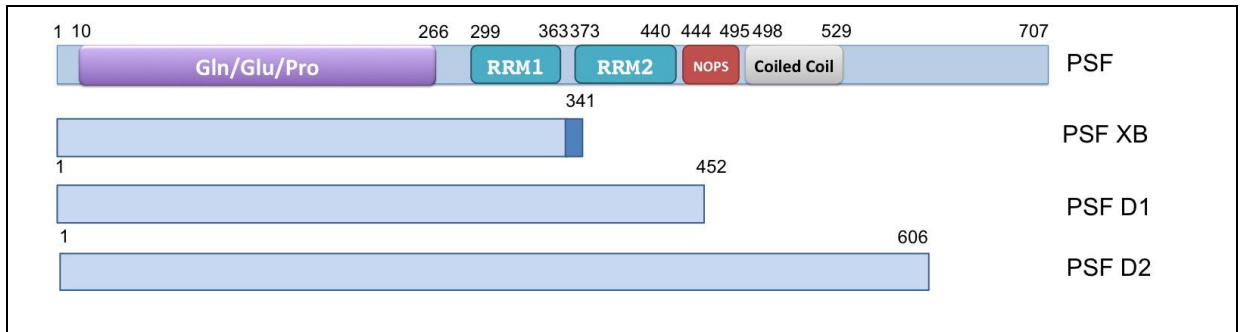


Figure 5-26 A schematic representation of the PSF wild type sequence and truncated proteins. PSF contains an N-terminal Gln/Glu/Pro-rich domain, two RRM domains (1,2), a coiled coil domain, a NOPS region and a C-terminal domain that include the NLS. The deletion mutants PSF XB, D1 and D2 are aligned with the PSpC-1 sequence.

5.7.4 Attempts to identify the cytoplasmic granules

CAV-9 infection clearly causes redistribution of paraspeckle proteins by translocation from the nucleus to cytoplasmic granules. In order to investigate the cytoplasmic granules to which the proteins were translocated, a number of cytoplasmic candidates that are associated with RNA were studied. It is believed that picornavirus infection causes rearrangement of cellular membrane into vesicles which then assemble into RNA replication complexes. During PV infection, the replication complexes may form the required supplements for rapid and efficient RNA replication. The formation of these complexes depends on several virus non-structural proteins (Egger et al., 2000). These complexes also help to segregate the products from templates during viral infection (Tao and Ye, 2010). In this study we examined the colocalisation of replication complexes and PSF, PSPC-1 and NONO at different time points (Figure 5-16-Figure 5-18). Complexes were labelled using a monoclonal dsRNA antibody and Alexafluor goat anti-mouse as a secondary antibody. The results showed that there is no localization between the complexes and paraspeckle proteins. This may suggest that the relocalisation of paraspeckle proteins is not involved in virus RNA replication directly. This is unexpected as a previous study found that NONO was needed for virus replication in the case of poliovirus (Lenarcic et al., 2013).

Enterovirus infection induces the cellular degradation process which is called autophagy. The induction or inhibition of autophagy causes alteration to enterovirus infection (Rhoades et al., 2011). Paraspeckle protein localization to autophagosomes was therefore also studied. The findings showed no clear colocalization between the paraspeckle

proteins and autophagosomes, as the punctuate structures distribution seen for paraspeckle proteins is largely lacking (Figure 5-24). However, some spots showed some colocalisation and this should be studied further.

It has been found that AUF-1 protein is cleaved during PV or rhinovirus infection by 2A^{pro}, 3C^{pro} or 3CD^{pro}, which also play a major role in picornavirus replication. It has been reported that the protein is mainly localized in the nucleus, but during PV infection there was an alteration of the AUF-1 distribution. 4 hr after infection there was a huge localization of AUF-1 to the cytoplasm displayed a distinct localization pattern (Rozovics et al., 2012). AUF-1 interacts with the 5'UTR of enteroviruses and cause degradation of the viral RNA. Under cellular stress condition it was found that AUF-1 translocates to stress granules. These stress granules are involved in mRNA translation inhibition (David et al., 2007). Several other RNA viruses are known to cause changes to stress granules and to another class of RNA-containing cytoplasmic structures, the P-bodies (reviewed by Reineke and Lloyd, 2013). Several proteins are known to be present in stress granules, including G3BP and TIA1. In our experiments, CAV-9 infection seemed to disrupt both stress granules and P-bodies formation, as the marker G3BP was located throughout the cytoplasm and not in spots in infected cells (Figure 5-19). P-bodies markers were also redistributed in infected cells, in this case to a diffuse pattern in the cytoplasm and nucleus (Figure 5-21-Figure 5-23). There was no colocalisation with PSPC-1 cytoplasmic granules.

It seems that the cytoplasmic granules are not P-bodies and are probably not stress granules. However, in a recent study on CBV-3 infection (Wu et al., 2014), it was found that stress granules containing G3BP and TIA1, as well as AUF-1, are produced early in

infection (3 hours), but while TIA1 remains in granules, G3BP seems to lose its punctate appearance later (6 hours), probably due to cleavage by CBV-3 3C^{pro}, as it is known that this occurs in enterovirus infections (Reineke and Lloyd, 2013). As we looked at G3BP only after 8 hours, it may be that we missed an early colocalisation with G3BP. It is important to do a G3BP timecourse/colocalisation with PSPC-1 and also to investigate if TIA1 colocalises with PSPC-1 and the other paraspeckle proteins. However, the other stress granule marker that we used, EGFP-N1HDAC6, did not colocalise with PSPC-1 at any time point.

5.7.5 Conclusion

The experiments performed have shown that redistribution of the DBHS paraspeckle proteins is probably not due to proteolytic processing. The redistribution seems to depend on the same parts of the protein that are needed for paraspeckle localization, which suggests that interactions between these proteins, which are known to involve regions like RRM2 and the coiled coil domain, are important to this process. The cytoplasmic structures which contain these proteins do not seem to correspond to any of the candidates we tested and could be previously unknown structures, or ones which are produced only during virus infection. It will be interesting to define what role these structures have in virus infection.

Chapter 6

General discussions

Most virus diseases cause self-limiting illnesses and no specific antiviral drug is required for therapy. In a few other cases there are effective vaccines. Currently, there are only antiviral drugs available to target four main viruses, HIV-1, herpes virus, hepatitis virus and influenza virus (Razonable, 2011). There are several drugs to treat HIV-1, and these target a number of different steps of virus replication. All anti-herpes viral drugs are based on the inhibition of viral replication and act on viral DNA polymerase. Interferon and/or combinations of nucleotide analogues can be used to treat virus hepatitis, especially that caused by hepatitis C. The most useful anti-influenza drugs target the virus neuraminidase protein and affect release from infected cells. However, there are some issues with the available antiviral drugs such as drug resistance. The major mechanisms for drug resistance are mutations in genes encoding the target of the drug (Razonable, 2011). Targeting cellular proteins or mechanisms may mean that resistance is less of a problem, because the target cannot change, although toxicity could be a problem.

The presence of many serotypes (over 250) is a problem for vaccines against members of the *Enterovirus* genus of *Picornaviridae*. The question is, is it possible to make a drug that targets all these related viruses? To do that we need to know more about how these viruses interact with the host cell. The thesis concentrated on the changes that occur to nuclear proteins when cells are infected with a typical enterovirus, CAV-9. Few enteroviruses, mainly PV and EV-71 have been studied in terms of nuclear protein redistribution and CAV-9 was used as it belongs to a different *Enterovirus* species from PV and EV-71 and so it is useful to find how general the mechanisms used in replication are, as this will give an idea of how useful they are for the design of antiviral drugs.

Several nuclear proteins have been shown now to be affected by RNA virus infection and have an effect on replication (Table 6-1). We found that CAV-9 had some minor effects on some of these proteins, particularly PML and nucleolin, but the clearest effect was on DBHS proteins which are key components of the paraspeckles. These nuclear structures have been little-studied in virus infected cells and our observation is novel.

There was a major relocalization in the paraspeckle proteins during viral infection and it would be interesting to understand what that means for cell gene expression and also how could the virus be using these proteins. Paraspeckles are involved in processes such as RNA processing, including splicing, RNA transport and retention in the nucleus. Picornaviruses affect transcription (through cleavage of transcription factors such as Oct-I and the TATA box binding transcription factor) and translation (cleavage of factors such as eIF4G, PAPB) (Castelló et al., 2011). Maybe they also affect processing and export of cell mRNA and inhibit gene expression through this pathway as well. The complete relocalisation of these proteins presumably means that their normal paraspeckle functions cannot take place. It would be interesting to analyse the effect of infection on splicing and RNA export. The functional significance of the proteins should be tested by knockdown of PSF, NONO or PSPC-1, in order to examine whether the virus grows better or not grows at all i.e. do the effects seen benefit the host or the virus? It was previously found that knock down of NONO decrease the amplification of PV and that as NONO is required for efficient translation and positive sense RNA synthesis (Lenarcic et al., 2013).

In this study we tried to investigate the mechanism of the redistribution. In several viruses, proteolytic digestion affects cell proteins, such as eIF4G which was cleaved by

rhinovirus 2A^{pro} which results in reduction of capped mRNA translation (Haghighat et al., 1996). Another protein cleaved by picornaviruses 3C^{pro} is PTB, which also inhibited the cellular translation (Kanda et al., 2010). La protein was also cleaved by PV 3C^{pro} (Shiroki et al., 1999). CAV-9 proteolytic constructs were made and analyzed. There was an issue with CAV-9 2A^{pro} as no cotransfected cells could be obtained. It may be useful to use an inducible system, e.g. Tet on/Tet off or a construct with a weaker promoter. 3C had a great effect on cells, including nuclear condensation, but the effect on the proteins being studied were not similar to redistribution seen in infected cells. In the case of the DBHS proteins, it was confirmed that the redistribution is not related to the proteolytic activity as seen in the Western blot results, as there was no cleavage of the proteins. So, proteolytic digestion may not be important. Non structural proteins such as CAV-9 3A and HPeV-1 2B caused relocalization of PSPC-1 to the nucleolus or peri-nucleolar caps. Although this was not similar to that seen in infected cells, it may indicate that these non-structural proteins may be able to affect the cell cycle or host-cell transcription, as PSPC-1 and NONO are relocated to similar structures when transcription is prevented (Fox et al., 2005) and during G1/S arrest (Shav-Tal et al., 2001). A link between these non-structural proteins and the nucleus has not been made before and so our work may open up a new area for research.

We produced several PSF mutants. Some of these prevented phosphorylation of sites known to be important in PSF relocalisation and one was a mutant where sumoylation was not possible. None of these had an effect on relocalisation during CAV-9 infection. Other mutants were deletion mutants. These confirmed the importance of sequences between positions 452 and 606 of PSF in paraspeckle localization and the same region is

also important in cytoplasmic granule localization in infected cells. Further mutants need to be made to find other parts of the protein involved in localization.

We also tried to study the cytoplasmic structures where the paraspeckle proteins are localized, but it seems like they do not relocate in these candidates and they might be novel structures. A mass spectrometry analysis is suggested to analyze PSF binding protein in infected cells, in order to examine whether those are novel structures and what else is in them. It would also be interesting to know if they contain NEAT-1 or virus RNA by performing FISH. Another experiment that should be performed is testing different viruses and examines the effect of these viruses on paraspeckles. It is known that infection by HPeV-1 also causes some relocalisation of PSPC-1, but this is within the nucleus and less obvious than that seen in CAV-9 infected cells (Mutabagani, 2012). However, as HPeV-1 and CAV-9 are quite far apart in the *Picornaviridae* tree, it suggests that paraspeckle proteins may be common targets during virus infections.

We have identified a novel redistribution of key proteins in the nucleus. If this is proved to be required by the virus, then it could be a potential drug target for the development of a new class of antiviral agents.

Table 6-1 A list of some nuclear proteins were affected by RNA virus infection and have an effect on replication

Nuclear protein	Nuclear location	Virus	Significance	Reference
PML	PML-NBs	PV	Stimulates PML phosphorylation and induces its movement from the nucleoplasm to the nuclear matrix	(Pampin et al., 2006)
PML	PML-NBs	EMCV	Decrease in the protein level by 3C ^{pro}	(El Mchichi et al., 2010)
Nucleolin	Nucleolus-dense fibrillar	PV	Relocalization from nucleus to the cytoplasm. Nucleolin stimulates viral IRES-mediated translation.	(Waggoner and Sarnow, 1998, Izumi et al., 2001)
B23	Nucleolus	EMCV	Shutdown of RNA Pol II transcription, and cap-dependent translation	(Aminev et al., 2003)
AUF-1	Nucleus	PV	Cleaved by the viral proteinase 3CD and AUF1 can then interact with the IRES	(Cathcart et al., 2013)
hnRNPA1	Nucleus	EV71	Relocalised from nucleus to cytoplasm and binds to IRES	(Lin et al., 2009a)

References

- ADAMS, M. J., LEFKOWITZ, E. J., KING, A. M. Q., BAMFORD, D. H., BREITBART, M., DAVISON, A. J., GHABRIAL, S. A., GORBALENYA, A. E., KNOWLES, N. J., KRELL, P., LAVIGNE, R., PRANGISHVILI, D., SANFAÇON, H., SIDDELL, S. G., SIMMONDS, P. A. & CARSTENS, E. B. 2015. Ratification vote on taxonomic proposals to the International Committee on Taxonomy of Viruses (2015). *Arch. Virol.*, 160, 1837-1850.
- AGOL, V. I. & GMYL, A. P. 2010. Viral security proteins: counteracting host defences. *Nature Reviews Microbiology*, 8, 867-878.
- AL-SUNAJDI, M., WILLIAMS, Ç. H., HUGHES, P. J., SCHNURR, D. P. & STANWAY, G. 2007. Analysis of a new human parechovirus allows the definition of parechovirus types and the identification of RNA structural domains. *Journal of virology*, 81, 1013-1021.
- AMINEV, A. G., AMINEVA, S. P. & PALMENBERG, A. C. 2003. Encephalomyocarditis viral protein 2A localizes to nucleoli and inhibits cap-dependent mRNA translation. *Virus research*, 95, 45-57.
- ARMER, H., MOFFAT, K., WILEMAN, T., BELSHAM, G. J., JACKSON, T., DUPREX, W. P., RYAN, M. & MONAGHAN, P. 2008. Foot-and-mouth disease virus, but not bovine enterovirus, targets the host cell cytoskeleton via the nonstructural protein 3Cpro. *Journal of virology*, 82, 10556-66.
- BACK, S., KIM, Y., KIM, W., CHO, S., OH, H., KIM, J. & JANG, S. 2002. Translation of polioviral mRNA is inhibited by cleavage of polypyrimidine tract-binding proteins executed by polioviral 3C(pro). *J Virol*, 76, 2529 - 2542.
- BANERJEE, R. & DASGUPTA, A. 2001. Interaction of picornavirus 2C polypeptide with the viral negative-strand RNA. *Journal of General Virology*, 82, 2621-2627.
- BARCO, A., FEDUCHI, E. & CARRASCO, L. 2000. Poliovirus Protease 3Cpro Kills Cells by Apoptosis. *Virology*, 266, 352-360.
- BARYGINA, V., VEIKO, V. & ZATSEPIN, O. 2010. Analysis of nucleolar protein fibrillarin mobility and functional state in living HeLa cells. *Biochemistry (Moscow)*, 75, 979-988.
- BELSHAM, G. J. 2009. Divergent picornavirus IRES elements. *Virus Research*, 139, 183-192.

- BERNARDI, R. & PANDOLFI, P. P. 2007. Structure, dynamics and functions of promyelocytic leukaemia nuclear bodies. *Nature reviews Molecular cell biology*, 8, 1006-1016.
- BERTRAND, L., LEIVA-TORRES, G. A., HYJAZIE, H. & PEARSON, A. 2010. Conserved residues in the UL24 protein of herpes simplex virus 1 are important for dispersal of the nucleolar protein nucleolin. *Journal of virology*, 84, 109-118.
- BLOM, N., HANSEN, J., BRUNAK, S. & BLAAS, D. 1996. Cleavage site analysis in picornaviral polyproteins: discovering cellular targets by neural networks. *Protein Science*, 5, 2203-2216.
- BOND, C. S. & FOX, A. H. 2009. Paraspeckles: nuclear bodies built on long noncoding RNA. *The Journal of cell biology*, 186, 637-44.
- BRAMLEY, T. J., LERNER, D. & SARNES, M. 2002. Productivity losses related to the common cold. *Journal of occupational and environmental medicine*, 44, 822-829.
- BRAND, P., LENSER, T. & HEMMERICH, P. 2010. Assembly dynamics of PML nuclear bodies in living cells. *PMC biophysics*, 3, 3.
- BROYLES, R. & ARNOLD, P. 2009. Viral Genetics: Enteroviruses. *Hub, Bright*.
- BUENZ, E. J. & HOWE, C. L. 2006. Picornaviruses and cell death. *Trends in microbiology*, 14, 28-36.
- BUXADÉ, M., MORRICE, N., KREBS, D. L. & PROUD, C. G. 2008. The PSF· p54nrb Complex is a novel Mnk substrate that binds the mRNA for tumor necrosis factor α . *Journal of Biological Chemistry*, 283, 57-65.
- CAMPANELLA, M., DE JONG, A., LANKE, K., MELCHERS, W., WILLEMS, P., PINTON, P., RIZZUTO, R. & VAN KUPPEVELD, F. 2004. The coxsackievirus 2B protein suppresses apoptotic host cell responses by manipulating intracellular Ca²⁺ homeostasis. *J Biol Chem*, 279, 18440 - 18450.
- CARRACEDO, A., ITO, K. & PANDOLFI, P. P. 2011. The nuclear bodies inside out: PML conquers the cytoplasm. *Current Opinion in Cell Biology*, 23, 360-366.
- CARTHY, C. M., GRANVILLE, D. J., WATSON, K. A., ANDERSON, D. R., WILSON, J. E., YANG, D., HUNT, D. W. C. & MCMANUS, B. M. 1998.

- Caspase Activation and Specific Cleavage of Substrates after Coxsackievirus B3-Induced Cytopathic Effect in HeLa Cells. *Journal of Virology*, 72, 7669-7675.
- CASTELLÓ, A., ÁLVAREZ, E. & CARRASCO, L. 2011. The multifaceted poliovirus 2A protease: regulation of gene expression by picornavirus proteases. *BioMed Research International*, 2011.
- CATHCART, A. L., ROZOVICS, J. M. & SEMLER, B. L. 2013. Cellular mRNA Decay Protein AUF1 Negatively Regulates Enterovirus and Human Rhinovirus Infections. *Journal of Virology*, 87, 10423-10434.
- CATHCART, A. L. & SEMLER, B. L. 2014. Differential restriction patterns of mRNA decay factor AUF1 during picornavirus infections. *The Journal of General Virology*, 95, 1488-1492.
- CHAKRABORTY, S., KUMAR, N., DHAMA, K., VERMA, A. K., TIWARI, R., KUMAR, A., KAPOOR, S., SINGH, S. V., KAPOOR, S. & JOSHI, R. 2014. Foot-and-mouth disease, an economically important disease of animals. *Advances in Animal and Veterinary Sciences*, 2, 1-18.
- CHANG, J.-T. 2015. Genome and Infection Characteristics of Human Parechovirus Type 1.
- CHANG, K. H., AUVINEN, P., HYYPIÄ, T. & STANWAY, G. 1989. The nucleotide sequence of coxsackievirus A9; implications for receptor binding and enterovirus classification. *Journal of General Virology*, 70, 3269-3280.
- CHASE, A. J. & SEMLER, B. L. 2012. Viral subversion of host functions for picornavirus translation and RNA replication. *Future virology*, 7, 179-191.
- CHERRA, S. J., KULICH, S. M., UECHI, G., BALASUBRAMANI, M., MOUNTZOURIS, J., DAY, B. W. & CHU, C. T. 2010. Regulation of the autophagy protein LC3 by phosphorylation. *The Journal of cell biology*, 190, 533-539.
- CHING, R. W., DELLAIRES, G., ESKIW, C. H. & BAZETT-JONES, D. P. 2005. PML bodies: a meeting place for genomic loci? *Journal of cell science*, 118, 847-54.
- CHIRAMEL, A. I., BRADY, N. R. & BARTENSCHLAGER, R. 2013. Divergent Roles of Autophagy in Virus Infection. *Cells*, 2, 83-104.

- COHEN, M. S., CHEN, Y. Q., MCCAULEY, M., GAMBLE, T., HOSSEINIPOUR, M. C., KUMARASAMY, N., HAKIM, J. G., KUMWENDA, J., GRINSZTEJN, B. & PILOTTO, J. H. 2011. Prevention of HIV-1 infection with early antiretroviral therapy. *New England journal of medicine*, 365, 493-505.
- CONG, R., DAS, S., UGRINOVA, I., KUMAR, S., MONGELARD, F., WONG, J. & BOUVET, P. 2012. Interaction of nucleolin with ribosomal RNA genes and its role in RNA polymerase I transcription. *Nucleic acids research*, 40, 9441-9454.
- COPELAND, A. M., ALTAMURA, L. A., VAN DEUSEN, N. M. & SCHMALJOHN, C. S. 2013. Nuclear Relocalization of Polyadenylate Binding Protein during Rift Valley Fever Virus Infection Involves Expression of the NSs Gene. *Journal of Virology*, 87, 11659-11669.
- CURRY, S., FRY, E., BLAKEMORE, W., ABU-GHAZALEH, R., JACKSON, T., KING, A., LEA, S., NEWMAN, J. & STUART, D. 1997. Dissecting the roles of VP0 cleavage and RNA packaging in picornavirus capsid stabilization: the structure of empty capsids of foot-and-mouth disease virus. *Journal of virology*, 71, 9743-9752.
- DALLDORF, G. & GIFFORD, R. 1951. Clinical and Epidemiologic Observations of Coxsackie-Virus Infection. *New England Journal of Medicine*, 244, 868-873.
- DALLDORF, G. & SICKLES, G. M. 1948. An Unidentified, Filtrable Agent Isolated From the Feces of Children With Paralysis. *American Association for the Advancement of Science. Science*, 61-4.
- DAMBARA, A., MORINAGA, T., FUKUDA, N., YAMAKAWA, Y., KATO, T., ENOMOTO, A., ASAI, N., MURAKUMO, Y., MATSUO, S. & TAKAHASHI, M. 2007. Nucleolin modulates the subcellular localization of GDNF-inducible zinc finger protein 1 and its roles in transcription and cell proliferation. *Experimental cell research*, 313, 3755-3766.
- DAVID, P. S., TANVEER, R. & PORT, J. D. 2007. FRET-detectable interactions between the ARE binding proteins, HuR and p37AUF1. *RNA*, 13, 1453-1468.
- DE BREYNE, S., BONDEROFF, J. M., CHUMAKOV, K. M., LLOYD, R. E. & HELLEN, C. U. 2008. Cleavage of eukaryotic initiation factor eIF5B by enterovirus 3C proteases. *Virology*, 378, 118-122.

- DE JONG, A., DE MATTIA, F., VAN DOMMELEN, M., LANKE, K., MELCHERS, W., WILLEMS, P. & VAN KUPPEVELD, F. 2008. Functional analysis of picornavirus 2B proteins: effects on calcium homeostasis and intracellular protein trafficking. *J Virol*, 82, 3782 - 3790.
- DE SILVA, U., ZHOU, Z. & BROWN, B. A. 2012. Structure of Aeropyrum pernix fibrillarin in complex with natively bound S-adenosyl-l-methionine at 1.7 Å resolution. *Acta Crystallographica Section F: Structural Biology and Crystallization Communications*, 68, 854-859.
- DELLAIRE, G. & BAZETT-JONES, D. P. 2004. PML nuclear bodies: dynamic sensors of DNA damage and cellular stress. *Bioessays*, 26, 963-977.
- DEN BOON, J. A., DIAZ, A. & AHLQUIST, P. 2010. Cytoplasmic Viral Replication Complexes. *Cell host & microbe*, 8, 77-85.
- DENISON, M. R. 2008. Seeking membranes: positive-strand RNA virus replication complexes. *PLoS Biol*, 6, e270.
- DESTOUCHES, D., PAGE, N., HAMMA-KOURBALI, Y., MACHI, V., CHALOIN, O., FRECHAULT, S., BIRMPAS, C., KATSORIS, P., BEYRATH, J. & ALBANESE, P. 2011. A simple approach to cancer therapy afforded by multivalent pseudopeptides that target cell-surface nucleoproteins. *Cancer research*, 71, 3296-3305.
- DONNELLY, M. L., LUKE, G., MEHROTRA, A., LI, X., HUGHES, L. E., GANI, D. & RYAN, M. D. 2001. Analysis of the aphthovirus 2A/2B polyprotein 'cleavage' mechanism indicates not a proteolytic reaction, but a novel translational effect: a putative ribosomal 'skip'. *Journal of General Virology*, 82, 1013-1025.
- DOUGHERTY, J. D., WHITE, J. P. & LLOYD, R. E. 2011. Poliovirus-mediated disruption of cytoplasmic processing bodies. *Journal of virology*, 85, 64-75.
- DYE, B. T. & PATTON, J. G. 2001. An RNA recognition motif (RRM) is required for the localization of PTB-associated splicing factor (PSF) to subnuclear speckles. *Experimental cell research*, 263, 131-144.
- EGGER, D., TETERINA, N., EHRENFELD, E. & BIENZ, K. 2000. Formation of the Poliovirus Replication Complex Requires Coupled Viral Translation, Vesicle Production, and Viral RNA Synthesis. *Journal of Virology*, 74, 6570-6580.

- EHRENFELD, E. & TETERINA, N. L. 2002. Initiation of Translation of Picornavirus RNAs: Structure and Function of the Internal Ribosome Entry Site. *Molecular Biology of Picornavirus*. American Society of Microbiology.
- EL MCHICHI, B., REGAD, T., MAROUI, M.-A., RODRIGUEZ, M. S., AMINEV, A., GERBAUD, S., ESCRIOU, N., DIANOUX, L. & CHELBI-ALIX, M. K. 2010. SUMOylation promotes PML degradation during encephalomyocarditis virus infection. *Journal of virology*, 84, 11634-11645.
- EMMOTT, E. & HISCOX, J. A. 2009. Nucleolar targeting: the hub of the matter. *EMBO Reports*, 10, 231-238.
- EVERETT, R. D. 2001. DNA viruses and viral proteins that interact with PML nuclear bodies. *Oncogene*, 20, 7266-7273.
- FLATHER, D. & SEMLER, B. L. 2015. Picornaviruses and nuclear functions: targeting a cellular compartment distinct from the replication site of a positive-strand RNA virus. *Frontiers in microbiology*, 6.
- FOX, A. H., BOND, C. S. & LAMOND, A. I. 2005. P54nrb forms a heterodimer with PSP1 that localizes to paraspeckles in an RNA-dependent manner. *Molecular biology of the cell*, 16, 5304-5315.
- FOX, A. H., LAM, Y. W., LEUNG, A. K. L., LYON, C. E., ANDERSEN, J., MANN, M. & LAMOND, A. I. 2002. Paraspeckles: a novel nuclear domain. *Current biology : CB*, 12, 13-25.
- FOX, A. H. & LAMOND, A. I. 2010. Paraspeckles. *Cold Spring Harbor Perspectives in Biology*, 2, a000687.
- FRAPPIER, L. 2010. andesioscienceonotdistributeandesioscienc eonotdistribute. 2, 58-62.
- FU, C., AHMED, K., DING, H., DING, X., LAN, J., YANG, Z., MIAO, Y., ZHU, Y., SHI, Y., ZHU, J., HUANG, H. & YAO, X. 2005. Stabilization of PML nuclear localization by conjugation and oligomerization of SUMO-3. *Oncogene*, 24, 5401-5413.
- GALIETTA, A., GUNBY, R. H., REDAELLI, S., STANO, P., CARNITI, C., BACHI, A., TUCKER, P. W., TARTARI, C. J., HUANG, C.-J., COLOMBO, E.,

- PULFORD, K., PUTTINI, M., PIAZZA, R. G., RUCHATZ, H., VILLA, A., DONELLA-DEANA, A., MARIN, O., PERROTTI, D. & GAMBACORTI-PASSERINI, C. 2007. NPM/ALK binds and phosphorylates the RNA/DNA-binding protein PSF in anaplastic large-cell lymphoma. *Blood*, 110, 2600-2609.
- GAO, X., KONG, L., LU, X., ZHANG, G., CHI, L., JIANG, Y., WU, Y., YAN, C., DUERKSEN-HUGHES, P. & ZHU, X. 2014. Paraspeckle Protein 1 (PSPC1) Is Involved in the Cisplatin Induced DNA Damage Response—Role in G1/S Checkpoint.
- GHISOLFI-NIETO, L., JOSEPH, G., PUVION-DUTILLEUL, F., AMALRIC, F. & BOUVET, P. 1996. Nucleolin is a sequence-specific RNA-binding protein: characterization of targets on pre-ribosomal RNA. *Journal of molecular biology*, 260, 34-53.
- GINISTY, H., SICARD, H., ROGER, B. & BOUVET, P. 1999. Structure and functions of nucleolin. *J Cell Sci*, 112, 761 - 772.
- GIORGI, C., ITO, K., LIN, H.-K., SANTANGELO, C., WIECKOWSKI, M. R., LEBIEDZINSKA, M., BONONI, A., BONORA, M., DUSZYNSKI, J. & BERNARDI, R. 2010. PML regulates apoptosis at endoplasmic reticulum by modulating calcium release. *Science*, 330, 1247-1251.
- GOLDSTAUB, D., GRADI, A., BERCOVITCH, Z., NOPHAR, Y., LURIA, S., SONENBERG, N., KAHANA, C., GOLDSTAUB, D. A. N. & GROSMANN, Z. 2000. Poliovirus 2A Protease Induces Apoptotic Cell Death Poliovirus 2A Protease Induces Apoptotic Cell Death.
- GONZÁLEZ-MAGALDI, M., POSTIGO, R., BEATRIZ, G., VIEIRA, Y. A., RODRÍGUEZ-PULIDO, M., LÓPEZ-VIÑAS, E., GÓMEZ-PUERTAS, P., ANDREU, D., KREMER, L. & ROSAS, M. F. 2012. Mutations that hamper dimerization of foot-and-mouth disease virus 3A protein are detrimental for infectivity. *Journal of virology*, 86, 11013-11023.
- GOODFELLOW, I. 2011. The genome-linked protein VPg of vertebrate viruses—a multifaceted protein. *Current opinion in virology*, 1, 355-362.
- GOODFELLOW, I., CHAUDHRY, Y., RICHARDSON, A., MEREDITH, J., ALMOND, J. W., BARCLAY, W. & EVANS, D. J. 2000. Identification of a cis-acting replication element within the poliovirus coding region. *Journal of virology*, 74, 4590-4600.

- GRADI, A., SVITKIN, Y. V., SOMMERGRUBER, W., IMATAKA, H., MORINO, S., SKERN, T. & SONENBERG, N. 2003. Human rhinovirus 2A proteinase cleavage sites in eukaryotic initiation factors (eIF) 4GI and eIF4GII are different. *Journal of virology*, 77, 5026-5029.
- GRANDE, M. A., VAN DER KRAAN, I., VAN STEENSEL, B., SCHUL, W., DE THÉ, H., VAN DER VOORT, H. T., DE JONG, L. & VAN DRIEL, R. 1996. PML-containing nuclear bodies: their spatial distribution in relation to other nuclear components. *Journal of cellular biochemistry*, 63, 280-91.
- GRUBMAN, M. J. & BAXT, B. 2004. Foot-and-mouth disease. *Clinical microbiology reviews*, 17, 465-493.
- GU, H. & ROIZMAN, B. 2009. The two functions of herpes simplex virus 1 ICP0, inhibition of silencing by the CoREST/REST/HDAC complex and degradation of PML, are executed in tandem. *Journal of virology*, 83, 181-7.
- HAGHIGHAT, A., SVITKIN, Y., NOVOA, I., KUECHLER, E., SKERN, T. & SONENBERG, N. 1996. The eIF4G-eIF4E complex is the target for direct cleavage by the rhinovirus 2A proteinase. *Journal of Virology*, 70, 8444-8450.
- HARVALA, H., KALIMO, H., DAHLLUND, L., SANTTI, J., HUGHES, P., HYYPIÄ, T. & STANWAY, G. 2002. Mapping of tissue tropism determinants in coxsackievirus genomes. *The Journal of general virology*, 83, 1697-706.
- HARVALA, H. & SIMMONDS, P. 2009. Human parechoviruses: biology, epidemiology and clinical significance. *Journal of Clinical Virology*, 45, 1-9.
- HAUGWITZ, M. 2002. Detect of protease activity in cell; obtain sample containing labeled enzymatic fusion protein, incubate with cell, detecting the subcellular position of label domain. Google Patents.
- HEIKKILÄ, O., SUSI, P., TEVALUOTO, T., HÄRMÄ, H., MARJOMÄKI, V., HYYPIÄ, T. & KILJUNEN, S. 2010. Internalization of coxsackievirus A9 is mediated by β 2-microglobulin, dynamin, and Arf6 but not by caveolin-1 or clathrin. *Journal of virology*, 84, 3666-3681.
- HELLEN, C. U. & DE BREYNE, S. 2007. A distinct group of hepacivirus/pestivirus-like internal ribosomal entry sites in members of diverse picornavirus genera: evidence for modular exchange of functional noncoding RNA elements by recombination. *Journal of virology*, 81, 5850-5863.

- HEYD, F. & LYNCH, K. W. 2010. Phosphorylation-dependent regulation of PSF by GSK3 controls CD45 alternative splicing. *Molecular cell*, 40, 126-137.
- HO, B.-C., YU, S.-L., CHEN, J. J., CHANG, S.-Y., YAN, B.-S., HONG, Q.-S., SINGH, S., KAO, C.-L., CHEN, H.-Y. & SU, K.-Y. 2011. Enterovirus-induced miR-141 contributes to shutoff of host protein translation by targeting the translation initiation factor eIF4E. *Cell host & microbe*, 9, 58-69.
- HU, Y. F., YANG, F., DU, J., DONG, J., ZHANG, T., WU, Z. Q., XUE, Y. & JIN, Q. 2011. Complete genome analysis of coxsackievirus A2, A4, A5, and A10 strains isolated from hand, foot, and mouth disease patients in China revealing frequent recombination of human enterovirus A. *Journal of clinical microbiology*, 49, 2426-34.
- HUGHES, P. J., HORSNELL, C., HYYPIÄ, T. & STANWAY, G. 1995. The coxsackievirus A9 RGD motif is not essential for virus viability. *Journal of Virology*, 69, 8035-8040.
- HUGHES, P. J. & STANWAY, G. 2000. The 2A proteins of three diverse picornaviruses are related to each other and to the H-rev107 family of proteins involved in the control of cell proliferation. *Journal of General Virology*, 81, 201-207.
- HUNT, R. 2010. Virology Chapter Ten Picornaviruses-Part One Enteroviruses and General Features of Picornaviruses.
- HUTTUNEN, M., WARIS, M., KAJANDER, R., HYYPIÄ, T. & MARJOMÄKI, V. 2014. Coxsackievirus A9 infects cells via nonacidic multivesicular bodies. *Journal of virology*, 88, 5138-5151.
- HYYPIÄ, T., HORSNELL, C., MAARONEN, M., KHAN, M., KALKKINEN, N., AUVINEN, P., KINNUNEN, L. & STANWAY, G. 1992. A distinct picornavirus group identified by sequence analysis. *Proceedings of the National Academy of Sciences*, 89, 8847-8851.
- INOUE, A., TSUGAWA, K., TOKUNAGA, K., TAKAHASHI, K. P., UNI, S., KIMURA, M., NISHIO, K., YAMAMOTO, N., HONDA, K.-I., WATANABE, T., YAMANE, H. & TANI, T. 2008. S1-1 nuclear domains: characterization and dynamics as a function of transcriptional activity. *Biology of the cell / under the auspices of the European Cell Biology Organization*, 100, 523-35.

- IZUMI, R. E., VALDEZ, B., BANERJEE, R., SRIVASTAVA, M. & DASGUPTA, A. 2001. Nucleolin stimulates viral internal ribosome entry site-mediated translation. *Virus research*, 76, 17-29.
- JANG, S., PESTOVA, T., HELLEN, C., WITHERELL, G. & WIMMER, E. 1989. Cap-independent translation of picornavirus RNAs: structure and function of the internal ribosomal entry site. *Enzyme*, 44, 292-309.
- JEANNE, M., LALLEMAND-BREITENBACH, V., FERHI, O., KOKEN, M., LE BRAS, M., DUFFORT, S., PERES, L., BERTHIER, C., SOILIHI, H. & RAUGHT, B. 2010. PML/RARA oxidation and arsenic binding initiate the antileukemia response of As₂O₃. *Cancer cell*, 18, 88-98.
- JUL-LARSEN, Å., GRUDIC, A., BJERKVIG, R. & BØE, S. O. 2010. Subcellular distribution of nuclear import-defective isoforms of the promyelocytic leukemia protein. *BMC molecular biology*, 11, 89.
- KANDA, T., GAUSS-MÜLLER, V., CORDES, S., TAMURA, R., OKITSU, K., SHUANG, W., NAKAMOTO, S., FUJIWARA, K., IMAZEKI, F. & YOKOSUKA, O. 2010. Hepatitis A virus (HAV) proteinase 3C inhibits HAV IRES-dependent translation and cleaves the polypyrimidine tract-binding protein. *Journal of viral hepatitis*, 17, 618-623.
- KERKVLIT, J., EDUKULLA, R. & RODRIGUEZ, M. 2010. Novel roles of the picornaviral 3D polymerase in viral pathogenesis. *Advances in virology*, 2010.
- KNOWLES, N., HOVI, T., HYYPIÄ, T., KING, A., LINDBERG, A., PALLANSCH, M., PALMENBERG, A., SIMMONDS, P., SKERN, T. & STANWAY, G. 2012. Picornaviridae. *Virus taxonomy: classification and nomenclature of viruses: ninth report of the international committee on taxonomy of viruses*, 855-880.
- KOLEHMAINEN, P., JÄÄSKELÄINEN, A., BLOMQVIST, S., KALLIO-KOKKO, H., NUOLIVIRTA, K., HELMINEN, M., ROIVAINEN, M., LAPPALAINEN, M. & TAURIAINEN, S. 2014. Human Parechovirus Type 3 and 4 Associated With Severe Infections in Young Children. *The Pediatric infectious disease journal*, 33, 1109-1113.
- KRENN, B., HOLZER, B., GAUDERNAK, E., TRIENDL, A., VAN KUPPEVELD, F. & SEIPELT, J. 2005. Inhibition of polyprotein processing and RNA replication of human rhinovirus by pyrrolidine dithiocarbamate involves metal ions. *Journal of virology*, 79, 13892-13899.

- KUDCHODKAR, S. B. & LEVINE, B. 2009. Viruses and autophagy. *Reviews in medical virology*, 19, 359-378.
- KUO, R.-L., KUNG, S.-H., HSU, Y.-Y. & LIU, W.-T. 2002. Infection with enterovirus 71 or expression of its 2A protease induces apoptotic cell death. *Journal of General Virology*, 83, 1367-1376.
- KWON, S., ZHANG, Y. & MATTHIAS, P. 2007. The deacetylase HDAC6 is a novel critical component of stress granules involved in the stress response. *Genes & development*, 21, 3381-3394.
- LAMOND, A. I. & SPECTOR, D. L. 2003. Nuclear speckles: a model for nuclear organelles. *Nature Reviews Molecular Cell Biology*, 4, 605-612.
- LAPEYRE, B., BOURBON, H. & AMALRIC, F. 1987. Nucleolin, the major nucleolar protein of growing eukaryotic cells: an unusual protein structure revealed by the nucleotide sequence. *Proceedings of the National Academy of Sciences*, 84, 1472-1476.
- LEE, H. H., KIM, H. S., KANG, J. Y., LEE, B. I., HA, J. Y., YOON, H. J., LIM, S. O., JUNG, G. & SUH, S. W. 2007. Crystal structure of human nucleophosmin-core reveals plasticity of the pentamer-pentamer interface. *Proteins: Structure, Function, and Bioinformatics*, 69, 672-678.
- LEE, M., SADOWSKA, A., BEKERE, I., HO, D., GULLY, B. S., LU, Y., IYER, K. S., TREWHELLA, J., FOX, A. H. & BOND, C. S. 2015. The structure of human SFPQ reveals a coiled-coil mediated polymer essential for functional aggregation in gene regulation. *Nucleic acids research*, gkv156.
- LEI, X., LIU, X., MA, Y., SUN, Z., YANG, Y., JIN, Q., HE, B. & WANG, J. 2010. The 3C protein of enterovirus 71 inhibits retinoid acid-inducible gene I-mediated interferon regulatory factor 3 activation and type I interferon responses. *Journal of virology*, 84, 8051-8061.
- LENARCIC, E. M., LANDRY, D. M., GRECO, T. M., CRISTEA, I. M. & THOMPSON, S. R. 2013. Thiouracil Cross-Linking Mass Spectrometry: a Cell-Based Method To Identify Host Factors Involved in Viral Amplification. *Journal of Virology*, 87, 8697-8712.
- LEPPARD, K. N. & DIMMOCK, J. 2004. Virus Interactions with PML Nuclear Bodies. *Proceedings of the National Academy of Sciences*, 84, 1-47.

- LI, M.-L., HSU, T.-A., CHEN, T.-C., CHANG, S.-C., LEE, J.-C., CHEN, C.-C., STOLLAR, V. & SHIH, S.-R. 2002. The 3C Protease Activity of Enterovirus 71 Induces Human Neural Cell Apoptosis. *Virology*, 293, 386-395.
- LIN, J., LI, M., HUANG, P., CHIEN, K., HORNG, J. & SHIH, S. 2008. Heterogeneous nuclear ribonuclear protein K interacts with the enterovirus 71 5' untranslated region and participates in virus replication. *Journal of General Virology*, 89, 2540 - 2549.
- LIN, J., SHIH, S., PAN, M., LI, C., LUE, C., STOLLAR, V. & LI, M. 2009a. hnRNP A1 Interacts with the 5'UTRs of Enterovirus 71 and Sindbis virus RNA and is Required for Viral Replication. *J Virol*.
- LIN, J.-Y., CHEN, T.-C., WENG, K.-F., CHANG, S.-C., CHEN, L.-L. & SHIH, S.-R. 2009b. Viral and host proteins involved in picornavirus life cycle. *Journal of Biomedical Science*, 16, 103.
- LIN, J.-Y., CHEN, T.-C., WENG, K.-F., CHANG, S.-C., CHEN, L.-L. & SHIH, S.-R. 2009c. Viral and host proteins involved in picornavirus life cycle. *Journal of biomedical science*, 16, 103.
- LLOYD, R. E. 2012. How do viruses interact with stress-associated RNA granules. *PLoS Pathog*, 8, e1002741-e1002741.
- LOBERT, P., ESCRIOU, N., RUELLE, J. & MICHIELS, T. 1999. A coding RNA sequence acts as a replication signal in cardioviruses. *Proc Natl Acad Sci USA*, 96, 11560 - 11565.
- LU, G., QI, J., CHEN, Z., XU, X., GAO, F., LIN, D., QIAN, W., LIU, H., JIANG, H., YAN, J. & GAO, G. F. 2011. Enterovirus 71 and Coxsackievirus A16 3C Proteases: Binding to Rupintrivir and Their Substrates and Anti-Hand, Foot, and Mouth Disease Virus Drug Design. *Journal of Virology*, 85, 10319-10331.
- LU, H. H., LI, X., CUCONATI, A. & WIMMER, E. 1995. Analysis of picornavirus 2A(pro) proteins: separation of proteinase from translation and replication functions. *Journal of Virology*, 69, 7445-7452.
- LUKONG, K. E., HUOT, M.-É. & RICHARD, S. 2009. BRK phosphorylates PSF promoting its cytoplasmic localization and cell cycle arrest. *Cellular signalling*, 21, 1415-1422.

- LYMBEROPOULOS, M. H. & PEARSON, A. 2010. Relocalization of upstream binding factor to viral replication compartments is UL24 independent and follows the onset of herpes simplex virus 1 DNA synthesis. *Journal of virology*, 84, 4810-4815.
- MAGGI, L. B., KUCHENRUETHER, M., DADEY, D. Y., SCHWOPE, R. M., GRISENDI, S., TOWNSEND, R. R., PANDOLFI, P. P. & WEBER, J. D. 2008. Nucleophosmin serves as a rate-limiting nuclear export chaperone for the Mammalian ribosome. *Molecular and cellular biology*, 28, 7050-7065.
- MÄKELÄ, M. J., PUHAKKA, T., RUUSKANEN, O., LEINONEN, M., SAIKKU, P., KIMPIMÄKI, M., BLOMQVIST, S., HYYPIÄ, T. & ARSTILA, P. 1998. Viruses and bacteria in the etiology of the common cold. *Journal of clinical microbiology*, 36, 539-542.
- MALCOLM, B. A. 1995. The picornaviral 3C proteinases: cysteine nucleophiles in serine proteinase folds. *Protein Science*, 4, 1439-1445.
- MARAMOROSCH, K., SHATKIN, A. J. & AND MURPHY, F. A. 2011. *Advances in virus research.*, USA., Academic press. .
- MARJOMÄKI, V., TURKKI, P. & HUTTUNEN, M. 2015. Infectious Entry Pathway of Enterovirus B Species. *Viruses*, 7, 6387-6399.
- MARTIN, A. & LEMON, S. M. 2006. Hepatitis A virus: from discovery to vaccines. *Hepatology*, 43, S164-S172.
- MASIUK, M. 2008. Nucleolin—characteristics of protein and its role in biology of cancers and viral infections. *Advances in Cell Biology*, 1, 1-19.
- MATTHEWS, D. A. 2001. Adenovirus protein V induces redistribution of nucleolin and B23 from nucleolus to cytoplasm. *Journal of virology*, 75, 1031-1038.
- MAY WANG, Q. & CHEN, S.-H. 2007. Human rhinovirus 3C protease as a potential target for the development of antiviral agents. *Current Protein and Peptide Science*, 8, 19-27.
- MCKNIGHT, K. & LEMON, S. 1998. The rhinovirus type 14 genome contains an internally located RNA structure that is required for viral replication. *Rna*, 4, 1569 - 1584.

- MCLEISH, N. J., WILLIAMS, Ç. H., KALOUDAS, D., ROIVAINEN, M. M. & STANWAY, G. 2012. Symmetry-Related Clustering of Positive Charges Is a Common Mechanism for Heparan Sulfate Binding in Enteroviruses. *Journal of Virology*, 86, 11163-11170.
- MELÉN, K., TYNELL, J., FAGERLUND, R., ROUSSEL, P., HERNANDEZ-VERDUN, D. & JULKUNEN, I. 2012. Influenza A H3N2 subtype virus NS1 protein targets into the nucleus and binds primarily via its C-terminal NLS2/NoLS to nucleolin and fibrillarin. *Virol J*, 9, 167.
- MOFFAT, K., HOWELL, G., KNOX, C., GRAHAM, J., MONAGHAN, P., RYAN, M. D., BELSHAM, G. J. & WILEMAN, T. 2005. Effects of Foot-and-Mouth Disease Virus Nonstructural Proteins on the Structure and Function of the Early Secretory Pathway : 2BC but Not 3A Blocks Endoplasmic Reticulum-to-Golgi Transport Effects of Foot-and-Mouth Disease Virus Nonstructural Proteins on
- MOREAU, B., BASTEDO, C., MICHEL, R. P. & GHALI, P. 2011. Hepatitis and Encephalitis due to Coxsackie Virus A9 in an Adult. *Case reports in gastroenterology*, 5, 617-622.
- MORIMOTO, M. & BOERKOEL, C. F. 2013. The role of nuclear bodies in gene expression and disease. *Biology*, 2, 976-1033.
- MUCKELBAUER, J. K., KREMER, M., MINOR, I., DIANA, G., DUTKO, F. J., GROARKE, J., PEVEAR, D. C. & ROSSMANN, M. G. 1995. The structure of coxsackievirus B3 at 3.5 Å resolution. *Structure*, 3, 653-667.
- MUEHLENBACHS, A., BHATNAGAR, J. & ZAKI, S. R. 2015. Tissue tropism, pathology and pathogenesis of enterovirus infection. *The Journal of pathology*, 235, 217-228.
- MUTABAGANI, M. 2012. *Intracellular events in human parechovirus infection*. PhD, University of Essex.
- NAGANUMA, T., NAKAGAWA, S., TANIGAWA, A., SASAKI, Y. F., GOSHIMA, N. & HIROSE, T. 2012. Alternative 3'-end processing of long noncoding RNA initiates construction of nuclear paraspeckles. *The EMBO Journal*, 31, 4020-4034.
- NAKAGAWA, S. & HIROSE, T. 2012. Paraspeckle nuclear bodies—useful uselessness? *Cellular and Molecular Life Sciences*, 69, 3027-3036.

- NARDELLA, C., LUNARDI, A., PATNAIK, A., CANTLEY, L. C. & PANDOLFI, P. 2011. The APL paradigm and the “co-clinical trial” project. *Cancer discovery*, 1, 108-116.
- NISHIMURA, Y., SHIMOJIMA, M., TANO, Y., MIYAMURA, T., WAKITA, T. & SHIMIZU, H. 2009. Human P-selectin glycoprotein ligand-1 is a functional receptor for enterovirus 71. *Nature medicine*, 15, 794-797.
- NYQUIST, H. 1928. Certain topics in telegraph transmission theory. *American Institute of Electrical Engineers, Transactions of the*, 47, 617-644.
- OBERSTE, M. S., MAHER, K., KILPATRICK, D. R. & PALLANSCH, M. A. 1999. Molecular Evolution of the Human Enteroviruses : Correlation of Serotype with VP1 Sequence and Application to Picornavirus Classification Molecular Evolution of the Human Enteroviruses : Correlation of Serotype with VP1 Sequence and Application to Picorna.
- OCHS, R., LISCHWE, M., SPOHN, W. & BUSCH, H. 1985. Fibrillarin: a new protein of the nucleolus identified by autoimmune sera. *Biology of the Cell*, 54, 123-133.
- OKUWAKI, M. 2008. The structure and functions of NPM1/Nucleophsmin/B23, a multifunctional nucleolar acidic protein. *Journal of biochemistry*, 143, 441-448.
- OLSON, M. O. & DUNDR, M. 2010. Nucleolus: Structure and Function. *eLS*.
- OTT, J. J., IRVING, G. & WIERSMA, S. T. 2012. Long-term protective effects of hepatitis A vaccines. A systematic review. *Vaccine*, 31, 3-11.
- PALMA, A. M. D., VLIEGEN, I., CLERCQ, E. D. & NEYTS, J. 2008. Selective Inhibitors of Picornavirus Replication. 1-62.
- PAMPIN, M., SIMONIN, Y., BLONDEL, B., PERCHERANCIER, Y. & CHELBI-ALIX, M. K. 2006. Cross Talk between PML and p53 during Poliovirus Infection: Implications for Antiviral Defense. *Journal of Virology*, 80, 8582-8592.
- PANJWANI, A., STRAUSS, M., GOLD, S., WENHAM, H., JACKSON, T., CHOU, J. J., ROWLANDS, D. J., STONEHOUSE, N. J., HOGLE, J. M. & TUTHILL, T. J. 2014. Capsid protein VP4 of human rhinovirus induces membrane permeability by the formation of a size-selective multimeric pore.

- PARK, N., KATIKANENI, P., SKERN, T. & GUSTIN, K. 2008. Differential targeting of nuclear pore complex proteins in poliovirus-infected cells. *J Virol*, 82, 1647 - 1655.
- PASSON, D. M., LEE, M., RACKHAM, O., STANLEY, W. A., SADOWSKA, A., FILIPOVSKA, A., FOX, A. H. & BOND, C. S. 2012. Structure of the heterodimer of human NONO and paraspeckle protein component 1 and analysis of its role in subnuclear body formation. *Proceedings of the National Academy of Sciences of the United States of America*, 109, 4846-4850.
- PATHAK, H. B., ARNOLD, J. J., WIEGAND, P. N., HARGITTAI, M. R. & CAMERON, C. E. 2007. Picornavirus Genome Replication ASSEMBLY AND ORGANIZATION OF THE VPg URIDYLYLATION RIBONUCLEOPROTEIN (INITIATION) COMPLEX. *Journal of Biological Chemistry*, 282, 16202-16213.
- PAUL, A. V., RIEDER, E., KIM, D. W., VAN BOOM, J. H. & WIMMER, E. 2000. Identification of an RNA hairpin in poliovirus RNA that serves as the primary template in the in vitro uridylylation of VPg. *Journal of virology*, 74, 10359-10370.
- PELLETIER, J. & SONENBERG, N. 1988. Internal initiation of translation of eukaryotic mRNA directed by a sequence derived from poliovirus RNA. *Nature*, 334, 320-325.
- POLACEK, C., BELSHAM, G. & MCINERNEY, G. FMDV-induced stress granules are disrupted by the viral L-protease. 18th International Picornavirus Meeting (Europic 2014), 2014
- PORTA, C., KOTECHA, A., BURMAN, A., JACKSON, T., REN, J., LOUREIRO, S., JONES, I. M., FRY, E. E., STUART, D. I. & CHARLESTON, B. 2013. Rational Engineering of Recombinant Picornavirus Capsids to Produce Safe, Protective Vaccine Antigen. *PLoS Pathogens*, 9, e1003255.
- PORTER, F. W. & PALMENBERG, A. C. 2009. Leader-induced phosphorylation of nucleoporins correlates with nuclear trafficking inhibition by cardioviruses. *Journal of virology*, 83, 1941-1951.
- RAKITINA, D., TALIANSKY, M., BROWN, J. & KALININA, N. 2011. Two RNA-binding sites in plant fibrillarin provide interactions with various RNA substrates. *Nucleic acids research*, gkr594.

- RAMOS-ECHAZÁBAL, G., CHINEA, G., GARCÍA-FERNÁNDEZ, R. & PONS, T. 2012. In silico studies of potential phosphoresidues in the human nucleophosmin/B23: its kinases and related biological processes. *Journal of cellular biochemistry*, 113, 2364-2374.
- RAWLINSON, S. M. & MOSELEY, G. W. 2015. The nucleolar interface of RNA viruses. *Cellular microbiology*, 17, 1108-1120.
- RAZONABLE, R. R. Antiviral drugs for viruses other than human immunodeficiency virus. Mayo Clinic Proceedings, 2011. Elsevier, 1009-1026.
- REICHELT, M., WANG, L., SOMMER, M., PERRINO, J., NOUR, A. M., SEN, N., BAIKER, A., ZERBONI, L. & ARVIN, A. M. 2011. Entrapment of viral capsids in nuclear PML cages is an intrinsic antiviral host defense against varicella-zoster virus. *PLoS Pathog*, 7, e1001266-e1001266.
- REINEKE, L. C. & LLOYD, R. E. 2013. Diversion of stress granules and P-bodies during viral infection. *Virology*, 436, 255-267.
- RHOADES, R. E., TABOR-GODWIN, J. M., TSUENG, G. & FEUER, R. 2011. Enterovirus infections of the central nervous system. *Virology*, 411, 288-305.
- ROSSMANN, M. G., HE, Y. & KUHN, R. J. 2002. Picornavirus-receptor interactions. *Trends in Microbiology*, 10, 324-331.
- ROZOVICS, J. M., CHASE, A. J., CATHCART, A. L., CHOU, W., GERSHON, P. D., PALUSA, S., WILUSZ, J. & SEMLER, B. L. 2012. Picornavirus modification of a host mRNA decay protein. *MBio*, 3, e00431-12.
- RYAN, M. D. & FLINT, M. 1997. Virus-encoded proteinases of the picornavirus supergroup. *Journal of General Virology*, 78, 699-724.
- SALOMONI, P. & BELLODI, C. 2007. New insights into the cytoplasmic function of PML.
- SAMAD, M. A., KOMATSU, T., OKUWAKI, M. & NAGATA, K. 2012. B23/nucleophosmin is involved in regulation of adenovirus chromatin structure at late infection stages, but not in virus replication and transcription. *Journal of general virology*, 93, 1328-1338.

- SAMAD, M. A., OKUWAKI, M., HARUKI, H. & NAGATA, K. 2007. Physical and functional interaction between a nucleolar protein nucleophosmin/B23 and adenovirus basic core proteins. *FEBS letters*, 581, 3283-3288.
- SANDRI-GOLDIN, R. M., HIBBARD, M. K. & HARDWICKE, M. A. N. N. 1995. The C-terminal repressor region of herpes simplex virus type 1 ICP27 is required for the redistribution of small nuclear ribonucleoprotein particles and splicing factor SC35 ; however , these alterations are not sufficient to inhibit host cell splicing . .
- SCHNEIDER, J., DAUBER, B., MELÉN, K., WOLFF, T., MELE, K. & JULKUNEN, I. 2009. Analysis of Influenza B Virus NS1 Protein Trafficking Reveals a Novel Interaction with Nuclear Speckle Domains Analysis of Influenza B Virus NS1 Protein Trafficking Reveals a Novel Interaction with Nuclear Speckle Domains □.
- SEILLIER, M., PEUGET, S., GAYET, O., GAUTHIER, C., N'GUESSAN, P., MONTE, M., CARRIER, A., IOVANNA, J. & DUSETTI, N. 2012. TP53INP1, a tumor suppressor, interacts with LC3 and ATG8-family proteins through the LC3-interacting region (LIR) and promotes autophagy-dependent cell death. *Cell Death & Differentiation*, 19, 1525-1535.
- SEIPELT, J., GUARNÉ, A., BERGMANN, E., JAMES, M., SOMMERGRUBER, W., FITA, I. & SKERN, T. 1999. The structures of picornaviral proteinases. *Virus research*, 62, 159-168.
- SHANNON, C. E. 1949. Communication in the presence of noise. *Proceedings of the IRE*, 37, 10-21.
- SHAV-TAL, Y., COHEN, M., LAPTER, S., DYE, B., PATTON, J. G., VANDEKERCKHOVE, J. & ZIPORI, D. 2001. Nuclear relocalization of the pre-mRNA splicing factor PSF during apoptosis involves hyperphosphorylation, masking of antigenic epitopes, and changes in protein interactions. *Molecular biology of the cell*, 12, 2328-2340.
- SHAW, P. & BROWN, J. 2012. Nucleoli: composition, function, and dynamics. *Plant physiology*, 158, 44-51.
- SHEN, M., REITMAN, Z. J., ZHAO, Y., MOUSTAFA, I., WANG, Q., ARNOLD, J. J., PATHAK, H. B. & CAMERON, C. E. 2008. Picornavirus Genome Replication IDENTIFICATION OF THE SURFACE OF THE POLIOVIRUS (PV) 3C DIMER THAT INTERACTS WITH PV 3Dpol DURING VPg URIDYLYLATION AND CONSTRUCTION OF A STRUCTURAL MODEL

- FOR THE PV 3C2-3Dpol COMPLEX. *Journal of Biological Chemistry*, 283, 875-888.
- SHINGLER, K. L., YODER, J. L., CARNEGIE, M. S., ASHLEY, R. E., MAKHOV, A. M., CONWAY, J. F. & HAFENSTEIN, S. 2013. The enterovirus 71 A-particle forms a gateway to allow genome release: a cryoEM study of picornavirus uncoating. *PLoS Pathog*, 9, e1003240.
- SHIROKI, K., ISOYAMA, T., KUGE, S., ISHII, T., OHMI, S., HATA, S., SUZUKI, K., TAKASAKI, Y. & NOMOTO, A. 1999. Intracellular redistribution of truncated La protein produced by poliovirus 3Cpro-mediated cleavage. *Journal of virology*, 73, 2193-2200.
- SMYTH, M. S. & MARTIN, J. H. 2002. Picornavirus uncoating. *Molecular Pathology*, 55, 214-219.
- SPECTOR, D. L. & LAMOND, A. I. 2011. Nuclear speckles. *Cold Spring Harbor perspectives in biology*, 3, a000646.
- STANWAY, G. & HYYPIÄ, T. 1999. Parechoviruses. *Journal of virology*, 73, 5249-5254.
- STANWAY, G., KALKKINEN, N., ROIVAINEN, M., GHAZI, F., KHAN, M., SMYTH, M., MEURMAN, O. & HYYPIÄ, T. 1994. Molecular and biological characteristics of echovirus 22, a representative of a new picornavirus group. *Journal of virology*, 68, 8232-8238.
- STEIL, B. P. & BARTON, D. J. 2009. Cis-active RNA elements (CREs) and picornavirus RNA replication. *Virus research*, 139, 240-252.
- SWEENEY, T. R., CISNETTO, V., BOSE, D., BAILEY, M., WILSON, J. R., ZHANG, X., BELSHAM, G. J. & CURRY, S. 2010. Foot-and-mouth disease virus 2C is a hexameric AAA+ protein with a coordinated ATP hydrolysis mechanism. *Journal of Biological Chemistry*, 285, 24347-24359.
- TACKEL, R. & MANLEY, J. L. 1995. The human splicing factors ASF / SF2 and SC35 possess distinct , functionally significant RNA binding specificities. 14, 3540-3551.

- TANG, S.-W., DUCROUX, A., JEANG, K.-T. & NEUVEUT, C. 2012. Impact of cellular autophagy on viruses: Insights from hepatitis B virus and human retroviruses. *J. Biomed. Sci*, 19, 92.
- TAO, Y. J. & YE, Q. 2010. RNA virus replication complexes. *PLoS Pathog*, 6, e1000943.
- THOMPSON, S. R. & SARNOW, P. 2000. Regulation of host cell translation by viruses and effects on cell function. 366-370.
- TOLSKAYA, E. A., ROMANOVA, L. I., KOLESNIKOVA, M. S., IVANNIKOVA, T. A., SMIRNOVA, E. A., RAIKHLIN, N. T. & AGOL, V. I. 1995. Apoptosis-inducing and apoptosis-preventing functions of poliovirus. *Journal of virology*, 69, 1181-1189.
- TOYODA, H., FRANCO, D., FUJITA, K., PAUL, A. V. & WIMMER, E. 2007. Replication of poliovirus requires binding of the poly (rC) binding protein to the cloverleaf as well as to the adjacent C-rich spacer sequence between the cloverleaf and the internal ribosomal entry site. *Journal of virology*, 81, 10017-10028.
- TOYODA, H., NICKLIN, M. J., MURRAY, M. G., ANDERSON, C. W., DUNN, J. J., STUDIER, F. W. & WIMMER, E. 1986. A second virus-encoded proteinase involved in proteolytic processing of poliovirus polyprotein. *Cell*, 45, 761-770.
- TRIAANTAFILOU, K. & TRIANTAFILOU, M. 2003. Lipid raft microdomains: key sites for Coxsackievirus A9 infectious cycle. *Virology*, 317, 128-135.
- TRITSCHLER, F., BRAUN, J. E., EULALIO, A., TRUFFAULT, V., IZAURRALDE, E. & WEICHENRIEDER, O. 2009. Structural basis for the mutually exclusive anchoring of P body components EDC3 and Tral to the DEAD box protein DDX6/Me31B. *Molecular cell*, 33, 661-668.
- TSUDA, Y., MORI, Y., ABE, T., YAMASHITA, T., OKAMOTO, T., ICHIMURA, T., MORIISHI, K. & MATSUURA, Y. 2006. Nucleolar protein B23 interacts with Japanese encephalitis virus core protein and participates in viral replication. *Microbiology and immunology*, 50, 225-234.
- TUTHILL, T. J., GROPELLI, E., HOGLE, J. M. & ROWLANDS, D. J. 2010. Picornaviruses. *Current topics in microbiology and immunology*, 343, 43-89.

- VAN KUPPEVELD, F., HOENDEROP, J., SMEETS, R., WILLEMS, P., DIJKMAN, H., GALAMA, J. & MELCHERS, W. 1997. Coxsackievirus protein 2B modifies endoplasmic reticulum membrane and plasma membrane permeability and facilitates virus release. *Embo J*, 16, 3519 - 3532.
- VETHANTHAM., V. & MANLEY, A. J. L. 2009. Emerging roles for SUMO in mRNA processing and metabolism. In: WILSON, V. (ed.) *SUMO Regulation of Cellular Processes*. College Station TX USA: Springer.
- VOLLBACH, S., MÜLLER, A., DREXLER, J. F., SIMON, A., DROSTEN, C., EIS-HÜBINGER, A. M. & PANNING, M. 2015. Prevalence, type and concentration of human enterovirus and parechovirus in cerebrospinal fluid samples of pediatric patients over a 10-year period: a retrospective study. *Virology journal*, 12, 1.
- WAGGONER, S. & SARNOW, P. 1998. Viral ribonucleoprotein complex formation and nucleolar-cytoplasmic relocalization of nucleolin in poliovirus-infected cells. *J Virol*, 72, 6699 - 6709.
- WANG, D., FANG, L., WEI, D., ZHANG, H., LUO, R., CHEN, H., LI, K. & XIAO, S. 2014a. Hepatitis A virus 3C protease cleaves NEMO to impair induction of beta interferon. *Journal of virology*, 88, 10252-10258.
- WANG, X., LIU, N., WANG, F., NING, K., LI, Y. & ZHANG, D. 2014b. Genetic characterization of a novel duck-origin picornavirus with six 2A proteins. *Journal of General Virology*, vir. 0.063313-0.
- WATTERS, K. & PALMENBERG, A. C. 2011. Differential processing of nuclear pore complex proteins by rhinovirus 2A proteases from different species and serotypes. *Journal of virology*, 85, 10874-10883.
- WESSELS, E., DUIJSINGS, D., LANKE, K., VAN DOOREN, S., JACKSON, C., MELCHERS, W. & VAN KUPPEVELD, F. 2006. Effects of picornavirus 3A Proteins on Protein Transport and GBF1-dependent COP-I recruitment. *J Virol*, 80, 11852 - 11860.
- WILLIAMS, Ç. H., KAJANDER, T., HYYPIÄ, T., JACKSON, T., SHEPPARD, D. & STANWAY, G. 2004. Integrin $\alpha\beta6$ is an RGD-dependent receptor for coxsackievirus A9. *Journal of virology*, 78, 6967-6973.
- WILSON, V. G. & ANDERSON, D. B. 2009. *SUMO regulation of cellular processes*, Springer.

- WORRALL, G. 2008. Common cold. *Canadian Family Physician*, 54, 573-574.
- WU, C., CAI, Q., CHEN, C., LI, N., PENG, X., CAI, Y., YIN, K., CHEN, X., WANG, X. & ZHANG, R. 2013. Structures of enterovirus 71 3C proteinase (strain E2004104-TW-CDC) and its complex with rupintrivir. *Acta Crystallographica Section D: Biological Crystallography*, 69, 866-871.
- WU, S., LIN, L., ZHAO, W., LI, X., WANG, Y., SI, X., WANG, T., WU, H., ZHAI, X. & ZHONG, X. 2014. AUF1 is recruited to the stress granules induced by coxsackievirus B3. *Virus research*, 192, 52-61.
- YAMAYOSHI, S., YAMASHITA, Y., LI, J., HANAGATA, N., MINOWA, T., TAKEMURA, T. & KOIKE, S. 2009. Scavenger receptor B2 is a cellular receptor for enterovirus 71. *Nat Med*, 15, 798-801.
- YANG, J., XIA, H., QIAN, Q. & ZHOU, X. 2015. RNA chaperones encoded by RNA viruses. *Virologica Sinica*, 30, 401-409.
- YANG, L., YE, S.-D., XIE, S., ALTUWAIJRI, S., NI, J., HU, Y.-C., CHEN, Y.-T., BAO, B.-Y., SU, C.-H. & CHANG, C. 2004. Androgen suppresses PML protein expression in prostate cancer CWR22R cells. 314, 69-75.
- YAROSH, C. A., IACONA, J. R., LUTZ, C. S. & LYNCH, K. W. 2015. PSF: nuclear busy-body or nuclear facilitator? *Wiley Interdisciplinary Reviews: RNA*.
- YAU, M., MOK, Q. & PRABHAKAR, P. 2011. Case Report A Fatal Case of Brainstem Encephalitis Caused by Human Parechovirus 人雙埃可病毒感染相關腦幹腦炎致死一例報告. *HK J Paediatr (New Series)*, 16, 56-60.
- YOUNESSI, P., A JANS, D. & GHILDYAL, R. 2012. Modulation of host cell nucleocytoplasmic trafficking during picornavirus infection. *Infectious Disorders-Drug Targets (Formerly Current Drug Targets-Infectious Disorders)*, 12, 59-67.
- YPMWONG, M. F., DEWALT, P. G., JOHNSON, V. H., LAMB, J. G. & SEMLER, B. L. 1988. Protein 3CD is the major poliovirus proteinase responsible for cleavage of the P1 capsid precursor. *Virology*, 166, 265-270.

- YU, Y., JI, H., DOUDNA, J. A. & LEARY, J. A. 2005. Mass spectrometric analysis of the human 40S ribosomal subunit: native and HCV IRES-bound complexes. *Protein science*, 14, 1438-1446.
- YU, Y., SWEENEY, T. R., KAFASLA, P., JACKSON, R. J., PESTOVA, T. V. & HELLEN, C. U. 2011. The mechanism of translation initiation on Aichivirus RNA mediated by a novel type of picornavirus IRES. *The EMBO Journal*, 30, 4423-4436.
- ZAKARYAN, H. & STAMMINGER, T. 2011. Nuclear remodelling during viral infections. *Cellular microbiology*, 13, 806-813.
- ZAUTNER, A., KÖRNER, U., HENKE, A., BADORFF, C. & SCHMIDTKE, M. 2003. Heparan sulfates and coxsackievirus-adenovirus receptor: each one mediates coxsackievirus B3 PD infection. *Journal of virology*, 77, 10071-10077.
- ZEICHHARDT, H., WETZ, K., WILLINGMANN, P. & HABERMEHL, K.-O. 1985. Entry of poliovirus type 1 and Mouse Elberfeld (ME) virus into HEp-2 cells: receptor-mediated endocytosis and endosomal or lysosomal uncoating. *Journal of general virology*, 66, 483-492.
- ZHANG, Q., CHEN, C.-Y., YEDAVALLI, V. S. R. K. & JEANG, K.-T. 2013. NEAT1 Long Noncoding RNA and Paraspeckle Bodies Modulate HIV-1 Posttranscriptional Expression. *mBio*, 4, e00596-12.
- ZHU, L., WANG, X., REN, J., PORTA, C., WENHAM, H., EKSTRÖM, J.-O., PANJWANI, A., KNOWLES, N. J., KOTECHA, A. & SIEBERT, C. A. 2015. Structure of Ljungan virus provides insight into genome packaging of this picornavirus. *Nature communications*, 6.
- ZOCHER, G., MISTRY, N., FRANK, M., HÄHNLEIN-SCHICK, I., EKSTRÖM, J.-O., ARNBERG, N. & STEHLE, T. 2014. A sialic acid binding site in a human picornavirus.
- ZOLOTUKHIN, A. S., MICHALOWSKI, D., BEAR, J., SMULEVITCH, S. V., TRAIISH, A. M., PENG, R., PATTON, J., SHATSKY, I. N. & FELBER, B. K. 2003. PSF Acts through the Human Immunodeficiency Virus Type 1 mRNA Instability Elements To Regulate Virus Expression. *Molecular and Cellular Biology*, 23, 6618-6630.

Appendix

A

```

anagcagaagacgggatcaaggtgaacttcaagatccgcccacaacatcgaggacgggcagg
X A E D G I K V N F K I R H N I E D G S
gtgcagctcgccgaccactaccagcagaacacccccatcggcgacggccccgtgctgctc
V Q L A D H Y Q Q N T P I G D G P V L L
cccgacaaccactacctgagcaccagtcggccctgagcaaaagacccccaacgagaagcgg
P D N H Y L S T Q S A L S K D P N E K R
gatcacatggctcctgctggagttcgtgaccgcccgggatcactctcggcatggacgag
D H M V L L E F V T A A G I T L G M D E
ctgtacaagtcgggactcagatctcggagctgggtgccttcggacaacaatccggggccgctc
L Y K S G L R S R A G A F G Q Q S G A V
tatgtgggcaactacagagtgatcaacagacacctggcaacacacacggattggcaaaat
Y V G N Y R V I N R H L A T H T D W Q N
tgcgtgtgggaggattacaatagagacctccttgtgagcagcactacagcgcagggtgtc
C V W E D Y N R D L L V S T T T A H G C
gatgtcatagctagatgccagtgatcaaccggggtgtacttttgtgcatccaagaacaag
D V I A R C Q C T T G V Y F C A S K N K
cactaccctgtttcattcgaaggccagggttagtgggaagccaagagatggaatactac
H Y P V S F E G P G L V E V Q E S E Y Y
cctaaagatatcaatcccattgtacttctggcagcaggatttccgaaccaggggactgtc
P K R Y Q S H V L L A A G F S E P G D C
ggtggcatcttaaggtgtgaacacggtgtcatagcgcgtgtaacctgggaggcgaaggt
G G I L R C E H G V I G I V T M G G E G
gttgtgggttttctgctgacgtgcgcgacctcttatgggttagaggatgacgctatggagcag
V V G F A D V R D L L W L E D D A M E Q
taaggatccaccggatctagataactgatcataatcagccataccacattttagtagaggtt
- G S T G S R - L I I I S H T T F V E V
ttacttggctttaaaaaacctcccacacctccccctgaaacctgaaacataaaaatgaatgca
L L A L K N L P H L P L N L K H K M N A
attgttgggttgaacttgtttattgcagcttataatgggttacaataaancaatagcatc
I V V V N L F I A A Y N G Y K - X N S I
acaaatttcacaataaancaattttttctactgcattctannt

```

B

```

agcagagggctgaagctgagggaacggccgaccactacgacgctgaggtcaagaccacctaaca
A E A E A E D G G H Y D A E V K T T Y K
gcccgaagcccgtgagctgcccgggacctacaagctcaccatcaagctgggacatcac
A K K P V Q L P G A Y N V N I K L D I T
ccccacaacaggactacaccatcgtggaacagctacgaacggccggagggccgacctc
S H N E D Y T I V E Q Y E R A E G R H S
accggccgcatggaggaactgtacaagtcgggactcagatctcggagcgggtgccttcgga
T G G M D E L Y K S G L R S R A G A F G
caacaatccggggccgctctatgtgggcaactacagagtgatcaacagacacctggcaaca
Q Q S G A V Y V G N Y R V I N R H L A T
cacacggattggcaaaattgctgtgggaggattacaatagagacctccttgtgagcagc
H T D W Q N C V W E D Y N R D L L V S T
actacagcgcacgggtgtgatgtcatagctagatgccagtgatcaaccgggggtgtacttt
T T A H G C D V I A R C Q C T T G V Y F
tgtgcatccaagaacaagcactaccctgtttcattcgaaggccagggttagtgggaagtc
C A S K N K H Y P V S F E G P G L V E V
caagagatggaatactaccctaaaagatatcaatcccattgtacttctggcagcaggattt
Q E S E Y Y P K R Y Q S H V L L A A G F
tccgaaccaggggactgtggtggcatcttaaggtgtgaacacgggtgtcatagggcatcgta
S E P G D C G G I L R C E H G V I G I V
accatgggaggcgaaggtgttgtgggttttctgctgacgtgcgcgacctcttatgggttagag
T M G G E G V V G F A D V R D L L W L E
gatgacgctatggagcagtaaggatccaccggatctagataactgatcataatcagccat
D D A M E Q - G S T G S R - L I I I S H
accacattttagtagaggttttacttggctttaaaaaacctcccacacctccccctgaaacctg
T T F V E V L L A L K N L P H L P L N L
aaacataaaaatgaatgcaattgttgggttgaacttgtttattgcagcttataatgggttac
K H K M N A I V V N L F I A A Y N G Y
aaataaagcaatagcatcacaaaatccacaataaagcatttttttctactgcattctagtc
K - S N S I T N F T N K A F F S L H S S
tgtgtgttgcacaaactcatcaatgtatcttaacgcgtaaatgtgtaagcgtttnatattt
C G L S K L I N V S - R V N C K R X Y F
gttaaaaattcgcgttaaaatfttgttaaatcagctcatttttttaccnatannngaaatc
V K I R V K F L L N Q L I F X X I X E I
ggcaaatcccttatnaatcaaaa
G K S L X N Q

```

C

```

agcagaagacggcatcaaggtgaacttcaagatccggccacaacatcgaggacggcagcgtg
A E D G I K V N F K I R H N I E D G S V
gagctcgccgaccactaccagcagaacacccccatcgccgacggccccgtgctgctgcc
Q L A D H Y Q Q N T P I G D G P V L L P
gacaaccactacctgagcaccagctccgcctgagcaaaagaccccaacgagaaagcagat
D N H Y L S T Q S A L S K D P N E K R D
cacatgggtcctgctggagttcgtgaccggccggggatcaactctcgggcatggaccagctc
H M V L L E F V T A A G I T L G M D E L
tacaagtcgggactcagatctcggagctgggccgatttgaattcgccgttgcaatgatg
Y K S G L R S R A G P A F E F A V A M M
aagagaaactcaagcacggtgaagactgagatgagcgaattcaccatgctgggcatctat
K R N S S T V K T E Y G E F T M L G I Y
gacaggtgggcccgtcttaccacggccacgtaagcctggaccaacctcctgatgaatgac
D R W A V L P R H A K P G P T I L M N D
caggaagtgggctgatggatgctaaggaattagtgagataaggatggcacaacactagaa
Q E V G V M D A K E L V D K D G T N L E
ctgacattgcttaaattaacaggaatgagaagttcagagacatcagaggcttcttagct
L T L L K L N R N E K F R D I R G F L A
aaggaggagatggaggtcaacgaagccgtgctagcaattaataaccagtaattttcccaac
K E E M E V N E A V L A I N T S K F P N
atgtacattccagtgggacaagtcacggactacggcttcttaaacctgggtggtacacc
M Y I P V G Q V T D Y G F L N L G G T P
actaagagaatgctcatgtacaactcccccaagagcaggtcagtcggcgagtgctc
T K R M L M Y N F P T R A G Q C G G V L
atgtccactggcaaagtcttgggaatccatgvtggtggaaatggtcatcaagggtttctca
M S T G K V L G I H V G G N G H Q G F S
gcagcatttctcaagcactacttcnatgatgaacaatnanggatccaccggatctagata
A A L L K H Y F X D E Q X X I H R I - I
actgatcataatcagccataccacattttagaggttttacttgctttaaaaaacctccc
T D H N Q P Y H I C R G F T C F K K P P
acacctccccngaantgaaacataaaatgaatgcaattg
T P P X E X E T - N E C N

```

D

```

agcagaggctgaagctgaaggacggggccactaccagcgtgaggtcaagcccacta
Q Q R L K L K D G G G H Y D A E V K T T T Y
aaggccaagaaagccgctgcagctgcccggccctacaacgtcaacatcaagttggatc
K A K K P V Q L P G A Y N V N I K L D I
acctccccacaacgaggactacacpatcgtggaacaglacgaacggccggaggccccc
T S H N E D Y T I V E Q Y E R A E G R H
ccaccggcggcatggaccgagctgtacaagtccggactcagatctcggagctgggccgca
S T G G M D E L Y K S G L R S R A G P A
tttgaattcgccgttgcaatgatgaagagaaactcaagcacggtgaagactgagatggc
F E F A V A M M K R N S S T V K T E Y G
gaattcaccatgctgggcatctatgacaggtgggcccgtcttaccacggccacgctaagcct
E F T M L G I Y D R W A V L P R H A K P
ggaccaacctcctgatgaatgaccaggaagtgggcccgtgatggatgctaaggaattagtg
G P T I L M N D Q E V G V M D A K E L V
gataaggatggcacaacactagaactgacattgcttaaattaacaggaatgagaagttc
D K D G T N L E L T L L K L N R N E K F
agagacatcagaggcttcttagctaaaggagatggaggtcaacgaagccgtgctagca
R D I R G F L A K E E M E V N E A V L A
attaataaccagtaaatcccaacatgtacattccagtgggacaagtcacggactacggc
I N T S K F P N M Y I P V G Q V T D Y G
ttcctaaacctgggtggtacaccactaagagaatgctcatgtacaactccccacaaga
F L N L G G T P T K R M L M Y N F P T R
gcaggtcagtcggcgagtgctcatgtccactggcaaagtcttgggaatccatggttgg
A G Q C G G V L M S T G K V L G I H V G
ggaaatggtcatcaaggtttctcagcagcacttctcaagcactacttcaatgatgaaca
G N G H Q G F S A A L L K H Y F N D E Q
taaggatccaccggatctagataactgatcataatcagccataccacattttagaggtt
- G S T G S R - L I I I S H T T F V E V
ttacttgctttaaaaaacctccccaccctccccctgaacctgaaacataaaatgaaatgca
L L A L K N L P H L P L N L K H K M N A
attgttggtttaacttggttatgtcagcttataatggntnacaaataaancaatancat
I V V V N L F I A A Y N X X Q I X Q X H
cacaatttcacaataaancattttttcactgcattctanttg
H N F T N K X F F S L H X X

```

Appendix 1 Translation results from the constructs encoding CAV-9 fusion proteins. A. pEGFP-2A, B. pmCherry-2A, C. pEGFP-3C and D. pmCherry-3C. Green and red highlighting shows the EGFP and mCherry proteins. Yellow shows the vector sequence after the CAV-9 insert. The sequence obtained for EGFP-3C had some ambiguities (N) close to the C-terminus, but the sequence chromatograph showed that the sequence is correct.

```

ctgnaaactgaaagacggcggccactaaggacgctgaggtcaagaccactacaaggccaa
X K L K D G G H Y D A E V K T T Y K A K
aaagccgtgcagctgcccagggactaccgcgacacatcaagtggaacatccctccca
K P V Q L P G A Y N V N I K L D I T S H
aaaggaactacacacatggtggaacactacgaacggcggcagggccgcaactccacggg
N E D Y T I V E Q Y E R A E G R H S T G
aaatgacggcgtgtaaacgtaaacgtaaacgtaaacgtaaacgtaaacgtaaacgtaaacg
G M D E L Y K S G L R S R A R E F K N E
cgggagttcaaaaatgaa
gctccttatgatggacaattggaacacatcatttctcaaatggcatatattactggttca
A P Y D G Q L E H I I S Q M A Y I T G S
acaactggccatgatgactcattgcccggttatcaacatgatgaaattatactccatggt
T T G H M T H C A G Y Q H D E I I L H G
cattccattaagtatttagaacaagaagatgaattgacactacattacaagaataaagtt
H S I K Y L E Q E D E L T L H Y K N K V
ttcccaattgaacaaccatctgttaccacaagtgacacttggtggttaaccaatggatttg
F P I E Q P S V T Q V T L G G K P M D L
gctatttctcaagtgttaagttgcctttcaggttcaagaaaaactctaaatattacaccaac
A I L K C K L P F R F K K N S K Y Y T N
aagattggaactgaaagtatgtaaatctggatgactgagcaaggcattattaccaaggaa
K I G T E S M L I W M T E Q G I I T K E
gtccaaagagtgaccattcaggtggcatcaagacaagggaaggaactgaaagcacaag
V Q R V H H S G G I K T R E G T E S T K
actatcagttatactgttaaatcttgcaaaaggaaatggtggtggcctacttatttcaaaa
T I S Y T V K S C K G M C G G L L I S K
gtagaaggtaacttcaaaatcctgggtatgcatattgctggttaatggtgaaatgggagta
V E G N F K I L G M H I A G N G E M G V
gctataccctttaattttcttaaaaatgacatgtctgatcaataaggatccaccggatct
A I P F N F L K N D M S D Q - G S T G S
agataactgatcataatcagccataccacattttagtagaggttttacttgctttaananac
R - L I I I S H T T F V E V L L A L X X
ctccacacctccccctgaacctgaaacataaanatgaatgcaattgttggtgtaacttg
L P H L P L N L K H X M N A I V V V N L
tttattgcagcttataatggttacaaataaagcaatagcatcacaatttcacaaataaa
F I A A Y N G Y K - S N S I T N F T N K
gcatttttttcaactgcattctagtgtggtttgtccaaactcatcaatgtatcttaacgc
A F F S L H S S C G L S K L I N V S - R
gtaaattgnaagcggttaatnntttgttaaaaattcnngttaaatTTTTGTAAATcannnc
V N X K R - X F V K I X V K F L L N X X
atTTTTtaaccaataaggccgaaatccgg
I F - P I R P K S

```

Appendix 2 Sequence translation results of fusion protein mCherry-3C. Red highlighting shows mCherry proteins. Yellow shows vector sequence after the HPeV-1 insert. Red box showing the HPeV-1 3C active site GXCG.